

idics

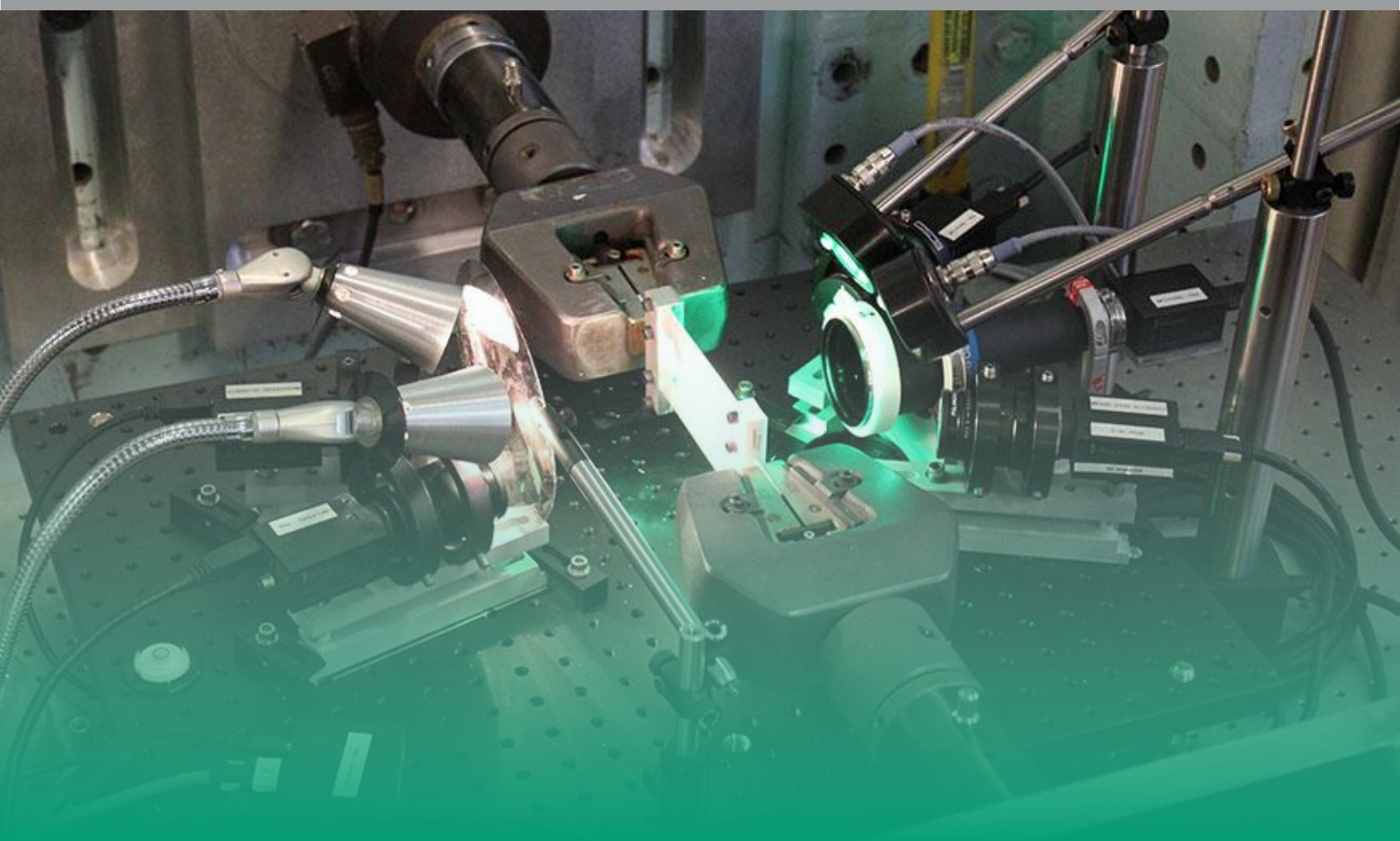
**INTERNATIONAL
DIGITAL IMAGE CORRELATION
SOCIETY**

A Good Practices Guide for Digital Image Correlation

Standardization Committee

October 2025

EDITION 2



Safety Disclaimer 0.1 — General Safety Disclaimer

This guide does not address the health or safety concerns regarding the application of DIC in a mechanical testing or laboratory environment. It is the responsibility of the laboratory and user to determine the appropriate safety and health requirements.

Copyright ©2018, 2025 by International Digital Image Correlation Society (iDICs)

Some rights reserved. This publication may be reproduced, distributed, or transmitted in any form or by any means, including photocopying, recording, or other electronic or mechanical methods, but only without alteration and with full attribution to the International Digital Image Correlation Society (iDICs). Exception is given in the case of brief quotations embodied in other documents with full attribution to the International Digital Image Correlation Society, but not in a way that suggests endorsement of the other document by the International Digital Image Correlation Society. For permission requests, contact the International Digital Image Correlation Society at info@idics.org.

DOI: 10.32720/idics/gpg.ed2

Electronic copies of this guide are available at www.idics.org.

Suggested citation: International Digital Image Correlation Society, Jones, E.M.C. and Iadicola, M.A. (Eds.) (2025). *A Good Practices Guide for Digital Image Correlation*, Edition 2. <https://doi.org/10.32720/idics/gpg.ed2>.



About this Guide

The International Digital Image Correlation Society (iDICs) was founded in 2015 as a nonprofit scientific and educational organization committed to training and educating users of digital image correlation (DIC) systems. iDICs is composed of members from academia, government, and industry, and develops world-recognized DIC training and certifications to improve industry practice of DIC for general applications, with emphasis on both research and establishing standards for DIC measurement techniques. More information can be found at www.idics.org.

To support this mission, the iDICs Standardization Committee was formed in part to develop guidelines for DIC practitioners. Details of the entire development and review process can be obtained through iDICs (info@idics.org), but they are summarized here. The working group on Good Practices, Reporting Requirements and Terminology (a subset of the committee) developed this Good Practices Guide for DIC. The working group was composed of expert DIC practitioners (see below), including representatives from many commercial DIC software packages, with diverse experience using DIC in a myriad of applications.

After a final draft of the guide was completed by the working group, a public comment period was opened in November 2017 through January 2018, during which any DIC practitioner could opt-in to review the Guide. In total, 100 people opted-in to the review process, 56 of whom returned official votes. Of the 56 received votes, 23 people voted “Approve without comment”, 32 people voted “Approve with comments and suggested revisions”, and 1 person voted “Disapprove with comments (at least one technical) and suggested revisions”. Over 500 comments were received (over 130 of which were technical comments), and the working group addressed each, either through revising the Guide, or through a written rebuttal. After that revision, the final version of the Guide and the working group responses to the comments were reviewed and approved by some of the members of the iDICs Executive Board, who did not participate in either the working group or the public comment period. Edition 1 of the Guide was officially released in October 2018.

During the public comment period for Edition 1 of the Guide, the Standardization Committee surveyed reviewers for what areas of the Guide needed to be prioritized for future improvement and expansion. Based on these results, the global DIC working group and the Figure-Examples-References working groups were formed. The Standardization Committee continued to collect editorial and technical comments about the entire Guide. Edition 2 of the Guide incorporates these additions and revisions.

Similar to Edition 1, a draft of Edition 2 was first reviewed by the Standardization Committee, and then opened for public comment in November 2022 through January 2023. In total, 59 people opted-in to review process, 40 of whom returned official votes. Of the 40 received votes, 11 people voted “Approve without comment”, and 29 people voted “Approve with comments and suggested revisions”. Over 600 comments were received (over 160 of which were technical comments), and the working groups and editors addressed each comment. The Standardization Committee and iDICs Executive Board reviewed the penultimate version of the Guide, and this final version was released in October 2025.

Contributors

The International Digital Image Correlation Society expresses sincere appreciation for the technical expertise and volunteered time of everyone who contributed to the creation and improvement of this Guide. Contributors and affiliations are shown for each edition at the time of publication (2018 for Edition 1 and 2025 for Edition 2).

Editors

Elizabeth M. C. Jones, Ph.D., Principal Member of Technical Staff, Sandia National Laboratories, United States of America

Mark A. Iadicola, Ph.D., Staff Scientist, National Institute of Standards and Technology, United States of America

Edition 1

Chair of Working Group

Elizabeth M. C. Jones, Ph.D., Principal Member of Technical Staff, Sandia National Laboratories, United States of America

Working Group Members

Rory P. Bigger, Senior Research Engineer, Southwest Research Institute, United States of America

Benoît Blaysat, Ph.D., Professor, Université Clermont Auvergne, France

Christofer Boo, Product Manager, Image Systems, Sweden

Manuel Grewer, Ph.D., Product Manager, LaVision GmbH, Germany

Jun Hu, Ph.D., Engineer, AK Steel, United States of America

Amanda R. Jones, Ph.D., Senior Member of Technical Staff, Sandia National Laboratories, United States of America

Markus Klein, GOM GmbH, Germany

Pascal Lava, Ph.D., Managing Director, Match ID, Belgium

Mark Pankow, Ph.D., Assistant Professor, North Carolina State University, United States of America

Kavesary Raghavan, Ph.D., PE, Senior Staff Engineer, AK Steel Corporation, United States of America

Phillip L. Reu, Ph.D., Distinguished Member of Technical Staff, Sandia National Laboratories, United States of America

Timothy Schmidt, Trilion/GOM, United States of America

Thorsten Siebert, Ph.D., R&D Manager, Dantec Dynamics GmbH, Germany
Micah Simonsen, Correlated Solutions, United States of America
Andrew Trim, Materials Engineering and Structural Dynamicist, Atomic Weapons Establishment, United Kingdom
Daniel Z. Turner, Ph.D., Center for Computing Research, Sandia National Laboratories, United States of America
Alessandro F. Vieira, Senior Instrumentation Engineer, Boeing, United States of America
Thorsten Weikert, GOM GmbH, Germany

Edition 2, Figures, Examples, and References

Chair of Working Group

Amanda R. Jones, Ph.D., Senior Member of Technical Staff, Sandia National Laboratories, United States of America

Working Group Members

Nathan Bechle, Ph.D., Engineer, U.S. Forest Service, United States of America
Sante DiCecco, Ph.D., Candidate, University of Waterloo, Canada
Jevan Furmanski, Ph.D., Staff Scientist, University of Dayton Research Institute, United States of America
Brian Harmon, Ph.D., Marketing Specialist, Correlated Solutions, United States of America
Mark A. Iadicola, Ph.D., Staff Scientist, National Institute of Standards and Technology, United States of America
Behrad Koohbor, Ph.D., Assistant Professor, Rowan University, United States of America

Edition 2, Global DIC

Chair of Working Group

Florent Mathieu, Ph.D., Managing Director, EikoSim, France

Working Group Members

Benoît Blaysat, Ph.D., Professor, Université Clermont Auvergne, France
Michel Coret, Ph.D., Professor, Ecole Centrale de Nantes, France
François Hild, Ph.D., Research Director, Ecole Normale Supérieure Paris-Saclay, France
Pascal Lava, Ph.D., Managing Director, MatchID, Belgium
Jean-Charles Passieux, Ph.D., Professor, INSA Toulouse, France
Jean-Noël Périé, Ph.D., Associate Professor, Université de Toulouse 3, France
Julien Réthoré, Ph.D., Research Director, Ecole Centrale de Nantes, France
Nicolas Swiergiel, Photomechanics Expert, ArianeGroup, France
Zixiang Tong, Graduate Student, The University of Texas at Austin, United States of America
Jin Yang, Ph.D., Assistant Professor, The University of Texas at Austin, United States of America

Conventions

In this guide, certain items are highlighted, set aside, or labeled separately from the main body based on the following conventions.

Recommendation 0.1 — Recommendation Convention

Recommendation text boxes are suggestions about specific actions a DIC practitioner should take, or specific decisions a DIC practitioner should make. Recommendations are intended to be ideal suggestions; in other words, for ideal DIC measurements within the scope of this document, a DIC practitioner would follow all recommendations.

Tip 0.1 — Tip Convention

Tip text boxes provide supplementary information that can be useful to a DIC practitioner, helping to design and execute DIC measurements. “Tips” are typically background information, targeted to either inexperienced DIC practitioners, or to experienced DIC practitioners working with advanced setups. “Tips” are differentiated from “Recommendations” in that “Tips” do not imply a specific action or decision that a DIC practitioner should follow.

Caution 0.1 — Caution Convention

Caution text boxes provide information about events, decisions, or features that could have negative impacts on DIC measurements. “Cautions” are often followed by “Recommendations”, which provide information on avoiding or mitigating the negative event, decision, or feature.

Example 0.1 — Example Convention

Example text boxes provide more detailed descriptions of topics using specific scenarios to demonstrate good practices.

Local-Global Flag 0.1 — Local-Global Convention

Local-Global text boxes indicate that a section or statement contains information specific to local DIC (such as mentions of subsets or step size) that should be dealt with carefully when using a global DIC method. Whenever a Local-Global text box appears in the body of the guide, the reader is referred to the Global DIC appendix in the main Good Practices Guide for details [\[1\]](#).

Footnote

Footnotes are reserved for brief remarks on topics that are outside of the scope of this edition of the guide. Their primary purpose is to inform the reader when the guidelines given in this guide are not applicable, to ensure that the guidelines are applied appropriately.

Appendix

Appendices are reserved for supplementary information that, due to length or complexity, would clutter and defocus the main body of text.

Contents

Front Matter	ii
Disclaimer	ii
Copyright	iii
About this Guide	iv
Contributors	v
Conventions	vii
1 Introduction	1
1.1 Aims and Basic Principles of DIC	1
1.2 Scope of this Guide	4
1.3 Scope for Common Mechanical Tests with DIC Measurements	5
2 Design of DIC Measurements	7
2.1 Measurement Requirements	7
2.1.1 Quantity-of-Interest	7
2.1.2 Region-of-Interest	7
2.1.3 Field-of-View	7
2.1.4 Position Envelope for Hardware	8
2.1.5 2D-DIC vs. Stereo-DIC	8
2.1.6 Stereo-Angle	11
2.1.7 Depth-of-Field	11
2.1.8 Spatial Gradients	12
2.1.9 Noise-Floor	17
2.1.10 Frame Rate and Image Acquisition Rate	17
2.1.11 Exposure Time	19
2.1.12 Synchronization and Triggering	20
2.2 Equipment and Hardware	20
2.2.1 Camera and Lens Selection	20
2.2.2 Camera and Lens Mounting	22
2.2.2.1 General Characteristics of Mounting System	22
2.2.2.2 Types of Mounting Systems	29
2.2.3 Aperture	29
2.2.4 Lighting and Exposure	30
2.2.4.1 Type of Lighting	32
2.2.4.2 Light Mounting	33

2.2.4.3	Contrast, Intensity, and Gain	34
2.2.5	Hardware Heating	35
2.3	DIC Pattern	37
2.3.1	Type of DIC Patterns	37
2.3.2	General Characteristics of DIC Patterns	38
2.3.2.1	Size	38
2.3.2.2	Variation	41
2.3.2.3	Density	42
2.3.2.4	Quality	43
2.3.2.5	Reflections	43
2.3.3	Characteristics of Applied Patterns	44
2.3.3.1	Non-Invasive	44
2.3.3.2	Bonding	45
2.3.3.3	Fidelity	47
2.3.3.4	Thickness	48
2.3.4	Patterning Techniques	48
3	Preparation for the Measurements	49
3.1	Pre-Calibration Routine	49
3.1.1	Review of Test Procedure	49
3.1.2	Cleanliness of Equipment	49
3.1.3	Camera Warm-Up	51
3.1.4	Synchronization	52
3.1.5	Application of the DIC Pattern	53
3.1.6	Pre-Calibration Review of System	53
3.1.6.1	Position Test Piece and Cameras	54
3.1.6.2	Verify Optical System	54
3.1.6.3	Lock Adjustable Components	54
3.1.6.4	Review Images	54
3.1.6.5	Accept the DIC System	56
3.2	Calibration	56
3.2.1	Purpose of Calibration	56
3.2.2	General Calibration Steps	57
3.2.2.1	Select Calibration Target	57
3.2.2.2	Clear Working Space	58
3.2.2.3	Adjust Lighting	59
3.2.2.4	Acquire Calibration Images	60
3.2.2.5	Calibrate System	63
3.2.2.6	Review Calibration Results	63
3.2.2.7	Review Calibration Parameters	64
3.3	Post-Calibration Routine	66
3.3.1	Images for Calibration Verification and Noise-Floor Analysis	66
3.3.1.1	Reset System	66
3.3.1.2	Adjust Lighting	66
3.3.1.3	Acquire Static Images	66
3.3.1.4	Review Images	67
3.3.1.5	Acquire Rigid-Body-Motion Images	67

3.3.2	Verification of Calibration	68
3.3.2.1	Intrinsic Parameters	68
3.3.2.2	Extrinsic Parameters	69
3.3.2.3	Absolute Distances	70
3.3.3	Post-Calibration Review of System	70
3.3.3.1	Noise-Floor	70
3.3.3.2	Heat Waves	71
3.3.3.3	Stability	71
3.3.3.4	Other Verifications	71
4	Execution of the Test with DIC Measurements	72
5	Processing of DIC Images	73
5.1	DIC Software	73
5.2	User-Defined Correlation Parameters	73
5.2.1	Reference Image	73
5.2.2	Pre-Filtering of Images	75
5.2.3	Matching Criterion	76
5.2.4	Subset Shape Function	77
5.2.5	Subset Weighting Function	78
5.2.6	Interpolant	78
5.2.7	Subset Size	78
5.2.8	Step Size	79
5.2.9	Thresholds	80
5.2.10	Initial Guess	80
5.3	User-Defined Post-Processing Parameters	80
5.3.1	Coordinate System	80
5.3.2	Data Filtering	81
5.3.3	Strain Calculations	81
5.4	Measurement Uncertainty (MU)	82
5.4.1	Overview	82
5.4.2	Standards for Measurement Uncertainty	82
5.4.3	Variance Errors	83
5.4.3.1	Iterations of the Noise-Floor Evaluation	84
5.4.3.2	Temporal vs. Spatial Variance Errors	84
5.4.3.3	Directional Components of the Noise-Floor	84
5.4.3.4	Quantifying Acceptable Noise-Floor for the Application	85
5.4.4	Bias Errors	86
5.4.5	Trade-Off Between Noise and Bias	86
5.4.6	Virtual Strain Gauge (VSG) Study	87
6	Reporting Requirements	94
6.1	DIC Hardware Parameters	95
6.1.1	Required	95
6.1.2	Recommended	96
6.2	DIC Analysis Parameters	96
6.2.1	Required	96

6.2.2	Recommended	97
7	Glossary and Acronyms	98
7.1	Acronyms and Initialisms	98
7.2	Units	99
7.3	Glossary	100
	References	113
A	Checklist and Flow Chart for DIC Measurements and Analysis	123
B	Focal Length, Field-of-View, Stand-Off Distance, and Aperture	128
B.1	Thin Lens Theory	128
B.2	Field-of-View and Stand-off Distance	128
B.3	Depth-of-Field	129
B.4	Reference Tables	129
C	Select Strain Calculation Methods	130
C.1	Subset Shape Function	130
C.2	Finite-Element Shape Functions	130
C.3	Strain Shape Function	131
C.4	Spline Fit	131
C.5	Hermite Method	131
C.6	Finite Difference Schemes	132
D	Global DIC	133
D.1	Introduction: What is global DIC?	133
D.2	Why use global or local DIC?	135
D.3	Global DIC Practical Implications	136
D.3.1	Mesh Definition and Positioning	136
D.3.2	Calibration	137
D.3.2.1	2D Global DIC	137
D.3.2.2	Stereo Global DIC	138
D.3.3	Crack Measurement	141
D.4	User-Defined Parameters	142
D.4.1	Matching Criterion	142
D.4.2	Element Shape Function Type	143
D.4.3	Element Size	143
D.4.4	Additional Regularization	144
D.5	Analysis Results for Global DIC Methods	146
D.5.1	Gray Level Residual	146
D.5.2	Uncertainty	146
D.5.3	Spatial Resolution	147
D.5.4	Strain Computation	148

List of Figures

1.1	2D-DIC vs. Stereo-DIC	2
1.2	Terminology Definitions	3
2.1	Out-of-Plane Errors in 2D-DIC	10
2.2	Schematic of test piece for spatial gradients example	13
2.3	Spatial gradient example strain results for FOV 1	14
2.4	Errors from spatial gradient example results for FOV 1	15
2.5	Spatial gradient example results for FOV 2	16
2.6	Image Acquisition Rate	18
2.7	Orientation of Cameras	26
2.8	Orientation of Cameras—Spatial Resolution	26
2.9	Orientation of Cameras—DOF	27
2.10	Orientation of Cameras—Summary	28
2.11	Lighting Trade-Offs	31
2.12	Heat Waves	37
2.13	Measuring Feature Size	39
2.14	Aliased Pattern	40
2.15	Pattern Variation	41
2.16	Pattern Density	42
2.17	Pattern Reflections	43
2.18	Pattern Degradation	46
3.1	Cleanliness of equipment	50
3.2	Pattern Defects and Image Issues	55
3.3	Lens Distortions	57
3.4	Calibration Volume	60
3.5	Calibration Target Orientations	61
3.6	Calibration Parameters	65
5.1	Reference image for stereo-DIC	75
5.2	VSG Example—Images to Analyze	88
5.3	VSG Example—Line Cut of Highest Strain Gradient	89
5.4	VSG Example—Effect of Step Size	90
5.5	VSG Example—Strain Noise	91
5.6	VSG Example—Noise vs. Bias	91
A.1	Flow chart of main steps for DIC measurements (part 1).	126
A.2	Flow chart of main steps for DIC measurements (part 2).	127
D.1	Comparison of global and local DIC	134
D.2	Self-Calibration for global DIC	139
D.3	Mesh Alignment for global DIC	140
D.4	Global DIC FE Mesh	140
D.5	Global DIC Element Shape Functions	144
D.6	Mechanical Regularization for Global DIC	145

D.7 Grey Level Residual for Global DIC	147
--	-----

List of Tables

2.1 Out-of-Plane Errors in 2D-DIC	10
2.2 Example calculation of physical pattern feature size.	39
5.1 DIC hardware parameters for the VSG study	87
5.2 DIC analysis parameters for the VSG study	92
6.1 DIC hardware reporting requirements	94
6.2 DIC analysis reporting requirements	95
B.1 Example reference table for FOV and DOF options.	129

List of Tips

Tip 0.1 — Tip Convention	vii
Tip 2.1 — FOV, lens focal length, and SOD	8
Tip 2.2 — Stereo-Angle	11
Tip 2.3 — Calculating and Measuring DOF	12
Tip 2.4 — DOF and Aperture	12
Tip 2.5 — Depth-of-Field for 2D-DIC	12
Tip 2.6 — Spatial Resolution	12
Tip 2.7 — Noise-Floor	17
Tip 2.8 — Frame Rate vs. Image Acquisition Rate	17
Tip 2.9 — Frame Rate and Image Brightness/Contrast	19
Tip 2.10 — Motion Blur	19
Tip 2.11 — Exposure Time and Frame Rate	20
Tip 2.12 — Exposure Time and Image Brightness/Contrast	20
Tip 2.13 — FOV, SOD, and DOF	20
Tip 2.14 — Camera and Lens Selection	21
Tip 2.15 — Low-Pass Filter	21
Tip 2.16 — Lens Selection	22
Tip 2.17 — Tape Moving Components on Lens	22
Tip 2.18 — Aligning Optical Axis for 2D-DIC	22
Tip 2.19 — Epipolar Error	23
Tip 2.20 — Vibration Detection	24
Tip 2.21 — Lens Aperture, DOF, and Image Brightness	29
Tip 2.22 — Lens Aperture, DOF, and F-Stop Number	29
Tip 2.23 — Aperture and DOF while Focusing	30
Tip 2.24 — Lighting trade-offs	30
Tip 2.25 — Cross-Polarized Light	32
Tip 2.26 — Luminescence	32
Tip 2.27 — Backlighting	33
Tip 2.28 — Pulsed Lighting	33
Tip 2.29 — Lighting Adjustments between Calibration and Test	33

Tip 2.30 — Image Contrast	34
Tip 2.31 — Heat Waves / Mirage Effect	36
Tip 2.32 — Natural DIC Pattern	38
Tip 2.33 — Camera-Limited vs. Lens-Limited Spatial Resolution	38
Tip 2.34 — Measuring Pattern Feature Size	38
Tip 2.35 — Physical Pattern Feature Size	39
Tip 2.36 — Confirming Pattern Feature Size	40
Tip 2.37 — Degradation of Patterns	43
Tip 2.38 — Verification of Pattern Quality	43
Tip 2.39 — Measurement Uncertainty due to Pattern Degradation	43
Tip 2.40 — Painted Pattern Debonding	45
Tip 2.41 — Paint Ductility	47
Tip 2.42 — Library of Patterning Techniques	48
Tip 2.43 — Verification of Patterning Technique	48
Tip 3.1 — Evaluating Cleanliness of Equipment	50
Tip 3.2 — Cleaning Camera Detectors and Lenses	51
Tip 3.3 — Camera Warm-Up	51
Tip 3.4 — Camera Synchronization	52
Tip 3.5 — Synchronization of Additional Signals	52
Tip 3.6 — Setting the Focus and Depth-of-Field	54
Tip 3.7 — Alternative Calibration Target Options	58
Tip 3.8 — Clear Working Space	58
Tip 3.9 — Lighting for Calibration	59
Tip 3.10 — Number of Calibration Images	62
Tip 3.11 — Review of Calibration Results	63
Tip 3.12 — User-Defined Inputs for Calibration	64
Tip 3.13 — Review of Calibration Parameters	66
Tip 3.14 — Rigid-Body-Motion Images	67
Tip 3.15 — User-Defined Parameters for Calibration Verification	68
Tip 3.16 — Improving the Calibration	68
Tip 3.17 — Acceptable Level of Epipolar Error	69
Tip 3.18 — Spatially-Resolved Epipolar Error	69
Tip 3.19 — Additional Influences of Epipolar Error	70
Tip 5.1 — Noise-Free Reference Image	74
Tip 5.2 — Reference Image for Stereo-DIC	74
Tip 5.3 — Low-Pass Image Pre-Filters	76
Tip 5.4 — SSD vs. ZNSSD	77
Tip 5.5 — Fourier Domain	77
Tip 5.6 — Gaussian Subset Weighting Function	78
Tip 5.7 — Subset Size	79
Tip 5.8 — Typical Displacement Noise-Floor	83
Tip 5.9 — Parameters Affecting VSG Size	88
Tip 5.10 — VSG Size Convergence	92
Tip 6.1 — Application-Dependent Reporting Requirements	94
Tip D.1 — Number of Fiducials	140
Tip D.2 — Fiducials and Calibration Target Images	140

Tip D.3 — Shape Error	141
Tip D.4 — Shape Functions for Correction Fields	143
Tip D.5 — Element Size and Number of Features	144
Tip D.6 — Shape Function	144
Tip D.7 — Validity of Kinematic Assumptions	146
Tip D.8 — Gray Level Residual and Image Noise	146

List of Recommendations

Recommendation 0.1 — Recommendation Convention	vii
Recommendation 2.1 — ROI and FOV	7
Recommendation 2.2 — Backdrop	8
Recommendation 2.3 — 2D-DIC Out-of-Plane Errors	9
Recommendation 2.4 — Telecentric Lens for 2D-DIC	9
Recommendation 2.5 — Stereo-Angle	11
Recommendation 2.6 — Camera Selection	21
Recommendation 2.7 — Lock Moving Components on Lens	22
Recommendation 2.8 — Camera and Lens Mounting Orientation	24
Recommendation 2.9 — Minimizing Vibrations	25
Recommendation 2.10 — Light Mounts	34
Recommendation 2.11 — Image Contrast	34
Recommendation 2.12 — Evaluation of DIC Pattern	38
Recommendation 2.13 — Pattern Feature Size Variation	40
Recommendation 2.14 — Mask Gripping Region	44
Recommendation 2.15 — Cleaning the Test Piece	45
Recommendation 3.1 — Maintaining Clean Equipment	50
Recommendation 3.2 — Fiducials	53
Recommendation 3.3 — Review Images via Correlation Results	55
Recommendation 3.4 — Calibration of 2D-DIC System to Correct Lens Distortions	57
Recommendation 3.5 — Selection of Calibration Target	57
Recommendation 3.6 — Metrologically Traceable Calibration Target	58
Recommendation 3.7 — Verification of Calibration	59
Recommendation 3.8 — Calibration Target Positions and Orientations	61
Recommendation 3.9 — Holder for Calibration Target	63
Recommendation 3.10 — Review of Calibration Parameters	64
Recommendation 3.11 — Static Images for Measurement Uncertainty Quantification	66
Recommendation 3.12 — Rigid-Body-Motion Images for 2D-DIC	67
Recommendation 3.13 — Rigid-Body-Motion Images for Stereo-DIC	68
Recommendation 3.14 — Evaluation of Lens Distortions	68
Recommendation 3.15 — Verification of Absolute Distances	70
Recommendation 3.16 — Abbreviated Noise-Floor Analysis	70
Recommendation 5.1 — Subset Size	79
Recommendation 5.2 — Coordinate System	81
Recommendation 5.3 — Variance Errors and Camera Noise	83
Recommendation 5.4 — QOI for VSG Study	88
Recommendation 6.1 — Reporting Requirements for Strain	96

List of Cautions

Caution 0.1 — Caution Convention	vii
Caution 2.1 — 2D Planar Assumption	8
Caution 2.2 — Telecentric Lens for stereo-DIC	9
Caution 2.3 — Large Stereo-Angles	11
Caution 2.4 — Camera Selection	21
Caution 2.5 — Interlaced Frames	21
Caution 2.6 — 2D-DIC Out-of-Plane Errors	23
Caution 2.7 — Rigid Camera Mounting	23
Caution 2.8 — Camera and Lens Mounting Balance	24
Caution 2.9 — Camera Heating	24
Caution 2.10 — Vibrations Increase Noise-Floor	24
Caution 2.11 — Vibrations Invalidate Calibration	25
Caution 2.12 — Diffraction and Aberrations	30
Caution 2.13 — Light Flicker	33
Caution 2.14 — Concerns with Lighting	33
Caution 2.15 — Evolution of Image Contrast	34
Caution 2.16 — Underexposure, Overexposure, and Glare	35
Caution 2.17 — Camera Gain	35
Caution 2.18 — Hardware Heating	35
Caution 2.19 — Fans	37
Caution 2.20 — Surface Coating on Test Piece	38
Caution 2.21 — Aliased Pattern Features	40
Caution 2.22 — Regular, Repeated, and Anisotropic Patterns	42
Caution 2.23 — Specular Reflections	44
Caution 2.24 — Pattern Compliance	45
Caution 2.25 — Destructive Patterning Methods	45
Caution 2.26 — Pattern Debonding	46
Caution 2.27 — Laser Speckle Patterns	47
Caution 2.28 — Pattern Thickness	48
Caution 3.1 — Cleaning Camera Detectors and Lenses	51
Caution 3.2 — Camera Warm-Up	52
Caution 3.3 — Camera Synchronization	52
Caution 3.4 — Pre-Calibration Review of System	53
Caution 3.5 — Accept the DIC System	56
Caution 3.6 — Calibration of 2D-DIC System	56
Caution 3.7 — Pre-Calibration Review	57
Caution 3.8 — Relative Motion between Cameras	59
Caution 3.9 — Lighting for Calibration	60
Caution 3.10 — Equipment Adjustments after Calibration	60
Caution 3.11 — Calibration Score	62
Caution 3.12 — High-Quality Calibration Images	62
Caution 3.13 — Calibration Score	66
Caution 3.14 — Recalibration of the System	67
Caution 3.15 — Adjusting Optical System Hardware during Calibration	68
Caution 3.16 — Evaluating Lens Distortions for 2D-DIC	69

Caution 4.1 — Static Reference Image	72
Caution 5.1 — Static Reference Image	74
Caution 5.2 — Low-Pass Image Pre-Filters	76
Caution 5.3 — Data Filtering	81
Caution 5.4 — VSG Study Line Cut	89
Caution 5.5 — Noise on Peak Strain Magnitude	89
Caution 5.6 — Peak Strain Magnitude Dependence on Step Size	90
Caution D.1 — Element Size	137
Caution D.2 — Mesh Position Uncertainty	138
Caution D.3 — Planar Assumption of 2D-DIC Calibration	138
Caution D.4 — Mesh Alignment	141
Caution D.5 — Initialization of the Calibration Problem	141
Caution D.6 — Shape Function and Element Size	143
Caution D.7 — Element Size and Shape Function	144
Caution D.8 — Regularization Implementation	146
Caution D.9 — Bias Errors Due to Regularization	146
Caution D.10 — Filtering of Displacements for Strain Calculations	148

List of Examples

Example 0.1 — Example Convention	vii
Example 2.1 — Estimating 2D-DIC Strain Errors due to Out-of-Plane Motion	9
Example 2.2 — Camera Selection Based on Strain Gradients	13
Example 2.3 — Image Acquisition Rate	17
Example 2.4 — Camera Orientation	25
Example 5.1 — Virtual Strain Gauge (VSG) Study	87
Example B.1 — FOV, SOD, and DOF	129

List of Local-Global Flags

Local-Global Flag 0.1 — Local-Global Convention	vii
Local-Global Flag 5.1 — Matching Criterion	76
Local-Global Flag 5.2 — Element Shape Function	78
Local-Global Flag 5.3 — Subset/Element Size	79
Local-Global Flag 5.4 — Step Size	79
Local-Global Flag 5.5 — Thresholds	80
Local-Global Flag 5.6 — VSG Size	88
Local-Global Flag 6.1 — Reporting Requirements	96

List of Safety Disclaimers

Safety Disclaimer 0.1 — General Safety Disclaimer	ii
---	----



1 — Introduction

1.1 Aims and Basic Principles of DIC

Within the scope of this guide, DIC is an optically-based technique used to measure the evolving full-field 2D or 3D coordinates on the surface of a test piece throughout a mechanical test. The measured coordinate fields can be used to calculate derived field quantities-of-interest (QOIs), such as displacements, strains, strain rates, velocities, and curvatures. Because DIC is a non-contact technique that is independent of the material being tested or the length-scale of interest, it can be used in a wide variety of applications to investigate and characterize the deformation of solids. Some common materials that are tested include metals, polymers, concrete, geological samples, biological tissues, battery electrodes, explosives, etc. Test pieces range from, for example, small coupons used in tensile tests up to entire sub-assemblies of aircraft. This versatility has led to a plethora of methodologies and software codes, both commercial and independently developed, to utilize the data captured from a DIC measurement. For a list of DIC software packages, see the iDICs website at <https://idics.org/resources/>.

The optical principles relevant to DIC are rooted in optical engineering theory and geometric optics, e.g. [2–4], as well as computer vision and photogrammetry techniques, e.g. [5, 6]. A complete introduction and description of the main theory and applications of DIC is presented in [7]. A practical guide to getting started with DIC is the series of articles in [8–31]. The reader is referred to these resources for a more thorough background of DIC. Here, the basic concepts of DIC are overviewed.

At the core level, DIC is based on optical flow [7, Sec. 5.2], [32], which dictates that the intensity of an image, or [gray level value](#), is conserved as the image is deformed. Grey level intensity conservation is expressed mathematically as:

$$F(\mathbf{x}) = G(\mathbf{x} + \mathbf{u}(\mathbf{x})), \quad (1.1)$$

where F is the intensity of the undeformed image (i.e. the image of the undeformed test piece), G is the intensity of the deformed image (i.e. the image of the deformed test piece), and $\mathbf{u}(\mathbf{x})$ is the displacement field at location \mathbf{x} . Since an exact equality can not be practically realized (due to, for instance, image noise, among other factors), an optimization problem is formulated to minimize the difference between F and G in order to estimate the full-field displacements \mathbf{u} that describe the motion between the two images. Moreover, the image intensities can be scaled and/or normalized to account for variations in lighting throughout a test, such that only the relative (and not the absolute) intensity and contrast need to be conserved [7, Sec. 5.4].

In practice, a high-contrast pattern on the surface of the test piece—either natural or applied—is imaged, leading to the grey level intensity distribution that is tracked in the images. A fundamental assumption in DIC measurements is that the pattern that is imaged follows the deformation of the underlying test piece. Thus, the images of the test piece taken throughout the test can be correlated

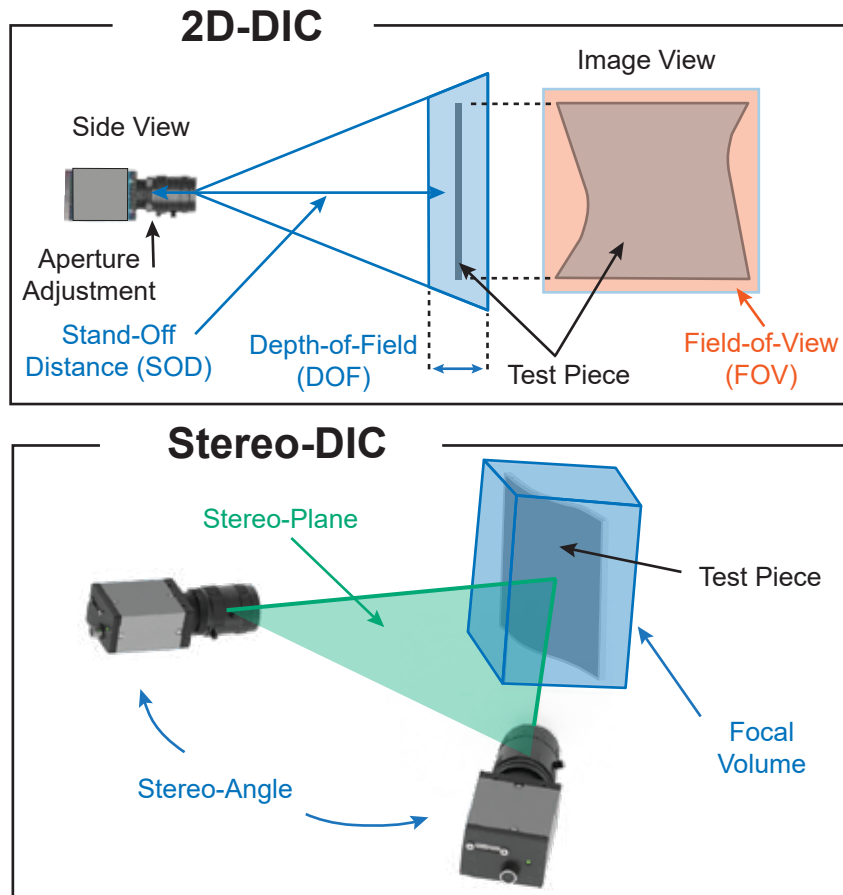


Figure 1.1: Schematic illustrating the differences between 2D-DIC and stereo-DIC. [Stand-off distance \(SOD\)](#), [field-of-view \(FOV\)](#), [depth-of-field \(DOF\)](#), [stereo-angle](#), [stereo-plane](#), and [focal volume](#) are also defined. See also the corresponding definitions in the glossary (Ch. 7).

to produce full-field coordinates representative of the shape, motion and deformation of the surface of the test piece. 2D coordinates of the surface can be measured using a single camera system, and this is referred to as 2D-DIC. 3D coordinate measurements of the surface require two cameras¹ oriented at a stereo-angle to perform 3D photogrammetry in addition to image correlation [7, Sec. 4.2], [33]; this is called stereo-DIC.² Fig. 1.1 shows a schematic of 2D-DIC and stereo-DIC. Before measurements are made, the camera/lens system is calibrated by imaging features of known separation lengths, i.e. a [calibration target](#) (Sec. 3.2). This calibration allows DIC software to correct for lens distortions and,

¹Stereo-DIC can be performed with a single camera using stereo optics, where the detector is split into two halves, and the two halves are taken as the primary and dependent images, respectively, or using mirrors to separate the image from a single camera into two image sets. Stereo-DIC can also be performed with more than two cameras, for instance to view a larger ROI of the test piece. Both of these configurations are advanced topics that are beyond the scope of the current edition of this guide.

²Stereo-DIC is often called 3D-DIC. However, to avoid confusion with digital volume correlation (DVC), this guide recommends the term stereo-DIC instead of 3D-DIC. See the Glossary entry "[Digital Image Correlation](#)" for more information.

for stereo-DIC, provides the location and orientation of the cameras in space with respect to each other, and to the test piece.

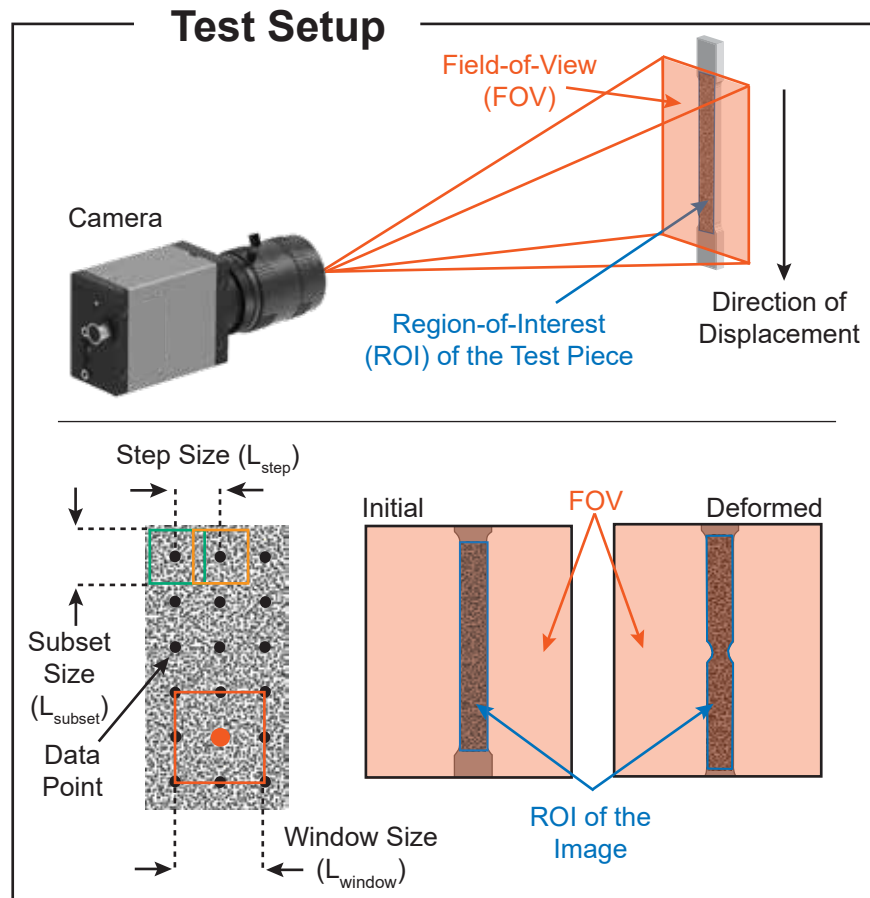


Figure 1.2: Schematic illustrating several terminology definitions, including the **ROI of the test piece**, **ROI of the image**, **subset** (orange square) and **subset size**, **step size**, **window size** (representing, for example, a **strain window** (red square) or a **filter window**), **field-of-view (FOV)**, and **data point** (also called interrogation or measurement point). See also the corresponding definitions in the glossary (Ch. 7).

There are many types of software developed to perform this correlation, but the two most common categories are local and global DIC methods. In a local method, the solution at a point depends only on a small subset of the image in the vicinity of that point, but is otherwise independent of the solution at all other points of interest. In a global method, all points of interest are inter-dependent and are solved for simultaneously. See Fig. D.1 for an illustration of the two methods. For the most part, the content of this guide is applicable to both methods, especially concerning the Design of DIC Measurements (Ch. 2), Preparation for the Measurements (Ch. 3), and Execution of the Test with DIC Measurements (Ch. 4); however, this guide is written from the perspective of local DIC when discussing the Processing of DIC Images (Ch. 5). Therefore, Appendix D has been written with global DIC users in mind to separately address the specifics of global DIC. Moreover, “Local-Global Flags” throughout this guide

denote sections or statements that contain information specific to local DIC and refer the reader to Appendix D for information specific to global DIC.

In brief, a software code analyzes a user-defined **region-of-interest (ROI) within the images** (Sec. 2.1.2), which contains a set of **data points**, also called interrogation points or measurement points. In local DIC, each data point is centered within a **subset** of the image (Sec. 5.2.7). The data points are typically defined at some regular spacing called the **step size** (Sec. 5.2.8), such that neighboring subsets may (or may not) overlap. The subsets are numerically correlated from the reference image (Sec. 5.2.1) acquired before motion/deformation to each subsequent image acquired during or after motion/deformation. See Fig. 1.2 for an illustration of some of these terminology definitions, as well as the glossary (Ch. 7). This correlation is performed by first approximating the pattern in each subset using an **interpolant function** (Sec. 5.2.6, [7, Sec. 5.6.1 and Sec. 10.2.3.2], [34, 35]), and then allowing that function to deform from the reference image based on a **subset shape function** (Sec. 5.2.4, [7, Sec. 5.3], [35, 36]). A **matching criterion** (Sec. 5.2.3, [7, Sec. 5.4], [37–39]) in conjunction with **subset weights** (Sec. 5.2.5, [7, Sec. 5.3.1]) is used to match each subset in the reference image with the corresponding subset in the deformed images. In stereo-DIC, the matching criterion, along with the parameters of the stereo-system calibration, are used to match subsets from one of the cameras to the other camera. The result of the correlation is the measured coordinates of the center of each subset. The process is similar for global DIC, with the primary difference being that the interpolant functions are defined on the entire ROI of the image simultaneously, often using a finite-element discretization, rather than on individual subsets (see Appendix D.1).

The calculation of derived field quantities is the final step in many DIC processing schemes. DIC provides access to kinematic QOIs, such as curvature, velocity, and acceleration. One of the most commonly derived QOIs is strain, which is computed from the displacement gradients with a **strain window** or **filter window** (Fig. 1.2, Sec. 5.3.3). The minimum resolution (also called the noise-floor) of the QOIs, as well as potential bias errors, are tied to both the measurement setup (e.g. camera selection, image contrast, DIC pattern feature size), and the data processing parameters (e.g. subset size, subset shape function, and virtual strain gauge for local DIC; and element shape function and element size for global DIC). Therefore, determination of the resolution of the QOIs through quantification of the measurement uncertainty completes the DIC data processing (Sec. 5.4). This leaves the user with a full-field description of displacements, and/or derived quantities, of a test piece subjected to a mechanical test, as well as the uncertainties of those measurements.

The last chapter of the guide aims to define critical reporting requirements (Ch. 6), which serve two main purposes: (1) reporting experimental parameters and/or analysis methods allows others to understand and repeat the experiment (2) accurate reporting yields credibility for the individual practitioner in terms of experimental procedures/ analysis as well as the community as a whole.

1.2 Scope of this Guide

The purpose of this document is to provide good-practice guidelines for conducting DIC measurements in conjunction with mechanical testing of a planar test piece under common laboratory test conditions. This guide is designed to be both a primer training document geared towards new practitioners of DIC (supplementing vendor-based or other formal training, and hardware- and software-specific documentation), as well as a reference for experienced users, to refresh their fundamental knowledge and skill sets, and assist them in troubleshooting DIC measurements. Appendix A provides a checklist of the major points to consider when designing, executing, and analyzing DIC measurements, while Fig. A.1 illustrates the steps of a typical mechanical test with DIC measurements in graphical form. Details for

each step of the checklist and the flow chart are presented in the body of each section of this guide. The goal of this guide is to aid DIC practitioners in achieving well planned, well executed, well analyzed, and well documented DIC measurements. Note that this guide does *not* provide any guidelines for the mechanical test itself; it focuses only on the complementary DIC measurements.

In developing this guide, we strove to include as many instructive and diagnostic suggestions as possible, while still keeping the document general, and independent of specific hardware or software packages. As this document is a guide and not a standard, the guidelines presented here are not strict requirements for DIC measurements, but rather are suggestions for good practices. However, some guidelines are considered to be crucial for reliable and trustworthy measurements, while others are recommendations that serve to increase confidence in the measurements. This guide attempts to delineate between crucial and recommended guidelines, and provide cautionary notes about the consequences of omitting each guideline.

This guide focuses on good practices for DIC measurement setup, image correlation, and basic post-processing of DIC data for strain computations. It does not cover other data processing, such as velocity, acceleration, curvature, etc., nor specific data analysis applications that utilize DIC data, such as finite-element model (FEM) validation, material identification, etc.

1.3 Scope for Common Mechanical Tests with DIC Measurements

This guide applies to the following conditions found in typical mechanical test arrangements and associated DIC setups. Additional considerations that are not discussed in the current edition of this guide may be necessary for test conditions outside of those listed here.

- Test piece size of approximately 50 mm to 1 m
- Planar test pieces undergoing nominally planar motion and/or deformation
- Strain range of approximately 0.05% (500 $\mu\text{m}/\text{m}$) to 60% (0.6 mm/mm)
- Quasi-static tests³
- General purpose laboratory testing with a well-controlled environment (e.g. room temperature of 10–35°C, and minimal vibrations)
- No special environmental conditions (e.g. no environmental chambers, no water tanks or pressurized vessels, no windows or viewports, no explosions or shock waves)
- Optical-based images (no images based on, for example, scanning electron microscopes, atomic force microscopes, or X-rays)

³Most guidelines presented here are applicable to both quasi-static and dynamic tests and are not limited to a certain range of test piece velocities or strain rates. However, there are some caveats to the applicability of this guide to dynamic tests. First, this guide is limited to typical machine vision cameras and excludes high-speed cameras, due to additional hardware complexity. High-speed cameras are defined here as cameras that record data in a burst to a RAM buffer on local camera memory that must be downloaded afterward. Second, special care and attention is often required when selecting a DIC pattern for dynamic tests, and this guide does not provide any guidelines, tips, or recommendations regarding this topic. Third, synchronization — both between cameras for stereo-DIC and between the camera(s) and other data of interest (e.g. force) — is often more complex for dynamic tests, but this guide only discusses the most basic need for camera synchronization for stereo-DIC. These and other features of dynamics tests are all beyond the scope of the current edition of this guide.

- 2D-DIC and stereo-DIC⁴
- Single DIC system: One camera for 2D-DIC and two cameras⁵ for stereo-DIC⁶
- Typical machine vision cameras and optical lenses (no images from, for example, microscopes, stereo microscopes, or high-speed cameras)
- Local, subset-based DIC algorithms in the main text, as well as global DIC algorithms in Appendix D

iDICs is continuously striving to improve and expand this guide. As such, there are several working groups focusing on relaxing the above restrictions and generalizing the scope of topics and applications covered by this guide. For more information on current efforts and/or to participate in a working group, please email the editors at guide@idics.org. All experience levels are welcome!

⁴Digital volume correlation (DVC) and other image processing techniques such as image stitching, photogrammetry data alignment, point tracking, object tracking, etc. are not discussed.

⁵See footnote 1 on page 2.

⁶The use of multiple cameras or multiple systems covering different regions-of-interest of a test piece, e.g. around a cylinder, is not discussed.

2 — Design of DIC Measurements

2.1 Measurement Requirements

Before conducting DIC measurements, clearly define the expectations and requirements of the mechanical test, and the objectives of the DIC measurements. The limits chosen here will be used later to assess if the analyzed results are within, approaching, or past the limits for which the DIC measurements were designed.

2.1.1 Quantity-of-Interest

Select the quantity-of-interest (QOI) such as shape, displacement, velocity, acceleration, strain, strain-rate, etc.

2.1.2 Region-of-Interest

Select the region-of-interest (ROI) of the test piece, and determine the expected motion and/or deformation of this region. The ROI may be a specific portion of the entire test piece (e.g. the gauge length and exposed end tabs of a uniaxial test piece). See Fig. 1.2 for a depiction of both the ROI of the test piece and the ROI of the image.

2.1.3 Field-of-View

Determine the required field-of-view (FOV) based on the ROI of the test piece and expected motion and/or deformation of the test piece. See Fig. 1.1 and Fig. 1.2 for a depiction of the FOV.

Recommendation 2.1 — ROI and FOV

Typically, the ROI of the test piece should almost fill the FOV to optimize the [spatial resolution](#) of the DIC measurements, while still remaining in the FOV throughout the test. For stereo-DIC, where the FOV is not the same in each camera, the effective FOV is the common FOV that is captured in both cameras, i.e. the portion of projected images to each camera of the same region of space. See Sec. 2.2.1 and Appendix B for more information about camera and lens selection, and Sec. 2.2.2 for more information about designing a camera mounting system to obtain the desired FOV.

2.1.4 Position Envelope for Hardware

Estimate the potential positions (i.e. the “position envelope”) for the cameras, mounting hardware, and lights to determine feasible stand-off distance (SOD) and location. See Fig. 1.1 for a depiction of the SOD. Determine what size and type of calibration target will be used (e.g. front-lit or back-lit) and how the mechanical test setup will need to be modified in order to calibrate the optical system (Sec. 3.2.2.2). Select (and purchase or fabricate if necessary) appropriate equipment for the camera support structure (Sec. 2.2.2).

Tip 2.1 — FOV, lens focal length, and SOD

For more information on the relationship between the FOV, lens focal length, camera detector size, and SOD, see Appendix B.

Recommendation 2.2 — Backdrop

Consider adding a stationary backdrop behind the test piece, to prevent any people or objects moving behind the test piece, or changing light reflections, from adversely affecting the images. A backdrop can also make the outline of the test piece more clear in the images, which can assist in precise identification of the ROI.

2.1.5 2D-DIC vs. Stereo-DIC

Determine if 2D-DIC or stereo-DIC will be used. See Fig. 1.1 for an illustration of a 2D-DIC setup and a stereo-DIC setup.

Caution 2.1 — 2D Planar Assumption

For 2D-DIC, the test piece is assumed to be planar, to remain planar throughout the test, to be perpendicular to the camera optical axis,^a and to maintain constant SOD throughout the test. Any inadvertent out-of-plane motion (i.e. due to test piece thinning or buckling, rotations or translations induced by misaligned grips, etc.) will cause errors in 2D-DIC [33, 40, 41].

Recommendation

Stereo-DIC is strongly recommended over 2D-DIC for all tests if possible, even tests in which a nominally planar test piece undergoes nominally planar deformation. 2D-DIC is recommended only if the geometry of the test setup cannot accommodate two cameras/lenses (i.e. when two cameras cannot physically fit into the position envelope available given the load frame and other equipment placement).^{b, c, d}

^aIf the intrinsic and extrinsic parameters of a 2D, single camera system are calibrated using a calibration target as described in Sec. 3.2, then an out-of-plane tilt of the test piece can be determined and corrected. However, this is an advanced topic that is outside the scope of the current edition of this guide.

^bLack of availability of two cameras/lenses due to cost can also prevent the use of stereo-DIC. However, this typically only applies to high-speed or ultra-high-speed cameras, which are outside the scope of the current edition of this guide, and not to typical machine-vision cameras.

^cStereo-DIC may be difficult on highly porous foams, because the natural pattern created by the pores can appear differently in the primary and dependent cameras (due to different perspectives, lighting, and shadows of each camera looking “into” the pores), and because applying a DIC pattern to the surface of the foam can be difficult. However, foams also often undergo large deformations, which induce large out-of-plane deformation.

Therefore, great care should be taken if using 2D-DIC on foam. More specific details about foam materials are beyond the scope of the current edition of this guide.

^aStereo-DIC may be difficult for small test pieces, as DOF of high magnification imaging systems can be limited. However, stereo-DIC is possible with conventional cameras and lenses and with stereo microscopes. More information about small test pieces is beyond the scope of the current edition of this guide.

Recommendation 2.3 — 2D-DIC Out-of-Plane Errors

If 2D-DIC must be used, estimate the expected out-of-plane motion/deformation of the test piece during the test (due to test piece thinning, for example) and the corresponding error of in-plane measurements as described in Example 2.1 and Sec. 5.4.4.

Recommendation 2.4 — Telecentric Lens for 2D-DIC

If 2D-DIC must be used, a bilateral telecentric lens is recommended to mitigate small errors due to out-of-plane translation [42]; out-of-plane rotations and large out-of-plane translations, however, will still cause errors in 2D-DIC measurements. The magnitude of out-of-plane translations for which a bi-telecentric lens can compensate depends on the FOV.

If a telecentric lens is not available or feasible, it is recommended to use a long focal-length lens, to maximize the SOD, and hence minimize errors caused by out-of-plane motion (see Example 2.1).

Caution 2.2 — Telecentric Lens for stereo-DIC

Although a telecentric lens is recommended for 2D-DIC, telecentric lenses may not be used for stereo-DIC.^a

^aThe use of telecentric lenses for stereo-DIC requires specialized camera and lens distortion models [43–45]. Most commercial DIC software packages assume a pin-hole camera model, which is incompatible with telecentric lenses. Therefore, the use of telecentric lenses for stereo-DIC is an advanced topic that is outside the scope of this edition of the guide.

Example 2.1 — Estimating 2D-DIC Strain Errors due to Out-of-Plane Motion

A key advantage of stereo-DIC over 2D-DIC is the ability to account for out-of-plane motion. In a 2D-DIC setup, only a single camera is used to capture the motion of a test piece. As a result, if the test piece moves out of plane, the correlation could interpret that motion as a false strain on the surface of the test piece. Some common examples of scenarios where false strain could occur include: imperfect alignment of the motion of a test piece with respect to the camera (i.e. the test piece is not or does not remain perfectly perpendicular to the camera digital detector), or thinning/buckling of the test piece during deformation.

For example, a simple pin hole model is shown schematically in Fig. 2.1. If a test piece of height h moves rigidly out of plane an arbitrary distance (Δd) further away from the camera (without deformation), the test piece height remains constant. However, the camera will detect a change in image scale, or magnification, where the size of the object in the image plane changes from m_1 to m_2 . Correspondingly, the angle defined by the stand-off distance and the test piece height also changes from α_1 to α_2 .

Schematic Top View of Experimental Setup

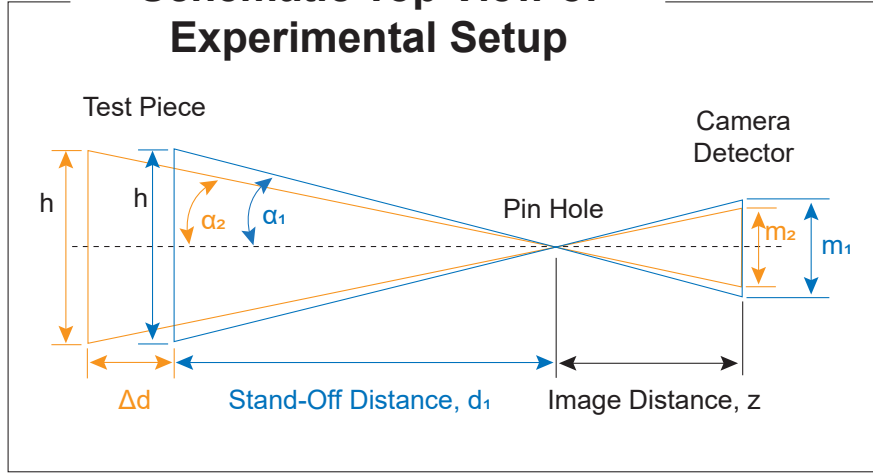


Figure 2.1: Schematic scenario where a test piece of height h moves away from the camera a distance of Δd , which leads to a change in image scale or magnification in the camera digital detector.

A simple estimate can be performed by using trigonometry to calculate the resultant change in magnification, which is approximately the false strain likely to be reported in a DIC correlation (Eqn. 2.1). If the test piece moves away from the camera as shown in Fig. 2.1, the false strain will be negative, implying that the test piece contracted. If the test piece moves towards the camera, the false strain will be positive, implying that the test piece expanded.

$$\tan(\alpha_1) = \frac{h/2}{d_1} = \frac{m_1/2}{z} \quad (2.1a)$$

$$\tan(\alpha_2) = \frac{h/2}{d_1 + \Delta d} = \frac{m_2/2}{z} \quad (2.1b)$$

$$\text{False Strain} \approx \frac{m_2 - m_1}{m_1} = \frac{d_1}{d_1 + \Delta d} - 1 \quad (2.1c)$$

The magnitude of this false strain is dependent on the experimental setup, specifically the stand-off distance d_1 , as can be seen in Eqn. 2.1. Table 2.1 shows that as the SOD increases, the false strain magnitude decreases. Thus, one possible method to reduce (limit) false strains in 2D-DIC is to select optics with longer focal lengths, which will require a longer SOD for a given constant FOV (see Sec. 2.2.1 and Appendix B). It is always recommended to estimate the magnitude of false strain for a 2D-DIC setup and compare the values obtained with both the noise-floor and the magnitude of a desired QOI.

Table 2.1: The effect of stand-off distance, d_1 , on false strain magnitude.

d_1	Δd	False Strain Magnitude
250 mm	1 mm	0.4%
500 mm	1 mm	0.2%
1000 mm	1 mm	0.1%

2.1.6 Stereo-Angle

For stereo-DIC, select the required stereo-angle. See Fig. 1.1 for a depiction of the stereo-angle.

Tip 2.2 — Stereo-Angle

The stereo-angle depends on geometry of the test setup and the QOI that is most important. Smaller stereo-angles lead to better in-plane displacement accuracy, at the cost of increased out-of-plane uncertainty. Alternatively, larger stereo-angles lead to better out-of-plane displacement accuracy, at the cost of increased in-plane uncertainty.

This relationship between stereo-angle and uncertainty is also affected by the focal length of the lens. Shorter focal length lenses require a larger stereo-angle to obtain the same out-of-plane uncertainty as longer focal length lenses.

The stereo-angle also affects the useable DOF. With smaller stereo-angles, the test piece will remain in focus in both cameras over a larger range of out-of-plane motions. Conversely, with larger stereo-angles, the allowable out-of-plane motion to keep the test piece in focus is reduced.

Recommendation 2.5 — Stereo-Angle

Typically, the stereo-angle should be between approximately 15–35° [15]. To reduce out-of-plane uncertainty and maximize useable DOF, short focal length lenses (ca. 8-12 mm) should have a larger stereo angle (ca. 35°), while long focal length lenses (ca. 35 mm or longer) should have a smaller stereo angle (ca. 15°) [46].

Caution 2.3 — Large Stereo-Angles

Experience has shown that large stereo-angles (greater than approximately 35°) may lead to difficulties in cross-correlation between the two cameras, due to large perspective differences in the images from each camera, especially with short focal length (wide angle) lenses.

2.1.7 Depth-of-Field

For stereo-DIC, determine the required depth-of-field (DOF) so that the entire ROI of the test piece remains in focus during the entire test, taking into account the expected out-of-plane motion of the test piece and the stereo-angle of the cameras. See Fig. 1.1 for a depiction of the DOF.

Tip 2.3 — Calculating and Measuring DOF

For a selected imaging setup, the approximate DOF can be calculated ahead of time as described in Appendix B, or measured in practice using a DOF target that has precise line pairs at a 45° angle to the optical axis or stereo-plane normal.

Tip 2.4 — DOF and Aperture

The DOF depends on the lens focal length, SOD, and lens aperture. However, the lens focal length and SOD are typically selected based on the ROI of the test piece (Sec. 2.1.2) and the position envelope of the hardware (Sec. 2.1.4). Once these two parameters are selected, the DOF is primarily controlled by the lens aperture (Sec. 2.2.3).

Tip 2.5 — Depth-of-Field for 2D-DIC

For 2D-DIC, the test piece is assumed to be planar and to remain planar with constant SOD. Therefore, DOF is not a large factor in the design of a 2D-DIC setup. However, having sufficient DOF helps ensure that the images will be in focus when the test piece is inserted into the load frame, and reduces sensitivity to alignment of the test piece and load frame with the optical axis of the imaging system. Additionally, having sufficient DOF will help ensure that focus will be maintained even during unexpected out-of-plane motion and/or deformation.

2.1.8 Spatial Gradients

Estimate the expected spatial gradients in the QOI, i.e. the rate at which the QOI varies spatially across the test piece, to determine the required [spatial resolution](#) of the DIC system. The spatial resolution is a function of measurement design parameters such as [image size](#) (also commonly called “camera resolution”) and FOV, and DIC processing parameters such as subset size and step size for local DIC, and element shape function and element size for global DIC.

Tip 2.6 — Spatial Resolution

If the spatial gradients of the QOI are higher than the maximum gradients that the DIC system can resolve, consider increasing the image scale of the optical system (i.e. increasing the magnification) by (1) using a camera with larger image size or by (2) reducing the ROI of the test piece to be a smaller portion of the test piece.^a

These tips assume that the spatial resolution of the DIC system is camera-limited, meaning that increasing the number of pixels across the ROI directly improves the spatial resolution of the DIC system. However, at high image magnification (small FOVs) or large image size, the imaging system resolution may be lens-limited, meaning that further increase in image magnification or image size will not improve the spatial resolution [47]. See Tip 2.33 for more information. Additionally, developing appropriate patterns for small FOVs and large image sizes may be challenging.

^aAlternatively, two DIC systems could be set up, one at a lower image magnification and with a larger FOV and larger DIC pattern features, to capture the overall motion and deformation of the test piece, and a second system at a higher magnification focused on a smaller ROI of the test piece with smaller DIC pattern features, to capture a localized region of sharp gradients. This advanced topic, however, is outside the scope of the current edition of this guide.

Example 2.2 — Camera Selection Based on Strain Gradients

The goal of this example is to determine the [detector array size](#) or [image size](#) required to accomplish a desired spatial resolution for a QOI. Image size also affects the minimum resolvable feature of a QOI (i.e. noise-floor) through the image scale, as described in [Tip 5.8](#), but capturing spatial gradients is typically more important. Finally, image size, and the corresponding detector array size, also impact the [pattern feature size](#) since the recommendation for minimum pattern feature size is 3-5 pixels (see [Section 2.3.2.1](#) and [Tip 2.35](#) for example calculations).

Knowledge about the expected spatial distribution of the QOI (e.g. displacement or strain) is necessary to assess whether the DIC system can capture the spatial gradients of a QOI. This information may come from engineering experience, numerical analysis (e.g. finite-element analysis (FEA)), or theoretical knowledge (e.g. elastic solution). This example utilizes theoretical knowledge to determine the expected strain distribution.

The mechanical test under consideration is a long rectangular test piece with a hole in the middle that is elastically stretched in the x-direction (long direction), as shown in [Fig. 2.2](#). The QOIs are the engineering strain along the x-axis, ε_{xx} , and engineering strain along the y-axis, ε_{yy} , from the edge of the hole to the edge of the test piece (black dotted lines in [Fig. 2.2](#), labeled “Line Slice X or Y”). It is assumed that having the measurement start one test piece thickness from the edge (boundary of the ROI, green short-dashed line in [Fig. 2.2](#)) is acceptable. It would be preferred to monitor the entire test piece length throughout the experiment, accomplishable using FOV 1, 220 mm along the x-axis, in [Fig. 2.2](#). If that is not possible, it would be acceptable to measure only the area close to the hole, as denoted by FOV 2, 110 mm along the x-axis, in [Fig. 2.2](#). Only elastic strains are considered here, so the analysis will assume an applied stress of 90% of the yield stress.

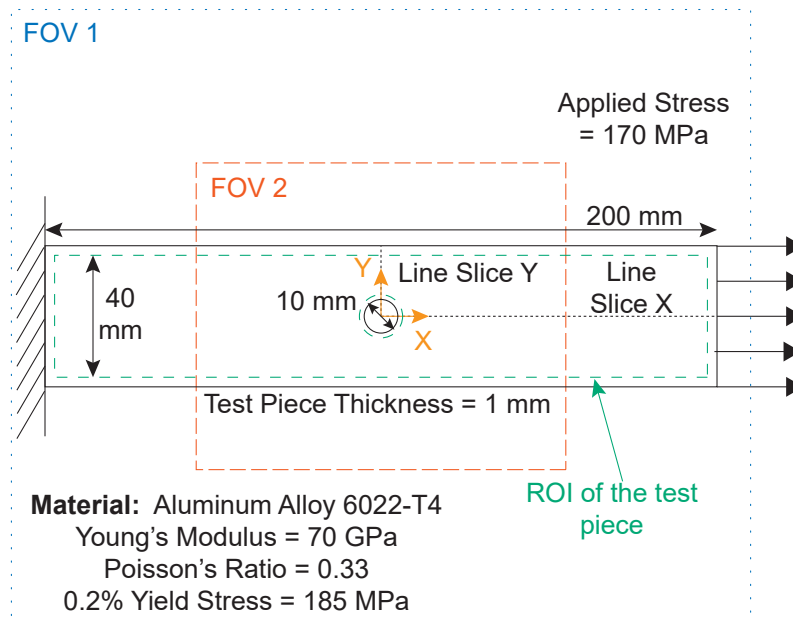


Figure 2.2: Schematic of test piece with two potential field-of-views (FOV 1 and FOV 2). The short-dashed green line is an example of the ROI of the test piece.

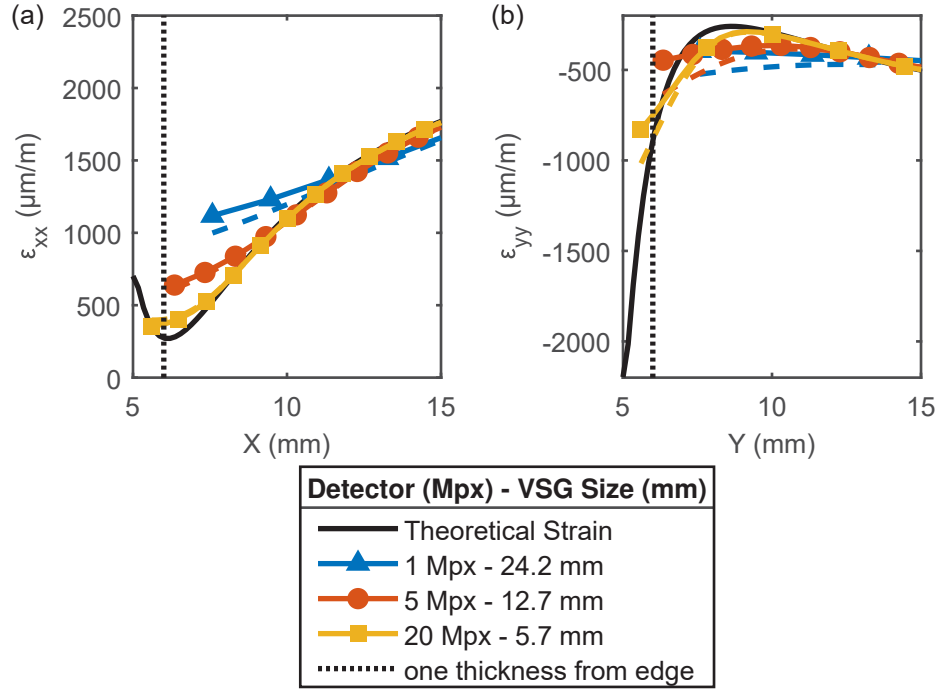


Figure 2.3: FOV 1 results for Method 1 (solid lines with symbols) and Method 2 (dashed lines). Strain profiles for ε_{xx} and ε_{yy} are shown in (a) and (b). Solid black lines are the theoretical strain profiles.

There are multiple cameras to choose from in this example, with detector array sizes (and resulting image sizes) of 1280 px \times 1024 px (1.3 Mpx), 2448 px \times 2048 px (5 Mpx), and 5472 px \times 3648 px (20 Mpx). Either FOV is achievable with these cameras given the proper lens selection and SOD, which is not shown here. For a nearly ideal pattern, a reasonable set of user-defined DIC analysis parameters are subset size of $L_{\text{subset}} = 31$ px (Sec. 5.2.7, Recommendation 5.1, and Tip 5.7), step size of $L_{\text{step}} = 11$ px (Sec. 5.2.8), and a Gaussian weighted strain filter window of size $L_{\text{window}} = 11$ data points.

The theoretical solution for this mechanical test, assuming plane stress, provides the “true” displacement and strain fields [48]. Two methods are compared to approximate the strain fields that would be obtained from DIC (though other options are also possible). Both of these methods could also be applied to a displacement or strain field extracted from a numerical analysis (e.g. FEA). The key to both methods is to estimate the DIC strains from the assumed “true” solution (e.g. theoretical or FEA), accounting for filtering effects from user-defined DIC analysis parameters such as subset size, subset shape function, step size, and strain or filter window.

The first method, Method 1, starts with the theoretical solution for the displacement fields. First, the image scale is calculated from the FOVs and image sizes stated earlier, and the displacements are computed at each pixel. Next, to approximate the effect of subset shape function attenuation bias of an affine subset shape function [7], the displacement results are averaged over the subset size. A moving average is used, so that the attenuated displacements are reported at each data point, separated by the step size, starting with a point one-half the subset size subset from the hole edge. Then, the engineering strains are computed by calculating the local gradient in displacements at each point to its neighboring points divided by the point spacing (central dif-

ference approximation). Finally, the strain values are smoothed using a moving Gaussian weighted filter over all the strain points. This results in a virtual strain gauge (VSG) size of 141 px according to Eqn. 7.3, which equates to 24.2 mm, 12.7 mm, and 5.7 mm for the 1.3 Mpx, 5 Mpx, and 20 Mpx image sizes, respectively, for FOV 1.

The second method, Method 2, starts with the theoretical solution for the strain fields that, again, are calculated at each pixel location similar to Method 1. To approximate the attenuation bias of DIC, the theoretical engineering strain values are simply smoothed with a moving Gaussian weighted filter over all pixel locations with a window size of the VSG length, L_{VSG} . Again, a moving window is used; however, since Method 2 does not assume a step size, the strains are reported at every pixel location that is at least as far from the edge of the test piece as in Method 1 (i.e. starting with a point one-half the subset size from the hole edge). This method will capture the general trends of the data smoothing, but not the discrete nature of the DIC data due to the step size spacing, nor the smoothing due to different subset sizes and subset shape functions. The VSG size used was 141 px as before, but this is not associated with a single combination of subset size, step size, and filter window size (i.e. many combinations of subset size, step size, and filter window size could result in that VSG size).

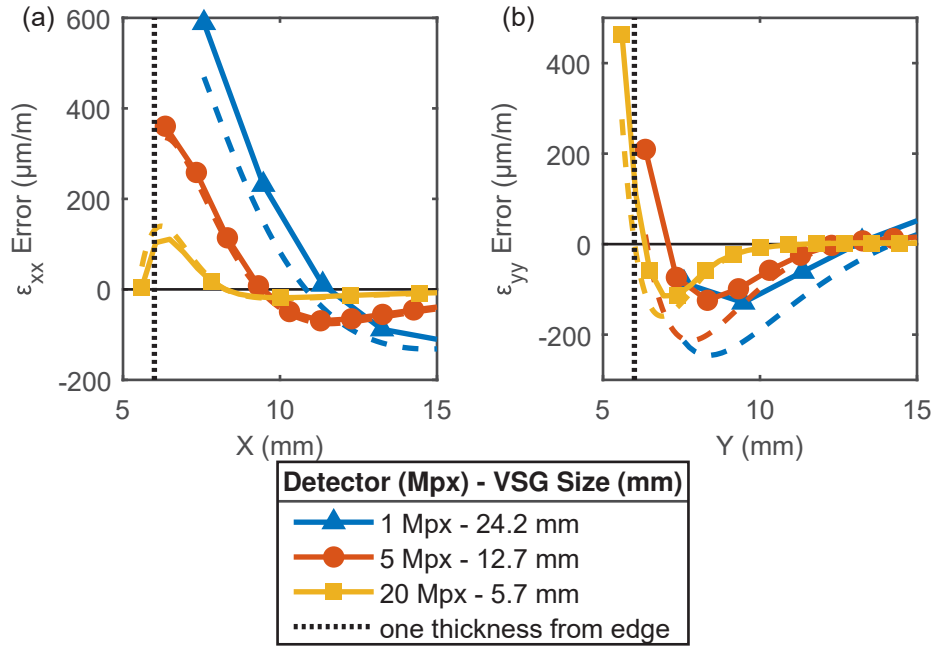


Figure 2.4: FOV 1 results for Method 1 (solid lines with symbols) and Method 2 (dashed lines). Strain error profiles are shown for ϵ_{xx} and ϵ_{yy} in (a) and (b), respectively.

Fig. 2.3a plots the results for ϵ_{xx} along the x-axis and Fig. 2.3b plots ϵ_{yy} along the y-axis, computed with Method 1 (solid lines with data points) and Method 2 (dashed lines), with the theoretical strains shown as solid black lines. Results are only shown from the edge of the hole to $x \leq 15$ mm and $y \leq 15$ mm, since the region near the hole has the highest strain gradients and thus is the most challenging region to accurately capture. The strain error (bias) is calculated as the measured strain minus the theoretical strain value, and is plotted for ϵ_{xx} and ϵ_{yy} in Fig. 2.4a

and Fig. 2.4b, respectively. As the image size is increased and VSG size (in terms of millimeters) is decreased, the DIC-estimated strain approaches the theoretical strain. That is, the peak strains near the hole are less attenuated, and the error is reduced. If none of the potential image sizes would meet the desired accuracy over the entire desired ROI for the test piece, then reducing the FOV (e.g. to FOV 2 in Fig. 2.2) might be considered, following Tip 2.6.

Therefore, the second FOV (FOV 2 in Fig. 2.2), that is half as wide, was similarly assessed for the same three image sizes. The results for the strain error with FOV 2 are presented in Fig. 2.5a and Fig. 2.5b, similar to Fig. 2.4a and Fig. 2.4b for FOV 1. By reducing the FOV to half the size, but keeping all DIC settings (in terms of pixels) the same (i.e. subset size of $L_{\text{subset}} = 31$ px, step size of $L_{\text{step}} = 11$ px, and strain filter window size of $L_{\text{window}} = 11$ data points), the VSG size (in terms of millimeters) is similarly reduced in half for each resolution (see legends in Fig. 2.4 and Fig. 2.5). With the smaller FOV and smaller VSG size (in terms of millimeters), the strain profile measured with DIC more closely matches the theoretical profile, with less attenuation of the peak strains in regions of high strain gradients. Additionally, since the subset size dictates the location of the first data point from the edge, and FOV 2 has a smaller subset size (in terms of mm) than FOV 1, the first data point from the hole edge is closer to the edge for FOV 2 than for FOV 1.

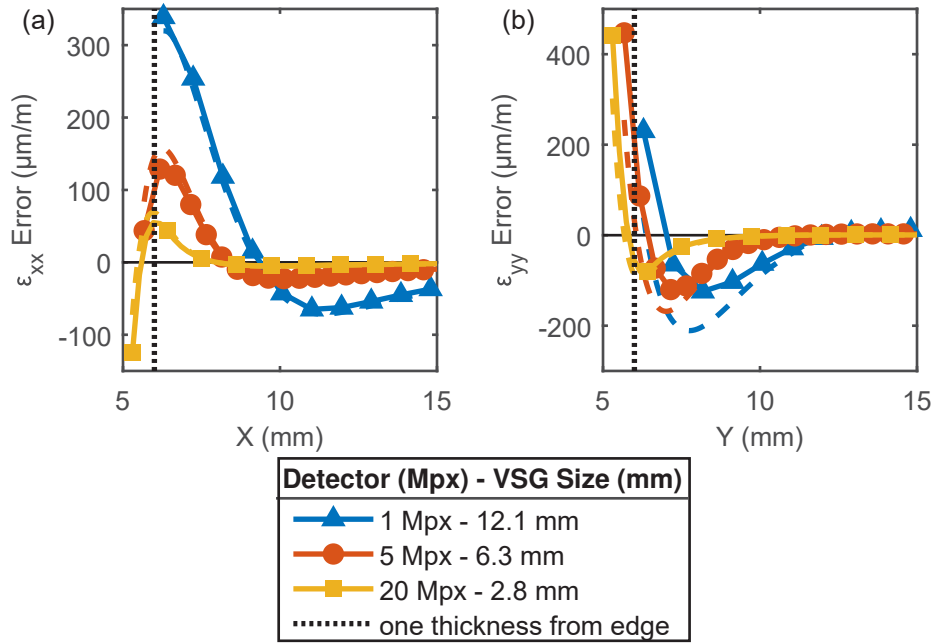


Figure 2.5: FOV 2 results for Method 1 (solid lines with symbols) and Method 2 (dashed lines). Strain error profiles are shown for ε_{xx} and ε_{yy} in (a) and (b), respectively.

Based on these results, a user could select the correct combination of camera (image size) and FOV for their intended measurement. For example, if the measurement needed to have a bias no greater than ± 150 $\mu\text{m/m}$ starting one thickness from the edge of the hole, then a 20 Mpx camera with either FOV could be used, or a 5 Mpx camera with the FOV 2 could be used. However, a 5 Mpx camera with FOV 1 would not meet this requirement, nor would a 1 Mpx camera with either FOV.

2.1.9 Noise-Floor

Determine the acceptable [noise-floor](#) for all QOIs. Justify and document the criteria used to establish this acceptable noise-floor.

Tip 2.7 — Noise-Floor

This threshold of an acceptable noise-floor is application-specific, and is often determined by a subject matter expert. The noise-floor can be evaluated during the design of the measurement to aid in the selection of different DIC hardware (i.e. camera and lens, patterning technique, lighting) and processing parameters (e.g. subset size and step size for local DIC, and element shape function and element size for global DIC). See Sec. 5.4 for more information.

2.1.10 Frame Rate and Image Acquisition Rate

Determine the desired [frame rate](#) and [image acquisition rate](#).

Tip 2.8 — Frame Rate vs. Image Acquisition Rate

As defined in the glossary, the [frame rate](#) is subtly different than the [image acquisition rate](#). The frame rate is the frequency at which a camera acquires or captures images, whereas the image acquisition rate is the frequency at which consecutive images are saved and analyzed. Often, the frame rate and the image acquisition rate are the same value. However, sometimes, the frame rate can be higher than the image acquisition rate. For instance, a camera may acquire images at 100 Hz, but only 1 of every 20 images are saved, leading to an image acquisition rate of 5 Hz. For DIC measurements, the image acquisition rate is typically the more important parameter, since the image acquisition rate governs the temporal resolution of the QOIs. Note that the image acquisition rate must be equal to or lower than the frame rate.

Example 2.3 — Image Acquisition Rate

There are several factors to consider when determining the desired image acquisition rate. This example describes some considerations for different scenarios:

1. The most important factor in determining an appropriate image acquisition rate is the desired temporal resolution of the QOIs. Because temporal resolution requirements are application-specific, no general guidelines for image acquisition rate and/or number of images to acquire during the test are given here. Some examples for specific applications include:
 - If the goal of the DIC measurements is to capture the elastic-plastic transition of a metal in a tensile test (region I (RI) in Fig. 2.6), or to capture the strain immediately before failure (region III (RIII) in Fig. 2.6), then the required image acquisition rate may be relatively high in order to adequately capture the rapidly evolving QOIs. Alternatively, if the goal is to characterize the plastic deformation of a ductile material (region II (RII) in Fig. 2.6), the image acquisition rate could be much slower since the QOI is changing slowly over time in this region. If all three regions are important, then there are several options for setting the image acquisition rate:

- The image acquisition rate could be updated for each region *in situ* during the test, so that a faster image acquisition rate is used for RI and RIII, but a slower image acquisition rate is used for RII.
- The cameras could be operated at a frame rate equal to the faster image acquisition rate required for RI and RIII, but only one out of every n images could be saved during RII, effectively lowering the image acquisition rate for RII.
- The cameras could be operated at a frame rate equal to the faster image acquisition rate required for RI and RIII, with all images saved during the test; then, images in RII could be decimated during post-processing, again effectively lowering the image acquisition rate for RII.

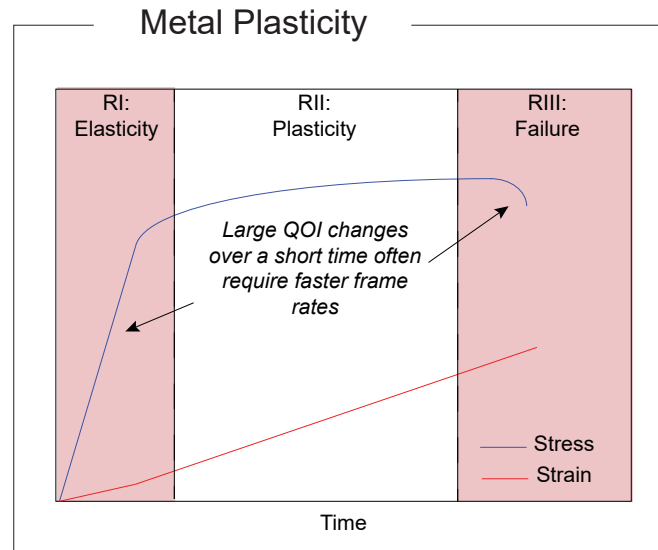


Figure 2.6: An example of factors to consider when determining the desired image acquisition rate, in this case for a tensile test of a ductile metal. Both engineering stress and engineering strain are depicted in this figure.

- If the test piece is cyclically loaded, the minimum image acquisition rate to resolve the correct frequency is determined by the Nyquist-Shannon sampling theorem. This theorem states that to measure an oscillating signal, the sampling frequency must be at least 2 times the frequency of oscillation. In practice, the image acquisition rate should be higher than 2 times the frequency of oscillation, to avoid zero-phase-locking (and thus measuring the deformation at various phases of the cycle) and to compensate for noisy signals. For modal analysis, an image acquisition rate of ca. 2.5 times the frequency of oscillation has been used successfully [49]. To be more conservative, an image acquisition rate of 5–10 times the frequency of oscillation is suggested.
2. The image acquisition rate also impacts temporal derivatives of QOIs, such as velocity and strain rate. To accurately estimate temporal derivatives using a discrete approximation (e.g. forward, backward, or central difference), a faster image acquisition rate than is needed for the base QOIs may be beneficial; however, if the image acquisition rate is much faster than the change in the QOI between frames, the temporal derivatives could be noisy.

3. A minor consideration when selecting the image acquisition rate is the amount of displacement between frames. If the displacement between frames is large, DIC algorithms may fail to locate the subset/element position in the deformed images. However, most DIC software allows for an initial guess (Sec. 5.2.10), which usually compensates for large displacements between images. The maximum displacement between frames that can be tracked is software-specific; however, a reasonable value (as a starting point) is approximately half of the subset/element size. For example, if the subset/element size is 25 px and the image scale is 20 px/mm, then the maximum displacement between two sequential frames should be less than approximately 0.63 mm. If the velocity of the test piece is approximately 1 mm/s, then the minimum image acquisition rate should be approximately 1.6 Hz.
4. Another minor consideration is the amount of data collected during the mechanical test. Gigabytes of data can quickly be accumulated during DIC measurements, so good data management is essential.

Tip 2.9 — Frame Rate and Image Brightness/Contrast

Ideally, the image acquisition rate is selected based on the desired temporal resolution of the QOIs and other considerations as described in Example 2.3. However, in some (usually more challenging) measurement configurations, an exposure time that is greater than the inverse of the desired frame rate (i.e. greater than the inter-frame period) may be necessary, which limits the maximum possible frame rate and thus maximum possible image acquisition rate. See Tip 2.24 for more information on the trade-offs between aperture (Sec. 2.2.3), exposure time (Sec. 2.1.11), external light (Sec. 2.2.4), and frame rate.

2.1.11 Exposure Time

Determine the maximum allowable exposure to limit motion blur.

Tip 2.10 — Motion Blur

The displacement, in pixels, per exposure is calculated as:

$$\text{Displacement per Exposure [px]} = \left(\text{Velocity} \left[\frac{\text{mm}}{\text{s}} \right] \right) \cdot \left(\text{Image Scale} \left[\frac{\text{px}}{\text{mm}} \right] \right) \cdot (\text{Exposure Time [s]}) \quad (2.2)$$

The most conservative estimate for the maximum allowable test piece motion over the course of the exposure time is the noise-floor (Sec. 2.1.9) of the displacement measurements [7, Sec. 10.1.4]. For typical DIC setups, this threshold is around 0.01 pixels (see Tip 5.8). In some fields such as machine vision, a threshold of 0.1–0.3 pixels is typically used, while dynamic tests often accept as much as 3 pixels of motion during the exposure time [50].^{a,b,c}

^aThe recommended thresholds for motion blur given here in terms of pixels assume an ideal pattern feature size of 3–5 pixels (Sec. 2.3.2). An alternative view is that the motion blur should be below a percentage of the mean feature size. For example, if a pattern is imaged with a 1 Mpx camera and the feature size is 3 pixels, then motion blur of 0.3 pixels corresponds to 10% of the feature size. If the same pattern is imaged with a 16 Mpx camera so that the feature size is now 12 pixels, the same amount of 10% blur corresponds to 1.2 pixels. If the subset size is correspondingly increased in the second case, the blur should affect the displacement results similarly.

^bIf the velocity of the test piece is constant throughout the duration of the test—such that the apparent size of the features remains constant—the effects of motion blur are less egregious than if the velocity changes during the test—such that the apparent size of the features changes. This scenario is typical of impact tests for example, where the test piece is moving at a fast velocity at the beginning of the test and then decelerates. Further discussion is outside the scope of the current edition of this guide.

^cIn scenarios where the required exposure time is intractably small, reduced test velocity or quasi-static loading may be viable approaches to mitigating motion blur, if the test is amenable to such modifications.

Tip 2.11 — Exposure Time and Frame Rate

While the exposure time is determined independently from the frame rate and image acquisition rate, the exposure time cannot be larger than the inverse of the frame rate (Sec. 2.1.10).

Tip 2.12 — Exposure Time and Image Brightness/Contrast

In addition to governing motion blur, the exposure time also affects the image brightness and contrast. Ideally, the exposure time should be less than or equal to the maximum allowable time to freeze motion. If the initially selected exposure time leads to unacceptably large motion blur, brighter and/or additional external light could be used. Then the exposure time could be decreased, while still obtaining sufficient image brightness and contrast (Sec. 2.2.4). See Tip 2.24 for more information on lighting trade-offs.

2.1.12 Synchronization and Triggering

For stereo-DIC, determine how the two cameras will be synchronized to each other. Determine how the DIC images will be synchronized to other measurements of interest, such as applied force or displacement, strain gauges, thermocouples, etc. Determine how all data acquisitions will be triggered at the start of the mechanical test.⁷

2.2 Equipment and Hardware

2.2.1 Camera and Lens Selection

Select a camera and lens⁸ pair to obtain the desired FOV (Sec. 2.1.3), SOD (2.1.4), DOF (Sec. 2.1.7), spatial resolution (2.1.8), noise-floor (Sec. 2.1.9), and temporal resolution (Sec. 2.1.10) determined in Sec. 2.1.

Tip 2.13 — FOV, SOD, and DOF

FOV, SOD, and DOF are all intertwined and must be selected together. Cameras and lenses cannot be selected independently, due to the combined detector array size and lens effect on the resulting image scale. For more information on the relationship between the FOV, lens focal length, camera detector array size, SOD, and DOF, see Appendix B. Additionally, more information on camera and lens selection is found in [13, 14].

⁷The method used to synchronize DIC images with other measurements of interest is dependent on the specific hardware and software of the mechanical test; therefore, no further information is given in this guide.

⁸The effects of anti-vibration features that some lenses have is outside the scope of the present version of the guide.

Tip 2.14 — Camera and Lens Selection

In most cases, experience is necessary to determine if a camera (e.g. noise level and detector dynamic range) or lens (e.g. resolution and distortions, see Recommendation 3.4, Fig. 3.3, and Recommendation 3.14) is of sufficient quality for DIC. Some qualification or verification of new hardware is recommended, by characterizing the baseline noise-floor of DIC results with the new hardware. Typically, this is done by DIC vendors for any hardware they provide, but DIC practitioners can verify the results, or evaluate independent hardware, by using the procedures outlined in Sec. 5.4.3.

Recommendation 2.6 — Camera Selection

Typically, machine-vision, monochromatic cameras with nearly square pixels are used for DIC.^a Also, detectors with global shutters (in which the data is read from all pixels simultaneously) are recommended over detectors with rolling shutters (in which the data is read from the detector row by row).

^aThe use of color cameras or the use of cameras that have pixels that are not square is possible; however, the use of these types of cameras requires complex analysis and is an advanced topic beyond the scope of the current edition of this guide.

Caution 2.4 — Camera Selection

Imaging systems that automatically adjust components of the lens and/or camera, such as auto-focus of the lens, or apertures that open/close with each image acquisition, are not appropriate for DIC measurements and should be avoided.

Caution 2.5 — Interlaced Frames

Some cameras (especially older digital video) have the ability to “interlace” frames to result in a smooth video that is more pleasing to the human eye. This feature combines every other row of the previous frame with the current frame, and is completely inappropriate for use in DIC.

Recommendation

When using new or unfamiliar camera hardware, it is recommended to verify that “interlacing” is not being used.

Tip 2.15 — Low-Pass Filter

Some cameras have a physical low-pass filter element (also called an anti-aliasing filter) adhered in front of the detector. This is more typical of single-lens reflex (SLR) or digital single-lens reflex (DSLR) cameras than of machine vision cameras. It is important to know whether or not the camera being used for DIC has a physical low-pass filter, in particular when deciding whether or not to pre-filter the images, as described in Sec. 5.2.2.

Tip 2.16 — Lens Selection

There are two main types of lenses used for stereo-DIC (and occasionally used for 2D-DIC), either fixed focal-length lenses or zoom lenses. With a fixed focal-length lens, the FOV or image scale is adjusted by adjusting the SOD. With a zoom lens, the FOV or image scale can be adjusted by adjusting either the SOD or the focal length of the lens. Thus, zoom lenses can be more flexible than fixed focal-length lenses. However, because of increased complexity of the optics in a zoom lens, lens distortions are often larger for zoom lenses. Also, many (though not all) zoom lenses do not have a way of locking the adjustment of the focal-length ring, making them more susceptible to inadvertent changes if the camera/lens is moved.

Recommendation 2.7 — Lock Moving Components on Lens

Lenses with the ability to lock moving components (e.g. focus ring, aperture ring, zoom setting (for a zoom lens)) are preferred, to reduce the likelihood of accidentally changing these components after they have been set to the desired position.

2.2.2 Camera and Lens Mounting

2.2.2.1 General Characteristics of Mounting System

Construct a sturdy camera and lens mounting system with the following general characteristics:

- Include sufficient degrees of freedom to allow for precise adjustment of the location and orientation of the camera(s)/lens(es) (i.e. translation or rotation stages, tripod adjustments, etc.).
- If the camera location and/or orientation need to be adjusted for calibration (Sec. 3.2.2.2), include the appropriate mechanisms in the mounting system (e.g. a bar that can rotate the camera(s) or a translation stage that can translate the camera(s)).
- Lock all moving components in the mounting system after the final position and orientation has been determined.

Tip 2.17 — Tape Moving Components on Lens

As mentioned in Recommendation 2.7, lenses with the ability to lock moving components (e.g. focus ring, aperture ring, zoom setting (for a zoom lens)) are preferred. However, if the only lens(es) available for the DIC measurement do not have locks for the moving components, masking tape can be used to lock the position of these adjustment rings. The rings should be taped after the imaging system is aligned and focused, but before the system is calibrated. Care must be taken during taping to not change the focus or other lens settings.

- For 2D-DIC, ensure the camera and lens optical axis is perpendicular to the surface of the test piece.

Tip 2.18 — Aligning Optical Axis for 2D-DIC

There are many possible methods for aligning the optical axis perpendicular to the surface of the test piece. A non-exhaustive list includes:

- For test pieces with rectangular cross sections (i.e. side faces are perpendicular to the front face of the test piece), ensure the side faces of the test piece are not visible in the image.
- Open the aperture to obtain a shallow DOF, and ensure the focus is consistent across the test piece.

Caution 2.6 — 2D-DIC Out-of-Plane Errors

See Sec. 2.1.5 for more information about the implications of out-of-plane motion in 2D-DIC.

- For stereo-DIC, mount the cameras such that the desired FOV, ROI of the image, and stereo-angle are achieved. Example 2.4 provides several considerations and recommendations regarding the orientation of the individual cameras and the stereo-rig.
- For stereo-DIC, mount both cameras rigidly together to avoid relative camera motion.⁹ See Sec. 2.2.2.2 for more information on common types of mounting systems.

Caution 2.7 — Rigid Camera Mounting

Any relative motion of one camera with respect to the second camera will induce errors in stereo-DIC measurements.^a If relative motion occurs, the camera system should be recalibrated.^b To avoid this problem, rigid mounting is critical!

^aIf both cameras move together rigidly with respect to the test piece, only rigid-body DIC displacements are affected. For most applications where rigid-body-motion is not important (e.g. strains are the QOI), this rigid-body displacement error is inconsequential.

^bRigid-body-motion of the stereo-camera *pair* can be corrected in post-processing if there is a fixed reference point somewhere in the FOV. However, correcting for relative motion of one camera with respect to the second camera requires adjusting the extrinsic parameters of the calibration (Sec. 3.2). Some DIC software packages offer a “calibration correction” that corrects the extrinsic parameters of a stereo-camera system based on certain assumptions and minimization of the [epipolar error](#) (Sec. 3.3.2.2). However, this type of correction is beyond the scope of the current edition of this guide.

Tip 2.19 — Epipolar Error

In stereo-DIC, the [epipolar error](#) is a good metric for indicating possible drift, misalignment, or vibrations in the camera/lens systems. For example, if the epipolar error of a series of static images was low immediately after calibrating the stereo system, but then increases over time, this could indicate drift of one or both imaging systems. If the epipolar error is cyclic over time, this could indicate vibrations affecting the imaging systems or this could also indicate heat waves.

- Mount the combined camera/lens system near its center of mass. If either the lens or the camera is substantially more massive than the other, mount to the more massive element. Consider mounting at two places along the optical axis instead of just one, to minimize the lever-arm effect.

⁹Test setups in which the cameras cannot be practically rigidly-mounted together, e.g. large-scale tests with large camera separation that require individual tripods for each camera, are outside the scope of this edition of the guide.

Recommendation 2.8 — Camera and Lens Mounting Orientation

Many commercial cameras, lenses, and mounts are designed to be used with the optical axis nearly horizontal. If the orientation of the optical axis is vertical, then verify the mounting, and reinforce it as needed to ensure the mount is effectively rigid in this orientation. Additionally, verify that the lens performs properly in this orientation, and that the focus or other settings do not drift.

Caution 2.8 — Camera and Lens Mounting Balance

Camera and lens systems that are not well balanced on their mounting are more likely to drift or become misaligned, thereby inducing errors into the DIC measurements.

Caution 2.9 — Camera Heating

If the lens (instead of the camera) is mounted to the mounting system, there is a risk that the heat produced by the camera will not be dissipated properly (Caution 2.18).

Recommendation

Monitor the camera temperature and ensure heat is being sufficiently dissipated.

- Stabilize and strain relieve camera cables to prevent the cables from pulling on the cameras or transferring ambient vibrations to the camera system. If the camera(s) will be moved for calibration (Sec. 3.2.2.2), ensure there is enough slack in the cables to accommodate the camera repositioning.
- Ensure that the camera support structure is stable. If necessary, add weights (e.g. sand bags) to tripods or other footing to prevent motion of the camera support structure.
- Minimize vibrations being transferred to the cameras.

Caution 2.10 — Vibrations Increase Noise-Floor

Any vibrations that are transferred to the cameras will directly increase the noise-floor of the DIC measurements. The amount of time and effort spent on minimizing vibrations is directly commensurate with the magnitude of the vibrations and the desired precision of the DIC measurements.

Tip 2.20 — Vibration Detection

Some vibrations — but not all — can be detected by the human eye by watching a live image stream, especially if the image is zoomed in so that individual pixels are visible. Camera and lens vibrations are more visible at larger SODs, and less visible for short SODs. Note that vibrations seen through the live image could be the result of vibrations of the camera/lens imaging system, or vibrations of the test piece.

Caution 2.11 — Vibrations Invalidate Calibration

A vibrating stereo-DIC system can result in temporal changes in the orientation between the cameras that will invalidate the calibration, even if vibrations are not visible to the human eye.

Recommendation 2.9 — Minimizing Vibrations

To reduce the effects of vibrations, the following precautions are recommended:

- Ensure the cameras and mounting system are not in direct contact with any vibrating components (i.e. fan, compressor, hydraulics, test machine, lights, etc.) [12].
- If a camera has a cooling fan, turn it off while actively acquiring images to reduce vibration effects from the fan, if doing so will not cause the camera to overheat.
- Verify there are no vibrations being transferred through the floor. Note that vibrations could come from equipment in other rooms in the building, and are often more pronounced on elevated floors compared to ground floor or basement.
- If vibrations are being transferred to the cameras, reinforce the mounting system and/or add damping.
- If the DIC measurement and test setup can accommodate different SODs and lenses of different focal lengths, use a shorter SOD and shorter focal-length lens.

Example 2.4 — Camera Orientation

The optimal camera orientation scheme in stereo-DIC depends both on the camera and test piece aspect ratios, as well as the direction of expected motion/deformation during the DIC test (Fig. 2.7).^a In this example, key concepts are illustrated using a tensile dog bone as the test piece.

Consider a test piece that is a long and narrow tensile dog bone. The ROI of the test piece is the gauge section of the dog bone, and the FOV includes the ROI of the test piece plus the expected deformation during the test, as specified in Sec. 2.1.3. Also consider a camera detector with a rectangular aspect ratio and image size of 1920 px × 1200 px. The camera should be aligned with the greater number of pixels (1920 px) allotted to the longer side of the test piece, as shown by the schematic with the green check mark in Fig. 2.8a. In Fig. 2.8b, the camera is rotated 90°, and while the image scale and spatial resolution remain the same, much less of the ROI of the test piece is captured in the FOV. Furthermore, many pixels are wasted on the outer edges of the image, not imaging the test piece. In Fig. 2.8c, the schematic shows the result of reducing the image scale (i.e. reducing the magnification) to cover an entire ROI. However, the spatial resolution is now degraded, since there are only 1200 px along the longer side of the ROI instead of 1920 px as with configuration (a), and a great number of pixels still are not imaging the test piece (again, wasted pixels).

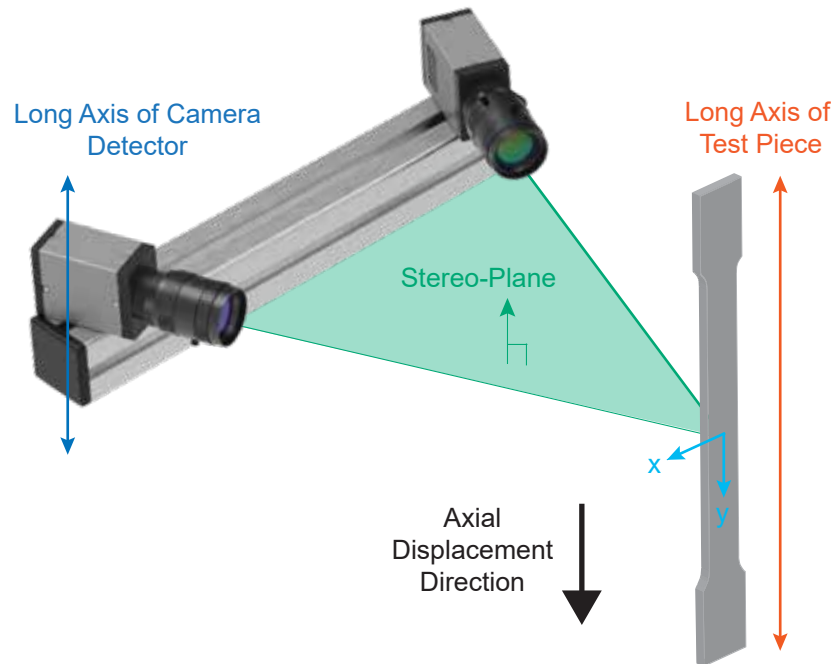


Figure 2.7: Schematic showing a setup for an example test piece (tensile dog bone) where the long axis of the camera detector is aligned both with the long axis of the tensile dog bone as well as the direction of deformation. Additionally, the long axis of the tensile dog bone is perpendicular to the stereo-plane (i.e. aligned with the normal of the stereo-plane).

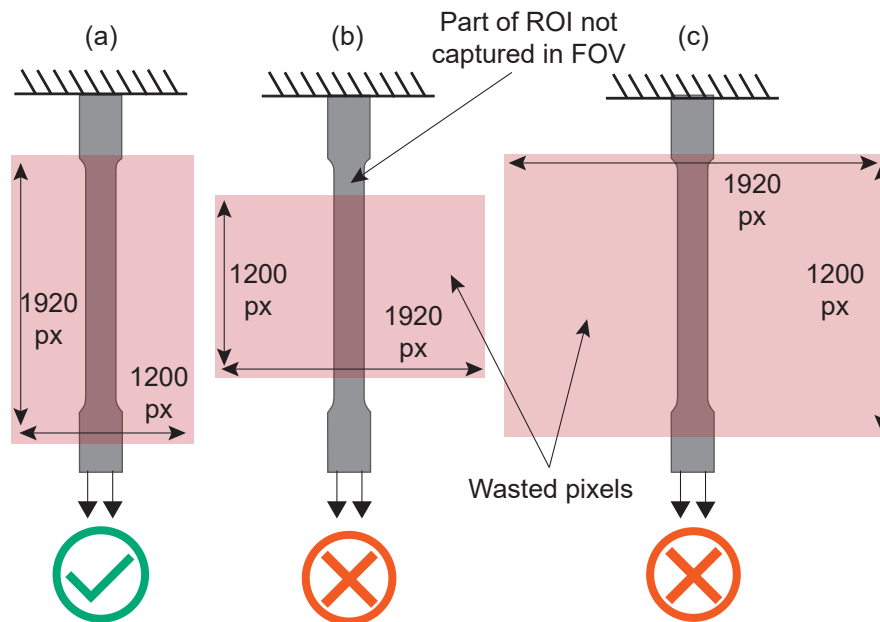


Figure 2.8: Schematics showing optimal (a) and non-optimal (b and c) orientations of a camera detector with a 1920 px to 1200 px aspect ratio with respect to a long and narrow test piece (here a tensile dog bone).

A second consideration involves the DOF. Both the initial undeformed test piece and the deformed test piece (or a test piece undergoing rigid-body-motion) should remain in the diamond shaped focal volume. For example, when oriented as in Fig. 2.9a, a long and narrow tensile dog bone will remain in the focal volume easily. However, if the tensile dog bone were rotated 90° and deformed as shown in the Fig. 2.9b, the images would become increasingly more blurry and out-of-focus for one of the cameras in the stereo-DIC setup. This degradation of image quality could eventually cause the images to fail to correlate as the test piece progressed outside of the focal volume.

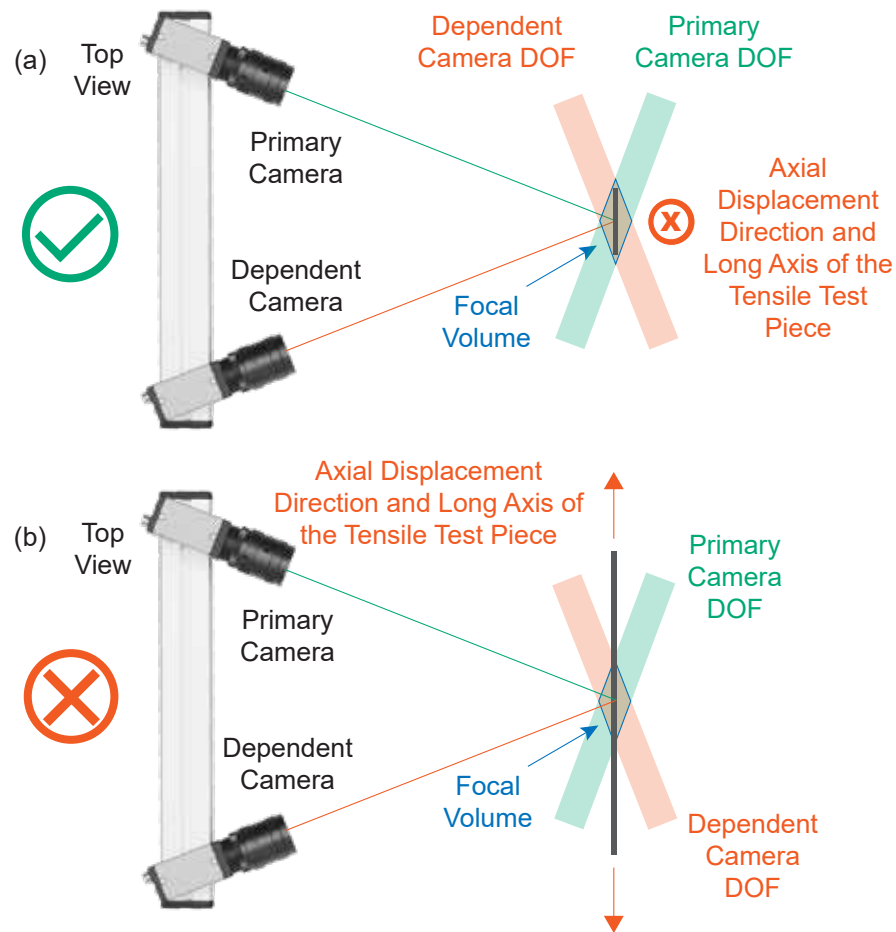


Figure 2.9: Schematics of an optimal (a) and non-optimal (b) orientation of a tensile dog bone test piece with respect to the focal volume covered by a set of stereo-DIC cameras.

In summary, a set of recommended orientations for a tensile dog bone with respect to a non-square (rectangular) camera detector is given in Fig. 2.10. Also included are two discouraged orientations; while these orientations are inferior, they may still be successfully employed if the available position envelope for the hardware does not allow the recommended orientations. As a final note, many cameras only feature mounting locations on one side of the housing, and as a result, the natural mounting location is not guaranteed to coincide with the ideal DIC setup. In these cases, adapters, such as 90° angle brackets, may need to be employed to rotate the cameras.

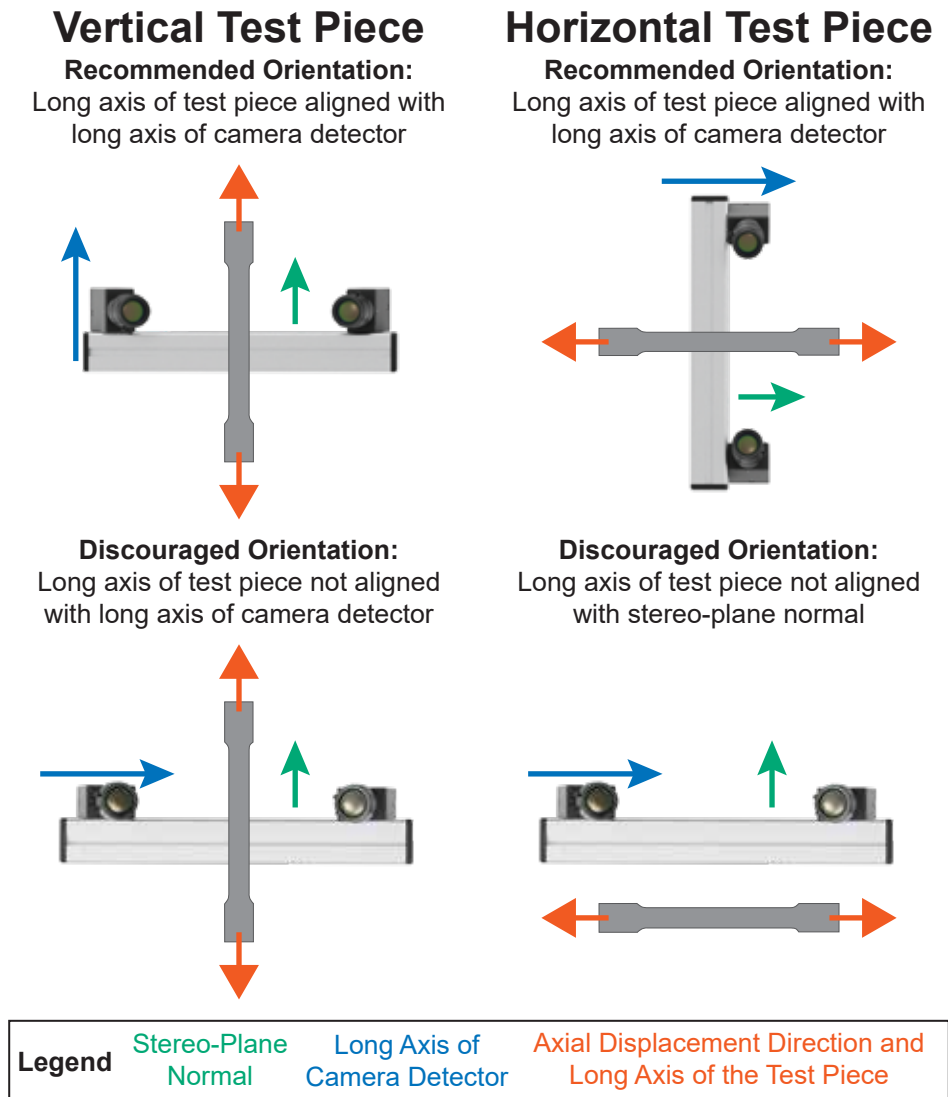


Figure 2.10: Summary of recommended and discouraged mounting configurations for the example of a tensile dog bone test piece (pulled axially).

^aThe recommended orientation may also depend on the shape of the test piece (e.g. planar versus cylindrical), but non-planar test pieces are beyond the scope of the current edition of this guide.

2.2.2.2 Types of Mounting Systems

There are many types of mounting systems for camera(s)/lens(es) that are appropriate for DIC, and the selection of a mounting system depends on the mechanical test setup and components available in each laboratory. A typical mounting system, appropriate for a large range of mechanical test setups, is often available with the purchase of commercial, turn-key DIC systems. Alternatively, custom mounting systems can be built from commercially-available products. For mechanical test setups with complicated geometry, restricted access, or uncommon camera(s) and/or lens(es), mounting system components may need to be specially designed and fabricated. Some common types of commercially-available systems include, but are not limited to:

- Typical optical hardware, such as 1-1/2 inch (38 mm) posts and associated mounting hardware, bolted to an optical table.
- Sturdy tripods. For stereo-DIC, a single bar is either mounted at each end to a tripod or mounted to a single tripod at the center of the bar. The two cameras are then mounted to the bar. In this way, the cameras are mounted rigidly together, and not on independent tripods.¹⁰
- Studio stands. Camera mounting with studio stands is similar to mounting with tripods, but studio stands have two advantages. First, their base is weighted, decreasing the likelihood that sandbags or other weights will be necessary to stabilize the system. Second, they are designed with several lockable degrees of freedom, allowing for easy adjustment of camera location and orientation.
- Systems of bars pre-fabricated to varying lengths and associated assembly and mounting hardware.

2.2.3 Aperture

Select the aperture on the lens to obtain desired DOF (Sec. 2.1.7). For stereo-DIC, the aperture should be the same in both cameras (as close as possible).

Tip 2.21 — Lens Aperture, DOF, and Image Brightness

In addition to governing the DOF, the aperture of the lens also governs how much light enters the optical system. However, typically the aperture is chosen based on the desired/required DOF, while exposure time (Sec. 2.1.11) and external light (Sec. 2.2.4) are adjusted in order to limit motion blur and obtain sufficient contrast. See Tip 2.24 for more information on lighting trade-offs.

Tip 2.22 — Lens Aperture, DOF, and F-Stop Number

Smaller apertures (larger f-stop numbers) equate to larger DOFs.

¹⁰Refer to footnote 9 on page 23.

Tip 2.23 — Aperture and DOF while Focusing

When focusing the camera-lens optical system, it is advantageous to have the aperture wide open (i.e. the lowest f-stop number, resulting in the shallowest DOF). After the focus is set, the aperture should be partially closed (i.e. f-stop number increased) to have the desired/required DOF. See Tip 3.6.

Caution 2.12 — Diffraction and Aberrations

Diffraction may become problematic at small apertures, while optical aberrations are accentuated by large apertures. See, for instance, Ref.[4].

Recommendation

Moderate lens apertures are recommended, to avoid accentuated lens distortions or diffraction limits at extreme apertures [47]. The recommended aperture size or f-stop number is dependent on the lens and the application, but typically a value in the range of $f/5.6$ – $f/11$ is recommended.

2.2.4 Lighting and Exposure

Given a pre-determined aperture (Sec. 2.2.3), select lighting and an exposure time (less than or equal to the maximum allowable exposure time, see Sec. 2.1.11) to have sufficient contrast between the lightest (white) and the darkest (black) regions of the DIC pattern. The contrast should be uniform over the entire ROI of the image, approximately the same in both cameras (for stereo-DIC), and constant in time. For typical stereo-DIC setups, the exposure time should also be the same for both cameras.¹¹

Tip 2.24 — Lighting trade-offs

There are many factors that are all intertwined and contribute together to obtaining sufficient contrast between the light and dark features of a DIC pattern. However, many of these factors additionally control other aspects of the DIC measurements as their primary function. These factors have been discussed individually in previous sections, but the trade-offs are summarized here and illustrated in Fig. 2.11:

- The lens aperture should be used to obtain the desired DOF, but it also affects lens resolution and governs how much light enters the optical system. An open aperture results in better lens resolution and brighter images, but results in a shallow DOF and accentuates optical aberrations. In contrast, a closed aperture results in a deep DOF, but poorer lens resolution, darker images, and potentially diffraction effects. See Sec. 2.2.3.
- The maximum exposure time should be chosen to limit motion blur, but exposure time also affects the image brightness. Longer exposure times produce brighter images, but potentially with motion blur. In contrast, shorter exposure times freeze motion, but produce darker images. See Sec. 2.1.11.

¹¹The exposure time is not strictly required to be the same in both cameras of a stereo-DIC setup. The exposure time may be adjusted for each camera independently to account for different sensitivities of the detectors, for instance, as long as each exposure time is short enough to limit motion blur as described in Sec. 2.1.11. However, this is an advanced topic outside the scope of the current edition of this guide.

- Given a pre-determined aperture and maximum exposure time, external lighting should be used to obtain sufficient contrast between the light and dark features of the DIC pattern. Lighting that is either too bright or too dark will result in images with poor contrast. If lighting is too bright, reduce either the light intensity, number of lights, or the exposure time. If lighting is too dark, brighter and/or additional lights should be added.

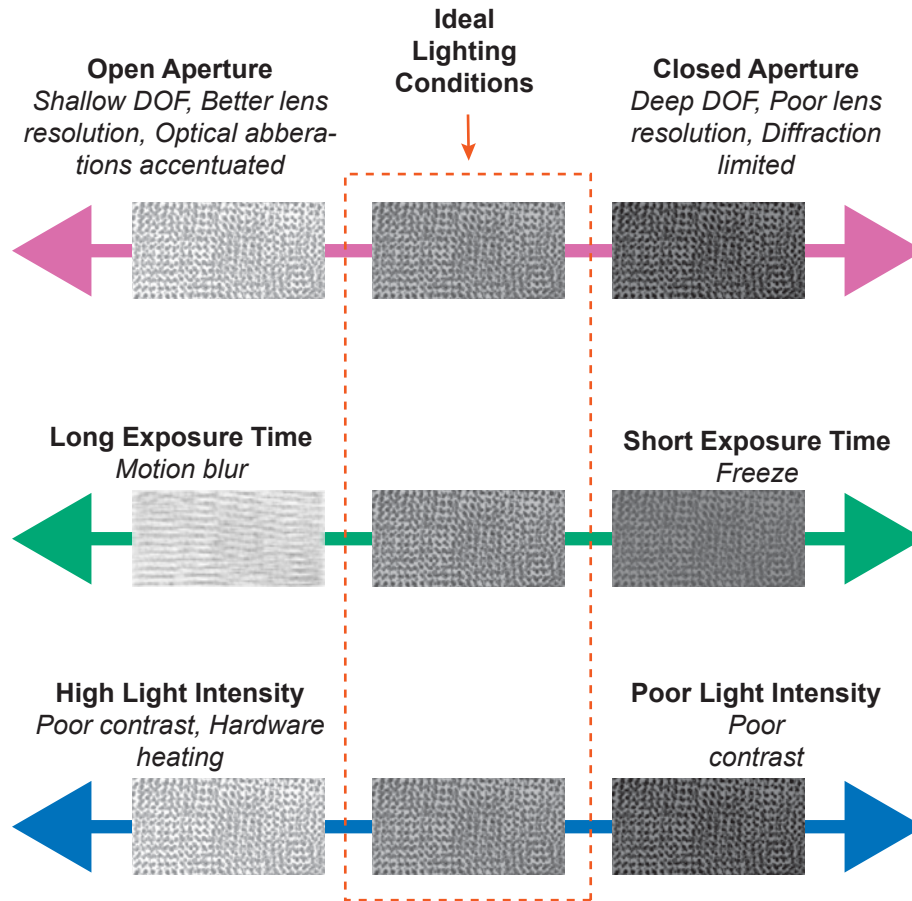


Figure 2.11: Illustration of lighting trade-offs regarding the aperture, exposure time, and light intensity. Note that the ideal conditions may not be in the center of the range for each factor.

In some (usually more challenging) measurement configurations, it may not be possible to fulfill all guidelines and recommendations related to lighting considerations simultaneously. For instance, if there is not sufficient external lighting, the exposure time may need to be increased to generate images with sufficient brightness and contrast. As a consequence, there may be more motion blur than desired, and the frame rate and/or image acquisition rate may be lower than desired. Alternatively, the aperture could be opened to increase the amount of light entering the optical system, but then the DOF would be reduced. In these situations, the DIC practitioner must determine an appropriate compromise between these factors.

2.2.4.1 Type of Lighting

In some cases (e.g. slow, quasi-static tests and moderate aperture), room lighting is sufficient. However, most of the time, additional lighting is required to have good contrast for a given aperture and exposure time. In these cases, white light or light of any wavelength or band of wavelengths will work, provided the camera and the lens are designed for that wavelength.¹² (It is recommended, though, to avoid lighting that has significant intensity in the infrared range, as this may increase the temperature of the test piece, and thus change the behavior of the test piece.) Diffuse lighting (instead of focused or spot lighting) is recommended to reduce glare caused by specular reflections (see Sec. 2.3.2.5). The main requirement for lighting is that it is uniform and constant, both across the FOV and in time, and does not heat the test piece.

Tip 2.25 — Cross-Polarized Light

Beyond diffuse light, another lighting approach to reduce specular glare is cross-polarized light [51].^a The key to a cross-polarized light system is to generate linearly polarized light that is incident onto the test piece, and then image only light that is linearly polarized 90° from the incident light.

Typically, a cross-polarized light system is accomplished as follows. First, place a linear polarizer in front of the light source; the absolute orientation of this polarizer is not important. Then place a linear polarizer in front of the lens (or lenses, for stereo-DIC), typically by screwing it into the filter threads on the front of the lens. View a live image and adjust the orientation of the polarizer on the lens until specular reflections are eliminated or minimized. This optimal orientation of the lens polarizer should be 90° from the light polarizer (i.e. if the light polarizer is oriented horizontally, the lens polarizer should be oriented vertically).

When unpolarized or randomly polarized light passes through a linear polarizer, the transmitted intensity is approximately half of the original light intensity (neglecting additional losses due to an imperfect polarizer). With cross-polarized light, the total light entering the camera is therefore reduced by a factor of approximately 4. To compensate for this reduction, brighter lights are typically necessary for cross-polarized light compared to unpolarized (randomly polarized) diffuse light. Alternatively, the exposure time may be increased as long as there is no motion blur (Sec. 2.1.11) or the aperture may be opened by two f-stops as long as there is still sufficient DOF (Sec. 2.1.7 and Sec. 2.2.3).

^aCross-polarized light is especially useful for curved surfaces or test pieces that are anticipated to undergo large rotations, but these topics are outside the scope of the current edition of this guide.

Tip 2.26 — Luminescence

Another lighting scheme involves a luminescent DIC pattern, based on fluorescence or phosphorescence of a material, rather than reflection of light [52, 53]. A DIC pattern can be created by applying the luminescent material directly to the test piece, and no base coat is needed. Luminescent patterns are typically excited by a short wavelength of light in the blue, near ultra violet (UV) or UV range, and then the pattern material emits light usually at a longer wavelength in

¹²Specific wavelengths of light can be advantageous over white light for some DIC measurements. For instance, blue light can be useful for test pieces that are heated and emitting significant levels of black body radiation in the visible wavelengths. Additionally, shorter wavelengths of light reduce diffraction effects and result in a smaller Airy disk spot size. However, these are advanced topics outside the scope of the current edition of this guide.

the visible range. A long-pass filter or band-pass filter is placed in front of the lens to block any reflected excitation light, thereby isolating only the luminescent emission from the pattern. Luminescent patterns and lighting schemes lead to high-contrast images with a very dark background, eliminate specular glare, minimize problems with shadows, and often reduce concerns of pattern degradation associated with a base coat.

Tip 2.27 — Backlighting

A transparent or translucent test piece may also be backlit, where light is shined from the back side through the test piece. Backlighting or transmission lighting does not generally suffer from reflections, but the transmitted intensity depends on the thickness and opacity of the test piece.

Tip 2.28 — Pulsed Lighting

Pulsed or strobed lighting may also be used, where the lights are programmed to turn on for a set duration or pulse length at a given frequency. Pulsed lighting may reduce the how much the lights heat the test piece and reduce the effects of heat waves by reducing the temperature of the lights themselves (Sec. 2.2.5). Additionally, the pulsed mode of some lights may provide a brighter light intensity than the same lights are capable of producing in a continuous mode.

Caution 2.13 — Light Flicker

Some lights may flicker (i.e. change intensity) at the same frequency as the alternating-current (AC) electrical supply (typically 50–60 Hz). Similarly, for some LED lights, the intensity of the light is controlled by varying the duty cycle of the light, again typically at 50 Hz. In either case, if the image acquisition rate is close to or faster than the AC electrical supply frequency or the duty cycle frequency, then the intensity of the light (and thus the contrast of the images) can vary between images.

Caution 2.14 — Concerns with Lighting

Especially when working with bright or intense lights, there may be safety concerns, for instance if laser illumination is used or if high-intensity lights become hot to the touch. Additionally, care should be taken to minimize effects of heat waves from hot lights (Sec. 2.2.5).

2.2.4.2 Light Mounting

Tip 2.29 — Lighting Adjustments between Calibration and Test

Often, different lighting and/or exposure is required to have good contrast for the test piece versus a calibration target (see Sec. 3.2 for information on DIC system calibration). Adjusting the light intensity, position, and/or the exposure time for calibration purposes is a common procedure and is acceptable as long as the camera, lens, and mounting are not disturbed (see Sec. 3.2.2.3), and the adjustments are reversed before the DIC measurements are made.

Recommendation 2.10 — Light Mounts

Numerous vendors supply lights that are integrated robustly onto the camera mounting system; often, these systems are designed to allow adjustment of the lights without disturbing the cameras. Alternatively, lights can be mounted on a separate frame than the cameras, or remote lighting control can be used, to reduce the possibility of unintentional camera motion when adjusting lights.

2.2.4.3 Contrast, Intensity, and Gain

Recommendation 2.11 — Image Contrast

Because DIC metrological properties rely highly on image gradients (and thus contrast), the better the contrast is (without the image being overexposed or underexposed), the less noisy the DIC results are. For an 8-bit image, the minimum contrast to have a displacement noise-floor of around 0.005 pixels is approximately 20% (50 grey-level counts between the light and dark features) [27], though contrast of at least 50% (130 counts) is typically preferred.^a

A preliminary noise-floor analysis can be performed to evaluate the image contrast (along with other factors such as the pattern quality), as described in Sec. 5.4.3. If the noise-floor is unacceptably high, then the lighting and related factors should be adjusted to improve image contrast, as described in Tip 2.24.

^aMore advanced users may optimize the contrast beyond simply the difference between the light (white) and dark (black) intensities. A well-spread distribution of intensities between these limiting white and black values may behave better than a bi-modal distribution. It can be advantageous to use only the lower portion of the dynamic range of the camera detector, as long as there is still sufficient contrast, because camera noise typically scales with intensity (though this can be camera-specific) [54].

Tip 2.30 — Image Contrast

There can be sufficient contrast in the image for DIC, even if the images “look” dark to the eye. This is especially true for camera detectors having larger dynamic ranges. Additionally, some monitors or displays may equalize the image contrast for visual aesthetics. Therefore, the actual grey-level counts should be evaluated quantitatively and not only assessed visually. A histogram of the grey-level counts is a useful tool for the evaluation.

Caution 2.15 — Evolution of Image Contrast

Contrast may change during the test, as the test piece is moved and/or deformed. Therefore, ensure there is sufficient contrast both at the beginning and throughout the duration of the test. Pre-testing extra test pieces may be required to confirm lighting and contrast throughout the test.

Recommendation

If the mean contrast in the image changes over time during the test, the zero-mean normalized sum of square difference (ZNSSD) matching criterion is recommended to compensate for contrast changes. See Sec. 5.2.3 for more information on matching criteria.

Caution 2.16 — Underexposure, Overexposure, and Glare

Ensure no regions-of-interest of the image are overexposed (i.e. the intensity at every pixel should be less than the maximum gray level of the camera detector) or underexposed (i.e. the intensity at every pixel should be greater than the minimum gray level of the camera detector), and there is no glare in the ROI (see Fig. 2.17 and Fig. 3.2). These conditions should be true both initially and as the test piece is translated and rotated within the [working volume](#) [16]. In stereo-DIC, check both images for glare, as glare could appear in only one of the two cameras. Keep in mind that glare can manifest as either points or as lines.

Caution 2.17 — Camera Gain

Do not increase the [gain](#) (sometimes referred to as the [exposure index](#) or the “ISO setting”) of the camera(s) in an attempt to increase the contrast or intensity. Increasing the gain increases camera noise, with no benefit for DIC [23].

2.2.5 Hardware Heating

Caution 2.18 — Hardware Heating

Almost all cameras, lights, and test frames become hotter than room temperature when run continuously. Camera heating can be larger when the frame rate is faster, and can increase when the cameras are actively acquiring and transferring images. Moreover, camera heating can be exasperated when the heat is not properly dissipated, such as when the lens (rather than the camera body) is mounted to the mounting system (Sec. 2.2.2.1). Even “cool” LED lights will warm up appreciably during use.

Hardware heating can negatively impact DIC measurements in several ways, including but not limited to:

- Changing the sizes and positions of the camera detector(s) and lens(es) due to thermal expansion of the components of the camera(s) and lens(es).
- Heating of the mounting structure, which, in stereo-DIC, can result in a change in the relative positions of the cameras during testing that negates the calibration.
- Inducing convective air currents (known colloquially as “heat waves,” “heat haze”, or the “mirage effect”) that refract light between the test piece and the imaging system.^a

Recommendation

To mitigate effects of thermal expansion of the camera(s), lens(es) and mounting structure, cameras should be turned on and operated at the target frame rate (Sec. 2.1.10) until they have reached a stable operating temperature. Calibration images and DIC measurement images should only be acquired after the cameras have reached thermal equilibrium. See Sec. 3.1.3 for more information on warming up the cameras.

It is recommended to minimize heat waves in the test setup before images are acquired, using one or more of the following preventative steps. Similar to camera vibrations (Sec. 2.2.2.1), the amount of time and effort spent on minimizing heat waves is directly commensurate with the magnitude of the errors caused by heat waves, and the desired precision of the DIC measurements.

- Mount lights *above* and *behind* the camera(s) if possible. Avoid mounting lights between the camera(s) and the test piece. In particular, avoid mounting lights below the camera/test piece plane.
- If lights are the source of heat waves and the test duration is short, keep lights off as much as possible to prevent them from heating up, and turn them on only for the test duration. If the test duration is long, pulse or strobe the lights so the lights are on only when images are being acquired (Tip 2.28), or add a fan onto the lights to cool them and homogenize the air temperature.
- If heat waves are caused by the camera(s), cool the camera(s) with a heat sink or a fan. Alternatively, place an air knife (a device that creates a sheet of high-intensity laminar air flow) in front of the cameras, to homogenize the air between the cameras and the test piece without blowing air directly onto the camera(s).

If heat waves cannot be satisfactorily minimized in the experimental setup, a longer exposure time may reduce errors in the DIC QOIs by essentially temporally filtering the heat waves. Alternatively, post-processing strategies can be employed to reduce errors, such as averaging images before correlation or applying temporal filters to the QOIs after correlation.^b However, details of the experimental setup, such as where the heat source is located relative to the test piece and the imaging system, influence the spatial and temporal frequencies of the heat waves and associated errors [58]. These frequencies may be in the same range as those for the QOIs. Therefore, filtering methods—either through the exposure time or post-processing—may have limited ability to remove the errors from heatwaves while retaining the underlying signal of interest [58]. Additionally, care should be taken to ensure that there is no motion blur when using a longer exposure time or averaging images (Sec. 2.1.11).

^aHeated test pieces may also induce heat waves, but heated test pieces are outside the scope of the current edition of this guide.

^bSpatial-temporal DIC is an approach to DIC that considers multiple images in a time-series simultaneously when performing the correlation [55, 56], opposed to the more typical “instantaneous DIC”, which considers each image individually. Spatial-temporal DIC can be useful to reduce errors caused by heat waves [57]. However, since most commercial DIC packages perform instantaneous DIC, spatial-temporal DIC is considered an advanced topic outside the scope of the current edition of the guide.

Tip 2.31 — Heat Waves / Mirage Effect

Even small temperature changes can generate heat waves between the test piece and the imaging system that refract light. The associated distortions, also known as “heat haze” or the “mirage effect”, cause errors in DIC measurements that manifest as spatially- and temporally-varying striations in the displacement and strain fields (Fig. 2.12).^a When animated in post-processing, these distortions can look similar to flames of a fire [58].

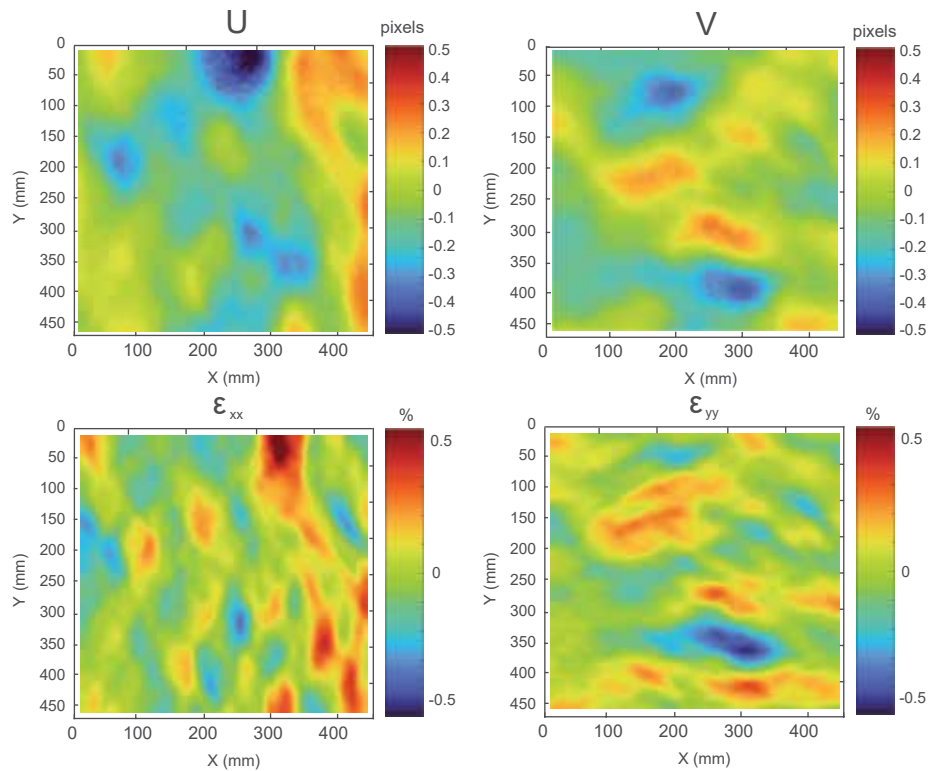


Figure 2.12: Illustration of the striations that appear in DIC data as a result of imaging through heat waves, for the horizontal and vertical in-plane displacements, U and V , and the horizontal and vertical normal strains, ε_{xx} and ε_{yy} [58].

^aNote that other types of gas or fluid flow between the camera and the specimen may cause a heterogeneous field of the index of refraction and result in similar errors in DIC measurements. However, these types of non-typical environmental conditions are outside the scope of the current edition of this guide.

Caution 2.19 — Fans

Beware of inducing camera motion by blowing air onto the camera(s) and/or transferring vibrations from a fan to the camera mounting structure. If using a fan to cool lights or camera(s), ensure that the reduction in errors due to reducing heat waves is more impactful than any increase in errors due to camera motion.

2.3 DIC Pattern

2.3.1 Type of DIC Patterns

One fundamental assumption of DIC is that the motion and deformation of the pattern that is imaged exactly replicates the underlying test piece motion and deformation. Sometimes, images of the surface of the test piece itself have a sufficient natural pattern that is adequate for DIC, and no artificial pattern needs to be applied.

Tip 2.32 — Natural DIC Pattern

As a first step, the test piece surface can be imaged, and the natural pattern can be evaluated to ascertain if it has the characteristics described in Sec. 2.3.2. If so, no applied DIC pattern is necessary.

Caution 2.20 — Surface Coating on Test Piece

Be cognizant of any surface coating that may be on the surface of the test piece, i.e. brittle mill scale on steel, brittle oxides, added coatings such as zinc coating on steel, etc. Such surface coatings may or may not move with or behave like the underlying material. Ensure that the pattern being imaged on the surface reflects the deformation of interest of the bulk material underneath.

Most of the time, a pattern must be applied to the test piece surface. Typically, though not exclusively, applied patterns consist of roughly circular “speckles” of a (preferably) uniform size but random locations.¹³

Recommendation 2.12 — Evaluation of DIC Pattern

The quality of a DIC pattern is often evaluated by manual, visual inspection of the images, where the DIC practitioner looks for the characteristics described in Sec. 2.3.2. More quantitative evaluation of a DIC pattern is typically not necessary outside of research activities, but can consist of metrics such as image gradients to evaluate contrast, and other image morphology methods to evaluate feature edges, shapes, sizes, and distribution [63, 64].

2.3.2 General Characteristics of DIC Patterns

Both natural and applied patterns should have the following general characteristics:

2.3.2.1 Size

For best spatial resolution, the optimum pattern feature size is 3–5 pixels [7, Sec. 10.1.3.1], [25, 47]. This guideline applies to both the light (white) and the dark (black) features as shown in Fig. 2.13.

Tip 2.33 — Camera-Limited vs. Lens-Limited Spatial Resolution

The guideline for pattern feature size of 3–5 pixels assumes the overall spatial resolution of the imaging system is limited by the camera, which is the case for most DIC applications. However, for a large image scale (i.e. high magnification) resulting from a small FOV and/or a large image size, the imaging system resolution may be limited by the lens resolution (resulting in a loss of image clarity), and larger feature sizes may be required [47]. See Tip 2.6 for more details.

Tip 2.34 — Measuring Pattern Feature Size

There are many definitions and methods of determining feature size [7, Sec. 10.1.3.1], [25, 61]. However, for features larger than one pixel, a rough, manual estimate, in which the DIC practitioner

¹³More advanced “optimized” pattern designs—including regular checkerboard pattern—are outside the scope of the current edition of this guide, but information can be found in [59–62].

zooms in on an image and approximates the feature size by eye, is quick and easy to perform and is typically sufficient, as shown in Fig. 2.13.

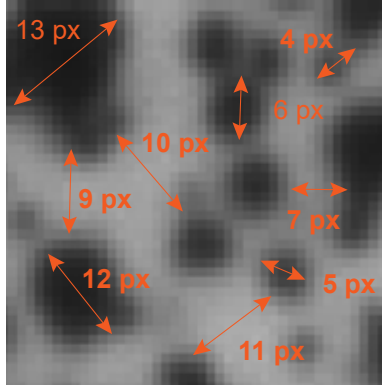


Figure 2.13: Illustration of a manual estimate of the feature sizes of a DIC pattern.

Tip 2.35 — Physical Pattern Feature Size

The physical pattern feature size, L_{physical} , is determined based on the image scale, S , and the apparent pattern feature size in the image, L_{image} , as follows:

$$L_{\text{physical}} = \frac{L_{\text{image}}}{S}. \quad (2.3)$$

The image scale in turn depends on both the FOV and the image size. To illustrate these dependencies, Table 2.2 shows the results for the cameras and FOVs from Example 2.2. For the example FOV 1 and the 2448 px wide image, the image scale is $S = 11.1$ px/mm. Therefore, a target pattern feature size in the image of $L_{\text{image}} = 5$ px equates to a physical feature size of $L_{\text{physical}} = 0.449$ mm. If the FOV is kept constant, but the image width is increased to 5472 px, then a smaller physical feature size of $L_{\text{physical}} = 0.201$ mm would be required to have the same pattern feature size in the image.

Table 2.2: Example calculation of physical pattern feature size based on FOV and camera selection in Example 2.2.

FOV in Example 2.2	FOV Width (mm)	Image Width (px)	Camera (Mpx)	Image Scale S (px/mm)	Feature Size in Image L_{image} (px)	Feature Size on Test Piece L_{physical} (mm)
1	220	1280	1.3	5.8	5	0.859
1	220	2448	5	11.1	5	0.449
1	220	5472	20	24.9	5	0.201
2	110	1280	1.3	11.6	5	0.430
2	110	2448	5	22.3	5	0.225
2	110	5472	20	49.7	5	0.101

Tip 2.36 — Confirming Pattern Feature Size

After the desired physical size of the DIC pattern features is calculated based on the image scale, the desired physical size can be confirmed by printing a synthetic pattern on paper using a typical office printer (if the printer has sufficient resolution for the desired pattern size) and imaging the pattern using the same optical system as the actual test, to ensure all features are 3–5 pixels in size.

Caution 2.21 — Aliased Pattern Features

Pattern features that are smaller than 3 px risk being aliased and adding error to DIC results [7, Sec. 10.1.3.1], [24, 47, 65]. A visualization of how an aliased pattern appears in a digital image is shown in Fig. 2.14. This error is more pronounced when displacements are small, due to a lower signal-to-noise ratio. When the pattern is compressed (e.g. applied compression in a given direction or transverse compression during applied tension), features that started at the lower end of the recommended range (e.g. 3 px) may become aliased. Features that are larger than necessary (i.e. larger than 5 px) will require larger subsets/elements (see Sec. 5.2.7) and thus will degrade spatial resolution of displacements and strains, but will otherwise not negatively effect the results (i.e. will not add noise).

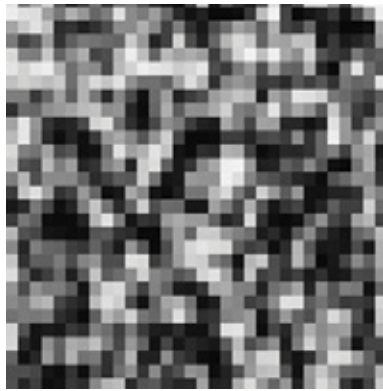


Figure 2.14: Photo showing how an aliased pattern appears in a digital image.

Recommendation

For many applications, if the selected patterning method results in a wide spread of feature sizes, then it is generally preferred to use features that are larger than optimal, to limit the number of aliased features. That is, added noise due to aliased features is typically worse than degraded spatial resolution due to large features.

Recommendation 2.13 — Pattern Feature Size Variation

In stereo-DIC, where the cameras are at an angle to the test piece, the image scale (on the surface of the test piece) is not constant over the FOV of each camera. To ensure that the smallest DIC pattern feature is not aliased at any location in the ROI of the image from either camera,

consideration must be given to the changing image scale across the ROI. Therefore, the location in the ROI of the image from either camera, where the image scale is smallest should be found and used to define the smallest allowable DIC pattern feature.^a

^aMore advanced users may take the varying image scale into account when designing an optimized DIC pattern. However, this advanced topic is outside the scope of the current edition of this guide.

2.3.2.2 Variation

The pattern should have sufficient random variation¹⁴ such that subsets/elements in different regions of the image can be uniquely identified, as shown in Fig. 2.15a.

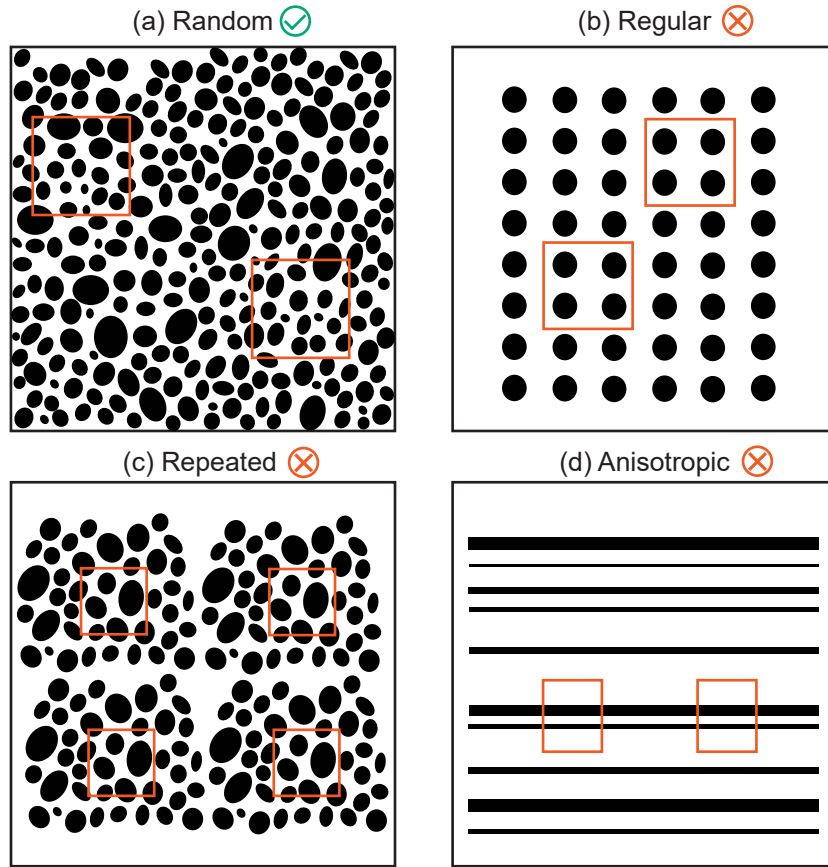


Figure 2.15: Illustrations of patterns with different types of variation. The orange boxes represent subsets/elements. In a random pattern (a), the subsets/elements are distinct throughout the pattern. In a regular pattern (b), one subset/element is indistinguishable from other identical subsets/elements. In a repeated pattern (c), a subset/element in one template may be erroneously matched to an identical subset/element in another template. In an anisotropic pattern (d), a subset/element is indistinguishable from other subsets along the direction of the pattern orientation.

¹⁴See footnote 13 on page 38.

Caution 2.22 — Regular, Repeated, and Anisotropic Patterns

Regular patterns (Fig. 2.15b) can be problematic for many DIC systems, since one subset/element is indistinguishable from another subset/element.^a

Repeated patterns (Fig. 2.15c) can arise when, for instance, a small template (e.g. stamp, sticker, stencil, or mask) is used to cover a large ROI of the test piece by repeating the template several times. With a repeated pattern, a point in one of the templates may be erroneously matched to a point in another template.

Anisotropic patterns (Fig. 2.15d), such as a series of period lines of different widths, can result in correlation of motion normal to the lines, but with no correlation of motion parallel to the lines. Anisotropic patterns should be avoided unless motion in only one direction is required.

Recommendation

If a regular, repeated, or anisotropic pattern is used, then some randomization should be added in addition to the pattern (e.g. adding some random marker dots, or rotating the template used to create the pattern and applying a second layer of the pattern). For regular and repeated patterns, an initial guess (Sec. 5.2.10) and/or bounds on the search area may also overcome the difficulties associated with the non-unique patterns.

^aSee footnote 13 on page 38.

2.3.2.3 Density

Pattern density should be approximately 50% (i.e. there should be approximately the same area of light (white) and dark (black) pixels in any intended subset/element of the ROI of the image) [7, Sec. 10.1.3.1], [29]. If round speckles are used, then a density closer to 25–40% can be expected due to the required minimum spacing between the round speckles. Sparse patterns with insufficient feature density require larger subsets/elements to prevent decorrelation, thus degrading the effective spatial resolution of the QOIs. Examples of pattern density are shown in Fig. 2.16.

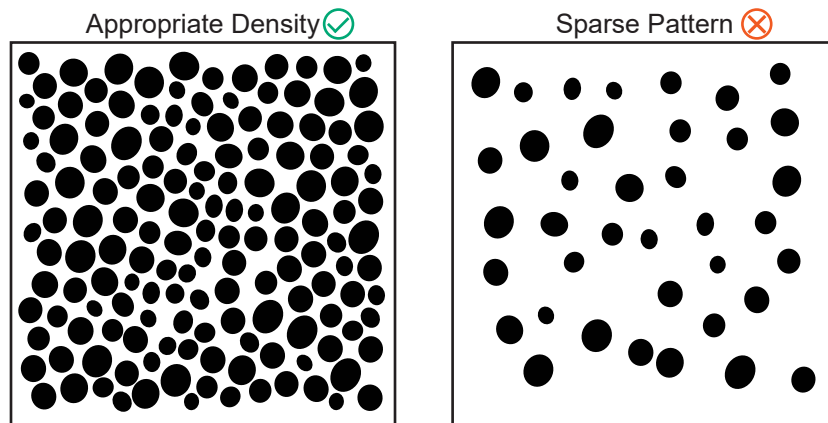


Figure 2.16: Images of a DIC pattern with appropriate or low (sparse) density.

2.3.2.4 Quality

Pattern quality degradation should be minimized and not permitted to result in decorrelation during the analysis.¹⁵

Tip 2.37 — Degradation of Patterns

For natural DIC patterns, sources of pattern degradation include, but are not limited to, significant morphological changes and development of slip bands on the surface of the test piece during plastic deformation. For applied DIC patterns, sources of pattern degradation include, but are not limited to, fading, cracking and debonding.

Tip 2.38 — Verification of Pattern Quality

Pretesting of extra test pieces may be required to verify the suitability of a pattern throughout the duration of the test.

Tip 2.39 — Measurement Uncertainty due to Pattern Degradation

Even at strains where decorrelation does not occur, pattern degradation can result in reduced correlation quality and increased uncertainty in the measurement [64].

2.3.2.5 Reflections

The pattern sheen should be matte and not glossy, to avoid glare and specular reflections (Fig. 2.17).

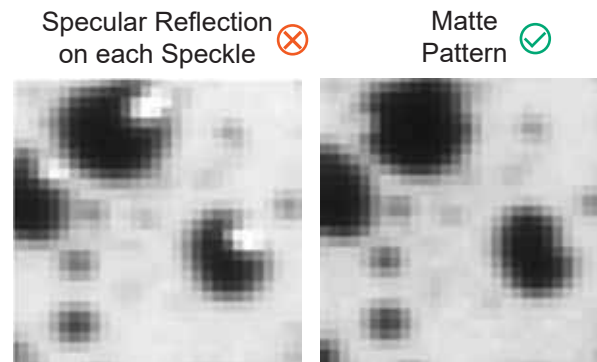


Figure 2.17: Examples of specular reflections on glossy speckles versus a matte pattern with no glare or reflections.

¹⁵Note that in tests involving large deformation (e.g. several hundred percent deformation in elastomers), a well-bonded applied pattern may deform so much that correlation is lost between the first image and an image later in the test, even if it does not debond or crack. In this case, incremental correlation may be used. This situation of large deformation, however, is outside the scope of the current edition of this guide and will not be discussed further.

Caution 2.23 — Specular Reflections

Specular reflections can often be hidden in an otherwise good DIC pattern (i.e. appearing as artificial bright spots that may evolve over time and/or appear differently in the two images of a stereo-DIC system) [66]. Specular reflections are dependent on the orientation and position of the test piece with respect to the light source and camera, and can change if the test piece is rotated or translated. Additionally, in stereo-DIC, specular reflections often look different in each camera, which effectively makes the DIC pattern different and uncorrelated in each FOV. Therefore, specular reflections should be avoided.

Recommendation

There are several lighting approaches to reduce specular reflections, including:

- Diffuse light (opposed to focused or spot light); see Sec. 2.2.4.1.
- Cross-polarized light; see Tip 2.25.
- Luminescent patterns; see Tip 2.26.
- Backlighting (for transparent or translucent test pieces); see Tip 2.27.

If specular reflections cannot be sufficiently minimized through the lighting, a photographic dulling spray can be applied to the DIC pattern. However, if a dulling spray is used, the DIC pattern should be carefully evaluated, to ensure that the spray does not degrade the pattern.

2.3.3 Characteristics of Applied Patterns

Applied patterns, regardless of the method used to create them (i.e. painting, applying an adhesive-backed foil or sticker, stamping or drawing with ink, applying a powder, transfer printing, etching, abrasion, etc.), should have the following additional characteristics, which do not necessarily apply to natural patterns.

Recommendation 2.14 — Mask Gripping Region

Only the ROI of the test piece should be patterned. Other regions—such as the grip region of a test piece in a tensile test or the surfaces that will contact platens in a compression test—should be masked so that the pattern is not applied to these areas. For tensile tests, masking the grip region will help increase grip force, reduce likelihood of the test piece slipping within the grips, and prevent clogging of the grips with the pattern material (e.g. paint). For compression tests, masking the surfaces that will contact the platens will help prevent uneven loading and prevent the pattern material from affecting friction.

2.3.3.1 Non-Invasive

The applied pattern should be non-invasive and not affect the behavior of the test piece.¹⁶

¹⁶As mentioned in Sec. 1.2 and Sec. 1.3, this guide focuses on mechanical testing, and thus this section focuses on the effect of the pattern on the mechanical properties of the test piece. However, in combined environment tests, other physical properties of the test piece should also be considered. For example, for a thermo-mechanical test, an applied

Caution 2.24 — Pattern Compliance

For mechanical tests, the applied pattern should be thin and compliant relative to the test piece. If the applied pattern is thick and/or stiff compared to the test piece, the pattern material may affect the mechanical response of the test piece. In this case, DIC measurements based on images of the pattern may reflect the deformation of the applied pattern, rather than the deformation of the underlying material of interest.

Caution 2.25 — Destructive Patterning Methods

In addition to *applying* material such as paint onto the surface of a test piece, material can also be *removed* to create a pattern, such as through abrasion or etching. With these destructive patterning methods, one must ensure that the effects on the properties of the test piece (e.g. stiffness, strength, failure strain, failure mode) are not altered.

2.3.3.2 Bonding

There should be good bonding between the test piece and the applied pattern.

Recommendation 2.15 — Cleaning the Test Piece

Before applying a DIC pattern, clean the test piece to promote good bonding between test piece and pattern. For example, for common metals (e.g. steel and aluminum), acetone can be used first to remove grease, cutting fluid, ink, etc. However, acetone leaves a residue after evaporating, so test pieces cleaned with acetone should always be subsequently cleaned with a solvent that does not leave a residue, such as isopropanol, methanol, or ethanol.

Additionally, if the surface is very smooth, consider roughening it with a very fine grit sand paper (similar to that used for preparing a surface for foil strain gauges) to promote adhesion of the applied pattern to the test piece surface, if such treatment will not alter the test piece properties.

Tip 2.40 — Painted Pattern Debonding

For paint-based patterns, especially on test pieces undergoing large deformations, debonding issues may be exacerbated when a solid base coat of paint is used. An alternative patterning approach is to forgo the solid base coat and apply only pattern features to the test piece. Disconnected (noncontiguous) pattern features may deform more conformally with the test piece than a solid coat of paint.

For instance, for metallic test pieces, one can apply white paint features onto the bare metal, with no base coat of paint, and then use cross-polarized light to create a high-contrast pattern (Tip 2.25). In this scenario, light specularly reflected from the bare metal will retain its polarization. Therefore, if the incident light is linearly polarized, and a linear polarizer on the lens is oriented at 90° from the incident light, no specularly reflected light from the bare metal will reach the camera detector. Thus, the bare metal appears black in the image. In contrast, diffusely re-

pattern should ideally not affect the thermal conductivity or emissivity of the test piece. Further discussion of combined environment tests is outside the scope of the current edition of this guide.

flected light from the paint will have random polarization. Therefore, a component of the diffusely reflected light will pass through the linear polarizer on the lens. Thus, the white paint is visible in the image.

Luminescent patterns (Tip 2.26) provide similar advantages to cross-polarized light. Individual (noncontiguous) pattern features of a luminescent material may be applied to the test piece with no base coat. With proper excitation light and filters, the luminescent features will emit light and be visible in the image while the uncoated background will appear black.

Both cross-polarized light and luminescence often create excellent DIC patterns that have high contrast and suffer less from debonding issues compared to patterns employing a solid base coat of paint.

Caution 2.26 — Pattern Debonding

Debonding of an applied pattern can be an insidious problem. In some cases, an applied pattern may locally debond from the test piece, yet remain intact and continue to deform independent of the test piece. In these cases, the fact that the pattern debonded may not be obvious. Some examples of pattern debonding and degradation are shown in Fig. 2.18.

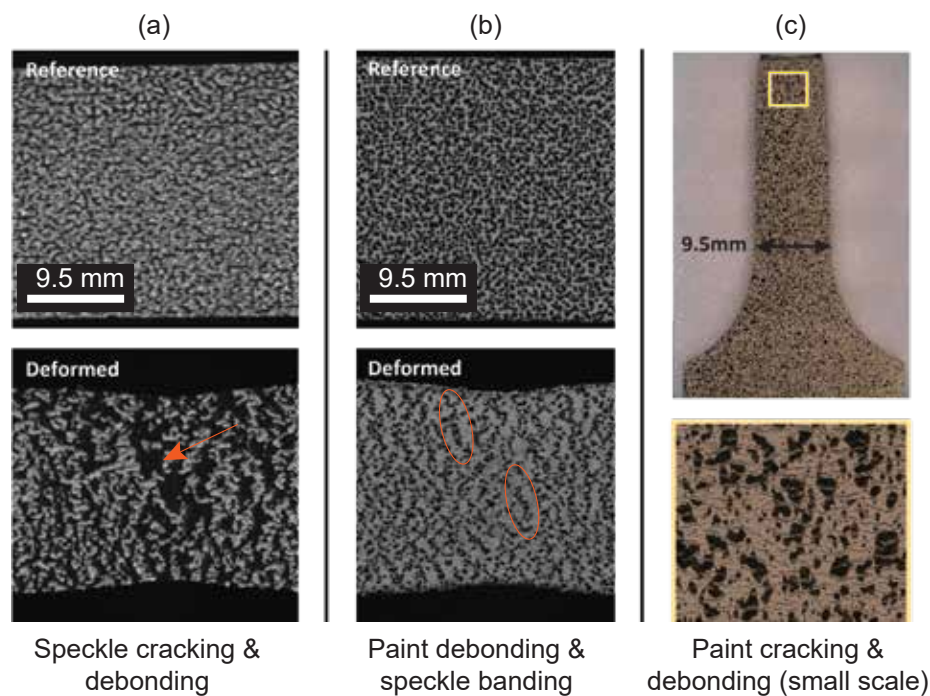


Figure 2.18: Examples of different debonding-related pattern degradations on 304L stainless steel tensile dog bone test pieces. (a) Individual features of a noncontiguous pattern of white features cracked. (b) A white base coat of paint debonded from the test piece yet remained intact and deformed independently of the test piece, resulting in semi-vertically aligned bands of the black features. (c) A paint-based pattern was embrittled at high temperatures and cracked when the test piece was deformed.

Recommendation

Inspect the test piece and applied pattern closely after the test, to look for any indications or evidence of pattern debonding. Executing a practice test beforehand can help build confidence in the patterning method (see Tip 2.43), but cannot completely replace carefully inspecting the actual test piece after testing.

2.3.3.3 Fidelity

The applied pattern should move and deform conformally with the test piece surface.

Tip 2.41 — Paint Ductility

For paint-based patterns, the ductility of the paint should be aligned with the expected deformation. That is, for test pieces that are expected to undergo large deformation, the paint should be as ductile as possible, so that it stretches with high fidelity with the underlying test piece without cracking or debonding. To accomplish this ductility, the test should be carried out shortly after a short drying period, when the paint has set, can be handled, and no longer shows wet glare (see Sec. 2.3.2.5), but before the paint is fully cured and brittle (e.g. within a few hours of painting). Alternatively, individual features (e.g. speckles) can be applied directly on the test piece, without a base coat of paint (see Tip 2.40).

On the other hand, if the test piece is brittle and observation of crack propagation is important, the paint should be as brittle as possible, while still not debonding or cracking independent of the test piece, so that the paint cracks at the same time as the test piece. In this case, the paint should be allowed to fully cure, and can even be baked (if baking does not alter the test piece properties) to make it more brittle. Alternatively, individual features (e.g. speckles) can be placed directly on the test piece, without a base coat of paint, so that cracking of the test piece can be observed directly.

If no base coat is used, and individual features are placed directly on the test piece, ensure that there is sufficient contrast and that there are no specular reflections (see Sec. 2.3.2.5).

Caution 2.27 — Laser Speckle Patterns

Usually, an interference-based laser speckle pattern is not recommended for DIC because this type of pattern will decorrelate from the motion of the test piece for large displacements. The decorrelation of laser speckles may introduce errors into the DIC measurements or could lead to false results.^a

^aThere are limited conditions in which a laser speckle pattern can be used for DIC, but this is an advanced topic that is outside the scope of the current edition of this guide.

2.3.3.4 Thickness

The pattern should be of uniform thickness.

Caution 2.28 — Pattern Thickness

In stereo-DIC, a pattern with a rough surface can result in the same portion of the pattern appearing substantially different between the two camera images, which can hinder cross-correlation between the two images. In both 2D-DIC and stereo-DIC, a pattern with areas of different thicknesses can result in artificial strain gradients across the transitions between the areas of different thicknesses.

2.3.4 Patterning Techniques

There are many different techniques available to create appropriate patterns for DIC, such as stencils, stamps, incomplete layers of paint (either using a commercial spray paint can, or using an air brush), printer toner or other fine powders, abrasion, and etching, to name a few. Tables 1 and 2 in [67] provide a summary of common patterning techniques and an evaluation of their respective advantages and disadvantages, as well as further references for more information on each method. Patterning techniques are limited only by the imagination. Often, patterning techniques are learned through on-the-job training by more experienced DIC practitioners, through training by a vendor when a new DIC system is purchased, or through classes taught by subject-matter experts.¹⁷ Due to the immense variety and nuances of patterning techniques, no guidelines are given here concerning the execution of specific patterning techniques.

Tip 2.42 — Library of Patterning Techniques

In order to facilitate the design of DIC measurements, creation of a table of patterning techniques and the resulting pattern size is recommended for each DIC practitioner or laboratory. Additionally, a library of physical chips with patterns created with different techniques is helpful when designing a new DIC measurement, because the size and contrast of different patterns can be quickly evaluated with the preliminary camera, lens, and lighting setup.

Tip 2.43 — Verification of Patterning Technique

Once a patterning technique has been selected, pattern a scrap test piece and image the pattern to verify that the pattern has the right size, variation, and density. Images should be taken in the test setup or in a mock setup that uses the same camera(s), lens(es), SOD, stereo-angle, etc. as the actual setup. The scrap test piece should be the same material as the actual test piece of interest, as patterning techniques can produce different results on different substrate materials. For example, spray-paint speckles may be larger on metal, where the paint droplets spread out, than on cardboard or paper, where the paint droplets soak into the material. Additionally, it is beneficial to execute a practice test and inspect the test piece afterwards to ensure the pattern did not degrade during testing (see Caution 2.26).

¹⁷iDICs offers DIC classes at their annual conference. For more information, see www.idics.org.

3 — Preparation for the Measurements

3.1 Pre-Calibration Routine

3.1.1 Review of Test Procedure

Before preparing for and executing the mechanical test with concurrent DIC measurements, review the overall test procedure. Some factors to consider are listed below, though there may be additional factors specific to an individual test:

- Evaluate the tentative testing procedure to be used, and ensure that the DIC pattern is preserved and undamaged during handling and gripping. Modify the testing procedure if necessary to reduce the likelihood of scratching or contaminating the pattern (e.g. oil on the surface of the test piece).
- Ensure the mechanical load frame is properly adjusted and calibrated.
- Review the timeline of the test process and ensure there is adequate time for all steps, such as warming up the cameras, warming up the load frame (if necessary), calibrating the DIC system, reviewing the calibration, preparing and patterning the test piece, testing the test piece, etc. Determine at what point in the test process the test piece should be patterned (if using an applied pattern).
- Ensure environmental conditions (e.g. temperature) will be stable during the course of the DIC calibration and mechanical test.¹⁸
- Consider adding a stationary backdrop behind the test piece, to prevent any people or objects moving behind the test piece or changing light reflections from adversely affecting the images.

3.1.2 Cleanliness of Equipment

Ensure there is no dirt, dust, or other foreign particles (e.g. water, marks, oil, smears, fingerprints) on the lens, camera detector, or calibration target.

¹⁸This consideration is more important for outdoor testing, though outdoor testing is outside the scope of this edition of the guide.

Recommendation 3.1 — Maintaining Clean Equipment

Keeping a clear lens filter (or linear polarizer if using cross-polarized light) on a lens as a semi-permanent addition to the lens protects the lens and makes cleaning easier. When lenses and cameras are not in use, lens caps and body caps should be used to protect the equipment. The amount of time that the camera detector and internal components of a lens are exposed to air (e.g. when changing lenses) should be minimized. If possible, disassembly of the lens-camera system and removal of lens and body caps should be performed in a clean environment. Store calibration targets in protective cases to keep them from getting dirty or damaged.

Tip 3.1 — Evaluating Cleanliness of Equipment

Image a white sheet of paper or other bright, solid background and look for any blurred spots or smears that could indicate dirt in the optical system (see Fig. 3.1). The image may need to be digitally magnified until individual pixels are visible, and image contrast may need to be digitally enhanced. Because the sheet of paper may not be perfectly clean itself, translate the sheet. If the spots/smears move with the paper, then the dirt is on the paper; if the spots/smears remain stationary, then the dirt is somewhere in the optical system. To determine if dirt is on the lens or detector, rotate the lens if possible. If the dirt rotates with the lens, the dirt is on the lens; otherwise, if the dirt remains stationary while the lens is rotated, the dirt is on the camera detector. Additionally, the external surface of the lens and the camera detector (with the lens removed) may be visually examined for the presence of dirt.

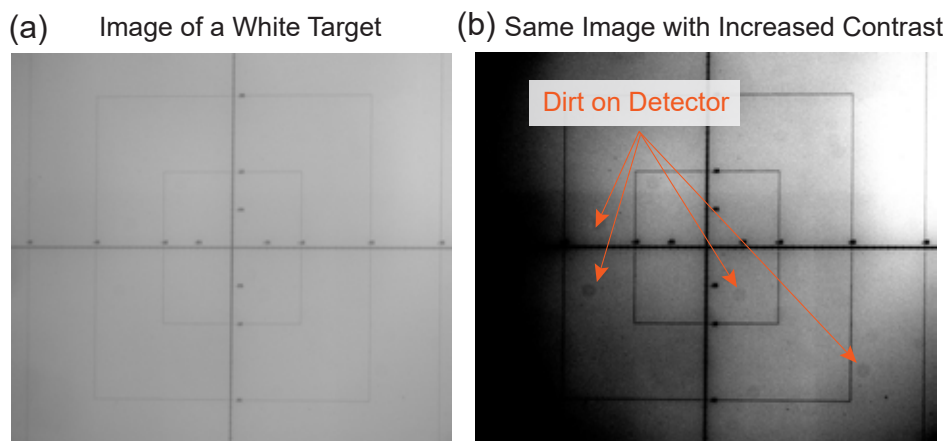


Figure 3.1: Image illustrating dirt on the detector and/or lens, when viewing a white target. (a) Original image contrast (i.e. intensity scaled across the full dynamic range of the image), where dirt is not easily visible. (b) Enhanced image contrast, clearly showing multiple specs of dirt as labeled by the arrows. (For clarity, not all spots are labeled.)

Tip 3.2 — Cleaning Camera Detectors and Lenses

Often, pressurized air, such as canned air or a bellows-type or bulb-type blower, is sufficient to remove dust or particles from the lens or detector. If canned air is used, the bottle should be kept upright and not shaken, to prevent propellant or condensate from being expelled from the can. Also, the canned air should first be sprayed away from the lens or detector, to ensure that no propellant or condensate is being emitted. Another tool that can be used to remove dust or particles is an optics cleaning brush.

To remove other contaminants such as oil, fingerprints, etc., lens paper and alcohol-based lens cleaning solution can be used to clean lenses. There are also specific products made to clean camera detectors, which consist of a swab that matches the camera detector size, and an appropriate cleaning fluid. Do not use denatured alcohol (also called methylated spirits) to clean a lens or detector; denatured alcohol can contain up to 4% water, which, while evaporating, can bind dirt onto the lens or detector. Always follow instructions from the manufacturer for cleaning lenses or camera detectors.

Caution 3.1 — Cleaning Camera Detectors and Lenses

Anytime the optical system is exposed (e.g. lens caps and/or body caps are removed and/or the lens is removed from the camera), be careful not to introduce dirt into the optical system. Be very careful when cleaning a lens or camera detector, as they can be easily, and irrevocably, damaged!

3.1.3 Camera Warm-Up

Turn on the camera(s) and acquire warm-up images at the target frame rate and image acquisition rate (Sec. 2.1.10) to allow the cameras to warm up to a stable operating temperature (see Caution 2.18). Once the cameras are warmed up, the warm-up images can be deleted. The camera(s) should reach a stable operating temperature before any calibration or test images are acquired and should remain at a constant temperature from the start of the calibration through the end of the DIC measurements. Refer to the DIC vendor manual for more information for vendor-supplied cameras.

Tip 3.3 — Camera Warm-Up

The time required for a camera to warm up to a steady temperature depends on the camera, mounting arrangement, laboratory environment, frame rate, and image acquisition rate. Moreover, the camera temperature rises some when a live feed is shown, but increases further when images are actually being acquired (i.e. saved to the computer).

Before using a new camera for DIC, monitor camera temperature during the warm-up period in the expected (or similar) mounting arrangement and laboratory environment, while acquiring images at the desired frame rate and image acquisition rate, and note the time required for the temperature to plateau. Some image acquisition software may report the camera temperature and indicate to the user when the temperature has stabilized. Typically, warm-up times range from several minutes to several hours.

For low-frequency frame rates, camera or software time-lapse functionalities may facilitate acquiring images at the desired rate over longer periods of time. For high-frequency frame rates and/or long-duration warm-up periods, images acquired during warm-up may need to be periodically deleted to avoid filling up the computer hard drive.

Use the determined warm-up time for all future DIC measurements that utilize the camera at the specified frame rate and image acquisition rate. If the camera, mounting arrangement, laboratory environment, frame rate, or image acquisition rate are changed, the warm-up time will need to be re-computed.

Caution 3.2 — Camera Warm-Up

If the cameras are not warmed up, errors can be introduced into DIC results due to thermal expansion of the cameras and lenses [68], and due to drift induced by thermal expansion of the camera mounts. See Sec. 2.2.5 for more information.

3.1.4 Synchronization

For stereo-DIC measurements, ensure the two cameras are synchronized to each other. For either 2D-DIC or stereo-DIC, review the data acquisition plan, and ensure any external signals (i.e. force, extensometers, strain gauges, etc.) are synchronized with the DIC camera(s).

Caution 3.3 — Camera Synchronization

Synchronization of the cameras in stereo-DIC is critical! Delay between the two cameras will result in errors in the DIC measurements.

Tip 3.4 — Camera Synchronization

Synchronization of two cameras in a stereo-DIC system can be verified in many different ways, including:

- Image a moving test piece that has a DIC pattern, correlate the images in the DIC software, and verify that the [epipolar error](#) is acceptable based on the DIC software documentation. See Sec. 3.3.2.2 for more information on the epipolar error.
- Image a strobe light set to the same frequency as the image acquisition rate.
- Image a dynamic event and ensure the event occurs in the same frame number in both cameras. (The speed of the dynamic event must be scaled appropriately with the image acquisition rate.)
- Measure the strobe or exposure signal from the cameras on an oscilloscope, if a strobe or exposure signal is output by the cameras.^a

^aHigh-speed cameras typically have both a sync-in port that receives a synchronization signal, as well as a sync-out port that provides the strobe or exposure signal. Machine vision cameras typically have a single synchronization port that can be used with commercial-off-the-shelf synchronization cables either to input a synchronization signal or to output the strobe signal, but not both simultaneously; however, custom cables may be able to be constructed to access both the sync-in and the sync-out pins simultaneously.

Tip 3.5 — Synchronization of Additional Signals

If additional signals (i.e. machine force, machine displacement, strain gauge signal, etc.) from other instruments used during a mechanical test are acquired and cannot be directly synchronized

or triggered with the DIC images, then one effective way to synchronize the signals through post-processing is as follows:

1. Trigger the cameras first, taking at least 10 images before starting the mechanical test.
2. Complete the test as planned.
3. After the test is complete, process the DIC images and extract the QOI. Plot the QOI versus image number or time. The QOI for images taken before the mechanical test commenced should be nominally zero (with some noise), whereas the images taken after the onset of the mechanical loading should increase with non-zero slope.
4. Fit lines to each of these two sections of the data and find the time where the lines intersect.
5. Subtract the time of the intersection from the time of all DIC measurements. This will effectively offset the times of the DIC measurements based on the correct time zero (i.e. the start of the test), even if it occurred in between DIC images.

3.1.5 Application of the DIC Pattern

If using an applied DIC pattern (as opposed to the natural surface of the test piece), apply the selected DIC pattern to the test piece.

Recommendation 3.2 — Fiducials

Apply two fiducial marks a known distance apart on a portion of the test piece that is within the FOV, but outside the critical ROI. Within reason, place the two fiducial marks as far apart as possible to improve the precision of the distance measurements. Assess the uncertainty in distance between the fiducials. These fiducials can be used to approximately verify the camera calibration, as described Recommendation 3.15. Other fiducial marks can also be useful. For example, fiducial marks for the center line axis of a test piece or the center of the gauge section can be used to rotate the DIC coordinate system and measurement results to the test piece coordinate system, as described in Sec. 5.3.1.

Experience has shown that the use of certain inks, such as red ultra-fine-point permanent markers, to draw fiducial marks or lines before painting, can result in bleeding of the lines through the paint in such a way that they are visible, but do not overly degrade the pattern with respect to image correlation. Alternatively, dotted or dashed fiducial marks made on top of the pattern can still be readily detectable by manual inspection of the images, but will not degrade the pattern.

3.1.6 Pre-Calibration Review of System

Caution 3.4 — Pre-Calibration Review of System

This is the time to make adjustments and fix any issues with the DIC measurement setup, so that the best possible images are obtained. Once calibration images are taken, very few aspects of the DIC system can be changed without re-taking calibration images. If any adjustments are made to the optical system hardware (cameras or lenses), then the previously acquired images must be discarded and an entirely new set of calibration images must be acquired. Care and time at this point in the test procedure can save tremendous time later on.

3.1.6.1 Position Test Piece and Cameras

Place the test piece in the load frame. Position the camera(s) to obtain the desired FOV, image ROI, and stereo-angle (for stereo-DIC). Set focus and aperture on the lens(es).

Tip 3.6 — Setting the Focus and Depth-of-Field

The test piece should be in the middle of the DOF^a and the focus should be constant across the ROI. To achieve these characteristics, first set the aperture wide open (low f-number). With the aperture open, the DOF is limited; thus it is easier to see when the test piece goes out of focus.

To determine when the test piece is in focus, digitally zoom-in on the image and inspect the edges of DIC pattern features. If the DIC pattern features have soft edges, it may be helpful to focus on printed text with sharp edges. Alternatively, some image acquisition software packages contain tools to automatically determine optimum focus.

Adjust the focus ring of the lens to sweep through the DOF to find the bounds of the DOF. Once the bounds have been established, set the focus to be in the middle of the DOF bounds. For stereo-DIC, the entire ROI may not be in focus when the aperture is wide open, due to the stereo-angle; in this case, bring the middle of the ROI into focus. Once the focus is set, decrease the aperture to have the desired DOF.

^aFor specimens that are anticipated to move out-of-plane in one direction, such as a bulge test, the test piece should be biased to be at the far side of the DOF at the beginning of the test, so that it stays within the DOF as it moves during the test. Further discussion of non-planar specimens is outside the scope of the current edition of this guide.

3.1.6.2 Verify Optical System

Verify FOV, focus, and DOF by translating the test piece within the [working volume](#) in which the test piece is expected to move and deform during the test.

3.1.6.3 Lock Adjustable Components

Adjust orientation of polarization filters if using cross-polarized light. Lock focal length (for a zoom lens), focus, and aperture rings if locks are included on the lenses. If locks are not available, consider fixing the moving components of the lens with tape (see [Tip 2.17](#)). Strain relieve any loose or hanging cables.

3.1.6.4 Review Images

Review the image of the pattern using either a live image or an acquired static image. Look carefully for the following defects, which are illustrated in [Fig. 3.2](#):

- Glare (e.g. glare from a glossy pattern, specular reflections, light reflecting from other objects directly into the lens)
- DIC pattern that is too sparse (i.e. fewer than 3 features (either dark or light) per intended subset size/element size), too coarse (i.e. features that are larger than 5 pixels), or too fine (i.e. features that are smaller than 3 pixels; see also [Fig. 2.14](#) for an illustration of aliased features)
- Defects in applied pattern (e.g. scratches, smudges, foreign objects)
- Out-of-focus regions of the image
- Poor contrast

- Non-uniform lighting (either across the FOV, in time, or between two cameras in stereo-DIC)
- Overexposed or underexposed regions
- Dirt or foreign object on lens or camera detector (see Fig. 3.1)
- Vibrations or other camera motion, some of which can be detected by zooming in on a live image and looking for non-random motion (see Caution 2.10, Tip 2.20, Caution 2.11, and Recommendation 2.9)

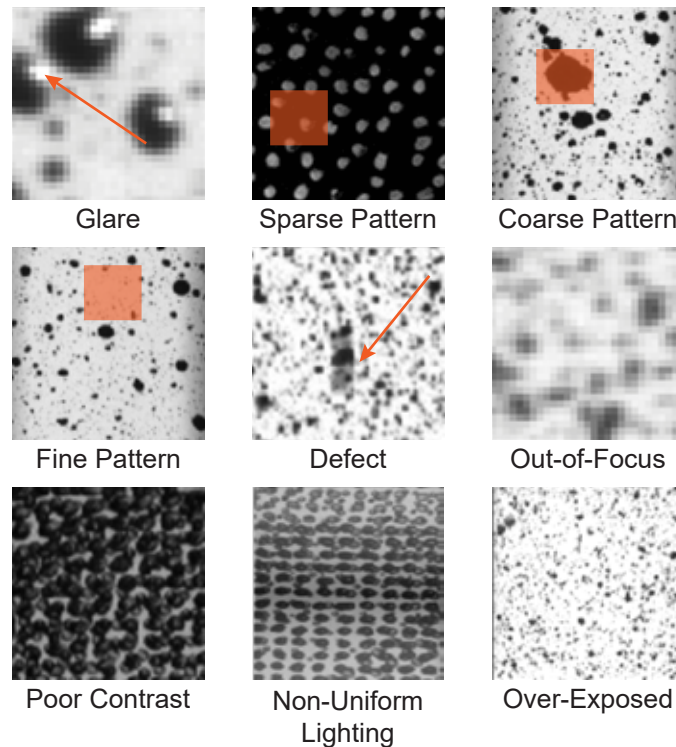


Figure 3.2: Examples of several types of defects/issues with the DIC pattern or the DIC images that should be corrected before testing. The red square represents an exemplar subset/element.

Recommendation 3.3 — Review Images via Correlation Results

For a more thorough check of the DIC system, correlate static images of the test piece, as correlation results can often elucidate issues that are not obvious from visual inspection of the images. For 2D-DIC measurements, check that sequential static images correlate. For stereo-DIC measurements, since at this point in time the stereo system has not yet been calibrated, use a 2D-DIC software to check that sequential images from each camera correlate.

If a certain region of the ROI in an image shows localized values of high correlation residual, look for the cause and remedy it before continuing. Some common sources of poor correlation results include (but are not limited to) the bulleted list above. As a diagnostic tool, the pattern may be translated, and a couple more images may be acquired. If the region of poor correlation moves with the test piece, then the cause is likely something on the test piece (e.g. poor DIC

pattern). If the region is at a fixed pixel location, then the cause is likely dirt or foreign object on the lens or camera detector (Sec. 3.1.2), fixed light scattered reflections into a lens or camera (Sec. 2.2.4, Sec. 2.3.2.5), or shadow on the test piece due to non-uniform lighting (Fig. 3.2).

Look for the presence of heat waves in the displacement fields. If significant heat waves are present, modify the test setup to minimize them. See Sec. 2.2.5 for more information.

3.1.6.5 Accept the DIC System

If the system is found to be acceptable, then proceed to calibration. If there are any unsatisfactory features in the images, including but not limited to the bulleted list in Sec. 3.1.6.4, adjust the DIC system to eliminate it. Then repeat this process iteratively as the system is modified, until satisfactory images are obtained.

Caution 3.5 — Accept the DIC System

Once satisfactory images are obtained, do not modify the system, and take care to not accidentally bump the camera(s), lens(es), or mounting system. Even the addition or removal of lens caps can subtly change the camera position or lens focus.

3.2 Calibration

3.2.1 Purpose of Calibration

The goal of calibration of a 2D-DIC system is to establish the image scale, i.e. the number of pixels in the image that corresponds to a certain physical distance on the test piece, and to correct for lens distortions.¹⁹ The goal of stereo-DIC calibration is to determine both the intrinsic camera parameters (i.e. image scale, focal length, image center, lens distortions, etc.) as well as the extrinsic parameters of the stereo-DIC system (i.e. stereo-angle, distance between cameras, distance from cameras to object, etc.).²⁰ With these calibrated camera parameters, 3D coordinates of measurement points can be reconstructed following triangulation principles, in which 3D points are projected to the respective image coordinates of the two images [69].

Caution 3.6 — Calibration of 2D-DIC System

If strains are the primary QOI, then calibration of a 2D system is often overlooked and considered unnecessary, since strain is a unitless quantity, and an image scale is not required to calculate strain. However, neglecting to correct lens distortions may add error to the measured displacements and result in additional error in the calculated strains [7, Sec. 3.1.2], [70].

¹⁹If the intrinsic and extrinsic parameters of a 2D-DIC (single camera) system are calibrated, then an out-of-plane tilt of the test piece can be determined and corrected [33]. However, this is an advanced topic that is outside the scope of the current edition of this guide.

²⁰Typically, both intrinsic and extrinsic parameters are calibrated simultaneously in a stereo-DIC system. However, some software allows for calibration of the intrinsic parameters of each camera-lens pair, and calibration of the extrinsic parameters of the stereo-system separately. However, this process is outside the scope of the current edition of this guide.

Recommendation 3.4 — Calibration of 2D-DIC System to Correct Lens Distortions

When using 2D-DIC, assess the magnitude of lens distortions for a given optical system, by acquiring and correlating images of a DIC pattern as it is translated in-plane across the FOV. It is important that the translation remain strictly perpendicular to the optical axis; otherwise, false strains due to out-of-plane motion will be convolved with lens distortions. If errors from lens distortions are negligible (i.e. insignificant compared to the overall noise-floor (Sec. 5.4.3)), then 2D-DIC calibration can be omitted. If errors from lens distortions are significant, however, calibration is strongly recommended, to determine the intrinsic camera parameters and correct lens distortions, as shown in Fig. 3.3.

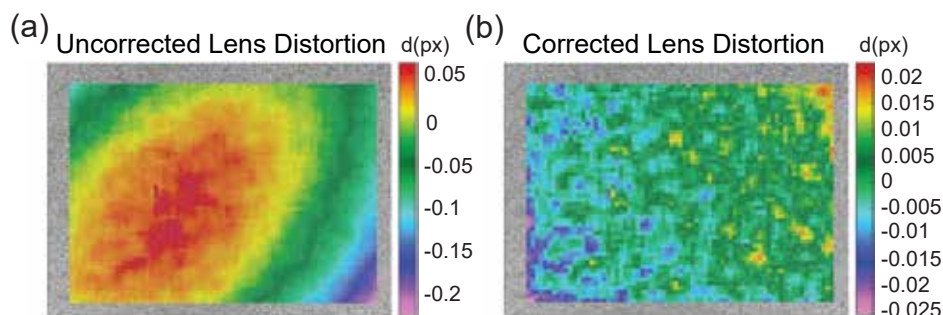


Figure 3.3: The displacement magnitude (after rigid-body-motion has been removed) when lens distortions are not corrected (a) or properly corrected (b).

If full calibration of a 2D-DIC system to correct lens distortions is omitted, a simplified calibration to establish the image scale is still recommended. An approximate image scale can be computed by dividing the image size by the FOV. Alternatively, the image scale can be calculated from images of a [resolution target](#). It is recommended to verify the image scale in both the vertical and horizontal directions.

3.2.2 General Calibration Steps

Caution 3.7 — Pre-Calibration Review

Before beginning the calibration process, be sure that all steps in the pre-calibration review of the DIC system (Sec. 3.1.6) have been completed.

3.2.2.1 Select Calibration Target

Select a [calibration target](#) of an appropriate size. Consult the manual of the DIC software for recommendations regarding the selection of an appropriate calibration target.

Recommendation 3.5 — Selection of Calibration Target

The calibration target should be approximately the same size as the FOV, or slightly smaller.

Tip 3.7 — Alternative Calibration Target Options

If no calibration target is available that is approximately the same size as the FOV, then two other options are possible.

- A first option is to use a smaller target; however, the target should not be smaller than approximately one half of the FOV.^a In this case, ensure that the features on the calibration target are still large enough to be resolved by the imaging system and extracted by the DIC software. Also, additional calibration images will be required in order to have a sufficient number of well-extracted features in the entire [calibration volume](#), which is discussed in [Sec. 3.2.2.4](#).
- A second option is to print the correctly sized target on computer paper using a typical office printer, and glue or tape the paper calibration target to a rigid plate. The accuracy of the image scale is directly related to the accuracy of the feature spacing; therefore, one guideline suggests that the feature spacing should be accurate to within 0.1 pixels [71].

^aTargets smaller than one half of the FOV may produce acceptable calibrations, but extra precautions are required, which are beyond the scope of the current edition of this guide.

Recommendation 3.6 — Metrologically Traceable Calibration Target

Scaling of DIC coordinates and displacements from pixels to physical units (e.g. millimeters) is completely dependent on accurate and precise measurements of the feature spacing on the calibration target. If the physical units are a critical aspect of the measurements to be made, it is recommended to use calibration targets that have been independently measured and are metrologically traceable to the International System of Units (SI).

3.2.2.2 Clear Working Space

Create a clear working space in which the calibration will be performed, so that the selected calibration target can be held, rotated, tilted, and translated as needed (requirements will be different for 2D-DIC and stereo-DIC calibration) at approximately the same SOD as the test piece.

Tip 3.8 — Clear Working Space

There are three strategies for creating a clear working space, which are listed in order of preference:

1. Remove the test piece from the load frame and move the grips back (if necessary). This option is preferred when possible, since any movement of the DIC system risks inadvertent alterations to the system which may invalidate the stereo-DIC calibration.
2. Move the DIC system. If moving the DIC system is necessary, then the following are recommended:
 - Move the system along only a single degree of freedom, such as translating the rig backwards away from the load frame, or rotating the bar on which the two cameras are mounted. Moving the system along two or more degrees of freedom (e.g. rotating and translating, or translating along two directions) is also permissible, but not preferred.

- If possible, calibrate the cameras in the same orientation (i.e. horizontal or vertical) as they will be mounted during the test. If the orientation is changed between the calibration and the test, the optics inside the lens may shift slightly, changing the focus, aperture, zoom, etc.
3. If it is too difficult to sufficiently clear the workspace prior to testing (e.g. because the test piece is impractical to remove or because the cameras are impractical to translate or rotate), calibration can be performed after the test is complete, as long as camera/lens settings such as aperture and focus are not adjusted and, for stereo-DIC calibration, if the two cameras move rigidly as a pair. If this approach is taken, it's recommended to attempt a preliminary calibration prior to inserting the test piece into the load frame to verify that the calibration procedure will be successful.

Caution 3.8 — Relative Motion between Cameras

If the stereo-DIC system is moved, it is imperative that the two stereo cameras are moved only as a rigid pair, and that there is no relative motion between the two cameras. Ensure that the two cameras are locked rigidly together during any adjustment of the position of the stereo rig. Any relative motion between the two cameras — even small changes on the micrometer scale — during calibration, or when repositioning the cameras after calibration, will result in errors in the DIC measurements.

Recommendation 3.7 — Verification of Calibration

Verification of the calibration (see Sec. 3.3.2) is strongly recommended after returning the test piece and/or stereo system to the position to be used for measurements, to ensure that no relative motion occurred between the two cameras during the repositioning of the test piece and/or stereo system.

3.2.2.3 Adjust Lighting

Ensure the contrast is sufficiently large and uniform across the entire calibration target, and that there is no glare for all desired positions and orientations of the target. These conditions should be true for both cameras for stereo-DIC. Adjust lighting and/or exposure time if necessary.

Tip 3.9 — Lighting for Calibration

The lighting and exposure for the actual DIC measurement images of the DIC pattern and for the calibration target are to a first order independent. If possible, the light wavelength or color temperature should remain the same for both calibration and DIC measurement images. However, there are many practical scenarios that require changes in lighting conditions between the calibration and the test. For example:

- Some calibration targets require back-lighting, which necessarily requires different lighting than that used for the images of the test piece during the mechanical test (unless the test piece is transparent or translucent and is also backlit during the test, see Tip 2.27).
- The lighting and/or exposure may need to be adjusted for different positions/orientations of the calibration target.

- Cross-polarized lighting (Tip 2.25) may be used to eliminate glare from the target.
- Calibration images may be acquired quasi-statically with one light source and a longer exposure time, while test images may be acquired at high-speed with a brighter light source and shorter exposure time.
- Luminescent patterns (Tip 2.26) usually require short wavelengths of light (blue to UV) to excite the pattern, but then are imaged at longer wavelengths with a long-pass filter or band-pass filter. Specialized calibration targets that also luminesce at similar wavelengths as the luminescent DIC pattern are required to use the same lighting for both calibration and the test. Alternatively, to use typical calibration targets, the wavelength of the light may need to be changed between the calibration and the test.

Caution 3.9 — Lighting for Calibration

Any changes in lighting should not disturb the cameras or their mounting. Refer to Sec. 2.2.4.2 for recommendations on mounting lights.

Caution 3.10 — Equipment Adjustments after Calibration

While lighting and exposure may be adjusted, aperture and focus may not be adjusted between calibration images of the calibration target and DIC measurement images of the DIC pattern.

3.2.2.4 Acquire Calibration Images

Acquire calibration images such that there are well-extracted features in the entire **calibration volume** (Fig. 3.4). For stereo-DIC, this calibration volume should, at a minimum, encompass the **working volume** in which the test piece is expected to move and/or deform during the test. To be more conservative, the calibration volume should encompass as much of the total **focal volume** of the stereo system (Fig. 3.4) as possible, while ensuring the calibration images remain in focus (see Caution 3.12).

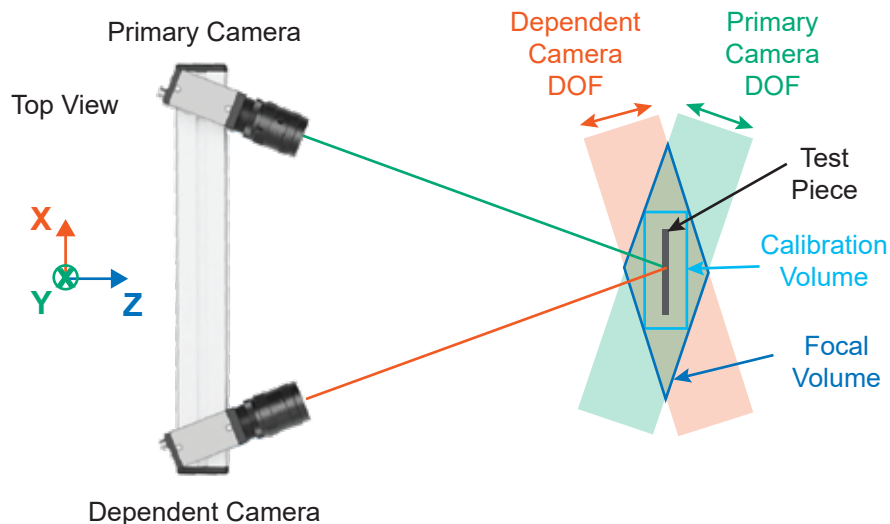


Figure 3.4: Schematic illustration of the stereo-DIC system **calibration volume** and **focal volume** in which calibration images should be acquired.

Recommendation 3.8 — Calibration Target Positions and Orientations

While there are slight variations for different software packages, typically the following positions and orientations of the calibration target are recommended^a for stereo-DIC calibration. See Fig. 3.4 and Fig. 3.5.

1. Rotate about the Y axis.
2. Rotate about the X axis.
3. Rotate about the Z axis.
4. Plunge towards and away from the cameras along the Z axis within the [calibration volume](#).
5. If the calibration target is smaller than the FOV, translate horizontally and vertically along the X and Y axes, so that features from the calibration target fill the entire FOV of each camera.
6. Rotate 90° about the Z axis and repeat the above steps.^b
7. Perform combinations of the above positions and orientations (e.g. rotate about the X and Y axes simultaneously while plunging along the Z axis).

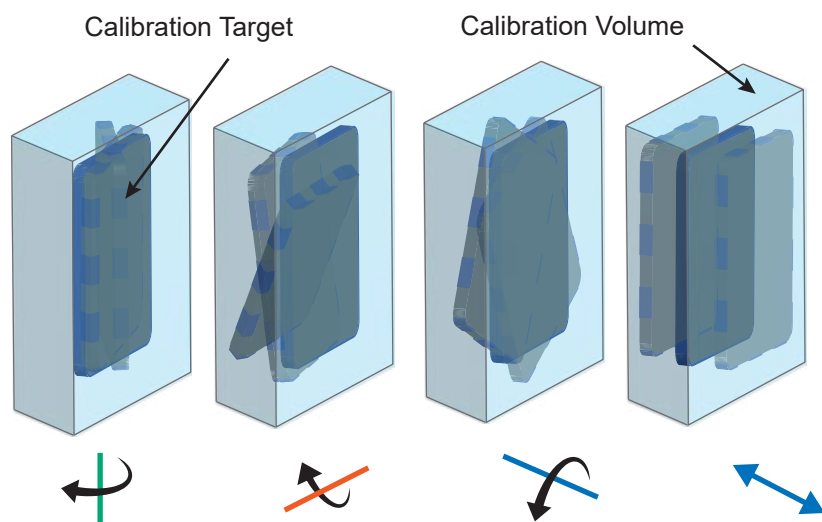


Figure 3.5: Schematic illustrating the recommended positions and orientations of the calibration target, including rotating about the three axes and plunging towards and away from the cameras within the [calibration volume](#).

^aThe Stereo-DIC Challenge is underway as of March 2023. Among other things, the Challenge seeks to explore the effects of the location and orientation of the calibration target, number of calibration images, etc. Recommendations for calibration based on this challenge may be included in a future edition of this guide.

^bManufacturing techniques of calibration targets vary, but some methods may result in a unidirectional stretch of the pattern on the calibration target. That is, features may have a slightly different spacing along the horizontal axis compared to the vertical axis. While using targets that have been independently measured is recommended (see Recommendation 3.6), rotating 90° about the optical axis is an additional precaution to help to compensate for any unidirectional stretch of the pattern on the calibration target.

Tip 3.10 — Number of Calibration Images

The number of calibration images required or recommended depends on the calibration target and DIC software, ranging from as few as 8 images up to 50–100 images. For stereo-DIC, three-dimensional calibration targets (targets that have features on two different planes) may require fewer images than two-dimensional calibration targets (targets that have features on only a single plane). Consult the user manual of the software for software-specific procedures.

Caution 3.11 — Calibration Score

For stereo-DIC, the calibration procedure is a minimization process that seeks to find the best set of intrinsic and extrinsic parameters, given a set of extracted calibration features. Different software packages have different metrics or “scores” for the final parameter values obtained by the minimization. Often, it is possible to have a better score with fewer images, or with a smaller volume filled by features from the calibration target. This scenario is analogous to obtaining a higher coefficient of determination (R^2 value) of a polynomial fit of a set of data points when fewer points are used. However, if a reduced number of data points is used in the minimization process, the final parameter values may not represent the optical system with high fidelity [71].

Recommendation

Take a sufficient number of images to have features that fill the [calibration volume](#), even if the calibration “score” is worse with more images covering a larger volume, compared to the score with fewer images covering a smaller volume.

Caution 3.12 — High-Quality Calibration Images

It is more important to have high-quality images (i.e. in focus, good contrast, no glare, filling the entire [calibration volume](#), etc.) than to have a large number of images. Take care to keep the calibration target within the [focal volume](#), so that the calibration target remains in focus, and ensure there is good contrast and no glare on the calibration images.

Recommendation

Some software packages show a live evaluation of the quality of the extraction of calibration target features and will only acquire an image if the features are extracted well. Others may show a live evaluation, but still allow poor quality images or images with poorly extracted features to be acquired. Other software packages extract features only after all calibration images have been acquired with no live evaluation during image acquisition. If using software that follows the second or third methodologies, a surplus of images can be acquired, allowing for some images and/or features to be excluded due to poor quality. Be careful, though, not to exclude all images from a certain region of the [calibration volume](#).

Recommendation 3.9 — Holder for Calibration Target

Ideally, a rigid calibration target holder is recommended to ensure that the calibration target is stationary when images are acquired. The rigid holder can be mounted on translation and rotation stages or on an adjustable and lockable ball-in-socket joint, to allow displacement and rotation of the target between images.

In cases where using a rigid calibration holder is not practical, holding calibration targets by hand is often also acceptable. If the calibration target is held by hand, hands should be braced against something rigid, and the exposure time should be limited to approximately 25 ms or less, to reduce motion blur. Holding calibration targets by hand is not recommended for large image scales (e.g. FOVs smaller than approximately 50 mm) since even small motions of the target can result in blurry images (Tip 2.10).

3.2.2.5 Calibrate System

Select an appropriate camera or lens-distortion model,²¹ and calibrate the system with the DIC software of choice. Refer to the manual of the software for details on the calibration process.

3.2.2.6 Review Calibration Results

Review the calibration results.

Tip 3.11 — Review of Calibration Results

This review is dependent on the software utilized; consult the user manual for specific suggestions for the DIC software. Some possible aspects of the calibration results to review (if the software provides access to these aspects) include:

- Check the images or features that were rejected and see if there was an obvious reason for rejection. This is particularly instructive for new users and/or experienced users working with new hardware setups. It can improve the ability of a practitioner to produce better quality calibration images in the future by learning what not to do (i.e. the user can see the effects of poor lighting or reflections, poor finger or holder placement that blocks key features of the target, defocused images, etc.).
- Verify that the remaining accepted images still fill the [calibration volume](#). (That is, make sure the rejected images were not all from the same region of the volume or from the same angle of the calibration target.)
- Verify that the features extracted from the accepted images are correct. (For example, sometimes the software will extract a feature that is actually dirt or glare on the calibration target.)
- Compare the calibration score from individual images to the score of the final calibration. Also compare the calibration score for a given image from each camera if using stereo-DIC. Consider removing images manually whose individual score is significantly higher than the

²¹Selection of the camera and lens-distortion model is an advanced topic and is both hardware- and software-specific; therefore, no further information is given in the current edition of this guide. Consult the DIC vendor for more information on selection of the appropriate settings for the software and hardware.

overall score, or significantly different between the two cameras. Alternatively, consider removing individual extracted features so that the individual score of the image is on par with the overall score.

- If possible, save a copy of the individual image calibration scores, in addition to the overall score and calibration results. This information can be useful in diagnosing problems later in the analysis, or problems with one camera and lens versus another.
- Some DIC software packages will alert the user to possible synchronization errors after the calibration procedure is complete. Synchronization errors typically only occur if the user is using a hand-held calibration target whose motion is not completely stopped when images are acquired, or if vibrations are causing significant camera motion when images are acquired. As a diagnostic tool, if a synchronization error or camera vibrations are suspected, one can try to calibrate the intrinsic parameters for each camera individually. If each camera can be calibrated individually with an acceptable calibration score, but the extrinsic parameters of the stereo-system cannot be calibrated, or if the calibration score of the stereo system is unacceptable compared to the scores of the individual camera calibrations, then a synchronization error, or camera vibrations (Sec. 2.2.2.1), are likely.

Tip 3.12 — User-Defined Inputs for Calibration

The amount of control the user has, and the number of user-defined inputs in the calibration procedure, varies with different DIC software packages. For example, some software allows the user to select the image intensity threshold for extracting features from the calibration target, or to define the lens distortion model that is used; other software is a black box (i.e. closed system) with calibration images as inputs, and a calibrated camera model and calibration score as outputs. If the DIC software has any user-defined settings, explore the effects of these settings on the calibration results.

3.2.2.7 Review Calibration Parameters

Compare the values of the calibration parameters to their corresponding physical values [21].²²

Recommendation 3.10 — Review of Calibration Parameters

Typical parameters to check include (Fig. 3.6):

- **Image center:** For most camera detector and fixed-focal length lens combinations, the intersection of the optical axis with the detector should be near the center of the detector array (e.g. if using a 5 Mpx camera that is 2448×2048 px², the calibrated image center should be close to $[C_x, C_y] = [1224, 1024]$). This result should be true for both cameras of the stereo-DIC pair, if the same type of camera and lens are used. Small variations from the detector center are to be expected, but non-physical values (e.g. negative values) or extreme values (e.g. near the detector edge) should be investigated and corrected when possible. When using a zoom lens, however, it is common for the optical axis to be far from the image center, due to the complexity of the optics inside of a zoom lens.

²²Individual parameters can be completely wrong vis-à-vis their corresponding physical values, yet together, the calibration parameters give an accurate triangulation, and accurate displacement results. Therefore, nonphysical parameters are not necessarily problematic [71]. However, this scenario typically only arises in complicated DIC measurement setups, and thus is outside of the scope of the current edition of this guide, which covers only typical laboratory conditions.

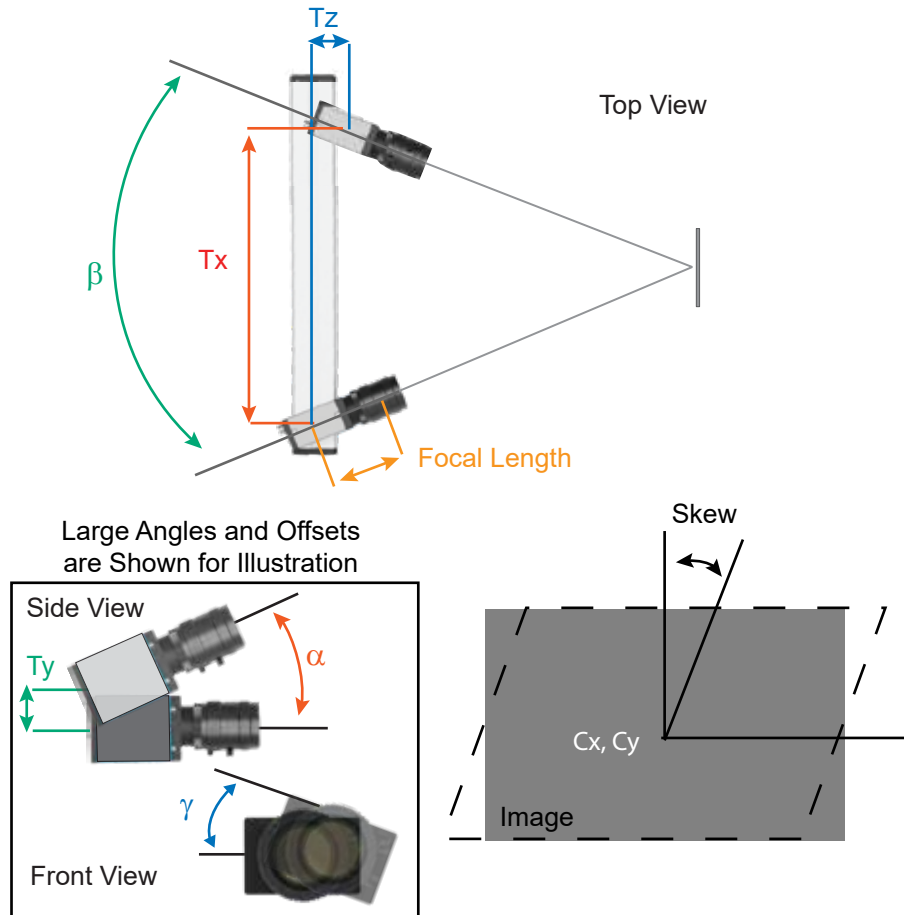


Figure 3.6: Schematic illustrating several typical calibration parameters, including intrinsic parameters such as the image center (C_x and C_y), lens focal length, and detector skew, and the extrinsic parameters of three rotations and translations that describe the relative position of the two cameras (α , β , γ , T_x , T_y , and T_z).

- **Lens focal length:** The calibrated focal length of the lens, in physical units, can be compared to the reported focal length of the physical lens. The two values may not be exactly equal, but they should be close.^a If the calibrated focal length of the lens is reported in pixels, it can be converted to physical units by multiplying by the camera detector pixel size in physical units.
- **Skew:** Skew represents a deviation from the right angle (90°) between the two axes of the camera detector. For modern detector manufacturing methods, the skew should be negligible. However, due to the covariance of the camera model parameters, especially for complex imaging setups, the skew parameter may be non-zero.
- **Angles:** The reported stereo-angle should be approximately the same as the physical angle between the two cameras (if using stereo-DIC). The other two angles should be approximately zero if the stereo-plane is perpendicular to the test piece, as described in Sec. 2.2.2 for typical orientation of the stereo-DIC system.

- **Distance between two cameras:** The reported straight line distance (i.e. the baseline distance) between the two cameras should be approximately the same as the distance between the two camera detectors (if using stereo-DIC).

^aNote that the calibrated focal length is usually the distance between the pinhole and the image plane, and thus it is not the same as the physical focal length. Additionally, the physical lens focal length reported by the lens manufacturer may be only a nominal value of the actual lens focal length (e.g. a lens manufacturer may call a certain lens a 50 mm lens, when in reality the focal length is 47.5 mm).

Tip 3.13 — Review of Calibration Parameters

Because the physical values are often hard to measure precisely, this review is a very broad assessment, to make sure the calibration parameters are in the correct range of values, rather than a very precise comparison between the calibration parameters and corresponding physical values. Additionally, tracking of these values for systems that are not changed/adjusted between calibrations can lead to user experience, and tighter ranges on what is considered acceptable.

Caution 3.13 — Calibration Score

The calibration score reported by the software can in some cases be misleading. Refer to Caution 3.11 in Sec. 3.2.2.4 for more details.

3.3 Post-Calibration Routine

The post-calibration routine described in this section has three purposes: to verify the calibration of the optical system, to acquire images for the noise-floor analysis (Sec. 5.4.3), and to perform a final review of the DIC system before conducting the mechanical test with DIC measurements.

3.3.1 Images for Calibration Verification and Noise-Floor Analysis

3.3.1.1 Reset System

Replace the test piece if it was removed to take calibration images. If the stereo-DIC system was moved to take calibration images, replace it to its normal position to view the test piece, and be sure to lock any moving components on the mounting system.

3.3.1.2 Adjust Lighting

If the lighting and/or exposure were adjusted for the calibration images, readjust lighting and/or exposure for the DIC pattern on the test piece.

3.3.1.3 Acquire Static Images

Acquire static images of the test piece.

Recommendation 3.11 — Static Images for Measurement Uncertainty Quantification

Ideally, the static images should be acquired at the same image acquisition rate and exposure time as that used for the test, and for the same duration of the test, in order to capture representative

sources of noise or error. For example, high-frequency vibrations may not be represented if images are acquired at a slow image acquisition rate. Alternatively, low-frequency errors, such as heat waves or camera drift, may not be represented if images are acquired over a short duration. Also, for some cameras, camera noise is a function of frame rate.

Acquiring static images at the same image acquisition rate and for the same duration as the test, however, doubles the amount of data that must be stored and processed, which can be non-trivial for many DIC measurements, in which gigabytes of images and processed data are accumulated. Therefore, the number and timing of static images is often a compromise between representing the noise sources present in the DIC measurement, and practical considerations of data size.

One possible strategy to minimize the number of images required for the noise-floor, while still representing all noise sources, is to acquire a burst of images at the desired image acquisition rate at the beginning and the end of the test duration time. In this way, both high-frequency and low-frequency error sources are captured in the static images.

3.3.1.4 Review Images

Perform a final review of the images from Sec. 3.3.1.3 as described in Sec. 3.1.6.4 and address any issues that are found.

Caution 3.14 — Recalibration of the System

If adjustments are made to the camera(s) or lens(es), the calibration process will have to be repeated. However, making adjustments to achieve the best-possible images is usually preferable to producing poor quality or even useless DIC measurements just to avoid recalibrating the system.

3.3.1.5 Acquire Rigid-Body-Motion Images

Rigidly translate and rotate the test piece and acquire additional images.

Tip 3.14 — Rigid-Body-Motion Images

The applied translations/rotations can either be applied by hand where the exact applied displacements are unknown, or with translation/rotation stages with micrometers, such that the applied displacements are known within the uncertainty of the stage.

Recommendation 3.12 — Rigid-Body-Motion Images for 2D-DIC

For 2D-DIC, capture both in-plane translations and out-of-plane translations and rotations. The two groups of images — in-plane translations versus out-of-plane motions — should be kept separate, so that the effects of in-plane versus out-of-plane motion can be analyzed independently. The in-plane images will be used to verify adequate correction of lens distortions (Sec. 3.3.2.1) and to calculate the noise-floor of QOIs. Because the visibility of uncorrected lens distortions depends on the magnitude of the translations, the test piece should be translated at least 10% of the FOV. The out-of-plane motions will be used to estimate the bias errors caused by out-of-plane motion during the mechanical test (Sec. 5.4.4).

Recommendation 3.13 — Rigid-Body-Motion Images for Stereo-DIC

At a minimum, translate the test piece within the [working volume](#) in which it is expected to move and/or deform during the test. For a more thorough review of the calibration, acquire additional images that cover the entire FOV and DOF of each camera. For additional recommendations for rigid-body translation studies, see also standards such as VDI-2626 standard [72] and ASD-STAN EN 4861 [73].

3.3.2 Verification of Calibration

Correlate the static and rigid translation images, and verify the calibration results using the methods described in this section. If the calibration is determined to be unsatisfactory based on any of the following metrics, improve the calibration before continuing. Otherwise, accept the calibration, and proceed to a post-calibration review of the system (Sec. 3.3.3).

Tip 3.15 — User-Defined Parameters for Calibration Verification

The final DIC user-defined parameters (Sec. 5.2)—such as subset size, step size, virtual strain gauge size for local DIC, or element size and element shape function for global DIC—will not be selected until after the actual mechanical test has been conducted and a noise-floor analysis has been completed (Sec. 5.4). Therefore, at this point, use default settings provided by the software, or expert judgment and past experience, to select reasonable parameters for the correlation of the static and translation images for purposes of verifying the calibration and performing a final review of the DIC system.

Tip 3.16 — Improving the Calibration

Improvement may require adjusting software-specific parameters in the calibration procedure, taking additional calibration images, or adjusting the optical system hardware (camera(s) or lens(es)).

Caution 3.15 — Adjusting Optical System Hardware during Calibration

If any adjustments are made to the optical system hardware (camera(s) or lens(es)), then the previously acquired calibration images must be discarded, an entirely new set of calibration images must be acquired, and both the calibration process and the post-calibration routine must be redone.

3.3.2.1 Intrinsic Parameters

The primary purpose for verifying intrinsic parameters is to verify that lens distortions are properly corrected. Correlate the translation images acquired in Sec. 3.3.1 and remove rigid-body-motion. Lens distortions often manifest as an elliptical shape in the displacement or strain contour plots, as shown in Fig. 3.3, though the actual shape depends on the nature or type of lens distortions.

Recommendation 3.14 — Evaluation of Lens Distortions

Evaluation of lens distortions is subjective. Compare the magnitude of the errors from lens distortions to the total noise-floor of the displacements and strains (see Sec. 5.4.3). If errors from

lens distortions are significant compared to the noise-floor, adjust the type and/or magnitude of the distortion correction in the calibration procedure. If distortions cannot be removed through the correction process in the calibration procedure, then either a custom correction procedure will need to be implemented, the choice of optical system (lens and camera) should be revisited, and/or the image ROI will have to be limited in size and motion to only the portion of the FOV with an acceptable level of distortion.

Caution 3.16 — Evaluating Lens Distortions for 2D-DIC

For 2D-DIC, it is important that the translation images are strictly perpendicular to the optical axis. Otherwise, false strains due to out-of-plane motion will be convolved with lens distortions, and the translation images cannot be used to verify lens distortions alone.

3.3.2.2 Extrinsic Parameters

Extrinsic parameters are applicable only for stereo-DIC, and are not applicable for 2D-DIC. The primary metric for verifying the extrinsic parameters is the [epipolar error](#). Depending on the DIC software, the epipolar error may be called by a different name, such as projection error, three-dimensional residuum, intersection error, or correlation deviation. There are slight differences in how these metrics are calculated in different software packages, but the basic principle is universal. To verify the extrinsic parameters, correlate the static images (and translation images if available) acquired in Sec. 3.3.1 and verify that the epipolar error is acceptable based on the DIC software documentation.^{23,24}

Tip 3.17 — Acceptable Level of Epipolar Error

There is not a single, fixed threshold for the epipolar error that separates “good” from “bad” calibrations. Rather, there is a direct relationship between epipolar errors and errors in DIC measurements, with larger epipolar errors resulting in larger errors in DIC measurements. As a rule of thumb, though, the epipolar error should typically be on the order of the calibration score; if the epipolar error is significantly larger than the calibration score, the cause of the large error should be investigated and rectified.

Tip 3.18 — Spatially-Resolved Epipolar Error

Some DIC software packages only report the average epipolar error over the image ROI, while others report the epipolar error for each subset. If the DIC software reports spatially-resolved epipolar error, then the epipolar error can additionally be used to evaluate the DIC pattern and lighting, similar to using the correlation residual in the first preliminary correlation as described in Recommendation 3.3.

²³See footnote [b](#) on page [23](#) for a note concerning correction of extrinsic parameters of a camera calibration.

²⁴If images of the calibration target were of a different image size than the static and rigid translation images of a DIC pattern, then the calibration images must be adjusted for cropping; failure to do so will result in an inflated value of the epipolar error. However, discussion of image cropping is beyond the scope of the current edition of this guide.

Tip 3.19 — Additional Influences of Epipolar Error

Uncorrected lens distortions and poor DIC patterns, in addition to the extrinsic parameters, will also influence the epipolar error. However, if the lens distortions are properly corrected and intrinsic calibration parameters are verified as described in Sec. 3.3.2.1, and the DIC pattern is high quality following the guidelines in Sec. 2.3 and free of defects mentioned in Sec. 3.1.6.4, then the epipolar error is primarily related to the extrinsic calibration parameters.

3.3.2.3 Absolute Distances

Verify that the DIC measurements are reporting accurate values for absolute distances.

Recommendation 3.15 — Verification of Absolute Distances

Some suggested metrics include, but are not limited to:

- **Fiducial Marks:** If fiducial marks of a known distance were placed on the test piece as recommended in Sec. 3.1.5, compare the distance between the fiducial marks calculated by the DIC software in the correlation of the static images or the translation images to the known distance. This is only an approximate assessment, since the calculated distance from the triangulation is known only to within ± 1 pixel at best, due to manual selection of the center of the fiducial marks, and there is some uncertainty in the known distance as well. However, it is a good sanity check to ensure that the correct target size was entered into (or identified by) the DIC calibration software.
- **Applied Displacements:** If the applied displacements are known for the rigid translation images, compare the DIC results to the applied displacements. This is typically only an approximate assessment, as precision on DIC results is often higher than precision of the “known” displacements if a typical micrometer translation stage is used.

3.3.3 Post-Calibration Review of System

Perform a final review of the DIC system. If any aspect of the DIC system is determined to be unsatisfactory based on the final review of the system, adjust the system and review it again. See Caution 3.15.

3.3.3.1 Noise-Floor

Perform an abbreviated noise-floor analysis and verify that the noise-floor values of the QOIs are acceptable.

Recommendation 3.16 — Abbreviated Noise-Floor Analysis

A full noise-floor analysis, as described in Sec. 5.4.3, can be time consuming, and also requires *a priori* knowledge of the test piece deformation, in order to select DIC user-defined parameters (Sec. 5.2), such as subset size, step size, virtual strain gauge size for local DIC, or element size and element shape function for global DIC. Therefore, at this point in time, before the mechanical test has been conducted, an abbreviated noise-floor analysis is recommended.

Compute the spatial standard deviation of the QOIs from the static images acquired previously (Sec. 3.3.1.3) using estimated DIC user-defined parameters based on vendor defaults, past experience, or expert judgment. If the static images were acquired at the desired image acquisition rate of the actual test, also compute the temporal standard deviation. Verify that the standard deviations (i.e. the noise-floor) are acceptable (Sec. 2.1.9).

3.3.3.2 Heat Waves

Look for the presence of heat waves in the displacement contour plots from the static images. If significant heat waves are present, modify the DIC measurement and/or mechanical test setup to minimize them. See Sec. 2.2.5 for more information.

3.3.3.3 Stability

If a significant amount of time passes between calibrating the DIC system and performing the mechanical test with DIC measurements, consider retaking static images and rechecking the camera calibration. Any increase in the epipolar error or noise-floor should be investigated and rectified.

3.3.3.4 Other Verifications

In addition to the guidelines outlined here, individual users or laboratories may have additional in-house procedures that include details specific to the mechanical test setups, equipment, and software that are commonly used in each laboratory. As a matter of good practice, it is recommended that in-house procedures be documented and that criteria be established to determine if a specific calibration and/or noise-floor (Sec. 5.4.3) is acceptable for the intended purpose of the DIC measurement. This will help prevent wasting time and resources to complete DIC measurements during a mechanical test, only to realize after the fact that the images are unsatisfactory.

4 — Execution of the Test with DIC Measurements

Once all details of the DIC measurement setup and mechanical test setup have been finalized, and the cameras have been calibrated, the actual mechanical test can be conducted, with concurrent imaging for DIC measurements. Before conducting the test, review all data acquisition systems, such as:

- The correct file name, location, and storage capacity for DIC images has been set.
- The correct test procedure or macro has been selected.
- Force signals and other measurement signals from the load frame are set to record and are synchronized with DIC images (Tip 3.5).
- Triggering of the load frame and/or DIC images is ready.

Caution 4.1 — Static Reference Image

Ensure at least one image is acquired of the test piece prior to any applied force or displacement.

- Lights are turned on, exposure is correct, and image acquisition rate is correct.

As this guide does not cover the mechanical test itself, no further guidelines are provided here for the actual execution of the test.

5 — Processing of DIC Images

5.1 DIC Software

Once the mechanical test has been performed and DIC images have been acquired, the images are processed using DIC software. There are both commercial (typically closed-source) DIC packages as well as independently developed (often open-source) software. The choice of software depends completely on the user, and the user is directed to the software manual for specific details on how to use the software. A list of DIC software packages is available on the iDICs website at <https://idics.org/resources/>.

As part of the DIC Challenge [74–76], a set of images to verify DIC software has been carefully designed and vetted. These images are available at <https://idics.org/challenge>. Users of closed-source DIC software can use these images to explore the “black box” (closed system) of the DIC software. Additionally, users and developers of independently developed DIC codes are strongly encouraged to verify their codes using these images, and to document the results of the verification.

5.2 User-Defined Correlation Parameters

There are many user-defined parameters in the DIC analysis procedure that must be selected. Here, some general comments are made, but detailed training — either on-the-job training by more experienced DIC practitioners, training by a vendor when a new DIC system is purchased, or classes taught by subject-matter experts²⁵ — is strongly recommended. Additionally, the user should refer to the manual for the DIC software of choice for more details that are specific to the software.

5.2.1 Reference Image

DIC tracks the motion, in a Lagrangian sense, of a set of data points defined on a reference image. There are three approaches for selecting a reference image:

1. **Single reference image:** The simplest and preferred approach for selecting a reference image is to use an image at the beginning of the series, of an undeformed test piece, prior to the application of any displacement or force. Motion or displacement of the data points is then tracked over time by correlation of subsequent images in the series back to the initial reference image.
2. **Incremental correlation:** In some cases, the DIC pattern may change significantly during the course of the test, such that the DIC pattern of the deformed test piece cannot be correlated back to the initial reference image of the undeformed test piece. In this situation, incremental correlation may be used, where each image is correlated to the previous image, rather than to the same,

²⁵iDICs offers DIC classes at their annual conference. For more information, see www.idics.org.

initial reference image of the undeformed test piece. Incremental correlation gives incremental displacements between each of the images; total displacements from the initial reference image of the undeformed test piece are computed by summation of the incremental displacements. The drawback to incremental correlation, though, is that errors in the total displacements are also summed, and thus errors typically increase with increasing number of images in the incremental correlation sequence.

3. **Partitioned correlation:** As a compromise between using a single reference image of the undeformed test piece and incremental correlation, the series of images may be partitioned into sub-series, and the images in each sub-series are correlated back to the image at the beginning of that sub-series. For example, let image 1 be the primary reference image of the undeformed test piece. Then, images 2-100 may be correlated back to image 1; images 101-200 may be correlated back to image 100; images 201-300 may be correlated back to image 200; etc. The total displacement of image 300, relative to image 1 of the undeformed test piece, is then given by the displacement of image 300 relative to image 200 plus the displacement of image 200 relative to image 100 plus the displacement of image 100 relative to image 1. By updating the reference image periodically instead of using the previous image, accumulation of errors is reduced.

Caution 5.1 — Static Reference Image

It is critical that the reference was acquired prior to any applied displacement or force. Otherwise, all DIC measurements correlated with respect to the reference image will be biased by an unknown amount.

Tip 5.1 — Noise-Free Reference Image

One can acquire a series of images of the stationary, undeformed test piece and average these images together. This averaged reference image can then be used as an approximately noise-free reference image. 100 images is concluded to be satisfactory, but a significant reduction in noise can be seen at 30–50 images [66, 77].

Tip 5.2 — Reference Image for Stereo-DIC

In stereo-DIC, typically a single image from one of the cameras is selected as the primary reference image. User-defined correlation parameters such as the ROI of the image and the subset size are defined on this single image. Next, the correlation can proceed one of two ways depending on the software, as illustrated in Fig. 5.1.

In Option 1, the matching criterion, along with the parameters of the stereo-system calibration, are used to match subsets from the primary reference image in the first camera to the corresponding dependent reference image from the second camera. Depending on the software, the subsets may be redrawn to be square in the dependent reference image. Then, succeeding images in the first camera series are compared back to the primary reference image of the first camera; in parallel, succeeding images of the second camera series are compared back to the dependent reference image of the second camera. In Option 2, all images from both camera series are compared back to the primary reference image of the first camera.

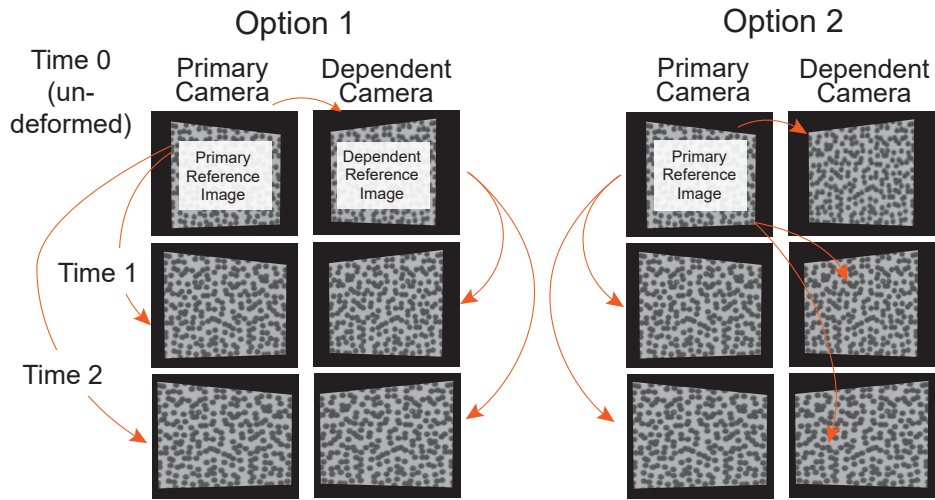


Figure 5.1: Schematic illustrating two different approaches to reference images and the correlation process for stereo-DIC with example showing left camera as primary and right camera as dependent.

There are advantages and disadvantages of both options, and both options are used in commercial DIC software. An advantage of Option 1 is that there is no perspective distortion involved when deformed images from each camera are compared to their respective reference images (either the independent reference image for the first camera or the dependent reference image for the second camera). The improved similarity between the reference and deformed images in this case can make the correlation easier and more accurate. An advantage of Option 2^a is that it requires only two correlation processes per time step while the first option requires three correlation processes. Additionally, when the subsets are redrawn in the first option to be square in the dependent reference image, the subsets may shift slightly to be centered at pixel locations and may overhang the ROI of the image, both of which may add small bias errors. Overall, though, the differences between the two options are considered to be minor for most applications, and either option is generally acceptable.

^aFor some software packages, the Option 2 is preferred when the geometry of the test piece is round (e.g. cylinders, spheres) or complicated. However, non-planar test pieces are outside the scope of the current edition of this guide.

5.2.2 Pre-Filtering of Images

Subset interpolants often perform better with smooth spatial gradients in image intensity. For this reason, applying a digital low-pass filter (e.g. a Gaussian filter) to the images prior to correlating them, to reduce high-frequency content by reducing random image noise and softening the edges of a particularly sharp DIC pattern, can be beneficial in some cases [78, 79].

Tip 5.3 — Low-Pass Image Pre-Filters

Low-pass filters are also known to mitigate the effects of aliased DIC pattern features (i.e. smaller than 3 pixels) in many cases (Fig. 2.14). Note, though, that physical anti-aliasing filters (see Tip 2.15) and digital low-pass filters are fundamentally different. The first prevents aliasing in the analog realm, so that no aliased information is encoded in the images. The second attempts to mitigate the effects of aliasing in the digital realm, after aliased information has been encoded in the images. See [65] for more details.

Caution 5.2 — Low-Pass Image Pre-Filters

Low-pass filtering can also have detrimental effects in some cases (e.g. low-pass filtering can bias the results) [78, 79]. Therefore, DIC practitioners should be judicious in the use of digital filters.^a

^aFurther discussion of pre-filtering of images is outside the scope of the current edition of this guide.

5.2.3 Matching Criterion

As mentioned in Sec. 1.1, conservation of intensity is the core principle of DIC. However, because Eqn. 1.1 cannot be satisfied exactly in practical applications (due to, for instance, image noise), a **matching criterion** is formulated. The basic matching criterion is the sum of square differences (SSD):

$$\chi_{\text{SSD}}^2 = \iint_{\Omega} [G(\mathbf{x} + \mathbf{u}(\mathbf{x})) - F(\mathbf{x})]^2 d\mathbf{x} \quad (5.1)$$

where $F(\mathbf{x})$ is the intensity of the undeformed image at location \mathbf{x} , $G(\mathbf{x} + \mathbf{u}(\mathbf{x}))$ is the intensity of the deformed image at location $\mathbf{x} + \mathbf{u}(\mathbf{x})$, $\mathbf{u}(\mathbf{x})$ is the displacement field describing the motion between the undeformed and deformed images, and Ω is the subset. An optimization algorithm is employed to find the displacement field $\mathbf{u}(\mathbf{x})$ that minimizes the matching criterion and thus minimizes differences in intensity between the two subsets.

In practical situations, the illumination of the test piece may fluctuate over time, leading to brightness and contrast changes in the image intensities. To counter these effects, more robust matching criteria have been developed, such as the zero-mean normalized sum of square differences (ZNSSD):

$$\chi_{\text{ZNSSD}}^2 = \iint_{\Omega} [c(\mathbf{x})G(\mathbf{x} + \mathbf{u}(\mathbf{x})) + b(\mathbf{x}) - F(\mathbf{x})]^2 d\mathbf{x} \quad (5.2)$$

where $c(\mathbf{x})$ accounts for spatially-varying change in the image contrast or lighting scale, and $b(\mathbf{x})$ accounts for spatially-varying change in the image brightness or lighting offset. Optimal values for $c(\mathbf{x})$ and $b(\mathbf{x})$ can be solved for in terms of the local mean of the intensity in each subset. More details on the ZNSSD and other matching criteria are found in [7, Sec. 5.4 and Table 5.1] and [39].

Local-Global Flag 5.1 — Matching Criterion

In local DIC, the matching criterion is computed for each subset individually. For global DIC, it is computed over the entire ROI of the image. See Appendix D.4.1.

Tip 5.4 — SSD vs. ZNSSD

Correlation criteria that compensate for changes in lighting, such as the ZNSSD, are typically more robust in practical experimental situations than non-normalized criteria, such as the SSD. Moreover, the ZNSSD also performs as well as the SSD in cases of steady and uniform light. One disadvantage of the ZNSSD, however, is that it is computationally more expensive, and thus may not be suitable for real-time applications.

Tip 5.5 — Fourier Domain

The cross-correlation function between two intensity fields of images can also be calculated in Fourier domain enabling the detection of subset displacements through operations involving the discrete Fourier transform (DFT) of both subsets [80–82]. Together with the implementation of subpixel displacement detection, this method may be more robust when faced with lower quality images in the absence of controlled experimental conditions [81, 83] and provide improvement in speed when large displacements are analyzed [84]. The advantage in speed is particularly significant when dealing with larger image ROIs [80, 83].

5.2.4 Subset Shape Function

The [subset shape function](#), is used to approximate the displacement field from the undeformed to the deformed image, as prescribed by optical flow through the matching criterion (Sec. 5.2.3, Eqn. 5.1, and Eqn. 5.2). Polynomial shape functions are common, with an affine (linear) and quadratic shape function shown in Eqn. 5.3:

$$\xi_{\text{affine}}(\mathbf{x}, \mathbf{p}) = \begin{bmatrix} x \\ y \end{bmatrix} + \begin{bmatrix} u \\ v \end{bmatrix} + \begin{bmatrix} \frac{\partial u}{\partial x} & \frac{\partial u}{\partial y} \\ \frac{\partial v}{\partial x} & \frac{\partial v}{\partial y} \end{bmatrix} \begin{bmatrix} \Delta x \\ \Delta y \end{bmatrix} \quad (5.3a)$$

$$\xi_{\text{quadratic}}(\mathbf{x}, \mathbf{p}) = \begin{bmatrix} x \\ y \end{bmatrix} + \begin{bmatrix} u \\ v \end{bmatrix} + \begin{bmatrix} \frac{\partial u}{\partial x} & \frac{\partial u}{\partial y} \\ \frac{\partial v}{\partial x} & \frac{\partial v}{\partial y} \end{bmatrix} \begin{bmatrix} \Delta x \\ \Delta y \end{bmatrix} + \begin{bmatrix} \frac{\partial^2 u}{\partial x \partial y} \\ \frac{\partial^2 v}{\partial x \partial y} \end{bmatrix} \Delta x \Delta y + \begin{bmatrix} \frac{\partial^2 u}{\partial x^2} & \frac{\partial^2 u}{\partial y^2} \\ \frac{\partial^2 v}{\partial x^2} & \frac{\partial^2 v}{\partial y^2} \end{bmatrix} \begin{bmatrix} (\Delta x)^2 \\ (\Delta y)^2 \end{bmatrix} \quad (5.3b)$$

where $\xi(\mathbf{x}, \mathbf{p})$ is the subset shape function, \mathbf{p} is a vector collecting the parameters of the subset shape function (e.g. $\mathbf{p} = [u, v, \frac{\partial u}{\partial x}, \frac{\partial u}{\partial y}, \frac{\partial v}{\partial x}, \frac{\partial v}{\partial y}, \frac{\partial^2 u}{\partial x^2}, \frac{\partial^2 u}{\partial y^2}, \frac{\partial^2 v}{\partial x^2}, \frac{\partial^2 v}{\partial y^2}, \frac{\partial^2 u}{\partial x \partial y}, \frac{\partial^2 v}{\partial x \partial y}]$ for a quadratic shape function), $\mathbf{x} = [x, y]$ is the location in the image, $\Delta x = x - x_{sc}$, $\Delta y = y - y_{sc}$, and x_{sc} and y_{sc} are the coordinates of the subset center [85]. The SSD [matching criterion](#) (Sec. 5.2.3, Eqn. 5.1) then becomes:

$$\chi_{\text{SSD}}^2 = \iint_{\Omega} [G(\xi(\mathbf{x}, \mathbf{p})) - F(\mathbf{x})]^2 d\mathbf{x} \quad (5.4)$$

where $(\mathbf{x} + \mathbf{u}(\mathbf{x}))$ is replaced by $\xi(\mathbf{x}, \mathbf{p})$, with similar modifications for other matching criteria. The optimization algorithm seeks to find the parameters in \mathbf{p} by minimizing the matching criterion. More details can be found in [7, Sec. 5.3] and [9, 85].

Some DIC software packages fix the subset shape function that is used, while others allow the user to choose this parameter. When selecting a shape function, there is a trade-off between noise filtering and accuracy [75]. Lower order shape functions cancel more noise, but have less overall accuracy. Higher order shape functions (for example, quadratic and above) are more accurate, but the standard deviation of the solution will be higher. There are two outlooks on this trade-off: One view is to use large subsets

with higher order shape functions. A second view is to use small, closely spaced subsets with low-order shape functions. Some software packages allow the subset shape function to vary spatially across the image, using lower order shape functions in regions of low displacement/strain gradients and higher order shape functions in regions of high gradients. An advanced user may explore the different options and combinations, and evaluate which is best for their application.

Local-Global Flag 5.2 — Element Shape Function

“Element shape function” in global DIC is analogous to “subset shape function” in local DIC. See Appendix D.4.2.

5.2.5 Subset Weighting Function

A [weighting function](#), can be used to weight pixels in the subset when computing the [matching criterion](#) (Sec. 5.2.3). For instance, the SSD matching criterion (Eqn. 5.4) then becomes:

$$\chi_{SSD}^2 = \iint_{\Omega} w(\mathbf{x}) [G(\xi(\mathbf{x}, \mathbf{p})) - F(\mathbf{x})]^2 d\mathbf{x} \quad (5.5)$$

where $w(\mathbf{x})$ is the subset weighting function. Similar modifications apply for other matching criteria.

The two most common subset weighting functions are uniform (each pixel in the subset is weighted equally) and Gaussian (pixels are weighted with a Gaussian distribution centered at the subset center). See [7, Sec. 5.3.1] for more details.

Tip 5.6 — Gaussian Subset Weighting Function

A Gaussian subset weighting function can improve the spatial resolution of the displacement measurements. It can also minimize errors due to pattern-induced bias (PIB) [86, 87]; see Sec. 5.4.4.

5.2.6 Interpolant

To obtain sub-pixel accuracy of DIC measurements, interpolation of image intensity between pixels is required. Therefore, the quality of interpolation has a significant influence on the precision and accuracy of DIC measurements. Most commercial DIC packages have optimized [interpolants](#), and further refinement is an advanced topic. For more information, the reader is directed to [10] and [7, Sec. 5.6.1].

5.2.7 Subset Size

A [subset](#) is the portion of the image that is used to calculate one coordinate value. Subsets are typically square or circular in the reference image. Broadly speaking, a subset should be large enough to contain sufficient information such that one subset can be distinguished from all other subsets in the ROI. The rule of thumb is that the subset should contain a minimum of three DIC pattern features [7, Sec. 10.1.3.1], [59]. If the features are in the optimum 3–5 pixel size range and the feature density is approximately 50%, then subsets of approximately $15 \times 15 \text{ px}^2$ are required (i.e. a minimum of three transitions between dark and light pattern features in all directions is achievable). If the features are larger and/or the feature density is sparse, the [subset size](#) will need to be increased.

Recommendation 5.1 — Subset Size

A larger subset size of 21×21 px² is recommended as a more practical minimum size for typical DIC measurements [9]. This is true particularly if the DIC pattern size and density is variable and not constant over the entire ROI.

Tip 5.7 — Subset Size

Larger subsets typically result in lower displacement noise, but often at the cost of increased spatial smoothing. Higher-order [subset shape functions](#) can be used to compensate for subset smoothing [7, Sec. 5.3], [35, 88], but may lead to increased random errors [89].

Local-Global Flag 5.3 — Subset/Element Size

“Element size” in global DIC is analogous to “subset size” in local DIC. See Appendix D.4.3.

5.2.8 Step Size

The [step size](#) controls the density of points at which DIC data is computed and, to some extent, influences the spatial resolution of the measurements. Typically, a step size of one-third to one-half of the subset size is recommended, so that neighboring subsets partially overlap, though this value can vary widely depending on specific applications [12, 90].

As a general rule, if the overlap is larger than about one-third of the subset size, then neighboring data points are typically considered as no longer independent, and decreasing the step size further does not improve the spatial resolution of the measurements. However, a small step size (in conjunction with a small subset size) may allow data to be obtained close to the edge or other critical feature of the test piece, even if the overlap is large and neighboring subsets are not independent.

Additionally, a small step size may be required to capture the peak *position* of a QOI (without interpolation) if it varies quickly across the ROI; see Example 5.1, specifically Fig. 5.4. (Note, however, that the peak *magnitude* of a spatially-varying QOI may still be damped or underestimated due to the low-pass-filter effect of DIC, if the spatial resolution is not sufficient to capture peaks in regions of high spatial gradients of the QOIs; again, see Example 5.1.) If the QOI varies slowly across the ROI, then a large step size can be used so as to reduce the number of data points, and thus reduce the computation time. (Even if the QOI varies slowly across the ROI, a maximum step size equal to the subset size is suggested, to generate quasi-continuous field data without interpolation.) Additionally, the step size also influences the virtual strain gauge size (Sec. 5.3.3 and Sec. 5.4.6).

Local-Global Flag 5.4 — Step Size

While subsets can overlap in local DIC, for [global DIC](#), [elements](#) are continuous with no overlap (though the support of the [element shape functions](#) may overlap with neighboring elements). Therefore, only the element size is needed to characterize the finite-element [mesh](#), and there is no equivalent term for [step size](#) in [global DIC](#).

However, when a [regularization](#) of [global DIC](#) is used, the cut-off wave it introduces may be interpreted as an equivalent of the [subset size](#), while the [element size](#) (in the case when a regular [mesh](#) of quadrilateral [elements](#) is used) becomes an equivalent of the [step size](#).

5.2.9 Thresholds

DIC software typically allows the user to select different thresholds that are used to determine the quality and confidence of the displacement results for each subset. The thresholds available are software-dependent, but two main thresholds include the value of the matching criterion and the epipolar error. The value of the matching criterion is a measure of how well each subset was matched between the reference image and a deformed image (or between the primary and dependent cameras for stereo-DIC). The epipolar error, which applies only to stereo-DIC, is a measure of how well the correlation results agree with the stereo calibration. Any measurement data points that are above the threshold values are removed from the reported results. Increasing the threshold values allows more data points to be retained, but at the cost of more uncertainty in the results.

Local-Global Flag 5.5 — Thresholds

Depending on the software implementation, individual elements may or may not be discarded based on thresholds such as for the matching criterion and epipolar error. In the case they are not discarded, one can still evaluate the magnitude of the gray level residual or matching criterion as a metric for the quality and confidence of the displacement results. See Appendix D.5.1.

5.2.10 Initial Guess

In many cases, the DIC software can correlate images based solely on the image intensity gradients resulting from the DIC pattern and, for stereo-DIC, the calibration. However, in some circumstances, an initial guess needs to be supplied in order to initialize the correlation process. An initial guess may be required if, for instance, the displacement between consecutive images is large (Example 2.3) or if a regular or repeated pattern is used (Caution 2.22); multiple initial guesses may be required if the test piece has complicated geometry, multiple ROIs, and/or fractures into multiple pieces.

The details of how an initial guess is generated are software-specific. Some methods of providing an initial guess include:

- The user manually identifies one or more approximate locations of material point(s) in each of the images.
- The image size is reduced by binning or resampling; these reduced images are correlated to provide initial guesses for the main correlation of the full-size images.
- The matching criterion is computed as the subset is translated in integer pixel displacements in the deformed image; the location of the best matching criterion value is taken as the initial guess.
- Other, more sophisticated methods of estimating initial guesses also exist [91, 92].

5.3 User-Defined Post-Processing Parameters

5.3.1 Coordinate System

The default coordinate system of the DIC data depends on the software. For 2D-DIC, the X and Y axes are typically aligned with the horizontal and vertical directions of the image, respectively. For stereo-DIC, common options include basing the coordinate system off of the primary camera position/orientation, centering the coordinate system between the two cameras, or defining the coordinate

system based on the location of fiducials in an image of the calibration target. For flat test pieces, a “best-plane fit” is often used, where the Z axis is set to be perpendicular to a plane that is fit to the 3D point cloud describing the undeformed test piece surface; then, the X axis is aligned with the horizontal direction of the image and the Y axis is perpendicular to the Z and X axes. After performing the image correlation, the user may define a DIC coordinate transformation in order to align the coordinate system to physically meaningful axes.

Recommendation 5.2 — Coordinate System

The default coordinate system may or may not correspond to a physically meaningful coordinate system. Additionally, if there are multiple ROIs of a test piece with a complicated geometry, different coordinate systems may be needed for different ROIs. Therefore, it is generally recommended to define an appropriate, physically meaningful coordinate system for every DIC analysis. As described in Recommendation 3.2, placing fiducials on the test piece assists in defining a coordinate system.

5.3.2 Data Filtering

After the initial correlation process, the DIC data may be filtered to reduce noise. There are innumerable methods for filtering the data, including methods in the temporal domain, spatial domain, and/or frequency domain. If any type of filtering is performed, this information should be reported, as specified by the reporting requirements in Sec. 6.2.

Caution 5.3 — Data Filtering

While filtering may reduce noise or variance errors, it could also introduce bias errors. See Sec. 5.4.5 for more information on evaluating the trade-off between noise and bias errors.

5.3.3 Strain Calculations

Strain is one of the most common QOIs for DIC measurements (though it is certainly not the only QOI). There are various strain tensors one can compute, such as engineering, Hencky (also called logarithmic or true), or Green-Lagrange, to name a few options; the appropriate tensor is application dependent.

There are also many different approaches to calculating strain from displacements, depending on the specific DIC software that is used. Brief descriptions of a few common approaches are provided in Appendix C. In each approach, there are different user-defined parameters that can be selected in the software. Refer to the user manual for explicit details about how strains are computed in the DIC software of choice.²⁶

One common and key element of all the approaches to strain computation is the [virtual strain gauge \(VSG\)](#). The VSG, broadly speaking, is the local region of the image that is used for strain calculation at a specific location. It is analogous to — though not directly equal to — the physical area that a foil strain gauge covers. The strain computed in DIC software is the average or weighted average of the strain within the VSG.

The exact size of the VSG depends on the method of strain computation used in the specific software. Even for a given method of strain computation, the exact size of the VSG is not well defined. However,

²⁶Alternatively, displacements can be exported from the DIC software, and strain may be computed by an advanced DIC practitioner, giving a higher degree of control on the strain calculation process.

there are several key variables that affect the VSG size, including step size, subset size, subset shape function, element size, element shape function type, strain window, strain shape function, pre-filtering of the displacements, post-filtering of the strains, and filter window. A useful approximation for the VSG size is given by Eqn. 7.3 in Ch. 7. Because many of these user-defined parameters are specified in terms of pixels, the VSG size can vary across the test-piece ROI, if the image scale varies (e.g. due to the stereo-angle). Spatial resolution of strain measurements is closely related to the VSG size, in addition to other DIC processing parameters. Sec. 5.4.6 provides more information about the effect of the VSG size on the noise and bias of strain measurements.

5.4 Measurement Uncertainty (MU)

5.4.1 Overview

There are two types of errors of DIC measurements, i.e. variance errors and bias errors. Variance errors (also called noise) refer to random errors centered with a mean about the true value of a QOI. Bias refers to an offset of the mean from the true value. The main sources of noise in DIC measurements are camera noise and matching errors during the correlation process. Bias can be introduced by smoothing over peaks in the QOI in regions of high spatial gradients, uncorrected lens distortions, improper camera calibration (e.g. if there was relative motion between cameras in a stereo system after calibration but before the mechanical test), unbalanced intensity gradients in the DIC pattern (so-called pattern-induced bias or PIB [86, 87]), and out-of-plane motion in 2D-DIC measurements, to name a few sources. Establishing the uncertainty of QOIs — considering both noise and bias errors — is critical for intelligent assessment and use of DIC results. Without uncertainty quantification, it is impossible to know if a reported QOI value is significant and relevant, or if it is the result of random noise and/or bias, and thus meaningless. However, bias is often not known, and variance errors computed from static images acquired *prior* to the test may not fully represent the variance errors present *during* the test. Therefore, the metrics available to a DIC practitioner for quantifying uncertainty often produce a *minimum* uncertainty of a QOI, rather than the true uncertainty.

The field of measurement uncertainty for DIC is rapidly evolving at this time. Sec. 5.4.2 summarizes some recently published standards and guides specific to measurement uncertainty for DIC, as well as others that are currently being developed. These standards and guides complement the information provided in Sec. 5.4.3 and Sec. 5.4.4, which describe some methods of quantifying noise and bias errors of DIC measurements. Other definitions exist for specific applications and for different QOIs. The key component, though, is to justify and document (see Ch. 6) some metric and value for the uncertainty of the QOIs.

5.4.2 Standards for Measurement Uncertainty

Recently, Verein Deutscher Ingenieure (VDI) published a standard, VDI-2626, outlining specific procedures for accepting and monitoring DIC systems, for both 2D-DIC and stereo-DIC, and quantifying some aspects of measurement uncertainty [72]. Specifically, VDI-2626 describes a “zero deformation” test, in which a rigid and stiff plate, patterned for DIC, is translated and rotated throughout the [calibration volume](#), similar to the description in Sec. 3.3.1.5. The metrics “zero deformation deviation” and “zero strain deviation” are then computed from either the displacement residual after rigid-body-motion is subtracted or from the strain field, respectively. VDI-2626 also describes procedures for evaluating absolute displacements and strains. Some DIC vendors are now developing equipment to assist DIC practitioners in applying the VDI-2626 procedures.

ASD-STAN, an associated body of the European Committee for Standardization (CEN), developed a recently published CEN standard, EN 4861 [73]. This standard uses a series of known rigid-body-motions to evaluate *in situ* the metrological performance of a DIC system to measure displacement fields, and by extrapolation strain fields. The standard uses a flat coupon with the same applied DIC pattern as the expected test piece, that is moved in two directions for 2D-DIC systems and three directions for stereo-DIC systems. A comparison is made between the measured and applied displacements at each data point in the ROI of the image. The result is a metrological assessment and classification of the field measurements of the system.

Other standardization bodies such as the ASTM International and the International Standards Organization (ISO) are also incorporating the use of DIC into their standards as non-contacting extensometers [93, 94] or in specific applications for particular test methods (e.g. [95, 96]).

Finally, the Measurement Uncertainty working group in iDICs is currently developing a measurement uncertainty guide (MUG) for DIC. The MUG is intended to be a compendium of various methods that can be used independently, or in combination with one another, to assess the measurement uncertainty under specific limitations. Once the MUG is complete and published, Sec. 5.4 here will be updated accordingly. Please contact info@idics.org for more information or to contribute to the MUG.

5.4.3 Variance Errors

The term “variance error” is used interchangeably with “noise”, and the process of quantifying the variance errors is often called a noise-floor analysis. The basic idea of a noise-floor analysis is to correlate images acquired under the same conditions as the test images, but of an undeformed test piece (i.e. either static images or images of rigid-body-motions). With no applied force or deformation on the test piece, all measured QOIs requiring deformation (e.g. strains) are errors. Any of those QOIs measured in the actual mechanical test that are smaller than the QOIs measured from the undeformed images are indistinguishable from the noise.

Tip 5.8 — Typical Displacement Noise-Floor

In general, for a well-controlled environment and an appropriate pattern (as described in Sec. 2.3), the noise-floor for in-plane components of DIC displacements, U and V , should be approximately 0.01 px. For stereo-DIC, the noise-floor for the out-of-plane displacement component, W , is normally about three times higher, or approximately 0.03 px. The noise-floor in engineering units can be computed by scaling these values by the [image scale](#) of the system. Note that the stereo angle and focal length of the lenses also affect these typical noise-floor values (see Tip 2.2).

Recommendation 5.3 — Variance Errors and Camera Noise

A significant source of variance errors in DIC measurements is driven by camera noise. Noise of the camera detector, i.e. fluctuations over time in the gray level intensity of a pixel observing a fixed object, directly contributes to noise in DIC results. Therefore, it can be useful to quantify the camera noise independent of quantifying the noise of the DIC results. This is typically only necessary when evaluating new hardware for its suitability for DIC (see Sec. 2.2.1) or if hardware damage is suspected. In the end, the noise-floor of the QOI is the critical metric, so one may choose to omit characterizing the noise of the camera itself.

5.4.3.1 Iterations of the Noise-Floor Evaluation

Evaluating the noise-floor is an iterative process that is typically performed several times, using sequentially more robust analysis procedures and metrics, during the design and execution of the DIC measurements. A rudimentary evaluation can be completed during the preliminary design of the measurements, to aid in the selection of the camera and lens, lighting, choice in patterning technique, etc. (Ch. 2). A second quick evaluation can be done during the pre-calibration review of the DIC system (Sec. 3.1.6.4), or the final review of the system (Sec. 3.3.3.1), before the mechanical test is performed. A third evaluation of the noise-floor is performed iteratively during the processing of DIC images after the mechanical test is performed, in order to evaluate the effect of user-defined parameters, and the trade-off between noise and bias (see Sec. 5.4.5).

For reporting purposes, the final, most thorough evaluation of the noise-floor must be done using the same conditions as the mechanical test, both in terms of physical conditions (e.g. camera and lens selection, lighting, camera temperature, cooling or mixing fans, test machine powered on) as well as data processing procedures (i.e. pre-filtering of images, subset size, step size, element size, element shape function, VSG size, temporal or spatial filtering of data, etc.). This means that the same user-selected DIC settings that are used for the analysis of the test piece images during motion/deformation must also be used for the analysis of the noise-floor images. Therefore, the final noise-floor analysis is typically completed *after* the mechanical test images are analyzed, but using images that were acquired immediately *before* the mechanical test.

5.4.3.2 Temporal vs. Spatial Variance Errors

Two different metrics can be used to quantify the variance error of QOIs: a spatial standard deviation and a temporal standard deviation. To quantify the spatial variation of the QOI, compute the standard deviation of the QOI for each undeformed image. Then average this spatial standard deviation over time for all the undeformed images. To quantify the temporal variation, compute the standard deviation of the QOI for each data point over time. Then average this temporal standard deviation for each data point over all the data points in the ROI of the image. Note that for an accurate evaluation of the temporal noise, the undeformed images must have been acquired at the same image acquisition rate and exposure time as the test images, as described in Recommendation 3.11.

While seemingly similar at first glance, these two different metrics of error provide different views of the noise-floor, emphasizing either spatially-varying or temporally-varying noise. It is recommended to compute both the spatial and the temporal standard deviation and evaluate if one is significantly larger than the other. However, the spatial and temporal standard deviations are typically similar, and either a single metric or the average of the two metrics can be selected to quantify the noise-floor.

5.4.3.3 Directional Components of the Noise-Floor

Typically, the standard deviation is similar between the two in-plane displacement components, U and V , while, for stereo-DIC, it is higher for the out-of-plane displacement, W (see Tip. 5.8). Similarly, the standard deviation is typically similar for the two in-plane strains, ε_{xx} and ε_{yy} , while it is lower for the shear strain, ε_{xy} . Similar trends affect other QOIs with directional components, such as velocity and strain rate. It is recommended to compute the standard deviation for the QOI in each direction, and select either the maximum or the average between the directions.

5.4.3.4 Quantifying Acceptable Noise-Floor for the Application

Given the standard deviation of the QOI, determine the noise-floor as a function of the standard deviation, using the experience of a subject matter expert. For example, some applications may require that all measurements with magnitudes of variation below three times the standard deviation be considered noise; other applications may loosen the requirement, so that only measurements with magnitudes of variation below one standard deviation be considered noise.

Depending on the application, different amounts of rigor may be employed when quantifying the noise-floor. Some examples include:

Abbreviated noise-floor: This option is performed with static images, typically acquired immediately prior to performing the mechanical test, and it captures primarily the effect of camera detector noise and environmental conditions. It is the quickest evaluation of the noise, but also the least conservative. Typically, true noise levels of QOIs extracted from the DIC measurements during the mechanical test are larger than the noise-floor computed from only static images. That is, an abbreviated noise-floor evaluation provides a lower bound on the true QOI noise or variance errors.

Extended noise-floor: This option is performed with rigid-body-motion images (Sec. 3.3.1.5). In addition to capturing effects of camera detector noise and environmental conditions, it also exercises the lens distortion model (Sec. 3.3.2.1). An extended noise-floor is more time-consuming to perform compared to an abbreviated noise-floor, and in some cases can be technically challenging to ensure pure rigid-body-motions. However, an extended noise-floor provides a more accurate estimation of the noise-floor during the test than the abbreviated noise-floor. One drawback, however, is that it does not account for pattern evolution (and possible degradation) that occurs during the mechanical test.

Deformed pattern noise-floor: This option strives to account for the effect of DIC pattern evolution (and possible degradation), along with changes to the environment or system, that may occur during the mechanical test. Depending on the specific details of the application, there are different ways to evaluate the noise-floor using the deformed DIC pattern. One option is to acquire a series of rigid-body-motion images using the deformed test piece after the mechanical test is finished [64]. However, the subset size and step size for the evaluation of the deformed pattern noise-floor may differ from the original reference image due to the amount of deformation already present. Another option is to quantify the variation in the strain field when the strain is homogeneous and uniform, e.g. for a tensile dog bone with a constant gauge section before any localization occurs; note, however, that it may not be straightforward to separate real strain heterogeneity from noise. The deformed pattern noise-floor is the most representative value of the variance errors for the QOIs extracted from the mechanical test. For strains, experience has shown that it can be orders of magnitude higher than the abbreviated noise-floor or extended noise-floor, for some applications.

In summary, there are many different options a DIC practitioner has when quantifying the noise-floor of the QOIs. There is no single correct procedure, as many choices are application dependent. This section provides many factors one should consider when computing the noise-floor. In the end, though, the critical factor is that a noise-floor should be computed and reported with the DIC measurements, and the process used to compute the noise-floor should also be reported (Ch. 6).

5.4.4 Bias Errors

Bias errors are often difficult to quantify, because the true value of a QOI is typically not known. However, some sources of bias can be evaluated as described below. It is important to note, however, that these evaluations are necessary but not sufficient to elucidate bias errors. Said another way, some bias errors may be detected through these evaluations, and if bias errors are detected, they should be reported; however, even if no bias errors are detected, unknown bias errors may still exist!

One metric of bias error of the QOI is the mean of the QOI from static images. A mean that changes over time could indicate a bias due to camera drift, heating of the camera (i.e. the cameras had not yet reached steady state during the camera warm-up), heat waves, vibrations, etc.

Bias errors due to uncorrected lens distortions can be evaluated from rigid-translation images, if the rigid-body-motion is approximately the same magnitude as the test piece motion and/or deformation during the actual test. Bias due to uncorrected lens distortions will typically manifest as an elliptical shape in the contour plots of strains (and of the displacements if the mean displacement or known applied displacement is subtracted from the field), as shown in Fig. 3.3. This type of bias is typically lower in the center of the FOV and higher near the edges, due to the mostly radial form of lens distortions.

For 2D-DIC, the bias error due to out-of-plane motion should be evaluated (see Example 2.1). Using rigid-body, out-of-plane translation and rotation images, compute the QOI (here, it is assumed that the QOI is in-plane strain) as a function of applied translation/rotation. The strain should be zero for rigid-body-motion, so any strain measured is a combination of bias and noise. Estimate the amount of out-of-plane translation/rotation that may have occurred or did occur during the test and report this. Compare the estimated bias error due to out-of-plane motion to the baseline noise-floor computed from static images (Sec. 5.4.3). If the bias error is larger than the variance errors, consider revising the mechanical test setup to reduce out-of-plane motion.

Bias can also be introduced into the QOI as a result of low-pass filtering, in the spatial domain, caused by the choices of user-defined parameters. This type of bias is described in more detail in Sec. 5.4.5. Finally, other factors, such as the image intensity interpolant, aliasing, noise, and pattern-induced bias (PIB) may cause spatially periodic bias errors that may not be visible in static images of an unloaded and stationary test piece [35, 78, 86, 87].²⁷

5.4.5 Trade-Off Between Noise and Bias

When selecting user-defined parameters (Sec. 5.2 and Sec. 5.3), there is often a trade-off between noise in the measurements and bias due to over-smoothing of the data [74, 75]. Large subset/element sizes, low-order subset/element shape functions, large VSG sizes, pre- or post-filtering of the data, etc. all reduce noise in the measurements, but at the expense of acting as low-pass spatial filters that potentially introduce bias to the measurements. Therefore, when selecting user-defined parameters, it is important to evaluate their effects on both noise and bias errors. Often, the final selection of parameter values is a compromise between noise and bias errors [74, 75, 97]. The choice between noisier but unbiased measurements versus smoother but underestimated measurements is application dependent; expert judgment is often required to determine which set of parameters produces appropriate results for a given test. In Sec. 5.4.6, a methodology and example are presented for evaluating the trade-off between noise and bias of strain, since strain is one of the most common QOIs of DIC measurements. Similar methods, though, can be applied to other QOIs.

²⁷For 2D-DIC, bias errors due to poor interpolants or aliasing may be evaluated by translating a flat test piece out-of-plane towards/away from the camera. This is an advanced topic and is not covered in this edition of the guide. For stereo-DIC, there are currently no standard procedures for detecting or evaluating these types of bias errors.

5.4.6 Virtual Strain Gauge (VSG) Study

Strain is a derived quantity, related to the spatial variation of the displacements. There are many different approaches to calculating strain from displacements, depending on the specific DIC software that is used, as described briefly in Sec. 5.3.3 and Appendix C. One common feature is the requirement that the user select, either directly or indirectly, the size of the VSG. A virtual strain gauge study is the process used to determine an appropriate and acceptable VSG size. It also elucidates if the peak strain magnitude is captured in regions of high spatial strain gradients, and aids in the determination of what the optimum balance is between capturing the peak strain magnitude (i.e. minimizing bias due to over-smoothing) and improving the strain resolution (i.e. minimizing the variance errors). Some DIC packages automate this process, while with others, the user must perform it manually.

Example 5.1 — Virtual Strain Gauge (VSG) Study

In this example, a VSG study is performed using the Stereo-DIC Challenge images from Sample 5: Tensile-Experimental, which can be downloaded freely at <https://idics.org/challenge/>. An overview of the experimental setup is reported in Table 5.1 following the reporting guidelines in Sec. 6.1; more details are found in the overview documents that accompany the images.

Table 5.1: DIC hardware parameters for the VSG study

Camera	FLIR (formerly PointGrey) Grasshopper 2 (Gras-50S5M)
Image Size	5 Mpx, 2448×2048 px ²
Lens	Edmund Optics, DG Series
Focal Length	35 mm
Aperture	f/8 (approximate)
Field-of-View	36.8×30.8 mm ² (approximate)
Image Scale	66.5 px/mm (approximate)
Stereo-Angle	28° (approximate)
Stand-Off Distance	190 mm (approximate)
Image Acquisition Rate	1 Hz
Exposure Time	10 ms (approximate)
Patterning Technique	Base coat of white paint (SEM primer) with black features on top
Pattern Feature Size	7 px (approximate)

The basic steps for a VSG study are as follows:

1. Perform an initial DIC analysis on all images of the mechanical test using predetermined DIC user-defined parameters, based on vendor defaults or past experience and expert judgment.
2. Select the reference image and the image of highest strain gradients determined in the previous step. See Fig. 5.2.

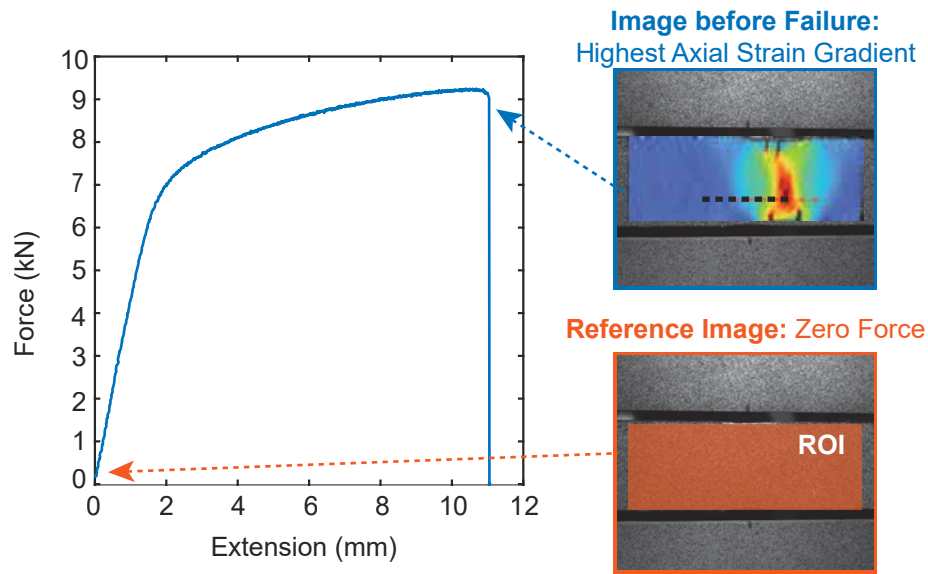


Figure 5.2: Example force-extension curve, where the reference image is selected at the beginning (zero force) and the image before failure is selected as the image with the highest axial true strain gradient.

3. Analyze these images with different DIC settings, varying the VSG size.

Tip 5.9 — Parameters Affecting VSG Size

There are many parameters that affect the VSG size (Eqn. 7.3), as described in Sec. 5.3.3. In this example, a simplified approach is used, where the subset size and step size were selected based on the recommendations in Sec. 5.2.7 and 5.2.8, respectively, and only the strain or filter window was adjusted. The strain tensor was also left as Hencky or true strain for the entirety of this example. However, some applications may require a more complete investigation of more or all of the user-defined parameters that affect the VSG size.

Local-Global Flag 5.6 — VSG Size

For details on the VSG size for global DIC, see Appendix D.5.4.

Recommendation 5.4 — QOI for VSG Study

It is recommended to investigate all three strain components (i.e. the axial strain, transverse strain, and shear strain). However, if only one strain component is the main QOI, an abbreviated VSG study can be done. In this example, the axial strain will be the main focus of the investigation.

4. Extract a line cut through the region of highest strain gradient. Plot the strain along the line for each of the analyses performed in the previous step. See Fig. 5.3.

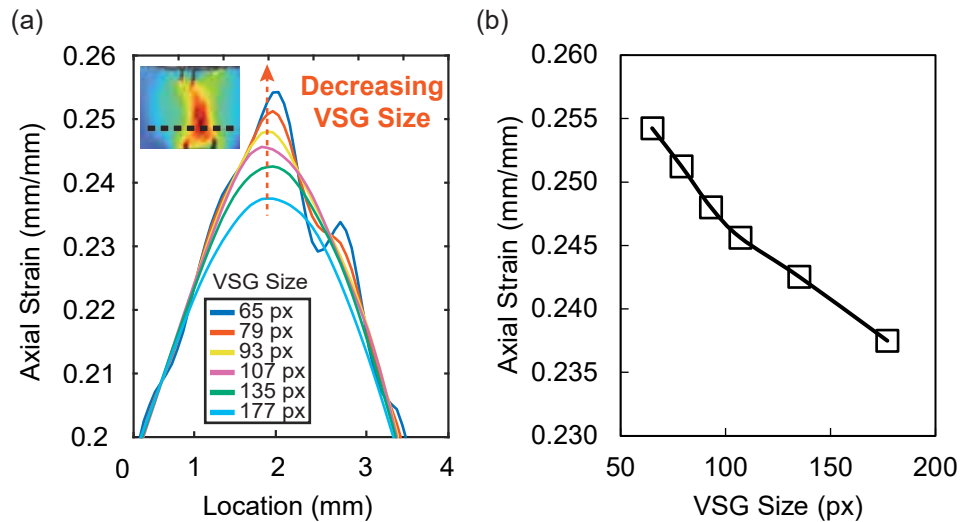


Figure 5.3: (a) Axial true strain as a function of location along a line cut (inset) for the image with the highest strain gradient. (b) Peak true strain magnitude as a function of VSG size. As the VSG size decreases, the peak magnitude increases.

As the VSG size decreases, the maximum strain magnitude along the line cut will typically increase. When the strain magnitude no longer increases as the VSG size decreases, the strain magnitude is said to be converged. Convergence is discussed more in Step 6.

Caution 5.4 — VSG Study Line Cut

Ensure that the line cut does not bridge a crack in the test piece. Computing strain across a crack is not physically meaningful.

Caution 5.5 — Noise on Peak Strain Magnitude

The measured peak magnitude is a combination of the true peak magnitude of the underlying strain field and the measurement noise. Therefore, the measured peak magnitude for small VSG sizes may be artificially inflated due to a higher noise-floor. See Step 5 for more information on the noise-floor. Additionally, the measured location of the peak may be incorrectly displaced from the true location of the peak, if the noise causes spurious peak values.

Caution 5.6 — Peak Strain Magnitude Dependence on Step Size

There is one aspect of the choice of step size and strain calculation method that is often not considered. Typically the strain values are only calculated at the center of each subset, which are spaced at the step size. Unfortunately, this can result in failing to sample the maximum strain magnitude location, if the step locations straddle the actual peak.

To illustrate this concept, Fig. 5.4 shows a hypothetical true strain profile in black. When a large step size is used (11 px in this example), the strain signal is undersampled. Depending on the starting location of the first data point (i.e. the “offset”), the true peak value (in black) could either be missed (Fig. 5.4a, yellow squares curve) or captured (Fig. 5.4b, red circles curve). Capturing the peak in this undersampled situation cannot be guaranteed *a priori* and is a matter of coincidence. When a small step size is used (3 px in this example), the sampling is sufficient, and the peak is captured reliably (Fig. 5.4c, green triangles curve).

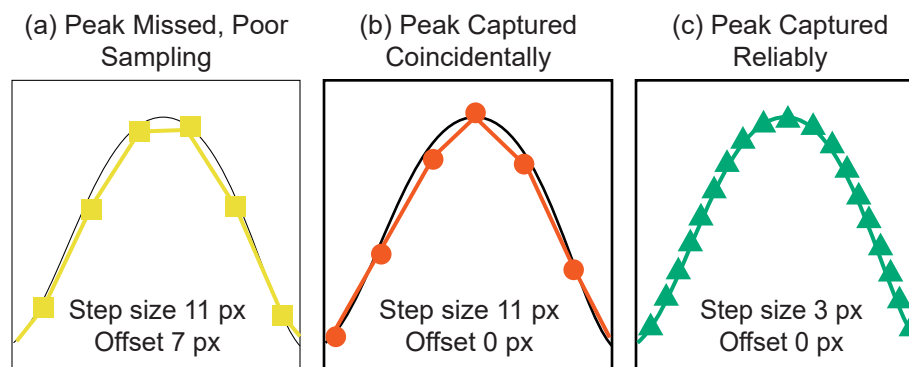


Figure 5.4: Schematic showing the effect of step size on the strain peak magnitude.

Although different selections of subset size, step size, and strain or filter window would change the value of this potential bias in the result, all systems that measure and report strains only at the step size interval risk under-reporting the magnitude of the largest strain in the underlying images, due to under-sampling. This uncertainty scales with the spatial frequency of the underlying strain field and the step size.

5. Compute the noise-floor for each of the analyses with different VSG sizes, using the same parameters used in Step 4.

Capturing images for the noise-floor is described in Sec. 3.3.1. The images could be static images or rigid-body-motion images of the test piece itself or a coupon with the same patterning method. These images are typically captured either immediately before or immediately after the mechanical test, with the same (or as similar as possible) environmental conditions as the mechanical test.

There are many factors to consider when quantifying the noise; see Sec. 5.4.3 for more details. In this example, an abbreviated noise-floor evaluation was performed for demonstration purposes. Ten static images, captured at the beginning of the mechanical test before force

was applied, were analyzed with the different VSG sizes. Then, one standard deviation of all points in the ROI for all 10 static images was computed and taken as the noise-floor. The noise-floor is shown in Fig. 5.5 as a function of the VSG size. As the VSG size decreases, the noise-floor will typically increase.

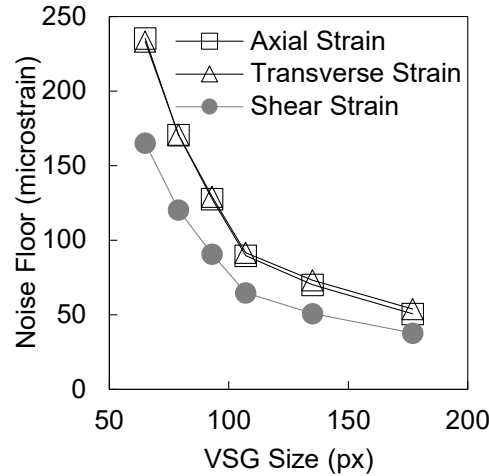


Figure 5.5: The noise-floor of the true strains as a function of VSG size. As the VSG size increases, the noise-floor decreases. Note: here the units of strain are microstrain ($\mu\text{m}/\text{m}$), as the random noise can be quite small compared to the absolute magnitude of the strains.

6. Plot the peak strain magnitude from Step 4 versus the noise-floor from Step 5, as shown in Fig. 5.6, to visualize the trade off between noise and bias errors.

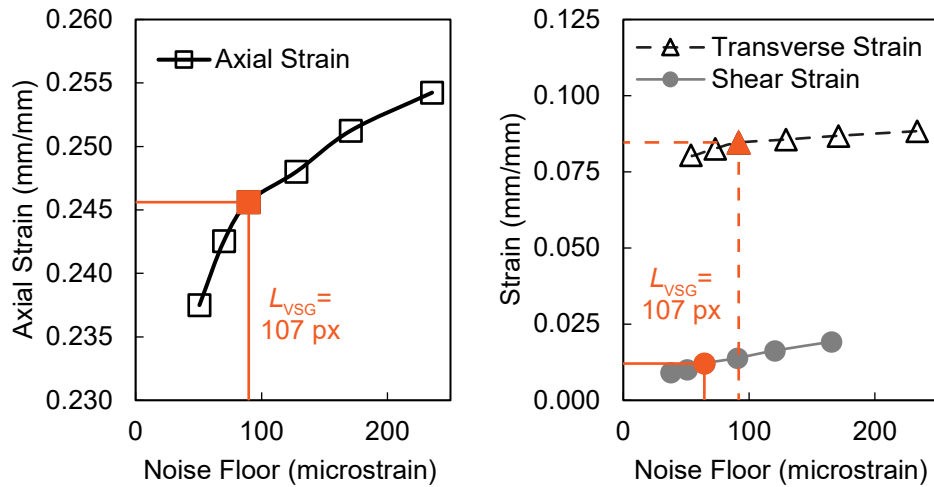


Figure 5.6: The peak true strain magnitude, for all three in-plane strains, as a function of noise-floor magnitude. The VSG size of 107 px is highlighted to illustrate the trade-offs between noise and bias for the three different in-plane strains.

In this example, the axial peak strain magnitude continues to increase as the noise increases (VSG size decreases), which is an example of the strain field not converging. If the maximum strain magnitude never converges, even with the smallest VSG allowed by the software, then the actual maximum strain magnitude is unknown. At best, one can report that the actual strain magnitude is greater than or equal to the maximum measured strain magnitude. That is, the reported strain is a lower bound on the actual strain magnitude.

Tip 5.10 — VSG Size Convergence

If the smallest VSG allowed by the software is not sufficient, the test could be repeated with a larger image scale (i.e. smaller FOV or higher image magnification). For a given set of user-defined parameters such as subset size, step size, strain or filter window size, etc. — all defined in terms of pixels in the DIC software — larger image scale would produce a smaller physical VSG size. See Sec. 2.1.8 for more information.

If the maximum strain magnitude converges with further decreases of the VSG size, then the actual maximum strain magnitude has been captured within the ultimate spatial resolution of the DIC system.^a In this example, the transverse strain magnitude does plateau with increasing noise (decreasing VSG size); if the transverse strain was the most important QOI, the user-defined parameters may be deemed sufficient.

Table 5.2: DIC analysis parameters for the VSG study

DIC Software [†]	[Manufacturer and Version number]
Image Filtering [†]	[Not reported here]
Reference Image	Single reference image (standard correlation)
Interpolant [†]	[Not reported here]
Matching Criterion	Zero-mean normalized sum of square differences (ZNSSD)
Subset/Element Size	37 px (0.56 mm)
Step Size	7 px (0.11 mm)
Subset Shape Function	Affine
Strain Window	11 data points
Virtual Strain Gauge Size ^{††}	107 px (1.61 mm)
Strain Formulation	Hencky
Strain Noise-Floor	90 $\mu\text{m}/\text{m}$ for ε_{xx}
	92 $\mu\text{m}/\text{m}$ for ε_{yy}
	65 $\mu\text{m}/\text{m}$ for ε_{xy}

[†]These parameters are vendor-specific and thus not included in this example.

^{††}The VSG size was estimated using Eqn. 7.3 (Sec. 7.3).

The final decision on which user-defined parameters and VSG size to use is application-dependent and often a matter of expert judgment. If capturing the highest strain peak magnitudes in regions of high strain gradients is critical for the DIC analysis, then a small VSG may be the best choice, even if the noise is large. On the other hand, if there are no high strain gradients, and/or a smoother strain field and/or reduced noise are more important than knowing the maximum strain at locations of high strain gradient, then a larger VSG may be the best choice. Alternatively, a combination of different VSG sizes for different portions of the test could be appropriate (e.g. a large VSG size early in the test when the signal-to-noise ratio for strains is low and strain gradients are small, and a small VSG size later in the test, when the strain signal-to-noise ratio is higher, and significant strain gradients have developed).

In this example, the final analysis parameters are reported in Table 5.2 following the reporting guidelines described in Sec. 6.2. These parameters were selected for illustrative purposes, to balance bias and noise errors (Fig. 5.6): with a VSG size of 107 px (1.61 mm), the transverse strain is nearly converged at a peak magnitude of $0.085 \text{ m/m} \pm 92 \text{ } \mu\text{m/m}$, and the reduction in noise for larger VSG sizes has diminishing returns. Note, however, that the axial and shear strains are not converged, and thus the peak magnitudes of $0.246 \text{ m/m} \pm 90 \text{ } \mu\text{m/m}$ and $0.012 \text{ m/m} \pm 65 \text{ } \mu\text{m/m}$, respectively, are lower bounds on the true peak magnitudes.

^aFor example, the macroscopic strain of a metal test piece may converge at the continuum level, yet highly-localized, microscopic strains of higher magnitude may exist at grain boundaries. This consideration is outside the scope of this edition of the guide.

6 — Reporting Requirements

With all the variables that must be selected in a mechanical test with DIC measurements, such as parameters of the physical system (i.e. camera, lens, patterning method, etc.) and parameters of the data analysis process (i.e. subset/element size, virtual strain gauge size, etc.), justification and documentation of the choices made is critical. The lists below present the minimum reporting requirements, as well as suggested and more detailed reporting recommendations. All documentation of DIC data — both internal reports and published journal articles — should contain this information. While the information may be documented in any format, one option is shown in Table 6.1 and Table 6.2. Note that more information may be necessary depending on the specific application.

Tip 6.1 — Application-Dependent Reporting Requirements

Depending on the application of the DIC data, some of the reporting recommendations may not be necessary; for example, if displacements were the QOI, then no information regarding the calculation of strains would be needed. In other cases, additional parameters not listed here may be important; for example, if accelerations were the QOI, then information on how the temporal displacement derivatives were calculated should be reported. The key is to document all relevant information!

Table 6.1: Example table that satisfies the basic reporting requirements for the DIC hardware parameters. Note that more information may be necessary depending on the specific application.

Camera	[Manufacturer and Model]
Image Size	2448 × 2048 px ²
Lens	[Manufacturer and Model]
Focal Length	35 mm
Aperture	f/8
Field-of-View	37.4 × 31.3 mm ²
Image Scale	65.4 px/mm
Stereo-Angle	25°
Stand-Off Distance	190 mm
Image Acquisition Rate	15 Hz
Exposure Time	50 ms
Patterning Technique[†]	Base coat of white spray paint with black ink stamped speckles
Pattern Feature Size	5 px (0.2 mm)

[†]A more complete description of the patterning technique may be appropriate in the main text.

Table 6.2: Example table that satisfies the basic reporting requirements for the DIC analysis parameters. Note that more information may be necessary depending on the specific application.

DIC Software	[Manufacturer, Package, and Version number]
Image Filtering	Gaussian filter with a 3×3 px ² kernel
Reference Image	Single image at zero force (standard correlation)
Interpolant	Bi-cubic spline
Matching Criterion	Zero-mean normalized sum-of-square differences (ZNSSD)
Subset/Element Size	21 px (0.32 mm)
Step Size	7 px (0.11 mm)
Subset Shape Function	Affine
Strain Window	15 data points
Virtual Strain Gauge Size (Eqn. 7.3)	119 px (1.79 mm)
Strain Tensor	Green-Lagrange
Strain Noise-Floor[†]	250 $\mu\text{m}/\text{m}$

[†]In the main text, also mention the method used to compute the noise-floor, as described in Sec. 5.4.3.

6.1 DIC Hardware Parameters

6.1.1 Required

- Camera manufacturer and model, and image size
- Lens manufacturer and model, focal length, and aperture

Note 1: If lens has a variable focal length, report both range and focal length used.

- FOV
- Image scale

Note 1: In stereo-DIC, where the cameras are at an angle to the test piece, the image scale is not constant across the FOV, and can be different in the two cameras. Therefore, the image scale of the ROI of the image should be reported, either as the average for the two cameras, if the scale is nearly the same, or for each camera individually, if the scale is significantly different in the two cameras.

- Stereo-angle

Note 1: Applicable for stereo-DIC; not applicable for 2D-DIC.

- SOD

Note 1: For stereo-DIC, the SOD should typically be approximately the same for both cameras; in this case, the average SOD can be reported.

- Image acquisition rate
- Exposure time
- Patterning technique
- Approximate pattern feature size

Note 1: Specify method used to determine feature size (see Tip 2.34). Note that both light (white) and dark (black) regions are considered features.

6.1.2 Recommended

- Image noise

6.2 DIC Analysis Parameters

6.2.1 Required

- DIC software manufacturer, package name, and version

Note 1: If an independently developed (non-commercial) DIC code is used, it is strongly recommended to verify the code using images from the DIC Challenge [74–76] (<https://idics.org/challenge/>). Any subsequent documentation of DIC measurements that use the code should refer to this verification.

- Image filtering, if applied
- Reference image
- Interpolant
- Matching criterion
- Subset size

Note 1: Preferably, report both in terms of pixels and in terms of physical units (e.g. millimeter) by scaling based on the image scale.

- Step size

Note 1: Preferably, report both in terms of pixels and in terms of physical units (e.g. millimeter) by scaling based on the image scale.

- Subset shape function (e.g. affine, quadratic)

Local-Global Flag 6.1 — Reporting Requirements

Subset size, step size, and subset shape function are all specific to local DIC. If a global formulation is used, report the analogous parameters of element size and element shape function. Since element size may vary across the ROI, report the average and standard deviation, or the average and minimum/maximum, and/or provide an image showing the finite-element mesh. See Appendix D.4 for more information.

- Data processing and filtering for QOIs

Recommendation 6.1 — Reporting Requirements for Strain

Strain is one of the most common QOIs. Typical parameters to report include:

- Pre-filtering of displacements (spatial and/or temporal), if applied
- Strain tensor (i.e. Lagrange, engineering, logarithmic, etc.)
- Strain window
- Virtual strain gauge size

Note 1: Preferably, report both in terms of pixels and in terms of physical units (e.g. millimeter) by scaling based on the image scale.

Note 2: One method of computing the VSG size is given in Eqn. 7.3. Other estimations of the VSG size may be more appropriate, depending on the strain calculation method used in the DIC software.

- Post-filtering of strains (spatial and/or temporal), if applied

- Noise-floor and bias of QOIs

Note 1: For 2D-DIC, bias caused by out-of-plane motion should be reported.

Note 2: There are many factors to consider when evaluating the noise-floor, and many possible approaches, as described in Sec. 5.4.3. For reporting purposes, state what method was used, and report the noise-floor value.

6.2.2 Recommended

- Calibration parameters, such as the following list. Note that models for calibration parameters are software-specific. The parameters listed here represent one particular model; relevant parameters for the selected model should be reported.

- Model number and serial number of calibration target used. (This information is useful for traceability and to elucidate any errors in measurements that may be associated with a specific, physical calibration target.)

- Image center

Note 1: Report for both cameras if using stereo-DIC.

- Focal length determined by the calibration

Note 1: Report for both cameras if using stereo-DIC.

- Lens distortion correction model and parameters

- Stereo-angle determined by the calibration

Note 1: Applicable for stereo-DIC; not applicable for 2D-DIC.

- Distance between cameras determined by the calibration

Note 1: Applicable for stereo-DIC; not applicable for 2D-DIC.

- Calibration quality metric(s)

7 — Glossary and Acronyms

7.1 Acronyms and Initialisms

CC: Cross-correlation

CCD: Charge-Coupled Device

CMOS: Complementary Metal Oxide Semiconductor

CSR: Current Session Reference

CSSD: Compensated Sum of Squared Difference

DFT: Discrete Fourier Transform

DIC: Digital Image Correlation

DOF: Depth-of-Field

DSLR: Digital Single-Lens Reflex

DVC: Digital Volume Correlation

EI: Exposure Index

FEA: Finite-Element Analysis

FOV: Field-of-View

FTCMOS: Frame Transfer CMOS

GCV: Generalized Cross-Validation

HS: High-Speed

IDIC: Integrated-DIC

iDICs: International Digital Image Correlation Society

IRIG: Inter-Range Instrumentation Group

ISIS: In-Situ Image Storage

ISO: International Organization for Standardization (though also used to refer to detector sensitivity, see [ISO](#) in the glossary)

LED: Light-Emitting Diode

LUT: Look-Up Table

NURBS: Non-uniform Rational B-splines

PIB: Pattern Induced Bias

QOI: Quantity-of-Interest

QE: Quantum Efficiency

REI: Recommended Exposure Index

ROI: Region-of-Interest

SI: International System of Units

SNR: Signal-to-Noise Ratio

SOD: Stand-Off Distance

SOS: Standard Output Sensitivity

SSD: Sum of Squared Difference

uCMOS: Ultra-High-Speed CMOS

UHS: Ultra-High-Speed

VSG: Virtual Strain Gauge

ZNSSD: Zero-mean Normalized Sum of Squared Difference

7.2 Units

Ampere [A]: Standard unit of electric current, representing the rate of flow of electric charge.

Electron charge [e]: Magnitude of the electric charge carried by a single electron.

Frames per second [fps]: Imaging rate of a camera.

Candela [cd]: Luminous intensity.

Decibel [dB]: A logarithmic unit used to measure the ratio of a power quantity to another.

Lumen [lm]: SI unit of luminous flux that describes the light produced by a source per unit of time. This unit is common for continuous lighting and flashbulbs.

Lumen-second [lm-s]: SI unit of light produced over time, or luminous energy. This unit is less common, but used for flash bulbs.

Lux [lx]: SI unit of illuminance or luminous flux per unit area, equal to one lumen per square meter. Lux is commonly used as a measure of light intensity (or luminous flux). This unit describes the amount of light incident on the object per unit area and is more common for continuous lighting, but can be used to describe strobed output as well.

Pixel [px]: See glossary definitions for an [image pixel](#) or [detector pixel](#). Standard SI prefixes are used, i.e. Mpx, Gpx, etc.

Pixels per second [px/s]: Rate at which data is transferred from the camera digital detector to the camera memory. Standard SI prefixes are used, e.g. Gpx/s.

Point or sample per second, Hertz [Hz]: Sampling frequency.

Volt [V]: Standard unit for electric potential.

Watt [W]: Standard unit of power or radiant flux.

Watt-second [W-s] or Joule [J]: A common unit of power output over a period of time. This unit is common for strobed/pulsed lighting.

7.3 Glossary

Binning, Image: The process of averaging [image data](#) from neighboring [pixels](#) in an image.

Note 1: Image binning performed during post-processing of the image should not be confused with [detector binning](#) performed during the image acquisition.

Note 2: Image binning reduces image noise but does not improve light sensitivity.

Binning, Detector: The process of combining charge from adjacent pixels on a [digital detector](#) during readout. Detector binning is performed prior to digitization in the on-chip circuitry.

Note 1: Binning performed on the camera [digital detector](#) should not be confused with [image binning](#) performed during post-processing of the image.

Note 2: Binning performed on the camera [digital detector](#) reduces noise, improves light sensitivity, and increases the maximum [frame rate](#), but degrades [spatial resolution of the detector](#).

Bit Depth, Detector [bits]: Number of bits of the analog to digital converter of a camera [digital detector](#) (e.g. 8-bit).

Note 1: The bit depth of the detector may not be the same as the [bit depth of the image](#) that the camera records, i.e. some conversion of bit depth may occur in the camera hardware or software.

Bit Depth, Image [bits]: Number of bits used to record the gray level at each [image pixel](#).

Note 1: The bit depth of the image may not be the same as the [bit depth of the detector](#), i.e. some conversion of bit depth may occur in the camera software.

Black Reference: The process of using a black image (i.e. captured with the shutter closed) to correct for fixed pattern noise due to persistent variations in light sensitivity between pixels. After performing a black reference, corrected images have a uniform pixel sensitivity.

Note 1: Depending on the camera software, the black reference may also be called current session reference (CSR), shading, session black, black calibration, etc.

Calibration Score: The residual of the bundle adjustment optimization process used to calibrate a DIC system.

Calibration Target: An object with features of specified size and/or spacing, used to calibrate the DIC system, i.e. determine intrinsic parameters (e.g. image scale, focal length, image center, lens distortions) and (for stereo-DIC) extrinsic parameters (e.g. stereo-angle, distance between cameras, distance from cameras to object).

Note 1: Calibration targets are often specific to DIC software packages. Some common types include: (1) a flat plate with circles or dots in a grid with known center-to-center dot spacing, which is often referred to as a “dot-grid calibration target”; (2) a plate with grooves or risers, so that dots are on multiple levels; (3) a plate with a checkerboard pattern.

Note 2: The calibration target should not be confused with a [resolution target](#) used to determine the [resolution of the imaging system](#).

Camera Throughput [px/s]: Rate at which [image data](#) can be read off the [digital detector](#).

Circular Buffer: A type of memory that is constantly recording over itself (overwriting earlier memory), until a trigger signal is received. A circular buffer allows images to be captured both before ([pre-trigger images](#)) and after a trigger signal is received by the camera.

Note 1: The term “ring buffer” is synonymous with “circular buffer”.

Note 2: A circular buffer is a typical feature of high-speed and ultra high-speed cameras. For low-speed cameras, this type of buffer may exist within the computer memory or camera hardware.

Chromatic Aberration: Lens defocus caused by different wavelengths of light being focused differently by the lens elements.

Data Filtering: Any further post-processing to spatially or temporally filter the DIC results (could include a Gaussian filter, median filter, etc.)

Data Point: A point at which DIC results (displacements, strains, etc.) are reported. Data points are typically reported at the center of subsets in local DIC and at the nodes of the mesh in global DIC. See Fig. 1.2 in the main Good Practices Guide.

Digital Image Correlation: Within the scope of this guide, Digital Image Correlation (DIC) is an optically-based technique used to measure the evolving full-field 2D or 3D displacements on the surface of a test piece, throughout a mechanical test of a material or structure.

Note 1: *2D-DIC* refers to the measurement of displacements in only two directions on the surface of the test piece, where one camera is oriented perpendicularly to a planar test piece.

Note 2: *Stereo-DIC* refers to the measurement of shape and displacements in three directions on the surface of the test piece, by using two (or more) cameras oriented at different angles. Stereo-DIC is sometimes called 3D-DIC, but should not be confused with digital volume correlation (DVC), which provides shape and displacement measurements throughout the volume of the test piece.

Depth-of-Field (DOF), L_{DOF} [mm]: The distance, along the optical axis, between the nearest and the farthest objects that are in acceptably sharp focus in an image. See Fig. 1.1 in the main Good Practices Guide.

Detector, Digital: An array of [pixels](#) used to acquire a digital image.

Note 1: A detector is typically (though not exclusively) contained within a “camera”, where the term “camera” encompasses the detector, additional electronic circuitry, synchronization/triggering hardware, lens mount, an outer housing, etc.

Note 2: The term “sensor” is often used interchangeably with the term “detector”.

Detector Array Size [px × px]: Total number of [pixels](#) contained in a [digital detector](#), typically reported as the width by height of the pixel array.

Note 1: Each [detector pixel](#) corresponds to an [image pixel](#); thus, the detector array size and the [image size](#) are the same, unless the image has been [windowed](#).

Note 2: “Camera resolution” is another term commonly used to refer to the array size of a detector. In this guide, however, the term “detector size” is preferred to avoid confusion with multiple other uses of the word “resolution”.

Detector Size, Physical [mm × mm]: Physical width and height of a [digital detector](#). The physical detector size is a function of the [detector array size](#) and the size of the [detector pixels](#).

Note 1: The physical size of a detector, L_{detector} (representing either the width or the height), is related to the [detector array size](#), N_{array} (again, representing either the width or the height), and the size of the [detector pixels](#), L_{pixel} , as $L_{\text{detector}} = N_{\text{array}} L_{\text{pixel}}$.

Note 2: This definition should not be confused with industry standard sizes given in nominal diagonal dimensions, e.g. 2/3 in. or 1 in.

Dynamic Range, Detector [dB]: The ratio of the largest possible light signal that can be measured (i.e. the full-well capacity of the pixel at saturation) divided by the lowest possible measurable signal (i.e. read-out noise). This term is represented in decibels and is defined mathematically by: $\text{dynamic range} = 20 \log_{10} (\text{full well capacity} / \text{read-out noise})$

Dynamic Range, Image [counts or gray levels]: Range of [gray levels](#) contained in the [image data](#). This can be graphically viewed in the image histogram. The image dynamic range is less than or equal to the [detector dynamic range](#).

Element (Global DIC): Sub-part of the [global DIC mesh](#) (in the topological sense of the finite-element method).

Note 1: The element in global DIC is analogous, but not exactly equal, to the [subset](#) in local DIC. See Fig. D.1 in the main Good Practices Guide.

Element Size, L_{element} [px] (Global DIC): Characteristic length of the [element](#) (for global DIC) in the reference image.

Note 1: Elements are typically triangular or quadrilateral. Because the element shape can be irregular and can vary across the ROI, the characteristic length of the element is typically the average side length of the element.

Note 2: Since element size may vary across the ROI, report the average and standard deviation, or the average and minimum/maximum, and/or provide an image showing the finite-element mesh.

Note 3: The element size in global DIC is analogous, but not exactly equal, to the [subset size](#) in local DIC. See Fig. [D.1](#) in the main Good Practices Guide.

Epipolar Error [px]: The distance between the location of a [data point](#), as determined by cross-correlation of a pair of images from the two cameras of a stereo-DIC system, and the epipolar line.

Note 1: Depending on the DIC software, the epipolar error may also be called projection error, three-dimensional residuum, intersection error, or correlation deviation.

Note 2: The epipolar line is determined by the extrinsic parameters of the stereo-camera calibration (i.e. stereo-angle, distance between two cameras). For more information on epipolar geometry, refer to [\[7, Sec. 4.2\]](#).

Exposure Index (EI): A camera setting that modifies the [tone curve or look-up table](#) applied to an image.

Note 1: The higher the EI, the brighter the image, and the higher the apparent sensitivity of the sensor.

Note 2: The application of a tone curve is a method used to digitally increase the apparent sensitivity or brightness of an image. Increasing the EI will also increase the noise in the image, and has no effect on the original raw data collected (i.e. it does not affect the sensor hardware since it is applied after the pixel data is collected).

Note 3: Exposure Index is closely related to [gamma](#), [gain](#), and [ISO setting](#).

Exposure Time [s]: Time during active acquisition of photons by the [pixel](#). Exposure time must be less than $1/(\text{frame rate})$.

Note 1: The exposure time may also be called exposure, integration time, or shutter-speed.

Fill Factor [%]: Photoreactive or light-sensitive area of a digital camera [detector pixel](#) that can receive photons and create photoelectrons, expressed as a percentage of the total area of the pixel.

Field-of-View (FOV) [mm × mm]: The region of space projected through a lens system onto a camera [digital detector](#) at a given [SOD](#). See Fig. [1.1](#) and Fig. [1.2](#) in the main Good Practices Guide.

Focal Length [mm]: A measure of how strongly a lens system converges light.

Note 1: A system with a shorter focal length bends light rays more sharply, bringing them to a focus in a shorter distance.

Note 2: The term “wide angle” lens refers to a lens with a short focal length.

Frame Rate [fps or Hz]: Frequency at which a camera acquires or captures images.

Note 1: The frame rate is typically expressed as frames per second (fps) or as a frequency of Hz.

Note 2: The frame rate can be equal to or higher than the [image acquisition rate](#).

Gain: Electronic amplification of a signal.

Note 1: For images specifically, the gain is the conversion between the number of electrons recorded by the [pixels](#) on the [digital detector](#) and the number of counts in the [gray-level](#) intensity of the image.

Gamma, γ : See [Exposure Index](#).

Ghosting: Residual image from a previous or later frame in the camera memory seen in the current image due to issues with the pixel wells bleeding or lack of pixel well emptying.

Global DIC Method: A category of DIC methods in which the full [image ROI](#) is represented using a global basis, for example, via a finite element formulation, and the full image ROI is analyzed together to seek the unknown deformation field.

Note 1: [Local DIC](#) is an alternative category of DIC methods.

Gray Level [counts]: The image intensity recorded by the image acquisition system, expressed as the number of counts of the digitizer.

Note 1: This value is proportional to the measured light intensity, but typically has no absolute calibrated relationship to the measured intensity. For DIC, this lack of calibration is acceptable, because the image is used for tracking the object motion, rather than measuring the light intensity at points on the object.

Note 2: Usually the number of counts is relative to the number of bits (quantization level) in the imaging analog-to-digital converter.

Gray Level Residual [counts] (Global DIC): Pixel-wise [gray level](#) difference between the image in the reference configuration and the image in the deformed configuration corrected by the measured displacement.

Note 1: The SSD (Sum of Squared Differences) of the gray level residual over the [image ROI](#) is generally the [matching criterion](#) that is minimized in [global DIC](#).

Image Acquisition Rate [fps or Hz]: Frequency at which consecutive images, or frames, are saved and analyzed.

Note 1: The image acquisition rate is typically expressed as frames per second (fps) or as a frequency of Hz.

Note 2: The image acquisition rate can be equal to or lower than the [frame rate](#).

Image Data: Recorded “images” of a test piece containing encoded information related to the displacement field including displacement gradients, nearly always a 2D or 3D numerical array of “intensity” or gray level data that will be used for correlation.

Image Filtering: Any type of image data processing done to modify the gray level values of the [pixels](#), most often a smoothing operation.

Note 1: *Analog Image Filtering* refers to filtering that is done in an analog fashion by modifying the physical optical system, e.g. with a blur filter assembled on the camera [digital detector](#) or by defocusing the lens.

Note 2: *Digital Image Filtering* refers to filtering that is done in a digital fashion as a post-processing step after the image has been acquired, e.g. a Gaussian filter.

Image Magnification: Ratio of the apparent size of an object and its true size. Magnification (or de-magnification) can be determined by the [detector pixel](#) size, the [detector array size](#), and the lens.

Image Noise [counts, gray levels, or percent of dynamic range]: Pixel-wise acquisition noise of the imaging system. This often varies depending on pixel intensity, camera temperature and optical intensity.

Image Scale, S [pixel/mm]: Number of optical elements ([pixels](#)) used to record an image of a region of physical length. The image scale can be used to convert from the [image pixel](#) size to physical units (e.g. meter).

Note 1: The image scale varies with position in an image. In 2D-DIC, with a single camera perpendicular to the test piece, the variation tends to be small, since the variation is the result of lens distortions or minor camera misalignment with the sample. In stereo-DIC, where the cameras are angled with respect to the surface of interest, the variation in image scale is much larger. This is the result of a combination of the lens distortions and the perspective effect (which is reversed in the left and right images). For stereo-DIC systems, the average image scale of the ROI shall be reported.

Image Size [px × px]: Total number of [pixels](#) contained in an image, typically reported as the width times the height of the image.

Note 1: Each [pixel in the image](#) corresponds to a [pixel in the detector](#); thus, the image size and the [detector array size](#) are the same, unless the detector has been [binned](#), the image has been [binned](#), or the image has been [windowed](#).

Note 2: “Camera resolution” is another term commonly used to refer to the size of an image or detector. In this guide, however, the terms “image size” and “detector array size” are preferred to avoid confusion with multiple other uses of the word “resolution”.

Integrated-DIC (IDIC): A [global DIC method](#) in which the sought displacement fields are mechanically admissible (i.e. constrained by a mechanical condition such as an analytical equation).

Interpolant: Interpolation function used to calculate the subpixel transformation within the [subset shape function](#) (in the case of local DIC methods) or [element shape function](#) (in the case of global DIC methods) subject to the [matching criteria](#) during the correlation calculation [7, Sec. 5.6.1 and Sec. 10.2.3.2], [34, 35].

ISO: Unit of measure of detector sensitivity. Higher numbers indicate more light sensitivity of the camera digital detector.

Note 1: “ISO” is also the abbreviation for the International Organization for Standardization.

Note 2: “ISO” can also be used to refer to the “ISO setting”, which is closely related to [gamma](#), [gain](#) and the [Exposure Index](#).

Local DIC Method: A category of DIC methods in which the full [image ROI](#) is subdivided into discrete [subsets](#). Each subset is analyzed independently.

Note 1: [Global DIC](#) is an alternative category of DIC methods.

Look-Up Table (LUT): A table that can be used to remap or alter the raw output counts from the camera [digital detector](#) by scaling them. Also called a “tone curve”.

Note 1: A look-up table is not a replacement for a detector calibration.

Luminance [cd/m^2]: Measure of the luminous intensity per unit area of light traveling in a certain direction.

Matching Criterion: Mathematical formulation used to calculate the quality metric of the calculated displacement field based on the underlying [image data](#) [7, Sec. 5.4], [37, 39].

Note 1: The matching criterion is also commonly referred to as “correlation criterion” or “cost function”.

Note 2: Common matching criteria include, but are not limited to, sum of square differences (SSD), normalized sum of square differences (NSSD), zero-mean normalized sum of square differences (ZNSSD), compensated sum-of-squared differences (CSSD), and cross-correlation (CC).

Mesh, Digital Image Correlation (Global DIC): A subdivision of the [image ROI](#) into [elements](#).

Motion Blur [px]: The distance in [pixels](#) that an object moves within a single frame capture or single [exposure time](#).

Node, Global DIC: Nodal point in the [global DIC finite-element mesh](#), or sampling measurement [data points](#) in the [global DIC](#) method.

Noise-Floor: [See [Resolution of a Quantity-of-Interest](#).]

Pattern Feature Size [px]: Characteristic length (e.g. diameter) of DIC pattern features in the [image data](#), reported in terms of [pixels](#). See Fig. 2.13 in the main Good Practices Guide.

Note 1: For DIC patterns that consist of primarily light or dark circular features (i.e. speckles), the pattern feature size is sometimes referred to as the “speckle size.”

Note 2: If a range of feature sizes exist in the image, the mean size and an indication of the distribution of sizes (e.g. minimum and maximum, or standard deviation) should be reported.

Note 3: Physical size of the features can be calculated by dividing by the [image scale](#).

Note 4: The spatial frequency of the pattern can be determined as the inverse of the pattern feature size (e.g. $1/(\text{pattern feature size})$).

Pixel, Image: Smallest addressable element in a digital image.

Note 1: Each image pixel corresponds to a physical [detector pixel](#) on the camera [digital detector](#), unless the detector has been [binned](#), the image has been [binned](#), or the image has been [windowed](#).

Note 2: The [gray level](#) or number of counts at each image pixel is related (possibly non-linearly) to the optical intensity or number of photons that impinged on the photoreactive or light-sensitive region of the [detector pixel](#).

Note 3: Often the term “pixel” is used on its own, and context typically is sufficient to distinguish between an image pixel and a [detector pixel](#).

Pixel, Detector: Physical region of the camera [digital detector](#) that corresponds to a single scalar element.

Note 1: A camera digital detector is typically comprised of millions of pixels configured in a rectangular array, e.g. a 5 Mpx camera digital detector, where “Mpx” stands for “mega-pixel”. Traditionally, “Mpx” has been shown as “MP” when referring to camera digital [detector array size](#), where the value has been rounded to 1 or 0.1 Mpx; here, the abbreviation “Mpx” is used.

Note 2: Each physical pixel on the camera digital detector corresponds to a [pixel on the image](#), unless the detector has been [binned](#), the image has been [binned](#), or the image has been [windowed](#).

Note 3: Often the term “pixel” is used on its own, and context typically is sufficient to distinguish between a detector pixel and an [image pixel](#).

Note 4: A detector pixel is comprised of a photoreactive or light-sensitive region and electronics or other non-active materials. The ratio of the light-sensitive area to the total area of the pixel is called the [fill factor](#).

Pre-Trigger Images: Images taken before the camera trigger. Pre-triggering is enabled by the [circular buffer](#) arrangement of the camera memory.

Note 1: Pre-triggering images is typically a feature of high-speed and ultra high-speed cameras.

Quantity-of-Interest (QOI): An attribute or property of a test piece that may be distinguished qualitatively and determined quantitatively [98], which a person seeks to characterize by performing a particular test.

Note 1: QOIs may be both direct measurements or derived quantities. With respect to DIC, common QOIs are kinematic measurements such as shape, curvature, displacement, velocity, acceleration, strain, strain-rate, etc.

Quantum Efficiency, QE [%]: The percentage of incident photons converted into photoelectrons by the [digital detector](#).

Note 1: Because the energy of photon is inversely proportional to its wavelength, QE is often measured over a range of wavelengths to characterize the detector efficiency at each photon energy level.

Note 2: QE can be computed from the [spectral response](#) according to Eqn. 7.1, where QE_λ is the quantum efficiency as a function of the wavelength λ , R_λ is the spectral response, h is the Planck constant, c is the speed of light in a vacuum, and e is the elementary charge.

$$QE_\lambda = \frac{R_\lambda}{\lambda} \frac{hc}{e} \approx \frac{R_\lambda}{\lambda} (1240 \text{ W nm A}^{-1}) \quad (7.1)$$

Region-of-Interest (ROI) of the Test Piece [mm × mm]: The portion of surface of the test piece that is used for analysis. See Fig. 1.2 in the main Good Practices Guide.

Note 1: The term “area-of-interest” is sometimes used interchangeably with the term “region-of-interest.”

Note 2: The region may be of any arbitrary shape, and may change shape in consecutive images.

Note 3: The term “region-of-interest” can refer to either a portion of the test piece or the corresponding portion of an image, and context typically is sufficient to distinguish between the two demarcations.

Region-of-Interest (ROI) of the Image [px × px]: The portion of the image corresponding to the [ROI of the test piece](#). See Fig. 1.2 in the main Good Practices Guide.

Note 1: The term “area-of-interest” is sometimes used interchangeably with the term “region-of-interest.”

Note 2: All QOIs are measured or derived using the [image data](#) that comes from the ROI of the image.

Note 3: The term “region-of-interest” can refer to either a portion of the test piece or the corresponding portion of an image, and context typically is sufficient to distinguish between the two demarcations.

Regularization, Global DIC: Technique used to diminish random errors in [global DIC](#) by adding an additional penalty term to the DIC [matching criterion](#).

Resolution, Imaging System [line pair/mm]: The ability of an imaging system to resolve detail in the object being imaged.

Note 1: Resolution of the imaging system is typically measured from images of a [resolution target](#).

Note 2: The resolution of the imaging system is a function of all optical components in the optical path, which may include the [digital detector](#), lens, intensifier, mirror, beam splitter, etc.

Note 3: The imaging system resolution is sometimes referred to as “optical resolution”.

Resolution, Lens [line pair/mm]: The ability of a lens to resolve detail in the object being imaged.

Note 1: The lens resolution is sometimes referred to as “optical resolution”.

Resolution, Detector [1/mm]: The ability of a [digital detector](#) to resolve detail in the object being imaged.

Note 1: For an image with [magnification](#) of unity, the Nyquist value of the detector resolution can be computed as $\frac{1}{2L_{\text{pixel}}}$, where L_{pixel} is the physical size of a [pixel on the detector](#). For images with non-unity magnification, the detector resolution in the object space is scaled based on the [image magnification](#) or [image scale](#).

Note 2: Detector resolution should not be confused with the [detector array size](#) or the [image size](#). Detector resolution here does not refer to the number of pixels on the [digital detector](#) or in the image.

Resolution, Spatial [px]: The minimum distance between two localized features that can be independently resolved.

Note 1: This definition might be counter intuitive, in that a smaller resolution value is desirable, whereas a larger resolution value is generally less desirable. These trends are opposite those of [image size](#) and [imaging system resolution](#).

Note 2: For the current edition of this guide, the concept of spatial resolution is defined as above; however, a unified method to determine the spatial resolution of DIC measurements is a current topic of interest for iDICs, and iDICs is actively exploring this concept in more detail.

Resolution Target: An object with features of specified width and/or spacing, used to determine the [imaging system resolution](#).

Note 1: Common resolution targets include the 1951 USAF target, the Siemens star, the NBS 1952 target and the NBS 1963A target, among others, which can be purchased from major optics companies. See https://en.wikipedia.org/wiki/Optical_resolution for more information.

Note 2: The resolution target should not be confused for a [calibration target](#) used to calibrate a DIC system.

Resolution, Temporal: Time interval between the start of consecutive frames.

Note 1: See [frame rate](#) and [image acquisition rate](#).

Note 2: Nyquist sampling rules apply.

Resolution of a Quantity-of-Interest: The threshold value of a QOI below which measurements are indistinguishable from noise, and above which measurements are significant.

Note 1: The phrase “Resolution of a QOI” is used interchangeably with the phrase “noise-floor” in this guide.

Note 2: The noise-floor is typically defined as a multiple of the standard deviation (either spatial or temporal) of the QOI computed under conditions in which the QOI should be zero.

Note 3: The noise-floor reflects only the random variance error of the QOI, and does not reflect any systematic bias errors that may be present in the QOI.

Ring Buffer: See [circular buffer](#).

Sensitivity, Detector [ISO]: Light sensitivity of the [pixels on the detector](#) to incoming photons. Typically defined by the camera manufacturer.

Note 1: The International Organization for Standardization (ISO) standard 12232 governing detector sensitivity details five possible methods to determine sensitivity; however the two most common are saturation-based, Ssat or Sat, and Standard Output Sensitivity, SOS.

Note 2: The unit for detector sensitivity is [ISO](#), which is separate from the International Organization for Standardization, which is also abbreviated as “ISO”.

Shape Function, Element (Global DIC): Interpolant used to describe the displacement field within an [element](#) when using [global DIC methods](#).

Shape Function, Strain: Analytic equation that is fit, in a least-squares sense, to the displacement data within the [strain window](#). Strains are computed from the derivatives of this equation.

Note 1: The strain shape function should not be confused with the [subset shape function](#) for or the [element shape function](#) for [global DIC](#).

Note 2: Not all methods of computing strain invoke a strain shape function.

Shape Function, Subset: Equation used to describe the displacement field within a [subset](#) [7, Sec. 5.3], [35, 36].

Note 1: Affine is the most common subset shape function, but higher ordered implementations are also used.

Note 2: The subset shape function should not be confused with the [strain shape function](#) or the [element shape function](#) for [global DIC](#).

Stand-Off Distance, SOD [m]: The distance between the aperture of the lens and the test piece. See Fig. 1.1 in the main Good Practices Guide.

Note 1: Stand-Off Distance is also often called “Working Distance”.

Note 2: In stereo DIC, the stand-off distance is the distance normal to the camera base line to the test piece in the stereo-plane.

Spectral Response, R_λ [Amps/Watt]: The relationship between the number of photoelectrons generated with respect to the visible spectrum of photons that are incident on the [digital detector](#).

Note 1: The [quantum efficiency](#) can be computed from the spectral response according to Eqn. 7.1.

Step Size, L_{step} [px]: The spacing of [pixel](#) grid points at which the subset displacements are calculated. That is, there will be a displacement solution at every step in the [ROI of the image](#). See Fig. 1.2 in the main Good Practices Guide.

Note 1: The step size is also sometimes reported as overlap, i.e. how much two neighboring [subsets](#) overlap when the step size is smaller than the [subset size](#). The overlap, L_{overlap} , is defined as a percentage of the [subset size](#), L_{subset} , in Eqn. 7.2.

$$L_{\text{overlap}} = \left(\frac{L_{\text{subset}} - L_{\text{step}}}{L_{\text{subset}}} \right) 100 \quad (7.2)$$

Note 2: While in [local DIC](#), subsets can overlap, for [global DIC](#), [elements](#) are continuous with no overlap. Therefore, only the [element size](#) is needed to characterize the finite-element [mesh](#), and there is no equivalent term for step size in [global DIC](#).

Stereo-Angle [°]: In a stereo-DIC system, the included angle between the optical axis of each of the two camera systems (i.e. camera and lens). See Fig. 1.1 in the main Good Practices Guide.

Stereo-Plane: In a stereo-DIC system, the plane formed by the optical axes of the two camera systems (i.e. camera and lens). See Fig. 1.1 in the main Good Practices Guide.

Subset: Portion of the image that is used to calculate one [data point](#) (e.g. 3D coordinate value (for stereo-DIC) or displacement value) in [local DIC](#). See Fig. 1.2 in the main Good Practices Guide.

Note 1: Center point displacement is commonly reported, although other parameters may be available via the [subset shape function](#).

Note 2: The subset in [local DIC](#) is analogous, but not exactly equal, to the [element](#) in [global DIC](#).

Subset Size, L_{subset} [pixel]: Length of the [subset](#) in the reference image in [local DIC](#). See Fig. 1.2 in the main Good Practices Guide.

Note 1: Subsets are typically square or circular (in the reference image), and thus a single length is sufficient to define the subset size. Some software, however, permits rectangular subsets; in this case, dimensions of both sides of the rectangle should be given to define the subset size.

Note 2: The subset size in [local DIC](#) is analogous, but not exactly equal, to the [element size](#) in [global DIC](#).

Virtual Strain Gauge (VSG): The local region of the image that affects the strain value at a specific location.

Note 1: The VSG is analogous to — but not exactly equal to — the physical area that a physical (e.g. foil) strain gauge would cover.

Virtual Strain Gauge Size, L_{VSG} [px]: Characteristic length of the [virtual strain gauge](#).

Note 1: Virtual strain gauges are typically square, circular, or hexagonal, and the size of the VSG is given by the characteristic length of the VSG (i.e. one side of the square, the diameter of the circle, or the effective diameter of the hexagon). The VSG size is specified in terms of the number of pixels that span the characteristic length of the VSG.

Note 2: The size of the VSG depends on the strain calculation method and user-defined parameters such as [step size](#), [subset size](#), [strain window](#), [filter window](#), [strain shape function](#), [weighting functions](#), and [subset shape function](#). An estimate for the size of the VSG, if $L_{\text{window}} > 0$, is given by Eqn. 7.3, where L_{window} is the [window size](#) (of either the [strain window](#) or of the [filter window](#)), L_{step} is the [step size](#), and L_{subset} is the [subset size](#).

$$L_{\text{VSG}} = (L_{\text{window}} - 1) L_{\text{step}} + L_{\text{subset}} \quad (7.3)$$

Note 3: To determine the VSG size in terms of physical units, the VSG size must be divided by the average [image scale](#).

Note 4: For [global DIC](#), the size of the VSG is less straightforward to estimate. Because the solutions for all [data points](#) in the ROI are solved simultaneously, it is difficult to clearly define a local region of the image that affects the strain at a specific location.

Volume, Calibration [mm³]: A portion of the [focal volume](#) in which images of the [calibration target](#) are acquired and for which the calibration parameters are valid. See Fig. 3.4 in the main Good Practices Guide.

Volume, Focal [mm³]: The volume over which a imaging system can produce an image with acceptably sharp focus. See Fig. 1.1 and Fig. 3.4 in the main Good Practices Guide.

Note 1: For a 2D-DIC system, this would be the volume within the [field-of-view](#) along the [depth-of-field](#).

Note 2: For a stereo-DIC system, this would be the overlapping volume within the [field-of-view](#) along the [depth-of-field](#) of both cameras.

Volume, Working [mm³]: The volume in which the test piece is expected to move and/or deform during the test.

Weighting Function: Mathematical device used to give some elements more influence on a result than other elements, based on the spatial location of the elements.

Note 1: Common weighting functions are square or uniform (which weights all elements equally) or Gaussian (which weights elements closer to the center point of interest more heavily than elements farther from the center point of interest).

Note 2: A *subset weighting function* is used to weight the [gray level](#) intensities of the [pixels](#) contained within the [subset](#) when performing subset matching.

Note 3: A *strain weighting function* is used to weight the displacement [data points](#) within the [strain window](#) when computing strain.

Note 4: A *filter weighting function* is used to weight the [data points](#) within a [filter window](#) when applying a spatial data filter.

Window, Filter: Local region of the [ROI of the image](#), containing a finite number of [data points](#), that is used for local spatial filters of DIC data.

Note 1: See [Window Size](#) for information about the filter window size.

Window, Strain: Local region of the [ROI of the image](#), containing a finite number of [data points](#), that is used to calculate strain.

Note 1: Not all methods of computing strain invoke a strain window.

Note 2: See [Window Size](#) for information about the strain window size.

Window Size, L_{window} [data point]: Characteristic length of a local region of [data points](#) (e.g. a [filter window](#) or a [strain window](#)). See Fig. 1.2 in the main Good Practices Guide.

Note 1: Strain windows and filter windows are typically square, circular, or hexagonal, and the size of the window is given by the characteristic length of the window (i.e. one side of the square, the diameter of the circle, or the effective diameter of the hexagon). The window size is specified in terms of the number of [data points](#) that span the characteristic length of the window. Windows are typically symmetric and centered at a data point; thus, window sizes are typically odd integers.

Note 2: The window size in terms of pixels, L_{window}^* , is given by Eqn. 7.4, where L_{window} is the window size in terms of data points, and L_{step} is the [step size](#).

$$L_{\text{window}}^* = (L_{\text{window}} - 1) L_{\text{step}} \quad (7.4)$$

Note 3: To determine the window size in terms of physical units, the window size in terms of pixels must be divided by the average [image scale](#).

Windowing: A reduction of the [image size](#) by cropping (i.e. discarding) pixels.

Note 1: Windowing can be used with a high-speed camera to allow the camera to acquire and store images at faster [frame rates](#).

Note 2: Windowing can also be used with both high-speed cameras and low-speed (machine-vision) cameras to eliminate unused pixels and reduce the file size of the images.

References

The references contained in this bibliography are provided for further reading on select topics covered in the guide. This list should not be presumed as comprehensive or consummate; additional (potentially better) references may exist, regarding any of the selected topics. Inclusion of these references in this bibliography should not be taken as endorsement by iDICs of these referenced works or their authors.

- [1] International Digital Image Correlation Society (Idics). *A good practices guide for digital image correlation*. 2nd ed. 2023. DOI: [10.32720/idics/gpg.ed2](https://doi.org/10.32720/idics/gpg.ed2).
- [2] J. E. Greivenkamp. *Field guide to geometrical optics*. Bellingham, Washington, USA: SPIE Press, 2004. DOI: <https://doi.org/10.1117/3.547461>.
- [3] W. Smith. *Modern optical engineering*. 4th ed. SPIE Press, 2007.
- [4] E. Hecht. *Optics*. 5th ed. Pearson Education Limited, 2017.
- [5] R. Hartley. *Multiple view geometry in computer vision*. Vol. 665. Cambridge university press, 2003.
- [6] R. Szeliski. *Computer vision: Algorithms and applications*. Springer Nature, 2022.
- [7] H. Schreier, J. J. Orteu, and M. A. Sutton. *Image correlation for shape, motion and deformation measurements*. Springer US, 2009. DOI: [10.1007/978-0-387-78747-3](https://doi.org/10.1007/978-0-387-78747-3).
- [8] P. Reu. “Introduction to digital image correlation: Best practices and applications”. *Exp. Tech.* 36.1 (2012), pp. 3–4. DOI: [10.1111/j.1747-1567.2011.00798.x](https://doi.org/10.1111/j.1747-1567.2011.00798.x).
- [9] P. Reu. “Hidden components of DIC: Calibration and shape function - part 1”. *Exp. Tech.* 36.2 (2012), pp. 3–5. DOI: [10.1111/j.1747-1567.2012.00821.x](https://doi.org/10.1111/j.1747-1567.2012.00821.x).
- [10] P. Reu. “Hidden components of 3D-DIC: Interpolation and matching - part 2”. *Exp. Tech.* 36.3 (2012), pp. 3–4. DOI: [10.1111/j.1747-1567.2012.00838.x](https://doi.org/10.1111/j.1747-1567.2012.00838.x).
- [11] P. Reu. “Hidden components of 3D-DIC: Triangulation and post-processing - part 3”. *Exp. Tech.* 36.4 (2012), pp. 3–5. DOI: [10.1111/j.1747-1567.2012.00853.x](https://doi.org/10.1111/j.1747-1567.2012.00853.x).
- [12] P. Reu. “Stereo-rig design: Creating the stereo-rig layout - part 1”. *Exp. Tech.* 36.5 (2012), pp. 3–4. DOI: [10.1111/j.1747-1567.2012.00871.x](https://doi.org/10.1111/j.1747-1567.2012.00871.x).
- [13] P. Reu. “Stereo-rig design: Camera selection-part 2”. *Exp. Tech.* 36.6 (2012), pp. 3–4. DOI: [10.1111/j.1747-1567.2012.00872.x](https://doi.org/10.1111/j.1747-1567.2012.00872.x).
- [14] P. Reu. “Stereo-rig design: Lens selection - part 3”. *Exp. Tech.* 37.1 (2013), pp. 1–3. DOI: [10.1111/ext.12000](https://doi.org/10.1111/ext.12000).
- [15] P. Reu. “Stereo-rig design: Stereo-angle selection - part 4”. *Exp. Tech.* 37.2 (2013), pp. 1–2. DOI: [10.1111/ext.12006](https://doi.org/10.1111/ext.12006).

- [16] P. Reu. “Stereo-rig design: Lighting-part 5”. *Exp. Tech.* 37.3 (2013), pp. 1–2. DOI: [10.1111/ext.12020](https://doi.org/10.1111/ext.12020).
- [17] P. Reu. “Calibration: Pre-calibration routines”. *Exp. Tech.* 37.4 (2013), pp. 1–2. DOI: [10.1111/ext.12026](https://doi.org/10.1111/ext.12026).
- [18] P. Reu. “Calibration: 2D calibration”. *Exp. Tech.* 37.5 (2013), pp. 1–2. DOI: [10.1111/ext.12027](https://doi.org/10.1111/ext.12027).
- [19] P. Reu. “Calibration: A good calibration image”. *Exp. Tech.* 37.6 (2013), pp. 1–3. DOI: [10.1111/ext.12059](https://doi.org/10.1111/ext.12059).
- [20] P. Reu. “Calibration: Stereo calibration”. *Exp. Tech.* 38.1 (2014), pp. 1–2. DOI: [10.1111/ext.12048](https://doi.org/10.1111/ext.12048).
- [21] P. Reu. “Calibration: Sanity checks”. *Exp. Tech.* 38.2 (2014), pp. 1–2. DOI: [10.1111/ext.12077](https://doi.org/10.1111/ext.12077).
- [22] P. Reu. “Calibration: Care and feeding of a stereo-rig”. *Exp. Tech.* 38.3 (2014), pp. 1–2. DOI: [10.1111/ext.12083](https://doi.org/10.1111/ext.12083).
- [23] P. Reu. “Speckles and their relationship to the digital camera”. *Exp. Tech.* 38.4 (2014), pp. 1–2. DOI: [10.1111/ext.12105](https://doi.org/10.1111/ext.12105).
- [24] P. Reu. “All about speckles: Aliasing”. *Exp. Tech.* 38.5 (2014), pp. 1–3. DOI: [10.1111/ext.12111](https://doi.org/10.1111/ext.12111).
- [25] P. Reu. “All about speckles: Speckle size measurement”. *Exp. Tech.* 38.6 (2014), pp. 1–2. DOI: [10.1111/ext.12110](https://doi.org/10.1111/ext.12110).
- [26] P. Reu. “DIC: A revolution in experimental mechanics”. *Exp. Tech.* 39.6 (2015), pp. 1–2. DOI: [10.1111/ext.12173](https://doi.org/10.1111/ext.12173).
- [27] P. Reu. “All about speckles: Contrast”. *Exp. Tech.* 39.1 (2015), pp. 1–2. DOI: [10.1111/ext.12126](https://doi.org/10.1111/ext.12126).
- [28] P. Reu. “All about speckles: Edge sharpness”. *Exp. Tech.* 39.2 (2015), pp. 1–2. DOI: [10.1111/ext.12139](https://doi.org/10.1111/ext.12139).
- [29] P. Reu. “All about speckles: Speckle density”. *Exp. Tech.* 39.3 (2015), pp. 1–2. DOI: [10.1111/ext.12161](https://doi.org/10.1111/ext.12161).
- [30] P. Reu. “Points on paint”. *Exp. Tech.* 39.4 (2015), pp. 1–2. DOI: [10.1111/ext.12147](https://doi.org/10.1111/ext.12147).
- [31] P. Reu. “Virtual strain gage size study”. *Exp. Tech.* 39.5 (2015), pp. 1–3. DOI: [10.1111/ext.12172](https://doi.org/10.1111/ext.12172).
- [32] B. K. P. Horn and B. G. Schunck. “Determining optical-flow”. *Artificial Intelligence* 17.1-3 (1981), pp. 185–203. DOI: [10.1016/0004-3702\(81\)90024-2](https://doi.org/10.1016/0004-3702(81)90024-2).
- [33] M. A. Sutton, J. H. Yan, V. Tiwari, H. W. Schreier, and J. J. Orteu. “The effect of out-of-plane motion on 2D and 3D digital image correlation measurements”. *Opt. Laser. Eng.* 46.10 (2008), pp. 746–757. DOI: [10.1016/j.optlaseng.2008.05.005](https://doi.org/10.1016/j.optlaseng.2008.05.005).
- [34] L. Luu, Z. Y. Wang, M. Vo, T. Hoang, and J. Ma. “Accuracy enhancement of digital image correlation with B-spline interpolation”. *Opt. Lett.* 36.16 (2011), pp. 3070–3072. DOI: [10.1364/ol.36.003070](https://doi.org/10.1364/ol.36.003070).
- [35] H. W. Schreier, J. R. Braasch, and M. A. Sutton. “Systematic errors in digital image correlation caused by intensity interpolation”. *Opt. Eng.* 39.11 (2000), pp. 2915–2921. DOI: [10.1117/1.1314593](https://doi.org/10.1117/1.1314593).
- [36] X. H. Xu, Y. Su, Y. L. Cai, T. Cheng, and Q. C. Zhang. “Effects of various shape functions and subset size in local deformation measurements using DIC”. *Exp. Mech.* 55.8 (2015), pp. 1575–1590. DOI: [10.1007/s11340-015-0054-9](https://doi.org/10.1007/s11340-015-0054-9).

- [37] A. Giachetti. “Matching techniques to compute image motion”. *Image Vis. Comput.* 18.3 (2000), pp. 247–260. DOI: [10.1016/s0262-8856\(99\)00018-9](https://doi.org/10.1016/s0262-8856(99)00018-9).
- [38] W. Tong. “An evaluation of digital image correlation criteria for strain mapping applications”. *Strain* 41.4 (2005), pp. 167–175. DOI: [10.1111/j.1475-1305.2005.00227.x](https://doi.org/10.1111/j.1475-1305.2005.00227.x).
- [39] B. Pan, H. M. Xie, and Z. Y. Wang. “Equivalence of digital image correlation criteria for pattern matching”. *Appl. Opt.* 49.28 (2010), pp. 5501–5509. DOI: [10.1364/ao.49.005501](https://doi.org/10.1364/ao.49.005501).
- [40] B. Pan, L. Yu, and D. Wu. “High-accuracy 2D digital image correlation measurements using low-cost imaging lenses: Implementation of a generalized compensation method”. *Meas. Sci. Technol.* 25.2 (2014), p. 025001. DOI: [10.1088/0957-0233/25/2/025001](https://doi.org/10.1088/0957-0233/25/2/025001).
- [41] L. Wittevrongel, M. Badaloni, R. Balcaen, P. Lava, and D. Debruyne. “Evaluation of methodologies for compensation of out of plane motions in a 2D digital image correlation setup”. *Strain* 51.5 (2015), pp. 357–369. DOI: [10.1111/str.12146](https://doi.org/10.1111/str.12146).
- [42] B. Pan, L. P. Yu, and D. F. Wu. “High-accuracy 2D digital image correlation measurements with bilateral telecentric lenses: Error analysis and experimental verification”. *Exp. Mech.* 53.9 (2013), pp. 1719–1733. DOI: [10.1007/s11340-013-9774-x](https://doi.org/10.1007/s11340-013-9774-x).
- [43] L. F. Wu, J. G. Zhu, H. M. Xie, and M. M. Zhou. “Single-lens 3D digital image correlation system based on a bilateral telecentric lens and a bi-prism: Systematic error analysis and correction”. *Opt. Laser. Eng.* 87 (2016), pp. 129–138. DOI: [10.1016/j.optlaseng.2016.02.006](https://doi.org/10.1016/j.optlaseng.2016.02.006).
- [44] K. Genovese. “Three-dimensional microscopic deformation measurements on cellular solids”. *J. Mech. Behav. Biomed. Mater.* 60 (2016), pp. 78–92. DOI: [10.1016/j.jmbbm.2015.12.043](https://doi.org/10.1016/j.jmbbm.2015.12.043).
- [45] L. F. Wu, J. G. Zhu, and H. M. Xie. “Single-lens 3D digital image correlation system based on a bilateral telecentric lens and a bi-prism: Validation and application”. *Appl. Opt.* 54.26 (2015), pp. 7842–7850. DOI: [10.1364/ao.54.007842](https://doi.org/10.1364/ao.54.007842).
- [46] E. Byrne and M. Simonsen. *Lens selection and stereo angle*. Web Page. Accessed Oct. 2023. URL: <https://correlated.kayako.com/article/78-lens-selection-and-stereo-angle>.
- [47] P. L. Reu, W. Sweatt, T. Miller, and D. Fleming. “Camera system resolution and its influence on digital image correlation”. *Exp. Mech.* 55.1 (2014), pp. 9–25. DOI: [10.1007/s11340-014-9886-y](https://doi.org/10.1007/s11340-014-9886-y).
- [48] J. R. Barber. *Elasticity*. Solid mechanics and its applications. Springer, 1992. DOI: [10.1007/978-94-011-2454-6](https://doi.org/10.1007/978-94-011-2454-6).
- [49] B. L. Witt and D. P. Rohe. “Digital image correlation as an experimental modal analysis capability”. *Exp. Tech.* 45 (2021), pp. 273–286.
- [50] E. Zappa, P. Mazzoleni, and A. Matinmanesh. “Uncertainty assessment of digital image correlation method in dynamic applications”. *Opt. Laser. Eng.* 56 (2014), pp. 140–151. DOI: [10.1016/j.optlaseng.2013.12.016](https://doi.org/10.1016/j.optlaseng.2013.12.016).
- [51] W. S. Lepage, S. H. Daly, and J. A. Shaw. “Cross polarization for improved digital image correlation”. *Exp. Mech.* 56.6 (2016), pp. 969–985. DOI: [10.1007/s11340-016-0129-2](https://doi.org/10.1007/s11340-016-0129-2).
- [52] B. Dong, C. Li, and B. Pan. “Fluorescent digital image correlation applied for macroscale deformation measurement”. *Appl. Phys. Lett.* 117.4 (2020), p. 044101. DOI: [10.1063/5.0016384](https://doi.org/10.1063/5.0016384).
- [53] E. M. Jones, A. R. Jones, and C. Winters. “Combined thermographic phosphor and digital image correlation (TP+DIC) for simultaneous temperature and strain measurements”. *Strain* 58.5 (2022), e12415.

- [54] B. Blaysat, M. Grédiac, and F. Sur. “On the propagation of camera sensor noise to displacement maps obtained by DIC - an experimental study”. *Exp. Mech.* 56.6 (2016), pp. 919–944. DOI: [10.1007/s11340-016-0130-9](https://doi.org/10.1007/s11340-016-0130-9).
- [55] G. Besnard, S. Guérard, S. Roux, and F. Hild. “A space–time approach in digital image correlation: Movie-DIC”. *Opt. Laser. Eng.* 49.1 (2011), pp. 71–81. DOI: [10.1016/j.optlaseng.2010.08.012](https://doi.org/10.1016/j.optlaseng.2010.08.012).
- [56] X. Wang, X. Liu, H. Zhu, and S. Ma. “Spatial-temporal subset based digital image correlation considering the temporal continuity of deformation”. *Opt. Laser. Eng.* 90 (2017), pp. 247–253. DOI: [10.1016/j.optlaseng.2016.10.021](https://doi.org/10.1016/j.optlaseng.2016.10.021).
- [57] M. Berny, T. Archer, A. Mavel, P. Beauchêne, S. Roux, and F. Hild. “On the analysis of heat haze effects with spacetime DIC”. *Opt. Laser. Eng.* 111 (2018), pp. 135–153. DOI: [10.1016/j.optlaseng.2018.06.004](https://doi.org/10.1016/j.optlaseng.2018.06.004).
- [58] E. M. C. Jones and P. L. Reu. “Distortion of digital image correlation (DIC) displacements and strains from heat waves”. *Exp. Mech.* 58.7 (2017), pp. 1133–1156. DOI: [10.1007/s11340-017-0354-3](https://doi.org/10.1007/s11340-017-0354-3).
- [59] S. Bossuyt. “Optimized patterns for digital image correlation”. *Imaging Methods for Novel Materials and Challenging Applications, Volume 3: Proceedings of the 2012 Annual Conference on Experimental and Applied Mechanics* (2012), pp. 239–248. DOI: [10.1007/978-1-4614-4235-6_34](https://doi.org/10.1007/978-1-4614-4235-6_34).
- [60] Y. L. Dong and B. Pan. “A review of speckle pattern fabrication and assessment for digital image correlation”. *Exp. Mech.* 57.8 (2017), pp. 1161–1181. DOI: [10.1007/s11340-017-0283-1](https://doi.org/10.1007/s11340-017-0283-1).
- [61] D. Lecompte, A. Smits, S. Bossuyt, H. Sol, J. Vantomme, D. Van Hemelrijck, and A. M. Habraken. “Quality assessment of speckle patterns for digital image correlation”. *Opt. Laser. Eng.* 44.11 (2006), pp. 1132–1145. DOI: [10.1016/j.optlaseng.2005.10.004](https://doi.org/10.1016/j.optlaseng.2005.10.004).
- [62] B. Blaysat, F. Sur, T. Jailin, A. Vinel, and M. Grédiac. “OpenLSA: An open-source toolbox for computing full-field displacements from images of periodic patterns”. *SoftwareX* 27 (2024). DOI: [10.1016/j.softx.2024.101826](https://doi.org/10.1016/j.softx.2024.101826).
- [63] G. Crammond, S. W. Boyd, and J. M. Dulieu-Barton. “Speckle pattern quality assessment for digital image correlation”. *Opt. Laser. Eng.* 51.12 (2013), pp. 1368–1378. DOI: [10.1016/j.optlaseng.2013.03.014](https://doi.org/10.1016/j.optlaseng.2013.03.014).
- [64] M. A. Iadicola. “Uncertainties of digital image correlation due to pattern degradation at large strain”. *Advancement of Optical Methods in Experimental Mechanics, Volume 3: Proceedings of the 2015 Annual Conference on Experimental and Applied Mechanics*. (2016), pp. 247–253. DOI: [10.1007/978-3-319-22446-6_31](https://doi.org/10.1007/978-3-319-22446-6_31).
- [65] P. L. Reu. “Using anti-aliasing camera filters for DIC: Does it make a difference?” *Advancement of Optical Methods in Experimental Mechanics, Volume 3: Proceedings of the 2017 Annual Conference on Experimental and Applied Mechanics*. (2018), pp. 89–92. DOI: [10.1007/978-3-319-63028-1_14](https://doi.org/10.1007/978-3-319-63028-1_14).
- [66] A. Peshave, F. Pierron, P. Lava, D. Moens, and D. Vandepitte. “Practical uncertainty quantification guidelines for DIC-based numerical model validation”. *Exp. Tech.* 49.3 (2025), pp. 437–457. DOI: [10.1007/s40799-024-00758-1](https://doi.org/10.1007/s40799-024-00758-1).
- [67] J. Yang, J. L. Tao, and C. Franck. “Smart digital image correlation patterns via 3D printing”. *Exp. Mech.* 61.7 (2021), pp. 1181–1191. DOI: [10.1007/s11340-021-00720-x](https://doi.org/10.1007/s11340-021-00720-x).

- [68] S. P. Ma, J. Z. Pang, and Q. W. Ma. “The systematic error in digital image correlation induced by self-heating of a digital camera”. *Meas. Sci. Technol.* 23.2 (2012), p. 7. DOI: [10.1088/0957-0233/23/2/025403](https://doi.org/10.1088/0957-0233/23/2/025403).
- [69] L. Yu and G. Lubineau. “Modeling of systematic errors in stereo-digital image correlation due to camera self-heating”. *Scientific reports* 9.1 (2019), p. 6567.
- [70] B. Pan, L. P. Yu, D. F. Wu, and L. Q. Tang. “Systematic errors in two-dimensional digital image correlation due to lens distortion”. *Opt. Laser. Eng.* 51.2 (2013), pp. 140–147. DOI: [10.1016/j.optlaseng.2012.08.012](https://doi.org/10.1016/j.optlaseng.2012.08.012).
- [71] P. L. Reu. “A study of the influence of calibration uncertainty on the global uncertainty for digital image correlation using a Monte Carlo approach”. *Exp. Mech.* 53.9 (2013), pp. 1661–1680. DOI: [10.1007/s11340-013-9746-1](https://doi.org/10.1007/s11340-013-9746-1).
- [72] Verein Deutscher Ingenieure (VDI). *Optical measuring procedures—digital image correlation: Basics, acceptance test, ad interim check*. Standard. 2019. URL: <https://www.vdi.de/en/home/vdi-standards/details/vdivde-2626-blatt-1-optical-measuring-procedures-digital-image-correlation-basics-acceptance-test-and-iterim-check>.
- [73] ASD-STAN. “Aerospace series—metrological assessment procedure for kinematic fields measured by digital image correlation”. CEN EN 4861 (2020).
- [74] P. L. Reu, E. Toussaint, E. Jones, H. A. Bruck, M. Iadicola, R. Balcaen, D. Z. Turner, T. Siebert, P. Lava, and M. Simonsen. “DIC challenge: Developing images and guidelines for evaluating accuracy and resolution of 2D analyses”. *Exp. Mech.* 58.7 (2017), pp. 1067–1099. DOI: [10.1007/s11340-017-0349-0](https://doi.org/10.1007/s11340-017-0349-0).
- [75] P. L. Reu, B. Blaysat, E. Andó, K. Bhattacharya, C. Couture, V. Couty, D. Deb, S. S. Fayad, M. A. Iadicola, S. Jaminion, M. Klein, A. K. Landauer, P. Lava, M. Liu, L. K. Luan, S. N. Olufsen, J. Réthoré, E. Roubin, D. T. Seidl, T. Siebert, O. Stamati, E. Toussaint, D. Turner, C. S. R. Vemulapati, T. Weikert, J. F. Witz, O. Witzel, and J. Yang. “DIC challenge 2.0: Developing images and guidelines for evaluating accuracy and resolution of 2D analyses”. *Exp. Mech.* 62.4 (2022), pp. 639–654. DOI: [10.1007/s11340-021-00806-6](https://doi.org/10.1007/s11340-021-00806-6).
- [76] W. Ahmad, J. Helm, S. Bossuyt, P. Reu, D. Turner, L. K. Luan, P. Lava, T. Siebert, and M. Simonsen. “Stereo-DIC challenge 1.0 – rigid body motion of a complex shape”. *Exp. Mech.* 64.7 (2024), pp. 1073–1106. DOI: [10.1007/s11340-024-01077-7](https://doi.org/10.1007/s11340-024-01077-7).
- [77] Z. Gao, X. Xu, Y. Su, and Q. Zhang. “Experimental analysis of image noise and interpolation bias in digital image correlation”. *Opt. Laser. Eng.* 81 (2016), pp. 46–53. DOI: <https://doi.org/10.1016/j.optlaseng.2016.01.002>.
- [78] B. Pan. “Bias error reduction of digital image correlation using gaussian pre-filtering”. *Opt. Laser. Eng.* 51.10 (2013), pp. 1161–1167. DOI: [10.1016/j.optlaseng.2013.04.009](https://doi.org/10.1016/j.optlaseng.2013.04.009).
- [79] Y. H. Zhou, C. Sun, Y. T. Song, and J. B. Chen. “Image pre-filtering for measurement error reduction in digital image correlation”. *Opt. Laser. Eng.* 65 (2015), pp. 46–56. DOI: [10.1016/j.optlaseng.2014.04.018](https://doi.org/10.1016/j.optlaseng.2014.04.018).
- [80] F. Barros, P. J. Sousa, P. J. Tavares, and P. M. Moreira. “Digital image correlation through image registration in the frequency domain”. *The Journal of Strain Analysis for Engineering Design* 53.8 (2018), pp. 575–583.

- [81] H. Lu, C. Huang, C. Wang, X. Wang, H. Fu, and Z. Chen. “Fast and noninterpolating method for subpixel displacement analysis of digital speckle images using phase shifts of spatial frequency spectra”. *Appl. Opt.* 53.13 (2014), pp. 2806–2814.
- [82] X. Tong, Z. Ye, Y. Xu, S. Gao, H. Xie, Q. Du, S. Liu, X. Xu, S. Liu, and K. Luan. “Image registration with fourier-based image correlation: A comprehensive review of developments and applications”. *IEEE Journal of Selected Topics in Applied Earth Observations and Remote Sensing* 12.10 (2019), pp. 4062–4081.
- [83] F. Barros, P. J. Sousa, P. J. Tavares, and P. M. Moreira. “A DFT-based method for 3D digital image correlation”. *Procedia Structural Integrity* 5 (2017), pp. 1260–1266.
- [84] A. A. Grebenyuk and V. P. Ryabukho. “Digital image correlation with fast fourier transform for large displacement measurement”. *Saratov fall meeting 2010: optical technologies in biophysics and medicine XII*. Vol. 7999. SPIE, pp. 68–72.
- [85] P. Lava, S. Cooreman, S. Coppieters, M. De Strycker, and D. Debruyne. “Assessment of measuring errors in DIC using deformation fields generated by plastic FEA”. *Opt. Laser. Eng.* 47.7-8 (2009), pp. 747–753. DOI: [10.1016/j.optlaseng.2009.03.007](https://doi.org/10.1016/j.optlaseng.2009.03.007).
- [86] S. S. Fayad, D. T. Seidl, and P. L. Reu. “Spatial DIC errors due to pattern-induced bias and grey level discretization”. *Exp. Mech.* 60.2 (2019), pp. 249–263. DOI: [10.1007/s11340-019-00553-9](https://doi.org/10.1007/s11340-019-00553-9).
- [87] F. Sur, B. Blaysat, and M. Grédiac. “On biases in displacement estimation for image registration, with a focus on photomechanics”. *J. Math. Imaging Vision* 63.7 (2021), pp. 777–806. DOI: [10.1007/s10851-021-01032-4](https://doi.org/10.1007/s10851-021-01032-4).
- [88] H. Lu and P. D. Cary. “Deformation measurements by digital image correlation: Implementation of a second-order displacement gradient”. *Exp. Mech.* 40.4 (2000), pp. 393–400. DOI: [10.1007/bf02326485](https://doi.org/10.1007/bf02326485).
- [89] L. P. Yu and B. Pan. “The errors in digital image correlation due to overmatched shape functions”. *Meas. Sci. Technol.* 26.4 (2015), p. 9. DOI: [10.1088/0957-0233/26/4/045202](https://doi.org/10.1088/0957-0233/26/4/045202).
- [90] X. D. Ke, H. W. Schreier, M. A. Sutton, and Y. Q. Wang. “Error assessment in stereo-based deformation measurements”. *Exp. Mech.* 51.4 (2011), pp. 423–441. DOI: [10.1007/s11340-010-9450-3](https://doi.org/10.1007/s11340-010-9450-3).
- [91] J. Q. Zhao, P. Zeng, L. P. Lei, and Y. Ma. “Initial guess by improved population-based intelligent algorithms for large inter-frame deformation measurement using digital image correlation”. *Opt. Laser. Eng.* 50.3 (2012), pp. 473–490. DOI: [10.1016/j.optlaseng.2011.10.005](https://doi.org/10.1016/j.optlaseng.2011.10.005).
- [92] Y. H. Zhou, B. Pan, and Y. Q. Chen. “Large deformation measurement using digital image correlation: A fully automated approach”. *Appl. Opt.* 51.31 (2012), pp. 7674–7683. DOI: [10.1364/ao.51.007674](https://doi.org/10.1364/ao.51.007674).
- [93] ASTM International. “Standard practice for verification and classification of extensometer systems”. ASTM E83-16 (2017).
- [94] International Standards Organization (ISO). “Metallic materials: Calibration of extensometer systems used in uniaxial testing”. ISO 9513:2012 (2012).
- [95] ASTM International. “Standard test method for determining forming limit curves”. ASTM E2218-15 (2016).
- [96] International Standards Organization (ISO). “Metallic materials: Determination of forming-limit curves for sheet and strip: Part 2: Determination of forming-limit curves in the laboratory”. ISO 12004-2:2021 (2021).

- [97] B. Blaysat, J. Neggers, M. Grédiac, and F. Sur. “Towards criteria characterizing the metrological performance of full-field measurement techniques”. *Exp. Mech.* 60.3 (2020), pp. 393–407. DOI: [10.1007/s11340-019-00566-4](https://doi.org/10.1007/s11340-019-00566-4).
- [98] JCGM Member Organizations. *International vocabulary of metrology—basic and general concepts and associated terms (VIM)*. 3rd ed. Vol. 200. BIPM, 2012.
- [99] Y. Wang, P. Lava, P. Reu, and D. Debruyne. “Theoretical analysis on the measurement errors of local 2D DIC: Part II assessment of strain errors of the local smoothing method—approaching an answer to the overlap question”. *Strain* 52.2 (2016), pp. 129–147. DOI: [10.1111/str.12174](https://doi.org/10.1111/str.12174).
- [100] J. Zhao, Y. Song, and X. Wu. “Fast Hermite element method for smoothing and differentiating noisy displacement field in digital image correlation”. *Opt. Laser. Eng.* 68 (2015), pp. 25–34. DOI: [10.1016/j.optlaseng.2014.12.010](https://doi.org/10.1016/j.optlaseng.2014.12.010).
- [101] J. Q. Zhao, P. Zeng, B. Pan, L. P. Lei, H. F. Du, W. B. He, Y. Liu, and Y. J. Xu. “Improved Hermite finite element smoothing method for full-field strain measurement over arbitrary region of interest in digital image correlation”. *Opt. Laser. Eng.* 50.11 (2012), pp. 1662–1671. DOI: [10.1016/j.optlaseng.2012.04.008](https://doi.org/10.1016/j.optlaseng.2012.04.008).
- [102] X. Li, G. Fang, J. Q. Zhao, Z. M. Zhang, and X. X. Wu. “Local Hermite (LH) method: An accurate and robust smooth technique for high-gradient strain reconstruction in digital image correlation”. *Opt. Laser. Eng.* 112 (2019), pp. 26–38. DOI: [10.1016/j.optlaseng.2018.08.022](https://doi.org/10.1016/j.optlaseng.2018.08.022).
- [103] X. Li, G. Fang, J. Q. Zhao, Z. M. Zhang, L. B. Sun, H. T. Wang, and X. X. Wu. “A practical and effective regularized polynomial smoothing (RPS) method for high-gradient strain field measurement in digital image correlation”. *Opt. Laser. Eng.* 121 (2019), pp. 215–226. DOI: [10.1016/j.optlaseng.2019.04.017](https://doi.org/10.1016/j.optlaseng.2019.04.017).
- [104] V. Rubino, N. Lapusta, A. J. Rosakis, S. Leprince, and J. P. Avouac. “Static laboratory earthquake measurements with the digital image correlation method”. *Exp. Mech.* 55.1 (2014), pp. 77–94. DOI: [10.1007/s11340-014-9893-z](https://doi.org/10.1007/s11340-014-9893-z).
- [105] V. Rubino, A. J. Rosakis, and N. Lapusta. “Full-field ultrahigh-speed quantification of dynamic shear ruptures using digital image correlation”. *Exp. Mech.* 59.5 (2019), pp. 551–582. DOI: [10.1007/s11340-019-00501-7](https://doi.org/10.1007/s11340-019-00501-7).
- [106] J. D. Hoffman and S. Frankel. *Numerical methods for engineers and scientists*. 2nd ed. Boca Raton: CRC press, 2018. DOI: [10.1201/9781315274508](https://doi.org/10.1201/9781315274508).
- [107] G. Besnard, F. Hild, and S. Roux. “Finite-element displacement fields analysis from digital images: Application to Portevin–Le Châtelier bands”. *Exp. Mech.* 46.6 (2006), pp. 789–803. DOI: [10.1007/s11340-006-9824-8](https://doi.org/10.1007/s11340-006-9824-8).
- [108] J. Van Beeck, J. Neggers, P. J. G. Schreurs, J. P. M. Hoefnagels, and M. G. D. Geers. “Quantification of three-dimensional surface deformation using global digital image correlation”. *Exp. Mech.* 54.4 (2013), pp. 557–570. DOI: [10.1007/s11340-013-9799-1](https://doi.org/10.1007/s11340-013-9799-1).
- [109] R. Fedele, L. Galantucci, and A. Ciani. “Global 2D digital image correlation for motion estimation in a finite element framework: A variational formulation and a regularized, pyramidal, multi-grid implementation”. *International Journal for Numerical Methods in Engineering* 96.12 (2013), pp. 739–762. DOI: [10.1002/nme.4577](https://doi.org/10.1002/nme.4577).
- [110] Y. Sun, J. H. Pang, C. K. Wong, and F. Su. “Finite element formulation for a digital image correlation method”. *Appl. Opt.* 44.34 (2005), pp. 7357–63. DOI: [10.1364/ao.44.007357](https://doi.org/10.1364/ao.44.007357).

- [111] L. Wittevrongel, P. Lava, S. V. Lomov, and D. Debruyne. “A self adaptive global digital image correlation algorithm”. *Exp. Mech.* 55.2 (2014), pp. 361–378. DOI: [10.1007/s11340-014-9946-3](https://doi.org/10.1007/s11340-014-9946-3).
- [112] L. Wittevrongel, P. Lava, S. V. Lomov, and D. Debruyne. “ C^n -continuity in digital image correlation: Implementation and validation of C^{-1} , C^0 and C^1 algorithms”. *Strain* 51.6 (2015), pp. 444–458. DOI: [10.1111/str.12156](https://doi.org/10.1111/str.12156).
- [113] L. Wittevrongel, D. Debruyne, S. V. Lomov, and P. Lava. “Implementation of convergence in adaptive global digital image correlation”. *Exp. Mech.* 56.5 (2016), pp. 797–811. DOI: [10.1007/s11340-016-0126-5](https://doi.org/10.1007/s11340-016-0126-5).
- [114] P. Cheng, M. A. Sutton, H. W. Schreier, and S. R. McNeill. “Full-field speckle pattern image correlation with B-spline deformation function”. *Exp. Mech.* 42.3 (2002), pp. 344–352. DOI: [10.1007/bf02410992](https://doi.org/10.1007/bf02410992).
- [115] J. Réthoré, T. Elguedj, P. Simon, and M. Coret. “On the use of NURBS functions for displacement derivatives measurement by digital image correlation”. *Exp. Mech.* 50.7 (2009), pp. 1099–1116. DOI: [10.1007/s11340-009-9304-z](https://doi.org/10.1007/s11340-009-9304-z).
- [116] F. Mortazavi, E. Ghossein, M. Lévesque, and I. Villemure. “High resolution measurement of internal full-field displacements and strains using global spectral digital volume correlation”. *Opt. Laser. Eng.* 55 (2014), pp. 44–52. DOI: [10.1016/j.optlaseng.2013.10.007](https://doi.org/10.1016/j.optlaseng.2013.10.007).
- [117] B. Wagne, S. Roux, and F. Hild. “Spectral approach to displacement evaluation from image analysis”. *Eur. Phys. J. Appl. Phys.* 17.3 (2002), pp. 247–252. DOI: [10.1051/epjap:2002019](https://doi.org/10.1051/epjap:2002019).
- [118] J. Yang and K. Bhattacharya. “Augmented Lagrangian digital image correlation”. *Exp. Mech.* 59.2 (2018), pp. 187–205. DOI: [10.1007/s11340-018-00457-0](https://doi.org/10.1007/s11340-018-00457-0).
- [119] J. Yang and K. Bhattacharya. “Fast adaptive mesh augmented Lagrangian digital image correlation”. *Exp. Mech.* 61.4 (2021), pp. 719–735. DOI: [10.1007/s11340-021-00695-9](https://doi.org/10.1007/s11340-021-00695-9).
- [120] F. Hild, S. Roux, R. Gras, N. Guerrero, M. E. Marante, and J. Flórez-López. “Displacement measurement technique for beam kinematics”. *Opt. Laser. Eng.* 47.3-4 (2009), pp. 495–503. DOI: [10.1016/j.optlaseng.2008.03.006](https://doi.org/10.1016/j.optlaseng.2008.03.006).
- [121] S. Roux and F. Hild. “Stress intensity factor measurements from digital image correlation: Post-processing and integrated approaches”. *International Journal of Fracture* 140.1-4 (2006), pp. 141–157. DOI: [10.1007/s10704-006-6631-2](https://doi.org/10.1007/s10704-006-6631-2).
- [122] J. C. Passieux, P. Navarro, J. N. Périé, S. Marguet, and J. F. Ferrero. “A digital image correlation method for tracking planar motions of rigid spheres: Application to medium velocity impacts”. *Exp. Mech.* 54.8 (2014), pp. 1453–1466. DOI: [10.1007/s11340-014-9930-y](https://doi.org/10.1007/s11340-014-9930-y).
- [123] X. Wang, Z. Pan, F. Fan, J. Wang, Y. Liu, S. X. Mao, T. Zhu, and S. Xia. “Nanoscale deformation analysis with high-resolution transmission electron microscopy and digital image correlation”. *Journal of Applied Mechanics* 82.12 (2015), p. 121001. DOI: [10.1115/1.4031332](https://doi.org/10.1115/1.4031332).
- [124] H. Leclerc, J.-N. Périé, S. Roux, and F. Hild. “Integrated digital image correlation for the identification of mechanical properties”. *Computer Vision/Computer Graphics Collaboration Techniques*. Ed. by André Gagalowicz and Wilfried Philips. Springer Berlin Heidelberg, pp. 161–171. DOI: [10.1007/978-3-642-01811-4_15](https://doi.org/10.1007/978-3-642-01811-4_15).
- [125] G. Besnard, H. Leclerc, F. Hild, S. Roux, and N. Swiergiel. “Analysis of image series through global digital image correlation”. *J. Strain Anal. Eng. Des.* 47.4 (2012), pp. 214–228. DOI: [10.1177/0309324712441435](https://doi.org/10.1177/0309324712441435).

- [126] J. Réthoré, S. Roux, and F. Hild. “An extended and integrated digital image correlation technique applied to the analysis of fractured samples”. *European Journal of Computational Mechanics* 18.3-4 (2012), pp. 285–306. DOI: [10.3166/ejcm.18.285-306](https://doi.org/10.3166/ejcm.18.285-306).
- [127] Z. Tomičević, F. Hild, and S. Roux. “Mechanics-aided digital image correlation”. *J. Strain Anal. Eng. Des.* 48.5 (2013), pp. 330–343. DOI: [10.1177/0309324713482457](https://doi.org/10.1177/0309324713482457).
- [128] J. Yang and K. Bhattacharya. “Combining image compression with digital image correlation”. *Exp. Mech.* 59.5 (2019), pp. 629–642. DOI: [10.1007/s11340-018-00459-y](https://doi.org/10.1007/s11340-018-00459-y).
- [129] R. Fouque, R. Bouclier, J.-C. Passieux, and J.-N. Périé. “Photometric DIC: A unified framework for global stereo digital image correlation based on the construction of textured digital twins”. *Journal of Theoretical, Computational and Applied Mechanics* (2022).
- [130] K. Han, M. Ciccotti, and S. Roux. “Measuring nanoscale stress intensity factors with an atomic force microscope”. *EPL (Europhysics Letters)* 89.6 (2010), p. 66003. DOI: [10.1209/0295-5075/89/66003](https://doi.org/10.1209/0295-5075/89/66003).
- [131] F. Mathieu, H. Leclerc, F. Hild, and S. Roux. “Estimation of elastoplastic parameters via weighted FEMU and integrated-DIC”. *Exp. Mech.* 55.1 (2014), pp. 105–119. DOI: [10.1007/s11340-014-9888-9](https://doi.org/10.1007/s11340-014-9888-9).
- [132] F. Hild and S. Roux. “Digital image correlation: From displacement measurement to identification of elastic properties - a review”. *Strain* 42.2 (2006), pp. 69–80. DOI: [10.1111/j.1475-1305.2006.00258.x](https://doi.org/10.1111/j.1475-1305.2006.00258.x).
- [133] J. C. Passieux, J. N. Périé, and M. Salaün. “A dual domain decomposition method for finite element digital image correlation”. *International Journal for Numerical Methods in Engineering* 102.10 (2015), pp. 1670–1682. DOI: [10.1002/nme.4868](https://doi.org/10.1002/nme.4868).
- [134] A. Ronovsky and A. Vasatova. “Elastic image registration based on domain decomposition with mesh adaptation”. *Advances in Electrical and Electronic Engineering* 15.2 (2017), pp. 322–330. DOI: [10.15598/aeae.v15i2.2281](https://doi.org/10.15598/aeae.v15i2.2281).
- [135] R. Vargas, A. Tsitova, F. Bernachy-Barbe, B. Bary, R. B. Canto, and F. Hild. “On the identification of cohesive zone model for curved crack in mortar”. *Strain* 56.6 (2020), e12364. DOI: [10.1111/str.12364](https://doi.org/10.1111/str.12364).
- [136] J. Réthoré, F. Hild, and S. Roux. “Extended digital image correlation with crack shape optimization”. *International Journal for Numerical Methods in Engineering* 73.2 (2008), pp. 248–272. DOI: [10.1002/nme.2070](https://doi.org/10.1002/nme.2070).
- [137] A. Charbal, J.-E. Dufour, A. Guery, F. Hild, S. Roux, L. Vincent, and M. Poncelet. “Integrated digital image correlation considering gray level and blur variations: Application to distortion measurements of ir camera”. *Opt. Laser. Eng.* 78 (2016), pp. 75–85. DOI: [10.1016/j.optlaseng.2015.09.011](https://doi.org/10.1016/j.optlaseng.2015.09.011).
- [138] T. Archer, P. Beauchêne, C. Huchette, and F. Hild. “Global digital image correlation up to very high temperatures with grey level corrections”. *Meas. Sci. Technol.* 31.2 (2020), p. 024003. DOI: [10.1088/1361-6501/ab461e](https://doi.org/10.1088/1361-6501/ab461e).
- [139] V. F. Sciuti, R. B. Canto, J. Neggers, and F. Hild. “On the benefits of correcting brightness and contrast in global digital image correlation: Monitoring cracks during curing and drying of a refractory castable”. *Opt. Laser. Eng.* 136 (2021), p. 106316. DOI: [10.1016/j.optlaseng.2020.106316](https://doi.org/10.1016/j.optlaseng.2020.106316).

- [140] J. E. Pierré, J. C. Passieux, and J. N. Périé. “Finite element stereo digital image correlation: Framework and mechanical regularization”. *Exp. Mech.* 57.3 (2016), pp. 443–456. DOI: [10.1007/s11340-016-0246-y](https://doi.org/10.1007/s11340-016-0246-y).
- [141] J. C. Passieux, F. Bugarin, C. David, J. N. Périé, and L. Robert. “Multiscale displacement field measurement using digital image correlation: Application to the identification of elastic properties”. *Exp. Mech.* 55.1 (2015), pp. 121–137. DOI: [10.1007/s11340-014-9872-4](https://doi.org/10.1007/s11340-014-9872-4).
- [142] D. Claire, F. Hild, and S. Roux. “Identification of a damage law by using full-field displacement measurements”. *International Journal of Damage Mechanics* 16.2 (2007), pp. 179–197. DOI: [10.1177/1056789506064940](https://doi.org/10.1177/1056789506064940).
- [143] M. Bornert, F. Brémand, P. Doumalin, J. C. Dupré, M. Fazzini, M. Grédiac, F. Hild, S. Mistou, J. Molimard, J. J. Orteu, L. Robert, Y. Surré, P. Vacher, and B. Wattrisse. “Assessment of digital image correlation measurement errors: Methodology and results”. *Exp. Mech.* 49.3 (2009), pp. 353–370. DOI: [10.1007/s11340-008-9204-7](https://doi.org/10.1007/s11340-008-9204-7).
- [144] B. Pan, B. Wang, G. Lubineau, and A. Moussawi. “Comparison of subset-based local and finite element-based global digital image correlation”. *Exp. Mech.* 55.5 (2015), pp. 887–901. DOI: [10.1007/s11340-015-9989-0](https://doi.org/10.1007/s11340-015-9989-0).
- [145] F. Hild and S. Roux. “Comparison of local and global approaches to digital image correlation”. *Exp. Mech.* 52.9 (2012), pp. 1503–1519. DOI: [10.1007/s11340-012-9603-7](https://doi.org/10.1007/s11340-012-9603-7).

A — Checklist and Flow Chart for DIC Measurements and Analysis

This appendix presents a checklist and flow chart of the main points to consider when designing, executing, and analyzing DIC measurements performed during mechanical testing of a planar test piece. Each of the steps listed in the checklist are expounded upon in the main body of this guide, and the flow chart (Fig. A.1) refers in parentheses to specific sections of the guide.

1. Design of DIC Measurements (2)

(a) *Measurement Requirements* (2.1)

- ☐ QOIs (2.1.1)
- ☐ ROI (2.1.2)
- ☐ FOV (2.1.3)
- ☐ Position Envelope for Hardware (2.1.4)
- ☐ 2D-DIC vs. Stereo-DIC (2.1.5)
- ☐ Stereo-Angle (2.1.6)
- ☐ DOF (2.1.7)
- ☐ Spatial Gradients (2.1.8)
- ☐ Noise-Floor (2.1.9)
- ☐ Frame Rate and Image Acquisition Rate (2.1.10)
- ☐ Exposure Time (2.1.11)
- ☐ Synchronization and Triggering (2.1.12)

(b) *Equipment Selection* (2.2)

- ☐ Camera and Lens (2.2.1)
- ☐ Mounting Equipment (2.2.2)
- ☐ Aperture (2.2.3)
- ☐ Lighting and Exposure (2.2.4)
- ☐ DIC pattern (2.3)

(c) *Mock Test (Optional)*

- ☐ Test DIC pattern technique on extra test piece(s).
- ☐ Evaluate DIC pattern behavior throughout mock test.
- ☐ Evaluate lighting/contrast throughout mock test.
- ☐ Evaluate data synchronization and triggering.

2. Preparation for the Measurements (3)

(a) *Pre-Calibration Routine* (3.1)

- ☐ Review test procedure (3.1.1).
- ☐ Check cleanliness of camera detector, lens, and calibration target (3.1.2).
- ☐ Warm-up cameras (3.1.3).
- ☐ Synchronize cameras to each other and to other data acquisition (3.1.4).
- ☐ Apply DIC pattern (3.1.5).

(b) *Pre-Calibration Review of System*(3.1.6)

- ☐ Position test piece in load frame (3.1.6.1).
- ☐ Position cameras for desired FOV and image ROI (3.1.6.1).
- ☐ Verify FOV, focus, DOF (3.1.6.2).
- ☐ Lock all moving parts of cameras, lenses, and mounting system (3.1.6.3).
- ☐ Adjust orientation of polarization filters if using cross-polarized light (3.1.6.3).
- ☐ Review static images (3.1.6.4), looking for:
 - Glare
 - DIC pattern that is too coarse, fine, or sparse
 - Defects in applied DIC pattern
 - Out-of-focus regions of the image
 - Poor contrast
 - Non-uniform lighting
 - Overexposed or underexposed regions
 - Dirt, smears, foreign object on lens or camera detector
 - Vibrations or other camera motion
- ☐ Adjust DIC system until high-quality images are obtained.

(c) *Calibration* (3.2)

- ☐ Select calibration target of appropriate size. (3.2.2.1).
- ☐ Create a clear working space in which to perform calibration (3.2.2.2).
- ☐ Lock all moving parts of cameras, lenses, and mounting system (3.2.2.2).
- ☐ Adjust lighting/exposure (3.2.2.3).
- ☐ Ensure there is uniform contrast and no glare as the calibration target is rotated, tilted, and translated (3.2.2.3).
- ☐ Acquire calibration images that have well-extracted features in the entire [calibration volume](#) (3.2.2.4).
- ☐ Calibrate the system (3.2.2.5).
- ☐ Review calibration results (3.2.2.6).
- ☐ Review calibration parameters (3.2.2.7).

(d) *Post-Calibration Routine* (3.3)

- ☐ Reset system: Position test piece in load frame (if removed for calibration) or reposition stereo-camera system (if moved for calibration) and lock any moving parts (3.3.1.1).
- ☐ Adjust lighting/exposure (3.3.1.2).

- ☐ Acquire static images (3.3.1.3).
- ☐ Review static images (3.3.1.4 and 3.1.6.4), looking for:
 - Glare
 - DIC pattern that is too coarse, fine, or sparse
 - Defects in applied DIC pattern
 - Out-of-focus regions of the image
 - Poor contrast
 - Non-uniform lighting
 - Overexposed or underexposed regions
 - Dirt, smears, foreign object on lens or camera detector
 - Vibrations or other camera motion
- ☐ Acquire rigid-body-motion images of test piece for noise-floor analysis (3.3.1.5).
- ☐ Verify calibration (3.3.2).
 - Intrinsic parameters (3.3.2.1)
 - Extrinsic parameters (3.3.2.2)
 - Absolute distances (3.3.2.3)
- ☐ Perform abbreviated noise-floor analysis and ensure the noise-floor is acceptable (3.3.3.1).
- ☐ Look for heat waves (3.3.3.2), system stability (3.3.3.3), and any other lab-specific system verifications (3.3.3.4).

3. Execution of the Test with DIC Measurements (4)

- ☐ Verify correct file name, location, and storage capacity for DIC images.
- ☐ Verify that the correct test procedure or macro has been selected.
- ☐ Verify force and other measurements of interest are set to record and are synchronized with DIC images.
- ☐ Verify triggering of load frame and DIC images.
- ☐ Verify that lights are on, exposure is correct, image acquisition rate is correct.
- ☐ Run the mechanical test with DIC measurements.

4. Processing of DIC Images (5)

- ☐ Select initial correlation and user-defined parameters.
- ☐ Perform initial correlation of images.
- ☐ Re-analyze images using different user-defined parameters. (For example, do a VSG study (5.4.6) if strain is the QOI.)
- ☐ Based on results of the different correlations, select a final set of user-defined parameters.
- ☐ Correlate all images using finalized parameters.
- ☐ Quantify variance and bias errors using finalized parameters (5.4).

5. Reporting Requirements (6)

- ☐ Justify and document selection of all choices in the test and analysis of DIC data.

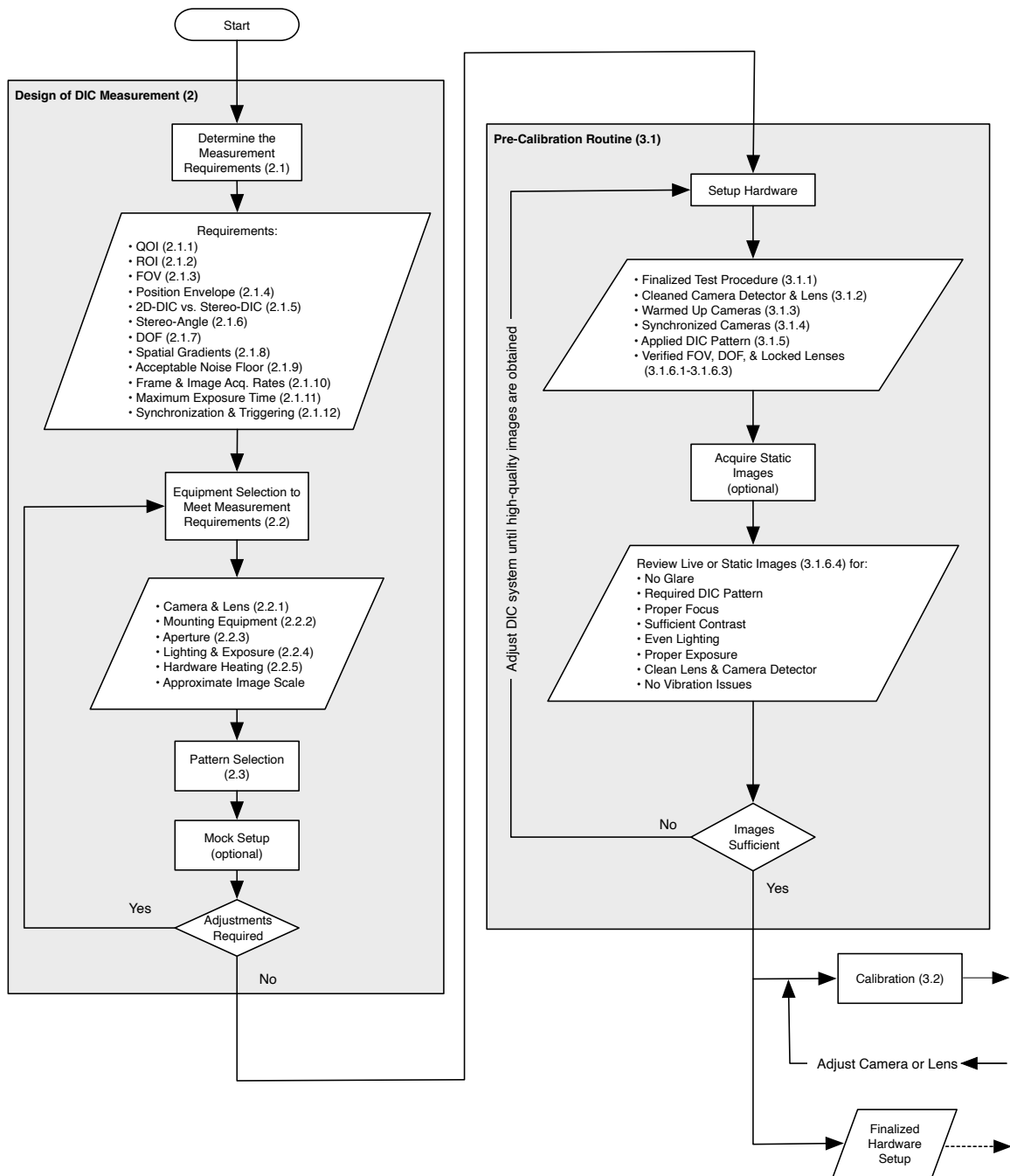


Figure A.1: Flow chart illustrating the main steps involved when conducting DIC measurements in conjunction with mechanical testing of a planar test piece (part 1).

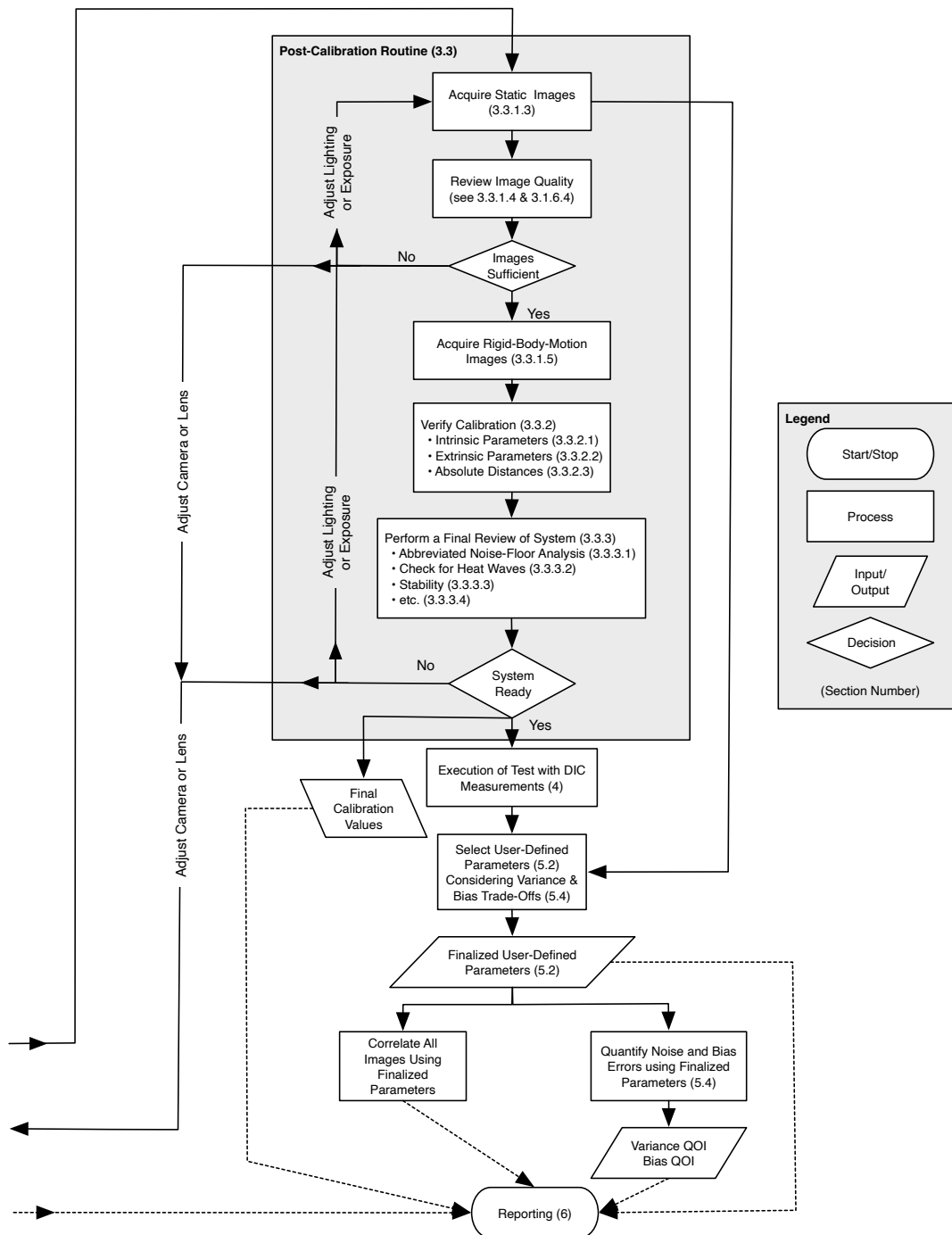


Figure A.2: Flow chart illustrating the main steps involved when conducting DIC measurements in conjunction with mechanical testing of a planar test piece (part 2).

B — Focal Length, Field-of-View, Stand-Off Distance, and Aperture

B.1 Thin Lens Theory

Thin lens theory^{28,29,30,31} defines a set of basic equations that may be used to approximate the relationships between FOV, SOD, lens focal length, camera physical detector size, lens aperture, and DOF. These equations are not exact, due to intricacies of real optical systems that are beyond the scope of the current edition of this guide, but they have proven to be close enough to use for setting up DIC in practical situations. They begin to break down in macro-lens photography situations, and should therefore not be relied upon for high accuracy when the FOV size shrinks to twice the detector size or smaller. In general usage, they are good for determining, for example, which lens from a kit of lenses to use, or for determining the approximate SOD.

B.2 Field-of-View and Stand-off Distance

In many typical DIC setups, the camera bar is set in a fixed location relative to a test fixture containing a patterned test piece (i.e. a fixed SOD), and it is desirable to calculate the FOV for a given lens, to determine if the ROI on the test piece will be imaged. The characteristic length of the FOV (L_{FOV}) can be closely approximated using the focal length of the lens(es) used (L_{FL}), the distance from the camera(s) to the patterned object (i.e. the SOD, L_{SOD}) and the width of the camera detector(s) (L_{CS}):

$$L_{\text{FOV}} = L_{\text{CS}} \left(\frac{L_{\text{SOD}} - L_{\text{FL}}}{L_{\text{FL}}} \right) \quad (\text{B.1})$$

Conversely, in some setups the required FOV is fixed by the test piece, and the lens focal length is fixed by the hardware on hand, but the distance to the test piece (i.e. SOD) may be adjusted by moving the camera bar. In this case, rearranging equation B.1 gives:

$$L_{\text{SOD}} = L_{\text{FL}} \left(\frac{L_{\text{FOV}}}{L_{\text{CS}}} + 1 \right) \quad (\text{B.2})$$

The width of the camera physical detector size is usually found in manufacturer specifications for the camera hardware. Sometimes, pixel size (typically in microns) is used instead. In the latter case, L_{CS} is simply the pixel size multiplied by one direction of the pixel array size. This is also true in cases where a cropped image, less than the full image size, is being used: simply multiply the width of the cropped

²⁸ *Thin Lenses* by Prof. Richard Fitzpatrick: <http://farside.ph.utexas.edu/teaching/3021/lectures/node140.html>

²⁹ *Lens (optics): Imaging properties* on Wikipedia: [https://en.wikipedia.org/wiki/Lens_\(optics\)#Imaging_properties](https://en.wikipedia.org/wiki/Lens_(optics)#Imaging_properties)

³⁰ *Lens Focal Length Calculator* by Iacopo Giangrandi: <http://www.giangrandi.ch/optics/focalcalc/focalcalc.shtml>

³¹ *Depth of field* on Wikipedia: https://en.wikipedia.org/wiki/Depth_of_field

image in pixels by the physical pixel size to obtain L_{CS} . If only the width of the physical detector size is in the specifications, it may be necessary to first calculate the detector pixel size by dividing L_{CS} by the width of the detector array size. Note that “binning” allowed by some cameras does not reduce L_{CS} , because it still utilizes the full detector, but combines data from multiple pixels to create a lower pixel count image (unless binning is used in addition to cropping of the image).

B.3 Depth-of-Field

Given a selected imaging setup, the DOF can be approximated according to:

$$L_{DOF} \approx 2F_s L_c \left(\frac{L_{SOD}}{L_{FL}} \right)^2, \quad (B.3)$$

where F_s is the f-stop number of the aperture, and L_c is the acceptable diameter of the circle of confusion. The circle of confusion is the optical spot on the camera detector caused by a cone of light rays from a lens not coming to a perfect focus when imaging a point source. In DIC, where the spatial resolution of the imaging system is often camera-limited (see Tip 2.33), a conservative diameter for the circle of confusion is approximately the physical size of the pixel on the detector.

B.4 Reference Tables

A practical use of these equations is building quick-reference tables for FOV, SOD, and DOF for a given set of hardware. Many online calculators^{32,33} are available to quickly solve for these parameters. Example B.1 shows how to create such a reference table for a given set of hardware.

Example B.1 — FOV, SOD, and DOF

Consider a 5 Mpx camera with an image size of 2448×2048 px², a physical detector width of $L_{CS} = 8.45$ mm, and a physical pixel size of $L_{px} = 3.45$ μ m. Assume the SOD is constrained by the position envelope for hardware (Sec. 2.1.4) to be $L_{SOD} = 1000$ mm. Three lenses are available with focal lengths of $L_{FL} = [35, 50, 75]$ mm. Assume a moderate aperture is used with an f-stop number of f/8 or $F_s = 8$ (see Caution 2.12), and that the acceptable circle of confusion is the size of the physical pixel on the detector, $L_c = L_{px} = 3.45$ μ m. Given these fixed parameters, Table B.1 presents the FOV and DOF for the different lens options, calculated using Eqn. B.1 and Eqn. B.3.

Table B.1: Example reference table for FOV and DOF options, given a fixed camera ($L_{px} = 3.45$ μ m), SOD ($L_{SOD} = 1000$ mm), f-stop number ($F_s = 8$), and circle of confusion ($L_c = L_{px}$).

Focal Length (L_{FL})	FOV Width (L_{FOV})	DOF (L_{DOF})
35 mm	230 mm	45 mm
50 mm	160 mm	22 mm
75 mm	100 mm	10 mm

³²Field of View Calculator (FoV) of Camera and Lens, Details and Calculator by Wayne Fulton: <http://www.scantips.com/lights/fieldofview.html>

³³Understanding Depth of Field, with Depth of Field Calculator, and Hyperfocal distance by Wayne Fulton: <https://www.scantips.com/lights/dof.html>

C — Select Strain Calculation Methods

Here, some general approaches for strain computation — representative of different approaches implemented in different DIC software packages — are briefly described. The effects of different user-defined parameters on the VSG size are highlighted.

C.1 Subset Shape Function

One approach is to compute the strain directly from the [subset shape function](#) and the deformed subset shape. In this method, the VSG size is approximately equal to the [subset size](#), giving rise to one of the smallest VSG sizes of all the strain computation methods. Additionally, no pre-filtering is applied to the displacements. The small VSG size and the lack of pre-filtering of displacements leads to high spatial resolution of the strain measurements, but noisy strain results.

After strains are calculated, they may be post-filtered to reduce the noise. A common type of post-filter is the mean of a local set of data points, often with a Gaussian [weighting function](#). The region of the data points that is included in this filter is called the [filter window](#). The VSG size can then be approximated by Eqn. 7.3 (under “Virtual Strain Gauge Size” in Sec. 7.3).

C.2 Finite-Element Shape Functions

A second approach closely follows the strain calculations used in finite-element analysis. A triangular or quadrilateral mesh is defined on the ROI of the reference image, using the displacement data points (provided at the center of the subsets) as the nodes of the mesh. Using finite-element shape functions defined over each element, the strain is computed from the deformed shape of each element. If a global DIC approach has been used, the computation can be done directly on the pre-existing finite-elements (see Appendix D.5.4).

At this point, the VSG size is small, approximately equal to the size of the elements (which is governed by the step size) plus the size of the subset. If no pre-filtering of the displacements was performed, the strain results from this method are usually noisy. Therefore, the strains are often post-filtered to reduce the noise. A common type of post-filter is the mean of a local set of data points, often with a Gaussian [weighting function](#). The region of the data points that is included in this filter is called the [filter window](#). The VSG size can then be approximated by Eqn. 7.3 (under “Virtual Strain Gauge Size” in Sec. 7.3).

As a slight variation to the above approach, instead of computing the strain on each triangular element individually using only the three nodes of the element, the strain can be computed in a least-

squares sense over a larger (i.e. hexagonal) region covering several triangular elements. This larger region is called the [strain window](#), and the VSG size be approximated by Eqn. 7.3 (under “Virtual Strain Gauge Size” in Sec. 7.3). In the least-squares regression, a [weighting function](#) may be applied to the displacement data points contained within the strain window, for instance with a Gaussian distribution centered at the center of the strain window and decaying towards the edges of the strain window. By computing the strain over a larger strain window using more data points, the strain results are less noisy, and post-filtering of the computed strains may not be necessary.

C.3 Strain Shape Function

A third approach is to fit a [strain shape function](#) to the displacements, which provides an analytical description of the displacement field [99]. The strains are then computed from the spatial derivatives of this analytical equation. Fitting the displacements to the strain shape function also serves to filter the displacements; thus, this fitting process can be considered as pre-filtering or smoothing the displacements before calculating the strains. The strain shape function is typically a polynomial or spline fit, and the order of the strain shape function effects the spatial resolution of the strain measurements.

The local region of the data points that is included in the fit is called the [strain window](#). Typically, strains are computed at the center of the strain window. A [weighting function](#) may be applied to the displacement data points contained within the strain window, for instance with a Gaussian distribution centered at the center of the strain window and decaying towards the edges of the strain window. The VSG size is approximated by Eqn. 7.3 (under “Virtual Strain Gauge Size” in Sec. 7.3).

C.4 Spline Fit

A fourth approach to strain calculations is to fit a spline to the entire displacement field, over the entire ROI. This approach is similar to the use of strain shape functions, except that here, the fit is global rather than local. This spline fit provides an analytical description of the strains over the entire ROI, which can be evaluated at any point in the ROI. Thus, strain measurements are not limited to the original DIC data point locations at the center of the subsets. The VSG size is less clearly defined, since there is no filter window or strain window, but it is related to the step size, subset size, element size, element shape function type and order of the spline.

C.5 Hermite Method

A fifth approach is to calculate the strain based on regularization by finding a best fitting surface to approximate the true displacement field concerning both the fitness and smoothness of resultant displacement/strain field. After using the fitting function, such as the Hermite shape function or polynomial, the regularization (for example the Tikhonov regularization) is utilized to tackle the ill-posed inverse problem in traditional least-squares regression, which comprises an additional regularization matrix and a regularization parameter. The regularization matrix is defined by summation of squared partial differential of fitting function, and the regularization parameter is normally determined by the generalized cross-validation (GCV) function. Thus, the strain is obtained by differentiation of the fitted surface.

This approach includes both global and local versions. The global method [100, 101] defines the fitting function typically with Hermite finite-elements on the whole ROI. It involves meshing and global regularization matrix assembly processes, and the strains are computed within the entire ROI at once.

For local methods [102, 103], as the special cases of global methods with only one element (also called the strain window), the generation of the regularization matrix is simple, and the strain is computed at the central point in the strain window, with strain computed at each data point in the ROI individually. In local methods, the parameters that effect the strain results include the order of the fitting function and window size.

C.6 Finite Difference Schemes

Another approach to compute the strain fields is by means of finite difference schemes [104, 105]. In the bulk of the body, away from boundaries or interfaces, the strain field can be computed using the central difference scheme [104–106]:

$$\varepsilon_{11}(i, j) = \frac{u_1(i, j + h) - u_1(i, j - h)}{2h} \quad (\text{C.1a})$$

$$\varepsilon_{22}(i, j) = \frac{u_2(i + h, j) - u_2(i - h, j)}{2h} \quad (\text{C.1b})$$

$$\varepsilon_{12}(i, j) = \frac{1}{2} \left(\frac{u_1(i + h, j) - u_1(i - h, j)}{2h} + \frac{u_2(i, j + h) - u_2(i, j - h)}{2h} \right) \quad (\text{C.1c})$$

where $u_1(i, j)$ and $u_2(i, j)$ are the displacement components expressed in pixels, in the x_1 and x_2 directions, respectively, for pixel (i, j) ; $2h$ is the [strain window size](#) in terms of pixels (see Eqn. 7.4). Note that the formulas reported above need to be adapted on the specific sign convention. For example, if the x_2 axis is taken positive in the upward direction, then $\varepsilon_{22}(i, j)$ and the first term of $\varepsilon_{12}(i, j)$ should have a minus sign in front, as the row index i in the matrices of the displacement components would increase in the opposite direction of the x_2 axis. Note also that the strains are computed in a coordinate system aligned with the image rows and columns. As mentioned in Sec. 5.3.1 and Recommendation 5.2, a coordinate transformation is likely to be required in order to express the strains in a coordinate system that is physically meaningful and aligned with the test piece.

If the displacement components are expressed in a physical unit instead of pixels, the same expressions can be used, provided the denominators are also converted into physical units by dividing them by the image scale [104]. Smaller strain window sizes correspond to smaller virtual strain gauge sizes. Conversely, larger strain windows may filter out noisy displacement data. As a note of caution, the central difference scheme is not suitable when computing strains close to boundaries or interfaces with displacement discontinuities. In the proximity of such features, the backward or forward difference scheme should be used instead so that strains are computed using displacements exclusively on one side of the boundary or interface [104].

D — Global DIC

D.1 Introduction: What is global DIC?

As explained in the main text of this guide, DIC (both local and global methods) uses an interpolant of the displacement field to perform correlation-based matching to aid in encompassing the effects of strain and perspective. The main difference between local and global DIC methods is the region of the image considered for the interpolation and the corresponding registration.

As described, the local or subset-based DIC method applies the correlation interpolant to a set of independent smaller subsets of the images, composed of a limited number of pixels, where continuity is not enforced between the neighboring subsets. The resulting displacements are only defined over a finite set of data points (typically centered in the subset), usually distributed over a regular grid built on the pixels. The lack of interaction between these subsets is the reason for the term “local method”. Determining a displacement between these points (e.g. for comparison with simulation results) requires subsequent interpolation.

In contrast, a global DIC method performs on an *a priori* chosen interpolant based on a set of shape functions to represent and solve the displacement field over the entire region of interest (ROI) of the image, and hence the term global. The displacement is then defined anywhere inside the ROI of the image. This approach allows the user to prescribe an *a priori* condition on the kinematic fields such as continuity. Currently, the most common and well known global DIC method relies on a finite-element description of the kinematics throughout the ROI of the test piece [107–110], as illustrated in Fig. D.1. This approach is referred to as finite-element based global DIC (FE-based global DIC). The user has then to define a measurement mesh that can either be built or imported from a simulation model. The degrees of freedom retrieved by the DIC software simply become the nodal displacements to be assessed. Then, the measured displacement can be calculated anywhere in the mesh from the FE shape functions.

As in local DIC, a code analyzes a user-defined region-of-interest (ROI) within the images, which contains a set of data points, also called interrogation or measurement, points. In finite-element based global DIC, data points are the nodes of a finite-element mesh. The mesh element size defines the spacing between these data points. The elements are numerically correlated from the reference image (before motion/deformation) to each subsequent image (during motion/deformation). This correlation is performed by first approximating the pattern in each element using an interpolant function, and then allowing that function to deform from the reference image based on an element shape function. A [gray level residual](#) (difference between reference configuration and deformed configuration gray levels) is minimized to match each element in the reference image with the corresponding element in the deformed images, while conserving continuity from the FE mesh. In stereo-DIC, the gray level residuals and the stereo-system calibration are used to match elements from one of the cameras to the other camera. The result of the correlation is the measured coordinates of each node of the mesh.

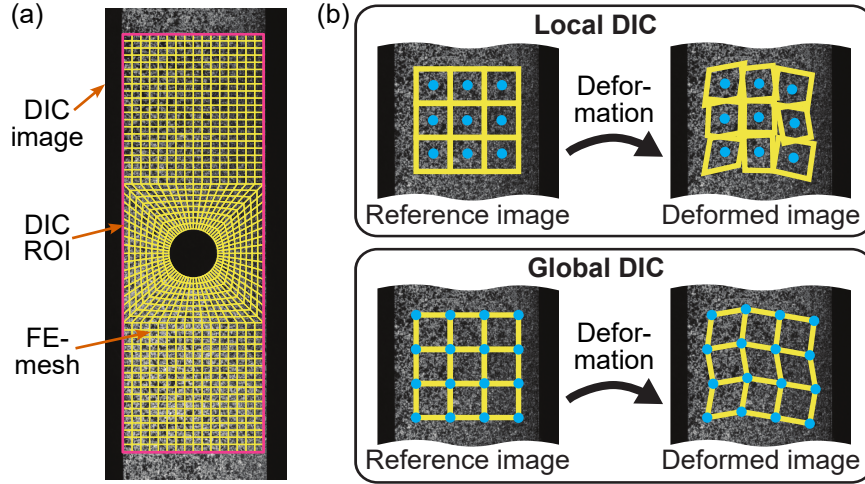


Figure D.1: (a) A representative FE-mesh over the whole ROI of the image in the FE-based global DIC. (b) Schematic comparison between local DIC subset and global DIC element.

Alternative global DIC methods also exist in the literature:

- Techniques exist to automatically select the shape function of each element to achieve the smallest error possible per degree of freedom, regardless of the original mesh [111–113].
- Some approaches involve imposing the continuity of the strain field in the whole ROI of the image (for example, by using splines [114, 115], or a spectral approach [116, 117], or adding global kinematic constraints as additional penalties onto the correlation cost function [118, 119]).
- For specific behaviors and/or geometries, analytical closed form solutions of the displacement field may be enforced. In this case (referred to as integrated-DIC), if the assumptions are correct, the user may additionally identify constitutive parameters of the test piece. Known examples include:
 - beams [120],
 - cracks [121],
 - rigid body [122],
 - diffusion interface [123], and
 - numerically precomputed solutions [124].
- Global versions of DIC might also encompass time in the solution minimization [125].

In this document, the term “global DIC” will be used to refer to the FE-based global DIC method, although in general “global DIC” is not limited to the FE-based method. Both 2D and stereo global DIC are considered here, the main difference being the calibration phase (see Sec. D.3.2).

D.2 Why use global or local DIC?

Local and global DIC approaches share a number of commonalities in their construction and their use, for which the reader of this appendix can directly refer to the main body of this guide. Main instances include:

- Measurement requirements: the same rules proposed in Sec. 2.1 of the main body of this guide apply.
- Hardware: the same advice proposed in Sec. 2.2 of the main body of this guide applies.
- Pattern quality: specific cases can arise in the case of small or very deformed FE elements in global DIC, but in general the user should be aware that advice given in Sec. 2.3 of the main body of this guide remains fully valid in global DIC.
- Pre- and post-calibration routine: the same advice proposed in Sec. 3.1 and Sec. 3.3 of the main body of this guide applies regarding general system set-up and measurement uncertainty best practices.
- Image series preparation and gray level interpolation: the same techniques described in Sec. 5.2.1 to 5.2.6 in the main body of this guide are also used in global DIC approaches, where “subset” is replaced by “element”.

Nevertheless, several factors have to be considered when selecting the type of DIC method for a given DIC measurement. Some of these factors favor using a global DIC method:

- (FE-based) global DIC has the advantage of being a natural counterpart to finite-element analysis (FEA). When comparing FEA results with experimental DIC data, it can be difficult to ensure spatial coincidence between these datasets. Using a global DIC method with the FE mesh that has been used in the simulation is a logical solution to this issue, allowing direct “node-to-node” comparison. Moreover, the kinematic fields are directly expressed in the coordinate system and in the units of the mechanical FE model. Note, however, that DIC-measured strain maps can include more noise than FEA results, and that a unified method for strain computation would have to be used before quantitative comparisons (see Sec. D.5.3 of this appendix).
- Global DIC guarantees the kinematic compatibility of the deformation field over the entire ROI, and regularization can further reduce the measurement noise. For example, because of its natural connection to FEA, global DIC allows mechanical regularization to be imposed in a straightforward way [126, 127], as discussed in Sec. D.4 of this appendix. In this case, global DIC can be less affected by local image contamination (for instance, in the case of a degrading DIC pattern, local image saturation, or visible particles moving between the lens and the test piece). Global DIC can fill in the missing local information from adjacent regions, while local DIC cannot correlate subsets where the image quality is poor [128].
- In general, global DIC allows the user to measure very complex geometries such as edges and holes,³⁴ where the user can provide a very close initialization of the shape of the measured test piece. It is often possible to measure displacements up to the edges of the ROI, which is useful if the user wants to limit the number of “lost” elements.

³⁴Global DIC can also accommodate complex 3D geometries such as ribs, and accommodate large angles between sets of cameras [129]. However, non-planar test pieces are outside the scope of the current edition of the guide.

- Global DIC provides direct access to the gray level residuals for each pixel within the ROI of the image. When plotted, the residuals can indicate where the kinematics are not rich enough to describe the deformation of the test piece from the images. For instance, one can imagine the situation where a crack initiates during the test. The discontinuity of the displacement field will result in strong concentrated residuals around the crack path. Such residual error maps are less robust at the pixel scale in local DIC packages.
- Although not in the scope of this appendix, less generic global DIC methods (i.e. integrated-DIC) allow the user to very closely match the anticipated test piece kinematics (beam, crack, etc.). Such methods can help regularize the observed kinematics in the case of a poor signal to noise ratio [130], or to identify directly simulation parameters without using a post-processing step [121, 124, 131, 132].

Conversely, local DIC methods have their own advantages:

- Local DIC is very generic and does not require the user to input any geometric features of the test piece. This approach enables the processing of image data for users who are using DIC even in cases where the measurement is not to be compared to (or regularized by) any mechanical model.
- Local DIC does not enforce displacement continuity within the measurement region, which can be important to some users in the case of studying crack opening for instance. Global DIC methods in these cases (remeshing, enrichment functions, integrated-DIC) are proven to be effective but are less straightforward and do not currently exist in commercial packages. Local DIC methods, to solve for cracks, also introduce additional operations such as subset-splitting to achieve higher accuracy.
- The local DIC method is parallelizable by nature; however, the global DIC method is not as easily parallelized (although the FE parallelization scheme is an option [133, 134]). Therefore, to track large-size images with fine spatial resolutions, local DIC can allow faster processing.
- In order to use an existing mesh for a displacement field measurement, global DIC methods often rely on a self-calibration procedure (see Sec. D.3.2.2.2) to be used. This procedure requires the mesh to be aligned to the image in order to use the test piece itself as a calibration object. Fitting an existing mesh to an image requires the ability to accurately locate fiducials (e.g. sharp angles or corners) that can be observed both in the images and the mesh (or its environment) to initialize this self-calibration procedure. If it is not possible to ensure this image/mesh correspondence, then the use of global DIC with an existing mesh is impractical.

D.3 Global DIC Practical Implications

D.3.1 Mesh Definition and Positioning

Using a mesh for a displacement field measurement has practical implications when defining the ROI of the test piece. Two situations can be encountered:

- The mesh can be defined directly on the image, in which case it is not derived from a simulation and the mesh generation is done in the similar way to the data point grid generated in the local DIC method. However, in the global DIC method, the nodes of the mesh—rather than the centers of the subsets—are selected.

- The mesh is loaded from a simulation file and is positioned on the images. Then the user selects either a group of surface elements that will constitute the ROI of the test piece, or a group of pixels per image that will constitute the ROI of the images.

The first kind of situation is very similar to the operations performed in a local DIC package: a regular grid is positioned on a reference image and is used as the ROI of this image. In this situation, no special positioning technique has to be used. The grid geometric parameters (especially the distance between nodes) can be chosen independently from the simulation. After the DIC computation, the result is provided on this grid, and then has to be exported by the user to the simulation reference system if a comparison to simulation results is to be made.

The second method allows the user to take advantage of an existing mesh, in order to perform a more direct comparison to simulation data without any post-processing. It also allows the use of mesh-based multi-camera measurement techniques in a direct fashion. To proceed with the calibration and measurement steps, the user will have to ensure a geometric correspondence between the mesh reference system and the image content (see Sec. [D.3.2](#) on 2D- and stereo-calibration).

Caution D.1 — Element Size

The consequence of this procedure is that the element size (in pixels) cannot be known precisely before this step is taken. In this context, the element size can be estimated at first, and fully validated only when the reference images have been taken. The user can then ask for a DIC mesh adaptation (refinement or coarsening) if the mesh does not fit their expectations about element size. To know more about mesh size validation, please refer to Sec. [D.4.3](#) of this appendix.

D.3.2 Calibration

Commercial packages have different calibration strategies, depending on the mesh definition options that were presented in Sec. [D.3.1](#). Options described here are available in commercial packages, but alternative routes exist.

D.3.2.1 2D Global DIC

D.3.2.1.1 New Mesh

In the case the user does not provide a pre-existing mesh, the user has to define a new mesh on the reference image. In this case, the DIC program builds its own mesh, which can be structured or unstructured, from the definition of a region of interest (ROI) in one image, similarly to what is done in local DIC. The procedure for calibrating a single camera in a global DIC program is very similar to what is described for local DIC in Recommendation [3.4](#) of the main body of this guide:

- If available, calibrate the camera via a simplified target calibration procedure, which allows for correction of optical distortions.
- Otherwise, the user can input a pixel-to-meter ratio that has been calculated based on fiducials of the image or (ideally) a resolution target.

D.3.2.1.2 Pre-Existing Mesh

In the case of using a pre-existing mesh, calibration for a single camera consists of:

- Aligning the mesh to the image via the use of fiducials as described in Sec. D.3.2.2.1. This step allows estimation of the camera intrinsic and extrinsic parameters that link the mesh coordinate system with the image coordinate system.
- Possibly correcting for distortions separately via a simplified target calibration procedure. It is always advised to correct for optical distortions whenever possible.

Caution D.2 — Mesh Position Uncertainty

In a commercial global DIC software, the mesh positioning uncertainty is on the order of the user's ability to pick a fiducial with a mouse-click (from one pixel to a few pixels depending on the geometry visibility and quality). This uncertainty should be taken into account when processing the results, possibly by performing user-sensitivity analyses to estimate results variability. Commercial packages use points as fiducials, but some other packages also allow using lines or curves.

Caution D.3 — Planar Assumption of 2D-DIC Calibration

When performing 2D-DIC calibration with a pre-existing mesh, the user assumes the points of the mesh that will be reprojected are contained within the same plane. If the ROI of the test piece mesh does not satisfy this condition, software packages may not allow the analysis to be performed.

D.3.2.2 Stereo Global DIC

D.3.2.2.1 New Mesh: Traditional Calibration Techniques

In the case the user does not provide a pre-existing mesh, the procedure for calibrating a stereo pair in a global DIC program is very similar to what is described for local DIC in Sec. 3.2 of the main body of this guide, with the use of a calibration target. For a two-camera DIC system, the mesh is usually created as a regular grid in the ROI of the primary camera. The mesh coordinate system is created based on an arbitrary origin and orientation, usually set by the first calibration image acquired by the primary camera. Good calibration practice follows advice given in Sec. 3.2 of the main body of this guide.

D.3.2.2.2 Pre-Existing Mesh: Self-Calibration

A stereo calibration consists in identifying a set of extrinsic and intrinsic camera parameters. The vast majority of calibration procedures in DIC rely on the use of a calibration target to provide a well-known object as a reference to determine the extrinsic stereo system parameters (see Sec. 3.2.2 of the main body of this guide). Alternatively, the calibration target can be replaced by the test piece itself, which geometry is assumed to be sufficiently well-known to calibrate the cameras.

The full self-calibration process is shown in Fig. D.2 and consists of four steps:

1. Pre-calibration, which aims to initialize the camera model associated with each camera by aligning the mesh to the object in the image (see Sec. D.3.2.2.1);

2. Camera calibration, which aims to update the camera model in total or in part (e.g. only extrinsic parameters) in a more robust way (see Sec. D.3.2.2.2.2);
3. Shape correction, to update the shape of the finite-element model to account for deviations from the nominal geometry when measuring the displacement fields (see Sec. D.3.2.2.2.3).
4. Possible iteration between the two last steps.

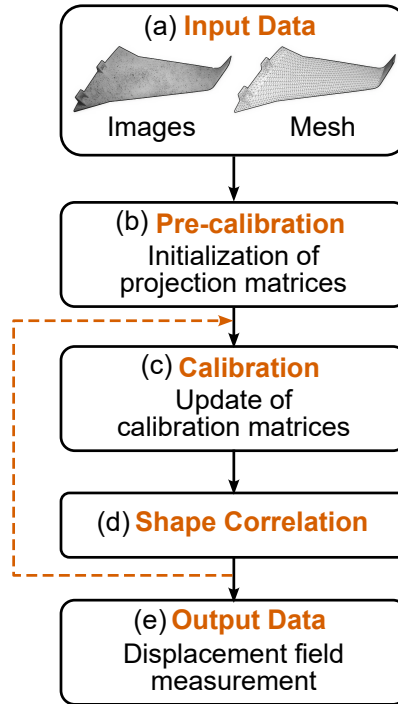


Figure D.2: Diagram summarizing the principle of the self-calibration algorithm, and illustration of the pre-calibration step with matching of 2D image points and 3D model points.

D.3.2.2.2.1 Pre-Calibration: Mesh Alignment

An important step for calibration is aligning the mesh to the images for each camera. Mesh/image correspondence is usually achieved by selecting fiducials that are visible in the image, with known coordinates in the mesh reference system. These fiducials can be either a part of the mesh (specific corner nodes or edges for instance) or elements of the environment with known coordinates with respect to the mesh. To achieve this pre-positioning step, the user has to select these fiducials in a way that they will be positioned in a 3D space encompassing the measurement area (depending on the software); see Fig. D.3. Once this correspondence is found, the mesh surface nodes are projected onto the images, and this part of the mesh can be superimposed (see Fig. D.4). Some DIC packages automatically remove elements that are not visible or for which the reprojected surface is too small.

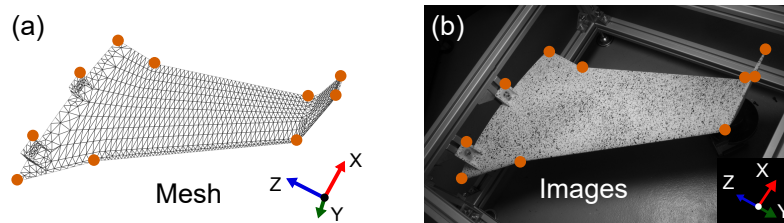


Figure D.3: Example of fiducial selection on the FE mesh (a) and in one of the reference images (b). See Tip D.1

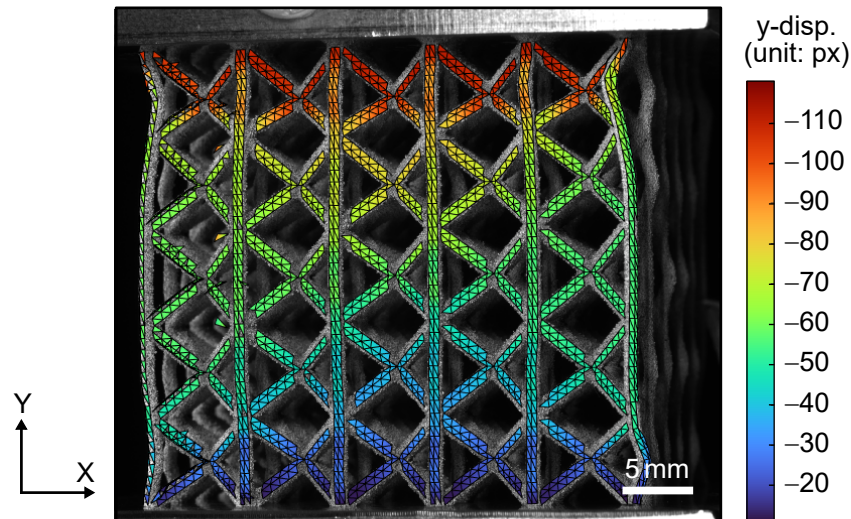


Figure D.4: A representative global DIC FE mesh over complex geometry— a lattice structure under compression (courtesy of L. Barrière, IRT Saint-Exupéry)

Tip D.1 — Number of Fiducials

Eight to ten fiducials are often recommended to ensure that both the translation and rotation of the mesh are aligned with the sample. These fiducials have to be well distributed in the 3D space and in the image to avoid bad conditioning of the inverse problem that solves for these projection matrix terms. It is good practice to prepare the list of fiducials in advance to make sure the calibration step will run smoothly. See Fig. D.3.

Tip D.2 — Fiducials and Calibration Target Images

In the case where the available fiducials do not cover the full ROI of the test piece, it is possible to add calibration target images to account for distortions and help pre-calibrate robustly.

Caution D.4 — Mesh Alignment

The first alignment step of the simulation data to the experimental results is only as good as a mouse click pixel selection. Errors of ± 1 pixel are typical. The mesh positioning step has a direct impact on the displacement measurement, since the measured displacement at the node will directly depend on this node position in the image. To the working groups' knowledge, existing literature does not study this question.

D.3.2.2.2.2 Self-Calibration: Extrinsic and Intrinsic Parameters Determination

The principle of self-calibration is to use the nominal geometry of the component, as defined in the finite-element mesh, to position and orient the camera system with respect to the 3D coordinate system of the model. A DIC algorithm then matches all images for each element to compute a residual, and minimizes this residual by searching for optimal extrinsic and/or intrinsic parameters. During this step, it is assumed that the observed geometry in the images matches the FE model shape that was provided in the original mesh, which is to be corrected in the next step.

Caution D.5 — Initialization of the Calibration Problem

The calibration operation consists in solving an ill-posed inverse problem by an iterative method. In some cases, bad initialization can prevent calibration from converging.

Recommendation

Therefore, it is preferable to initialize the problem with a set of parameters fairly “close” to the final solution to ensure algorithmic robustness. This initialization is partly determined by the pre-calibration step, which is therefore a crucial step to obtain a robust calibration. Calibration target images can also be used to robustly calibrate camera parameters, which the software can then realign on the imported geometry. When in doubt, refer to the software vendor as algorithm solutions are software-specific.

Tip D.3 — Shape Error

When measuring a part with a shape defect, a tolerance of 1% of the field-of-view is generally considered acceptable. For instance, if the FOV is 100 mm, the user may expect that a 1 mm shape error does not have a strong effect on calibration. The user should consult the vendor to understand the capability to overcome the large shape defects during the self-calibration procedure.

D.3.2.2.2.3 Shape Correction

Once the extrinsic and intrinsic parameters are determined and fixed, the FE shape can be corrected. A DIC algorithm then matches all images for each element to compute a residual, and minimizes this residual by searching for optimal nodal positions for all nodes of the ROI of the test piece.

D.3.3 Crack Measurement

When a crack occurs in a displacement field, global DIC tends to show results even for the element(s) intersected by the crack. In local DIC, non-converged subsets (which are intersected by cracks) are often

discarded. Recall that the global DIC method may enforce continuity, which is completely inappropriate when a crack exists. Therefore, the measurements in this zone are not usable, but the location of the cracks can then be detected from the resulting gray level residual field.³⁵ Meshes accounting for the presence of such cracks can be subsequently re-constructed [135], or the kinematic basis of elements passing crack paths can be further enriched [136]. Alternative local DIC approaches introduce subset splitting to solve the same kind of issues.

D.4 User-Defined Parameters

A finite-element (FE) discretization of the displacement field in the whole ROI of the image is adopted. The value of the displacement at any point is obtained from the nodal displacements of the element it belongs to and the shape functions. The continuity of the displacement field is thus enforced at any location inside the ROI of the image. As presented in Sec. D.3.1, the user has to generate a mesh and place it onto the image. This mesh can be loaded from FE codes or created by the user. In both cases, the user has to validate the mesh is suited to follow the speckle pattern, which can be done by looking at the parameters discussed in the following sections. It is to be noted that parameter choices have to be further validated with an uncertainty quantification approach.

D.4.1 Matching Criterion

The fundamental sum of squared differences (SSD) matching criterion for global DIC is the same as for local DIC (Sec. 5.2.3, Eqn. 5.1) and is repeated here for clarity:

$$\chi_{\text{SSD}}^2 = \iint_{\Omega} [G(\mathbf{x} + \mathbf{u}(\mathbf{x})) - F(\mathbf{x})]^2 d\mathbf{x}, \quad (\text{D.1})$$

where $F(\mathbf{x})$ is the intensity of the undeformed image at location \mathbf{x} , $G(\mathbf{x} + \mathbf{u}(\mathbf{x}))$ is the intensity of the deformed image at location $\mathbf{x} + \mathbf{u}(\mathbf{x})$, $\mathbf{u}(\mathbf{x})$ is the displacement field describing the motion between the undeformed and deformed images, and Ω is the entire ROI of the image. Additionally, a compensated SSD (CSSD) can be used to account for changes in lighting, using a similar definition as the ZNSSD for local DIC (Eqn. 5.2) [137–139]:

$$\chi_{\text{CSSD}}^2 = \iint_{\Omega} [c(\mathbf{x})F(\mathbf{x}) + b(\mathbf{x}) - G(\mathbf{x} + \mathbf{u}(\mathbf{x}))]^2 d\mathbf{x} \quad (\text{D.2})$$

While sharing the same fundamental roots as the matching criteria for local DIC, there are several key differences in how these criteria are implemented in global DIC:

- When using global DIC, the matching criterion is solved in the same mathematical process for all pixels of the ROI of the image, opposed to locally for each subset as in local DIC. Therefore, Ω in Eqn. D.1 or Eqn. D.2 is the entire ROI of the image opposed to the subset.
- The displacement field, $\mathbf{u}(\mathbf{x})$, is approximated by [element shape functions](#) (Sec. D.4.2) associated with an interconnected mesh, instead of independent [subset shape functions](#) (Sec. 5.2.4).
- For the CSSD, the brightness and contrast correction fields, $b(\mathbf{x})$ and $c(\mathbf{x})$, can be decomposed over a set of shape functions, ϕ , with corresponding degrees of freedom, b_i and c_i , as:

³⁵The processing of gray level “cracks” is outside the scope of the current edition of this guide.

$$b(\mathbf{x}) = \sum_i b_i \phi_i(\mathbf{x}) \quad (\text{D.3a})$$

$$c(\mathbf{x}) = \sum_i c_i \phi_i(\mathbf{x}) \quad (\text{D.3b})$$

Tip D.4 — Shape Functions for Correction Fields

Brightness and contrast typically have lower spatial-frequency than the displacement fields. Therefore, shape functions for the correction fields are often chosen to encompass larger zones than the finite-element shape functions that are used for capturing displacement fields (Sec. D.4.2).

D.4.2 Element Shape Function Type

Global DIC packages allow the user to pick shape functions for the mesh elements that are used for the measurement (see Fig. D.5). Usually finite-element shape functions are the typical choice, since they can be imported from the original FE simulation mesh. In this case, the displacement field, $\mathbf{u}(\mathbf{x})$, is decomposed as a sum of finite-element shape functions as:

$$\mathbf{u}(\mathbf{x}) = \sum_i u_i N_i(\mathbf{x}), \quad (\text{D.4})$$

where u_i are degrees of freedom of the global problem and $N_i(\mathbf{x})$ the element shape functions. DIC computations are usually performed by assembling gray level data from evaluation points contained in each projected element (in stereo-DIC) or pixels (in 2D-DIC).

Caution D.6 — Shape Function and Element Size

Just like in a FE computation, measuring displacements with higher order (e.g. quadratic) elements allows the description of smooth changes in the displacement/strain field more accurately, but the higher order shape functions also require solving an inverse problem with more degrees of freedom (assuming the element size is constant). The consequence is that higher order elements must encompass more pixels than linear elements to achieve the same uncertainty level (see Sec. D.5.2 for more details about uncertainties). A global displacement interpolation based on non-uniform rational B-splines (NURBS) offers an alternative to higher order finite-element shape functions when increasing the continuity of the solution is a critical issue [115], though NURBS are currently not available in commercial DIC software packages at the time of publication.

D.4.3 Element Size

The element size plays a similar role as the subset size in local DIC methods. The element size should be at least of the order of the feature size of the DIC pattern [59]. As the mesh is often imported from a simulation model, it should be emphasized that element size can vary in the ROI of the image.

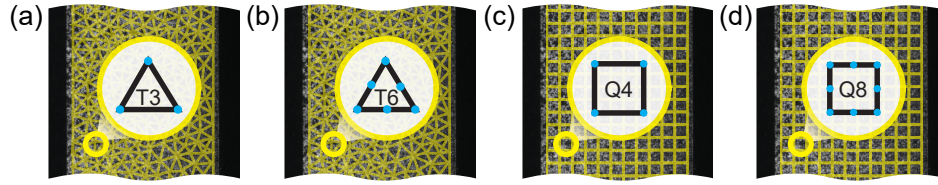


Figure D.5: Examples of global DIC element shape functions: (a) linear triangle, (b) quadratic triangle, (c) quasi-linear quadrangle, and (d) quadratic quadrangle

Tip D.5 — Element Size and Number of Features

As with local DIC and subsets, it is generally accepted that elements should contain approximately 3–5 image features in order for them to be computed with a correct convergence. This value may vary depending on the type and size of elements being used but is generally a good starting point to determine if a mesh can be used directly conjointly with a series of images.

Caution D.7 — Element Size and Shape Function

Without mechanical regularization (see Sec. D.4.4), the user will have to make a trade-off between small element sizes to capture very high displacement gradients and high measurement uncertainties that increase with decreasing element sizes. The element size and element shape function type cannot be chosen independently. A higher order element should encompass more pattern features than a linear element, as higher order elements require solving a larger number of degrees of freedom. Rules of thumb described in the main body of the guide for subset size (Sec. 5.2.7) can also be applied here.

Tip D.6 — Shape Function

As global DIC meshes often come from a simulation mesh, a logical approach can be to use the same shape functions in the DIC measurements as in the simulation. Refer to the DIC vendor manual for more information on these matters.

D.4.4 Additional Regularization

Using a refined simulation mesh for a measurement can be a problem when the size of the reprojected elements are too small in the ROI of the image. To overcome this problem, mechanical regularization has been introduced in global DIC analyses [126, 127, 140]. This regularization technique is a “mechanical filter” within the DIC algorithm. It requires the measured displacement field to locally follow a mechanical regularity imposed on the displacement and strain fields in the absence of cracks (see Fig. D.6).

The weight associated with the regularization term leads to a length scale that defines the cut-off frequency of this mechanical filter. If this regularization length is less than the element size, the latter controls the uncertainty level and the interpolation error. Otherwise, the regularization length becomes the primary length to consider and plays a similar role as the element size.

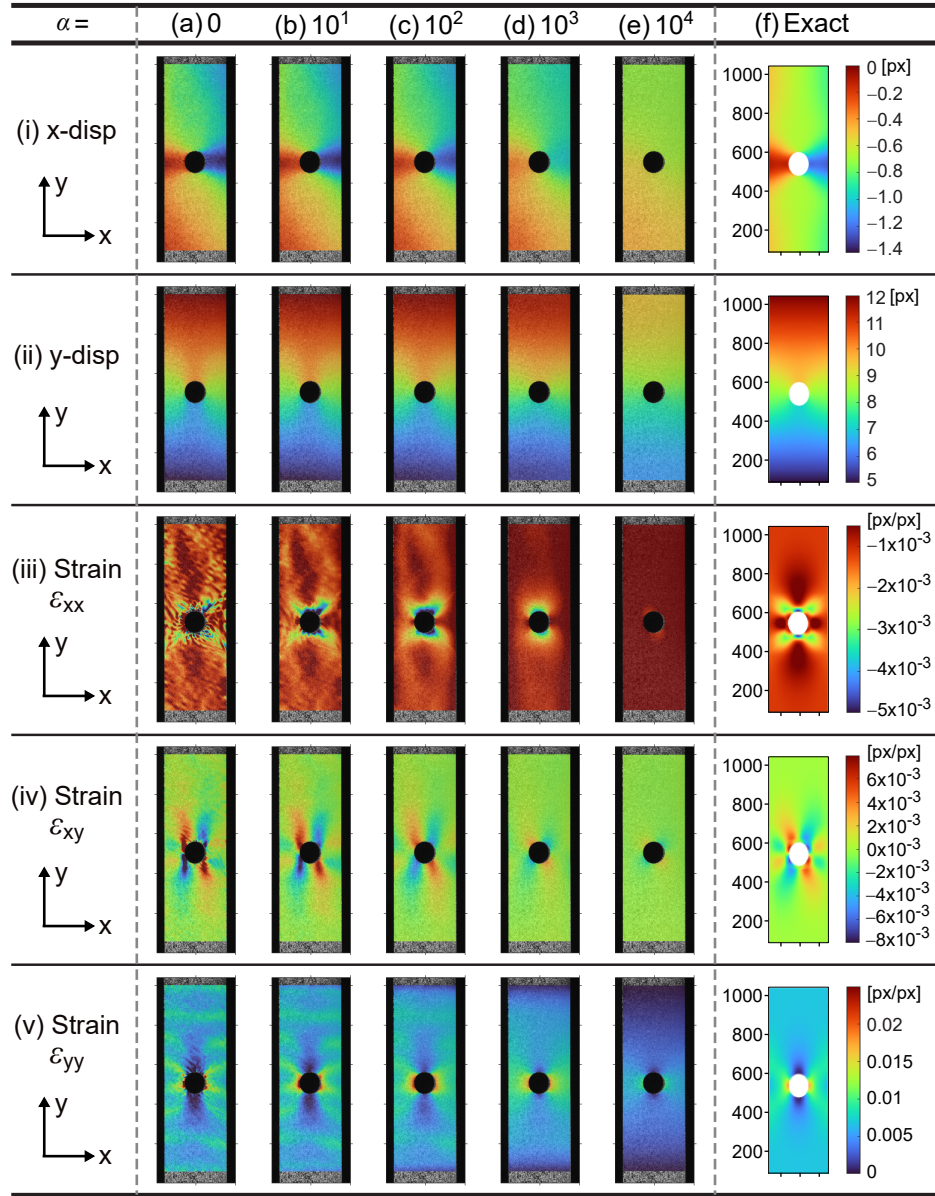


Figure D.6: Mechanical regularization method effect on an open hole tensile test in the Y-direction: displacement and strain fields with (a) no mechanical (or additional) regularization and (b), (c), (d), and (e) with increasing regularization lengths. As a “mechanical” filter, regularization allows the removal of high-frequency components that are not mechanically admissible (see (a) versus (b)). Conversely, choosing a too large regularization length can also remove useful mid-frequency content (see (d) and (e)). Data in (a-e) columns were computed using images “oht_cfrp_00” and “oht_cfrp_11” from DIC Challenge 1.0, Sample 12 [74, 141]. Column (f) “Exact” results were obtained from a finite element simulation by assuming linear elasticity.

Caution D.8 — Regularization Implementation

Regularization is highly dependent on the chosen implementation, and the user should refer to the DIC vendor manual to choose the correct regularization length for their problem and for more information on these matters.

Caution D.9 — Bias Errors Due to Regularization

Regularization will force a solution to follow the solution required by the regularization. Bias errors may be introduced if regularization is used inappropriately.

D.5 Analysis Results for Global DIC Methods

D.5.1 Gray Level Residual

The gray level residuals allow the user to check if the measured displacement field obtained after convergence of the algorithm is a valid solution to correct the deformed images by this displacement field with respect to the reference image. Residuals can be reported by camera for stereo-DIC or directly on the mesh. In the first case, each residual field corresponds to the difference between the corrected deformed image and the reference for each camera. In the case where the residual is given per element, it is generally computed as the difference between the speckle pattern defined on the 3D mesh as the mean value of the reference images and the mean values of the advected deformed images. Gray level residual fields examples are provided in Fig. D.7.

Tip D.7 — Validity of Kinematic Assumptions

The user can check the validity of the kinematic assumptions (e.g. displacement continuity or cracks) using the gray level residual.

Tip D.8 — Gray Level Residual and Image Noise

Ideally, after a measurement, the residual level should be close to the noise present in the image, assuming there are no other sources of error (i.e. camera position-dependent lighting issues, pattern degradation), and the kinematic assumptions are correct (Tip D.7).

D.5.2 Uncertainty

In global DIC, the uncertainty at each node of the FE mesh can be estimated either:

1. Analytically, through the inverse of the correlation matrix and using the noise level given by the camera detector [121]. This approach is valid if the camera sensor noise can be well approximated as white Gaussian noise, and the uncertainty in the displacement field is due only to this noise.
2. Experimentally or numerically, through the measurement of a known displacement applied to the test piece [143]. Usually this displacement is based on rigid body, stretch, shear or even harmonic motions. This route was followed in the DIC Challenge, where numerically-generated images were also used to evaluate uncertainties [74, 75], or in other measurement uncertainty guidelines [72, 73].

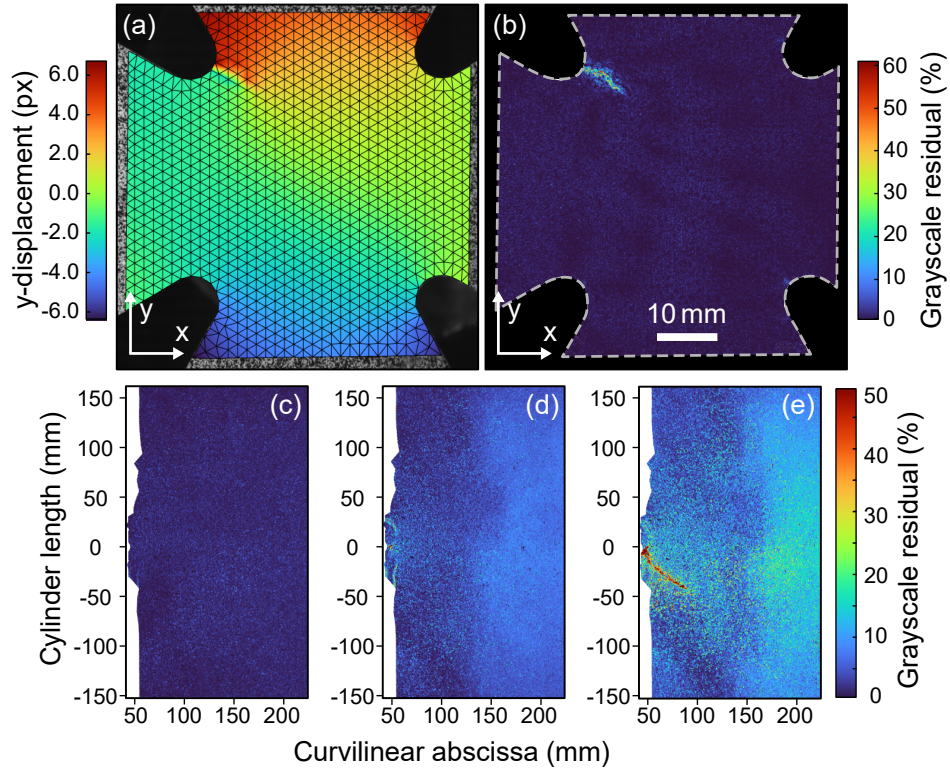


Figure D.7: Gray level residual field examples [142]. (a) Magnitude of displacement field (left) and gray level residual field (right) of a composite cross test piece (courtesy of F. Hild, LMT-Cachan). Localized increases in residuals highlight the crack path, with a characteristic size depending on chosen element size and regularization options. (b)-(d) Residual field of a crack propagation experiment in a steel tube (courtesy of EDF). Increases in the residual moving from (b) to (d) characterized with larger spatial wavelengths indicate other errors, for instance due to lighting evolutions.

Method 1 is derived from the global DIC equations, but its results remain theoretical. From a general point of view, measurement uncertainty should be reasonably similar between local and global DIC, and it is recommended to use Method 2. The main body of this guide presents usual techniques to quantify measurement uncertainties (see Sec. 5.4 of the main body of this guide). Differences between DIC techniques for global DIC include varying element size and element shape function instead of subset size, subset shape function, and step size.

D.5.3 Spatial Resolution

Some authors also address the question of spatial resolution and compare local and global DIC methods [54, 97, 144, 145]. These matters are current areas of research, and a consensus on how to define spatial resolution in global DIC has not been reached at the time of publication. The DIC Challenge 2.0 [75] attempts to tackle this issue and can be consulted for the most recent results and discussion at the time of publication.

D.5.4 Strain Computation

As for any DIC analysis, several definitions for strain calculations can be chosen. Strain computation in global DIC may use the same kind of techniques already available in local DIC methods (see Sec. 5.3.3 of the main body of this guide). For global FE-based DIC, the most direct way is to analytically take the derivatives of the existing element shape functions in order to construct the local deformation gradient, from which various strain descriptors can be calculated. This approach allows for a one-to-one matching with usual strain calculations of FE simulations. It is also usually possible to apply some kind of filter to compensate for the naturally noisy data. To extract a local strain value, some packages also allow interpolations of the displacement field in a selected region before deriving a strain.

Caution D.10 — Filtering of Displacements for Strain Calculations

Similar to the local DIC method, users should be aware of the implications of using any kind of filter or transformation of the raw measured data (i.e. the displacements). The use of filtering, mechanical regularization or virtual strain gauges should always be handled with care since these settings may have a strong influence on the extracted quantity value and noise-floor (as defined in the main body of this guide). Users should refer to the DIC vendor manual and training for more information on these matters.